ZooKeys 626: 1–43 (2016)
doi: 10.3897/zookeys.626.9681
http://zookeys.pensoft.net

RESEARCH ARTICLE

A peer-reviewed open-access journal
ZooKeys
Launched to accelerate biodiversity research

A new species of *Illacme* Cook & Loomis, 1928 from Sequoia National Park, California, with a world catalog of the Siphonorhinidae (Diplopoda, Siphonophorida)

Paul E. Marek[1], Jean K. Krejca[2], William A. Shear[3]

1 *Virginia Polytechnic Institute and State University, Department of Entomology, Price Hall, Blacksburg, Virginia, USA* **2** *Zara Environmental LLC, 1707 W FM 1626, Manchaca, Texas, USA* **3** *Hampden-Sydney College, Department of Biology, Gilmer Hall, Hampden-Sydney, Virginia, USA*

Corresponding author: *Paul E. Marek* (paulemarek@gmail.com)

Academic editor: *R. Mesibov* | Received 25 July 2016 | Accepted 19 September 2016 | Published 20 October 2016

http://zoobank.org/36E16503-BC2B-4D92-982E-FC2088094C93

Citation: Marek PE, Krejca JK, Shear WA (2016) A new species of *Illacme* Cook & Loomis, 1928 from Sequoia National Park, California, with a world catalog of the Siphonorhinidae (Diplopoda, Siphonophorida). ZooKeys 626: 1–43. doi: 10.3897/zookeys.626.9681

Abstract

Members of the family Siphonorhinidae Cook, 1895 are thread-like eyeless millipedes that possess an astounding number of legs, including one individual with 750. Due to their cryptic lifestyle, rarity in natural history collections, and sporadic study over the last century, the family has an unclear phylogenetic placement, and intrafamilial relationships remain unknown. Here we report the discovery of a second species of *Illacme*, a millipede genus notable for possessing the greatest number of legs of any known animal on the planet. *Illacme tobini* **sp. n.** is described from a single male collected in a cave in Sequoia National Park, California, USA. After 90 years since the description of *Illacme*, the species represents a second of the genus in California. Siphonorhinidae now includes *Illacme* Cook & Loomis, 1928 (two species, USA), *Kleruchus* Attems, 1938 (one species, Vietnam), *Nematozonium* Verhoeff, 1939 (one species, South Africa) and *Siphonorhinus* Pocock, 1894 (eight species, India, Indonesia, Madagascar, Vietnam).

Keywords

California Floristic Province, paleoendemic, endemic, marble, mesovoid shallow substratum, Kaweah River, foothills, Sierra Nevada forest ecoregion, California interior chaparral and woodlands ecoregion

Introduction

The genus *Illacme* is the sole representative of the Siphonorhinidae in the Western Hemisphere. Its closest known relative, *Nematozonium filum* Verhoeff, 1939, is endemic to the Drakensburg Mountains of South Africa (Shelley and Hoffman 2004, Hamer 1998). The current geographical distribution of the Siphonorhinidae in California, Wallacea, Sundaland, Himalayas, Indo-Burma, and southern Africa likely represents remnants of its former range and an ancient radiation predating the breakup of Pangaea more than 200 million years ago (Marek and Bond 2006). There is molecular phylogenetic evidence for monophyly of its order Siphonophorida (Regier et al. 2005, Brewer and Bond 2013, Fernandez et al. 2015). In contrast, it is unclear whether the Siphonorhinidae is a natural group. Because there are so few species in the Siphonorhinidae and little is known about the family from a basic α-taxonomic and a biological perspective, the discovery of a novel species provides significant new data. Here we describe a new species of the genus *Illacme* from a marble cave in Sequoia National Park and provide a world catalog and map of species in the family Siphonorhinidae.

The Siphonorhinidae are members of the subterclass Colobognatha that contains the orders Platydesmida, Polyzoniida, Siphonocryptida, and Siphonophorida (Shear 2011). The Colobognatha are diminutive in size, with most individuals less than 30 mm in length, about a millimeter or less in trunk width, and possessing an oval or circular cross-section. The Platydesmida, Polyzoniida, and Siphonocryptida are typically wider than the Siphonophorida, and are dorsoventrally flattened in segmental cross-section. Some taxa possess elongated paranota further adding to the flattened appearance, and appear platyhelminth-like (e.g., *Brachycybe*, *Hirudicryptus*, *Octoglena*, *Platydesmus*). In contrast, most individuals in the order Siphonophorida are pale thread-like millipedes that are even confused with nematodes by the unaccustomed observer. These millipedes possess the greatest number of leg-bearing trunk segments of any animal. One female specimen of *I. plenipes* Cook & Loomis, 1928 possesses a superlative 192 diplosegments. The trunk rings are translucent and lightly pigmented and lack the heavy cuticle that many chilognathan diplopods possess. Despite the delicate nature of their exoskeleton, siphonophoridans have a variety of cuticular adornments—including spines, tubercles, and silk-secreting setae (Read and Enghoff 2009, Marek et al. 2012).

The rings of colobognath millipedes are uniform in appearance throughout the length of the trunk, except those of some Platydesmida (genus *Andrognathus*) with anteriorly projecting ozopores on the fifth ring and Platydesmida and Siphonocryptida with color patterns that vary antero-posteriorly (Shear and Marek 2009, Enghoff 2011). The cephalic morphology of colobognaths is generally regarded as highly derived relative to other Diplopoda, making it difficult to draw homology to known structures (Enghoff et al. 2015). The orders Siphonocryptida and Polyzoniida possess a cluster of simple eyes; in Platydesmida and Siphonophorida eyes are absent. However, a few platydesmidan taxa possess pigmented patches on the cuticle where the eyes would normally occur. The Colobognatha (meaning "abbreviated jaw") are characterized by reduced mouthparts. Their heads are often small in relation to the trunk and appear

triangular in anterior view, while other millipedes have larger, subspherical heads supporting musculature required for strong chewing action by the mandibles. This modification reaches a pinnacle in the Siphonophoridae, which have heads drawn out into long beaks, and mandibles that are highly simplified and styliform, with gnathochilarial components fused and reduced. The Siphonorhinidae possess mouthparts somewhere in between with components that remain identifiable and able to be homologized with those of other non-colobognath millipedes.

In contrast with their derived cephalic morphology, the order Siphonophorida possesses a primitive trunk architecture for helminthomorph diplopods, including unfused rings composed of a free sternite, pleurite, and tergite. The siphonorhinid mouthparts are presumed to be ancestral to the highly derived siphonophorid beak, and based on these features, siphonorhinids are hypothesized to be a basal sister group to the remaining siphonophoridan taxa. Based on molecular phylogenetics, the Siphonophorida are sister to a clade formed by exemplars of the Polyzoniida and Platydesmida (Regier et al. 2005, Sierwald and Bond 2007). However, the family Siphonorhinidae has yet to be sampled by recent phylogenomic estimations of the class Diplopoda (Brewer and Bond 2013, Fernandez et al. 2015).

Illacme species and their colobognathan relatives exhibit true anamorphosis (euanamorphosis), whereby six-legged hatchlings develop into adulthood in coordination with the addition of new segments (Enghoff et al. 1993). The addition of new segments lengthens the body and adds legs, which develop shortly after segment formation. This process continues beyond attainment of sexual maturity for an indeterminate amount of time, and imparts high variability and a very large number of segments in euanamorphic taxa. A paratype female of *I. plenipes* collected by O.F. Cook in 1926 possesses 192 segments and 750 legs (Cook and Loomis 1928). The age of this exceptionally segmented individual is unknown, but likely to be several years. While diplosegmentation and sequentially repeated leg-bearing segments serve to provide force for burrowing, the superlative segment count in *I. plenipes* seems unwarranted and perhaps serves another function. The role is unclear, and several hypotheses have been suggested including: burrowing in deeper soil, clinging to rocks, or lengthening the gut to digest low nutrient food (Marek et al. 2012). As in the highly elongate geophilomorph centipedes, the long, flexible body may be an adaptation to negotiating narrow, pre-existing spaces in the soil.

In the western U.S. (Arizona, California, Texas), Siphonophorida occur in moist refugia within more arid habitats. However, many tropical siphonophoridans occur in mesic habitats and in rainforests that are continuously wet. The microhabitats of siphonophoridan species are usually within deep substrata and individuals are frequently discovered beneath large stones (e.g., *I. plenipes* in California) and embedded inside large decaying logs (e.g., *Siphonophora* species in Central America). Persistence in these microhabitats is consistent with their morphology, including a lack of eyes, depigmented exoskeleton, shortened legs, and an elongate flexible body. The Siphonophorida in Arizona and California are found in relatively mesic oak woodlands in mountain foothills, including those of the Coast Ranges (CA), Sierra Nevada (CA), and Madrean Sky Islands (AZ).

Methods and results

From 2002 to 2004, scientists led formal biological surveys of caves in Sequoia and Kings Canyon National Parks for invertebrates, including arachnids, myriapods, and hexapods. From 2006 to 2009 several follow up visits yielded incidental collections, and among these specimens was one sample of *I. tobini* sp. n. from Lange Cave, collected by JKK on 9 October 2006. Three years after this discovery, myriapod specialists made three additional expeditions to Lange Cave and surrounding habitats to search for additional material for description of the species. Collecting effort was focused within the cave, and surface searches around the cave entrance were carried out. More intensive searches were conducted at the the confluence of Cave, Yucca, and Cascade creeks—the general area where *I. tobini* sp. n. was discovered. During field expeditions by PEM from 2010–2012, 63 additional localities in the foothills of the Sierra Nevada from El Dorado National Forest southward to the Tehachapi Mountains were explored for *I. tobini* sp. n. Using techniques previously developed for *I. plenipes* (and applied to *I. tobini* sp. n.), the undersides of large stones were examined. The bases of decaying logs and leaf litter were also searched, albeit an improbable microhabitat since previous collections of U.S. siphonophoridans were rarely encountered in these areas. Live millipedes were collected by hand, or in some cases lifted with a paintbrush or forceps if necessary. In spite of all of this additional effort, field biologists found no additional specimens.

Lange Cave is 240 km east of its congener *I. plenipes* that occurs in San Benito County California (Fig. 1). The single live specimen was sacrificed and preserved in 80% ethanol. Forty segments from the midbody were removed and preserved in 100% ethanol and archived at -20 °C nine years later in an attempt to preserve DNA. The remnants of the holotype (anterior and posterior sections) were removed, dried at room temperature, and mounted on a standard SEM pin stub mount (Ø12.7 mm × 8 mm pin height) with double sided carbon conductive tape. Specimens were coated with 10 nm of platinum and palladium metals with a Leica EM ACE600 high vacuum coater (Wetzlar, Germany), and stored with silica gel desiccant until ready for examination.

Genomic DNA was extracted and purified from half of the ethanol-preserved tissue from the midbody section using a Qiagen DNeasy tissue extraction protocol. The remaining half of the tissues have been retained in the VTEC frozen tissue collection. Standard kit protocol was followed and the DNA was eluted from the spin column with one round of 50 µL AE buffer. Genomic DNA was archived at -20 °C in the freezer collections at the VTEC. A segment of the cytochrome c oxidase I gene (COI), was amplified using polymerase chain reaction and the thermal cycling steps of Hebert et al. (2003) and with the universal DNA barcoding primers LCO1490 and HCO2198 of Folmer et al. (1994). Polymerase chain reaction of the COI barcoding region of the single *I. tobini* sp. n. individual and visualization of amplifications on a 12% agarose gel, did not indicate the presence of DNA based on comparison with the negative and positive controls. A second PCR was repeated with the amplification product from the

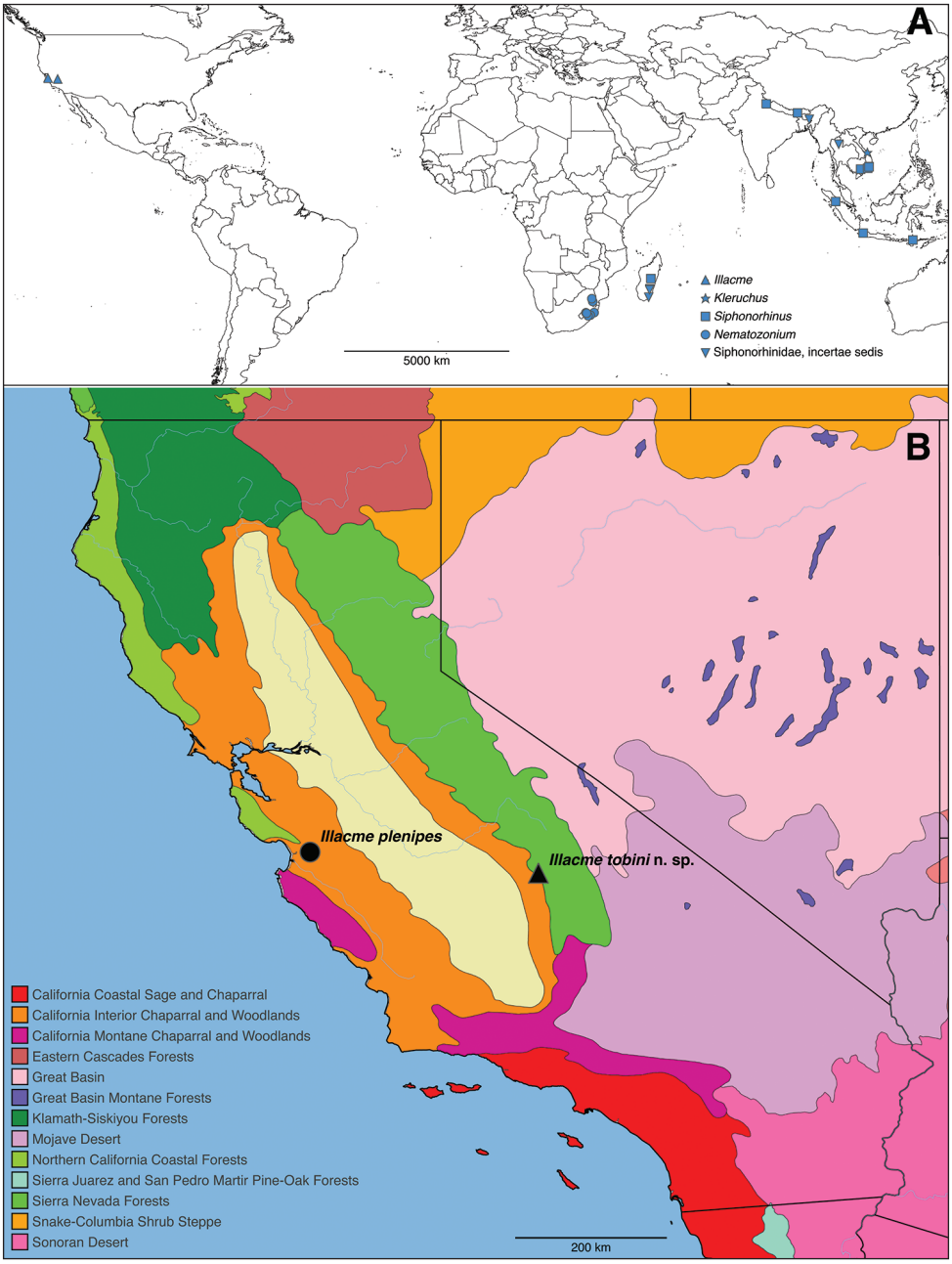

Figure 1. A Distribution of the millipede family Siphonorhinidae, and **B** of the genus *Illacme*. Terrestrial ecoregions according Olson et al. (2001).

first reaction, in case a low concentration of DNA from *I. tobini* sp. n. was present. The second reaction showed the same results and a lack of DNA based on comparison with the controls.

Descriptive taxonomy

For comparison with *I. tobini* sp. n., we examined the 17 known specimens of *I. plenipes* from the Smithsonian Institution (USNM), Florida State Collection of Arthropods (FSCA), Virginia Museum of Natural History (VMNH), and Virginia Tech Insect Collection (VTEC). The *I. tobini* sp. n. specimen label information was databased in Symbiota Collections of Arthropods Network (http://symbiota4.acis.ufl.edu/scan/portal/). Due to the sensitivity of its cave habitat, locality details are withheld publicly on SCAN, and are available upon request from the authors. The following dimensions were measured for *I. plenipes* and *I. tobini* sp. n.: (1) body length: from anterior margin of labrum to posterior margin of paraprocts, BL; (2) head width, HW; (3) head length, HL; (4) interantennal socket width, ISW; (5) antennomere 6 width, AW; (6) collum width, CW; (7) metazonite width at 1/4 length of body, W1; (8) metazonite length at 1/4 length of body, L1; (9) metazonite height at 1/4 length of body, H1; (10) first apodous metazonite width, AS1; (11) anterior gonopod article 7 width, A7W; and (12) posterior gonopod article 7 width, P7W. The 12 measurements refer to 1–10, 17 and 18 used in Marek et al. (2012). Specimens were measured from digital scanning electron and light micrographs using the segmented line measurement tool in ImageJ64 (Rasband 2011). Measurements are recorded in millimeters and this unit is hereafter excluded throughout the paper. The number of segments were counted and legs calculated using the formula $l = ((p + a) \times 4)–(a \times 4)–(10)$, where l is the number of legs, p is the number of podous tergites (each bearing four legs), a is the number of apodous tergites (without legs), and 10 is the number to be subtracted because the first tergite (the collum) is legless and second through fourth tergites (the millipede thorax) each have two legs. Examination of specimens were accomplished with a Leica M125 stereomicroscope with eyepiece reticules (Wetzlar, Germany). Scanning electron micrographs were taken of palladium/platinum coated structures with an FEI Quanta 600 FEG environmental SEM (Hillsboro, Oregon). The figures are of male specimens, unless otherwise indicated, and Figs 2–6, 8–11, 15–17, 18, and 19 show *I. tobini* sp. n. and *I. plenipes* (VTEC catalog # SPC000932) side by side for comparison. The identification and terminology of antennal sensilla followed that of Nguyen Duy-Jacquemin (1974) and Chung and Moon (2006). Terminology of mouthparts is from Silvestri (1903) and Koch (2015). Museum abbreviations follow Marek et al. (2014), and supplemental abbreviations are the following: HT = holotype; PT = paratype; LT = lectotype; ST = syntype; nec = but not; and sic = misspelling. The National Geospatial-Intelligence Agency GEOnet Names Server (NGA GNS) was used to query names of historical type localities for their geographical coordinates, using the "include historical records" option (http://geonames.nga.mil/gns/html/). The elevation of the type locality was determined from a U.S. Geological Survey quadrangle topographic map: Giant Forest Quadrangle, 7.5-minute series (USGS 2015). The uncompressed and uncropped scanning electron micrographs of *I. tobini* sp. n. are archived in the Dryad Data Repository at http://dx.doi.org/10.5061/dryad.tk0b8 under a public domain CC0 Creative Commons license.

Taxonomy

Class Diplopoda de Blainville in Gervais, 1844
Subclass Chilognatha Latreille, 1802/1803
Infraclass Helminthomorpha Pocock, 1887
Subterclass Colobognatha Brandt, 1834
Order Siphonophorida Hoffman, 1980
Family Siphonorhinidae Cook, 1895

Genus *Illacme* Cook & Loomis, 1928

Family placement. The genus *Illacme* is placed in the family Siphonorhinidae based on the following characters: Head pear-shaped (♂) or triangular (♀), not elongate or beak-shaped, as in the Siphonophoridae (Fig. 2A–F). Antennae elbowed between antennomeres 3, 4 (Figs 2B; 3A, B). Antennomeres 5, 6 with apical dorsal cluster of 7 or 8 basiconic sensilla (Bs_2) in slight depression, not in defined circular pits, as in the Siphonophoridae (Figs 2B, D; 3A, B). Antennomere 1 set deep in cranium, not entirely visible dorsally as in Siphonophoridae (Figs 2A, B; 2E; 3C, D). Antennomere 2 longer than wide, conical, not doughnut-shaped and wider than long as typical in Siphonophoridae. Anterior margin of collum straight, not emarginate medially as in Siphonophoridae. Sterna with prominent midline triangular projections, oriented ventrally (Figs 3E, F; 4A, B). Posterior gonopods with distal podomere divided into 2–4 branches with one branch spike-like (Figs 4C, D, E, F; 5A–D). See also diagnoses of *Illacme* in Shelley (1996b, pg. 23), Marek et al. (2012, pg. 85), and Enghoff et al. (2015, pg. 386), and of Siphonorhinidae in Shelley and Hoffman (2004, pg. 218), Wesener (2014, pg. 417), and Enghoff et al. (2015, pg. 386).

Diagnosis. Adults of *Illacme* are distinct from other siphonorhinid genera (and commonly encountered millipedes co-occurring with *I. tobini* sp. n. and *I. plenipes*) based on the combination of the following characters: Body light cream-colored, thread-like, extremely narrow and long (max. width: ♂ 0.55, ♀ 0.64; max. length: ♂ 28.16, ♀ 40.40). Adult individuals with 84–192 segments, and with 318–750 legs. Body covered with many long delicate setae, imparting a velvety appearance (Figs 5E, F; 6A, B). Antennae elbowed between antennomeres 3, 4 (Figs 2B; 3A, B). Antennomeres 5, 6 enlarged, appearing much larger relative to other articles (Figs 2B, D, 3A, B). Head pear-shaped in males or triangular or chevron-shaped in females, eyeless (Fig. 2C–F). Genae slightly convex (♂) or straight (♀), not concave (imparting a teardrop-shaped head) as in *Nematozonium filum*, *Siphonorhinus* sp. (Wesener 2014), and the family Siphonophoridae (Shelley 1996, Shelley and Hoffman 2004). Mouthparts (gnathochilarium, mandibles) and labrum tightly appressed, tapered anteriorly to rounded apex—not beak-shaped, as in the Siphonophoridae (Figs 2A–F; 3C, D). Labrum with a deep medial slit, margins lined with teeth (Figs 6C–F; 7A–F). Denticulate shelf-like carina, projecting dorsally from labrum-epistome margin (Figs 6E, F; 7D; 8A, B). 9th and 10th leg pairs modified into gonopods, each comprising 7 podomeres (Figs 4C, D; 8C–F; 9A–F). Anterior gonopod thick, bulkier than posterior

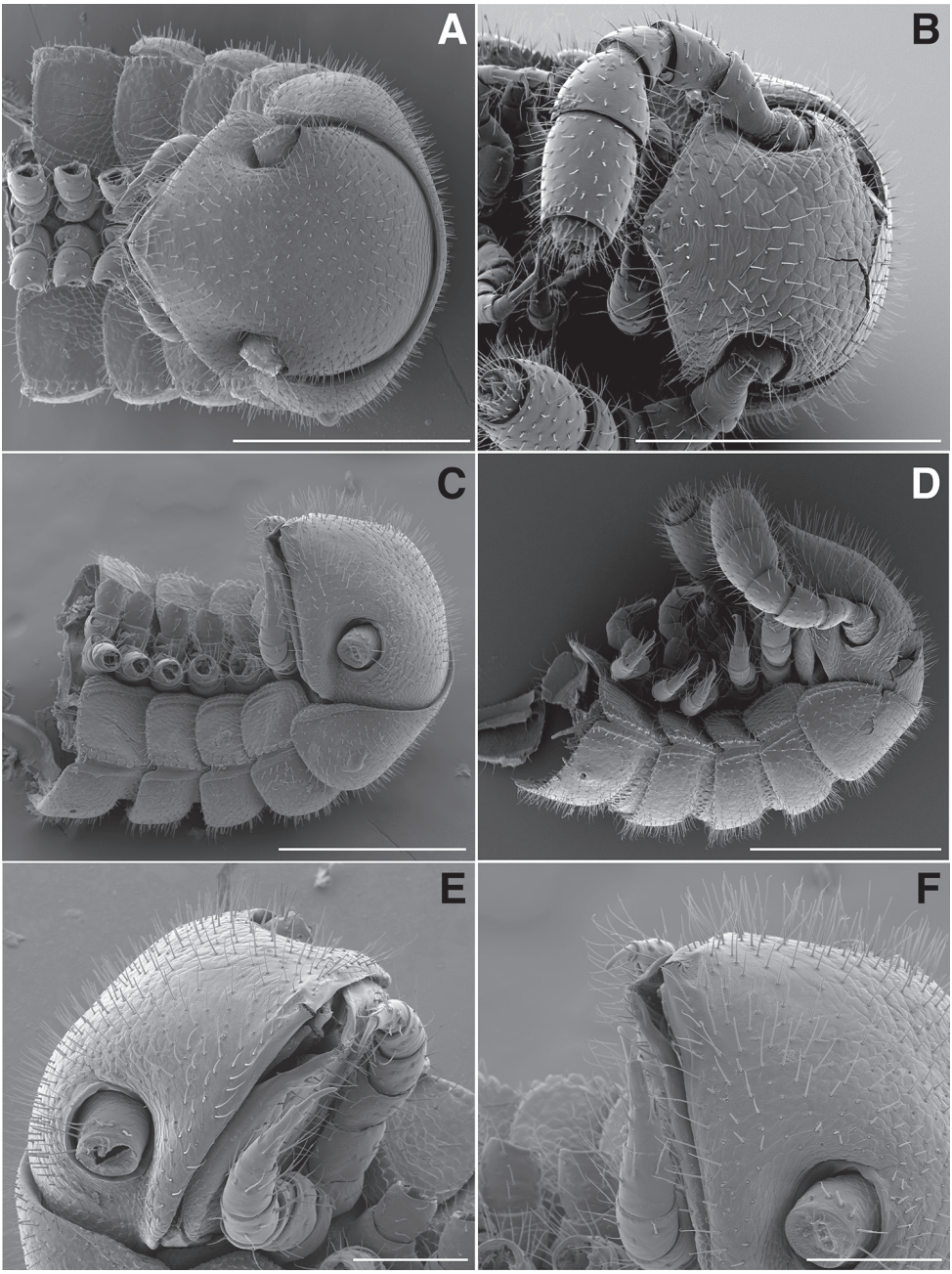

Figure 2. A Dorsal view of head, antennae and rings 1–5 of *I. tobini* sp. n. (scale bar 300 μm) **B** the same of *I. plenipes* (scale bar 300 μm) **C** Lateral (right) view of head and rings 1–5 of *I. tobini* sp. n. (scale bar 300 μm) **D** the same of *I. plenipes* (scale bar 300 μm). *Illacme tobini* sp. n.: **E** anterolateral (right) view of head and first leg pair (scale bar 100 μm) **F** lateral (left) view of head and first leg pair, antennae broken off at base (scale bar 100 μm). (Catalog #s: *I. tobini* sp. n. MPE00735, *I. plenipes* SPC000932.)

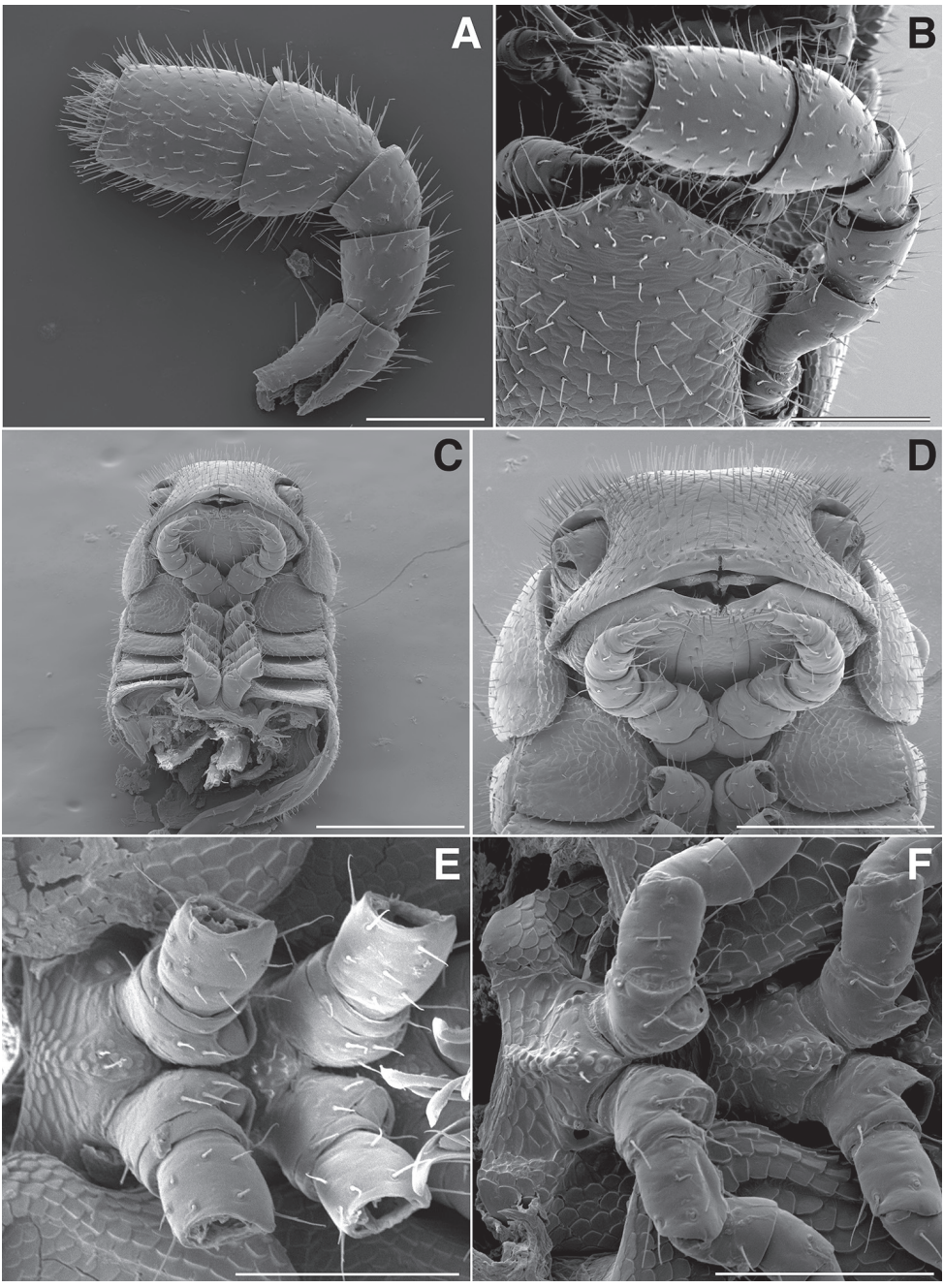

Figure 3. A Lateral (right) view of antenna of *I. tobini* sp. n. (scale bar 100 μm) **B** the same of *I. plenipes* (scale bar 100 μm). *Illacme tobini* sp. n.: **C** ventral view of head and rings 1–5 (scale bar 300 μm) **D** the same of head and rings 1–3, magnified view (leg pairs 2–6 broken off at prefemur-femur joint) (scale bar 200 μm) **E** Ventral view of rings 6 and 7 with sternites, pleurites and leg bases of *I. tobini* sp. n. (scale bar 100 μm) **F** the same of *I. plenipes* (scale bar 100 μm). (Catalog #s: *I. tobini* sp. n. MPE00735, *I. plenipes* SPC000932.)

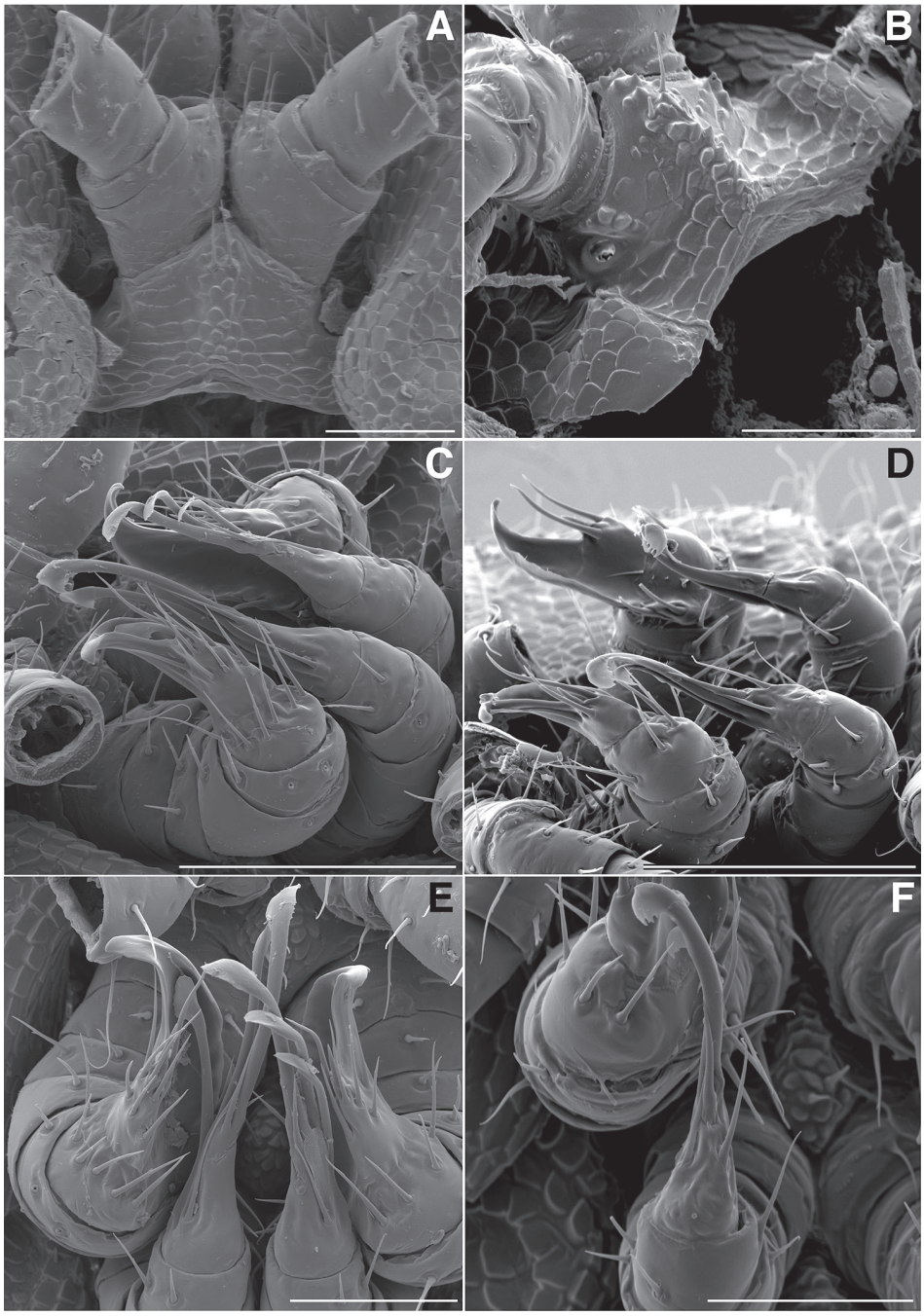

Figure 4. A Anterior view of ring 6 sterna of *I. tobini* n. sp (scale bar 50 μm) **B** anterolateral (left) view of the same of *I. plenipes* (scale bar 50 μm) **C** Lateral (right) view of gonopods (leg pairs 9 and 10) of *I. tobini* sp. n. (scale bar 100 μm) **D** the same of *I. plenipes* (scale bar 100 μm) **E** Ventral view of gonopods of *I. tobini* sp. n. (centered on right posterior gonopod, leg-pair 10) (scale bar 50 μm) **F** the same of *I. plenipes* (scale bar 50 μm). (Catalog #s: *I. tobini* sp. n. MPE00735, *I. plenipes* SPC000932.)

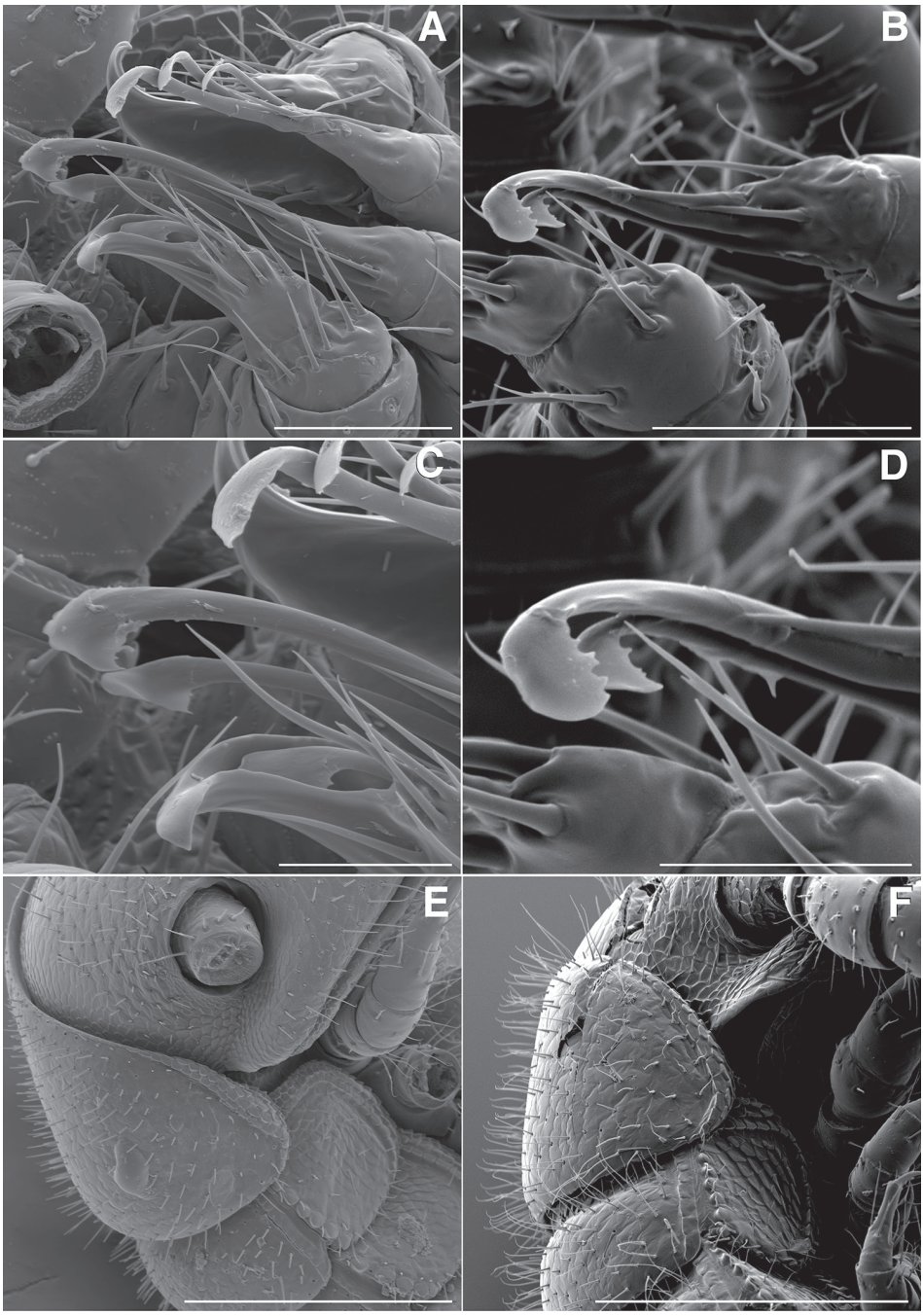

Figure 5. A Lateral (right) view of gonopods of *I. tobini* sp. n. (centered on right posterior gonopod) (scale bar 50 μm) **B** the same of *I. plenipes* (scale bar 50 μm) **C** Lateral (right) view of right posterior gonopod apex of *I. tobini* sp. n. (scale bar 25 μm) **D** the same of *I. plenipes* (scale bar 25 μm) **E** Lateral (right) view of head, collum, and rings 2, 3 of *I. tobini* sp. n. (scale bar 200 μm) **F** the same of *I. plenipes* (scale bar 200 μm). (Catalog #s: *I. tobini* sp. n. MPE00735, *I. plenipes* SPC000932.)

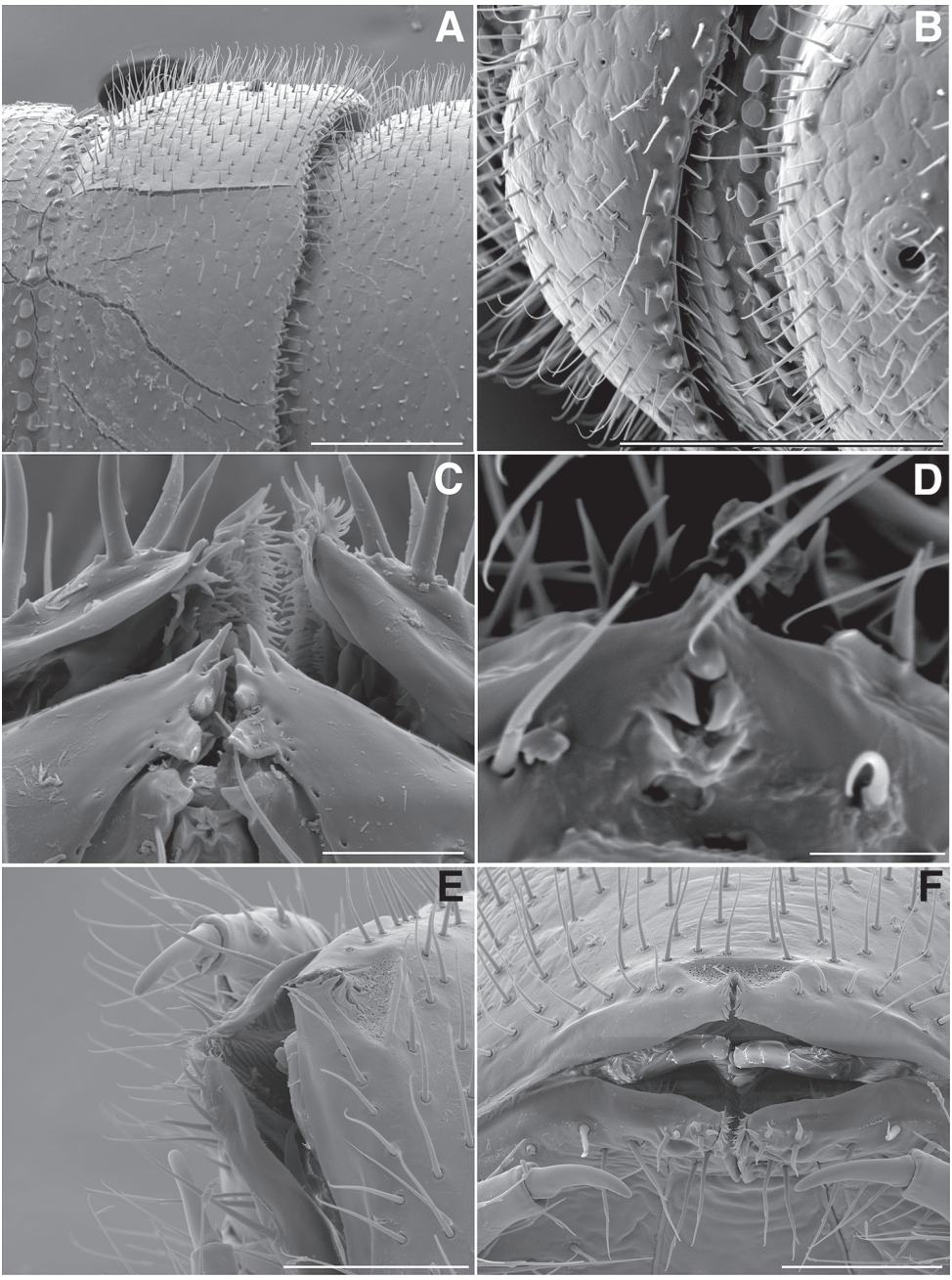

Figure 6. A Dorsolateral (left) view of tenth prozonite and metatergite of *I. tobini* sp. n. (scale bar 100 μm) **B** the same of *I. plenipes* (scale bar 100 μm) **C** Dorsal view of anterior region of head and labrum of *I. tobini* sp. n. (scale bar 10 μm) **D** the same of *I. plenipes* (the gnathochilarial apices can be seen projecting beneath the medially split labrum) (scale bar 10 μm). *Illacme tobini* sp. n.: **E** anterolateral (left) view of head and first leg pair (scale bar 50 μm) **F** anterior view of head with gnathochilarium open showing flabellate mandibles (scale bar 50 μm). (Catalog #s: *I. tobini* sp. n. MPE00735, *I. plenipes* SPC000932).

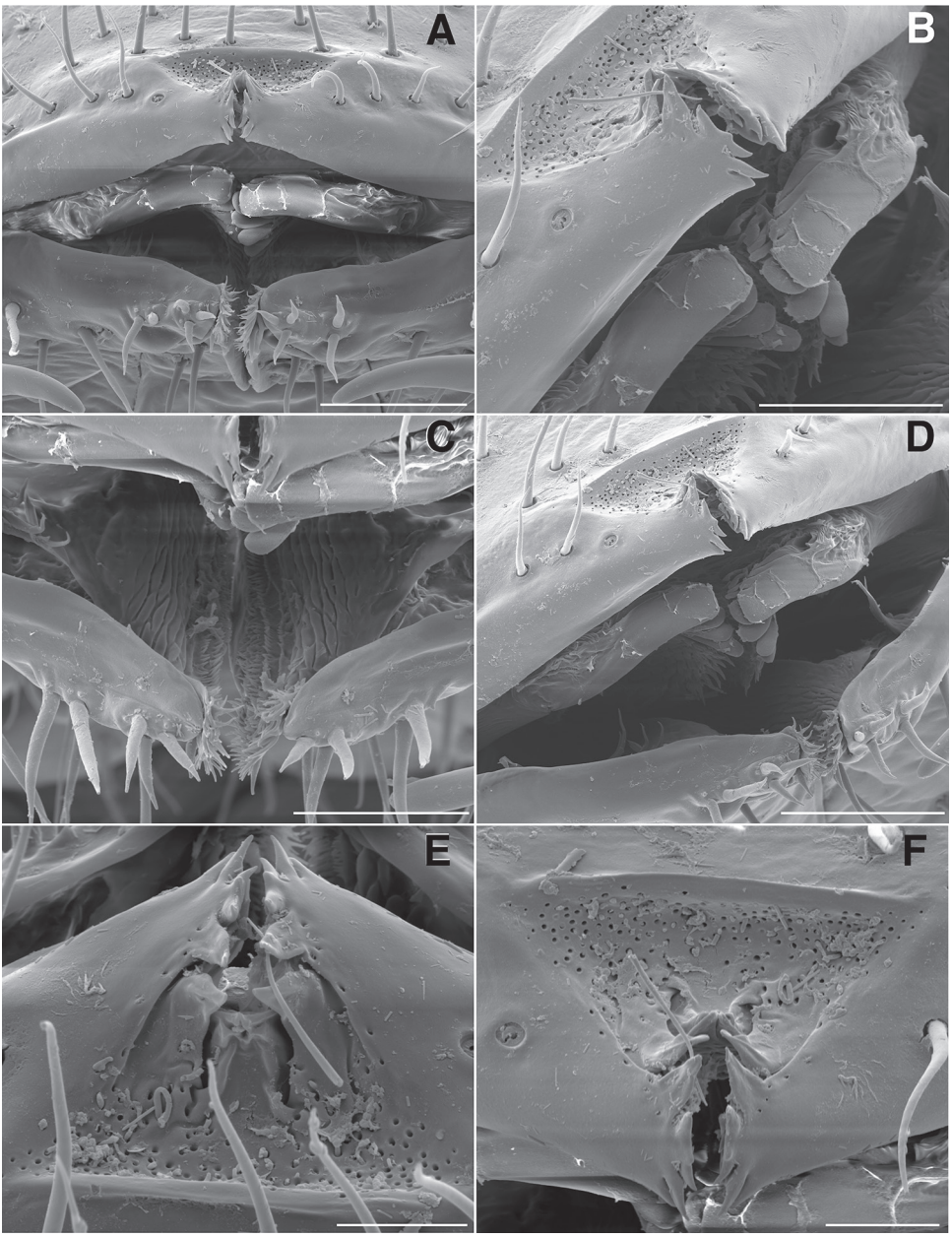

Figure 7. *Illacme tobini* sp. n.: **A** anterior view of head with gnathochilarium open showing flabellate mandibles (scale bar 30 μm) **B** anterolateral (right) view of head with gnathochilarium open showing mandibles and pectinate lamella with numerous rows of jagged ventrally projecting serrulae (scale bar 20 μm) **C** dorsal view of V-shaped endochilarial frontal body with fringed lobes (spatulae) protruding through gnathochilarial stipes (scale bar 20 μm) **D** anterolateral (right) view of open mouth and keel-shaped pectinate lamella of the mandible nested in V-shaped groove of the endochilarium (scale bar 30 μm) **E** dorsal view of labrum with deep medial incision (scale bar 10 μm) **F** anterior view of labrum with heavily porous surface (scale bar 10 μm). (Catalog #: *I. tobini* sp. n. MPE00735.)

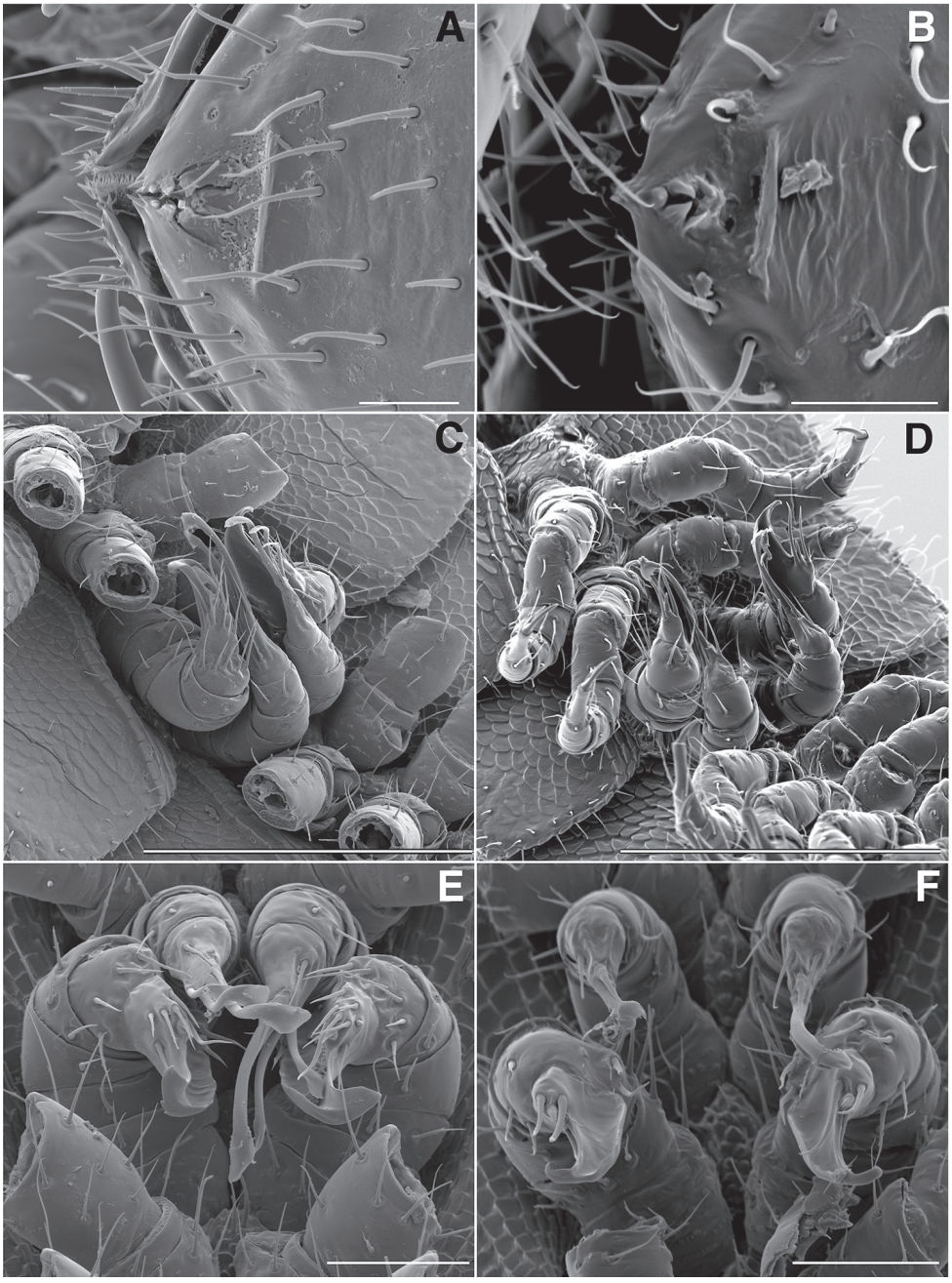

Figure 8. A Dorsal view of anterior region of head and labrum of *I. tobini* sp. n. (scale bar 20 μm) **B** the same of *I. plenipes* (scale bar 20 μm) **C** Ventrolateral (right) view of gonopods of *I. tobini* sp. n. (scale bar 200 μm) **D** the same of *I. plenipes* (scale bar 200 μm) **E** Anteroventral view of gonopods of *I. tobini* sp. n. (scale bar 50 μm) **F** the same of *I. plenipes* (scale bar 50 μm). (Catalog #s: *I. tobini* sp. n. MPE00735, *I. plenipes* SPC000932.)

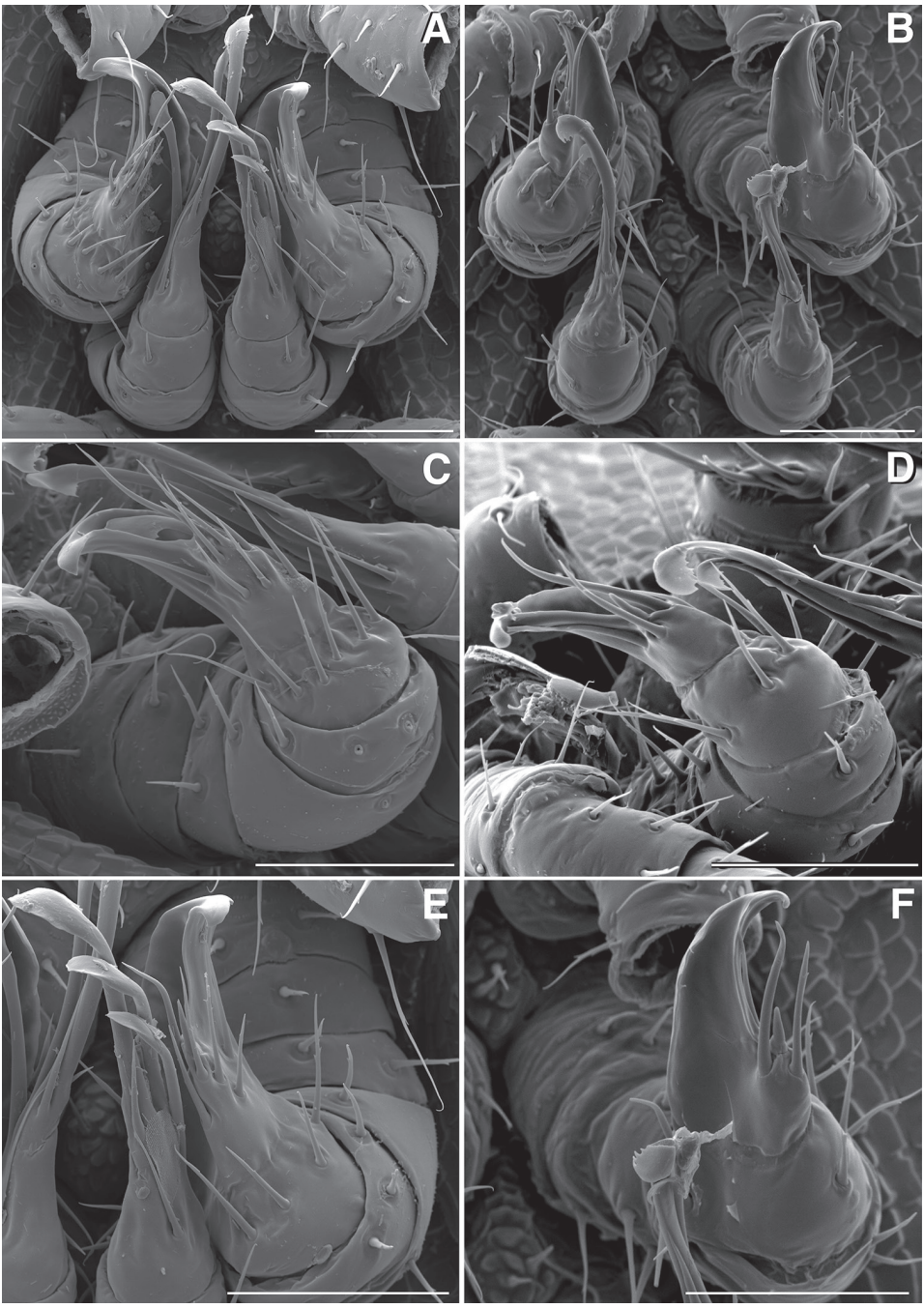

Figure 9. A Ventral view of gonopods of *I. tobini* sp. n. (scale bar 50 μm) **B** the same of *I. plenipes* (scale bar 50 μm) **C** Lateral (right) view of right anterior gonopod (leg-pair 9) of *I. tobini* sp. n. (scale bar 50 μm) **D** the same of *I. plenipes* (scale bar 50 μm) **C** Ventral view of gonopods of *I. tobini* sp. n. (centered on right anterior gonopod) (scale bar 50 μm) **D** the same of *I. plenipes* (scale bar 50 μm). (Catalog #s: *I. tobini* sp. n. MPE00735, *I. plenipes* SPC000932.)

gonopod (Figs 4C, D; 8C–F). Anterior gonopodal apex (podomere 7, A7—Fig. 4C, D) spade-shaped; at rest, cupped sheath-like around posterior gonopodal stylets (podomere 7, P7—Figs 4E, F; 9A–F). Posterior gonopodal podomere 7 deeply divided, comprising a bundle of 3 (*I. plenipes*) or 4 (*I. tobini* sp. n.) stylus-shaped articles; one article spike-shaped (Fig. 4E, F); other siphonorhinid taxa with 2 stylus-shaped articles and a small spine (*Nematozonium filum*) or 2 articles without spine (*Siphonorhinus* species and *Kleruchus olivaceus* Attems, 1938). 2, 3 dorsal-most, longest articles laminate distally and recurved laterally, with denticulate posterior margins appearing saw-like (Fig. 5A–D). Ventral-most, shortest article acuminate distally, spike-like.

Illacme tobini Marek, Shear & Krejca, 2016, sp. n.

http://zoobank.org/65D9B6C5-A148-4CC0-8509-D32364B7034F

Material examined. ♂ holotype (Virginia Tech Insect Collection, VTEC catalog # MPE000735) from United States, California, Tulare County, Sequoia National Park, Lange Cave, a marble cave near intersection of Yucca and Cave Creeks, Elevation 1231 m, 9 October 2006, from within cave (Coll: J. Krejca). Exact coordinates withheld due to species rarity and habitat sensitivity.

Diagnosis. Adult males of *I. tobini* sp. n. are distinct from *I. plenipes*, its sole congener, based on the combination of: Metazonites wider than prozonites with slightly enlarged paranota (Fig. 10A), not subequal in width as in *I. plenipes* (cf. Fig. 10B). Peritreme without the 2 large backwards projecting spines (Fig. 10C) as in *I. plenipes* (cf. Fig. 10D), ozopore ringed with ca. 15 setae. Ozopores nearer to margin, oriented dorsolaterally (Fig. 10A), not dorsally as in *I. plenipes* (cf. Fig. 10B). Metazonite posterior margin (limbus) lined with quadrate posteriorly projecting spines (Fig. 10E), not anchor-shaped as in *I. plenipes* (cf. Fig. 10F). Posterior margin sinuate, with anteriorly curved paramedial margins (Fig. 10A), not straight as in *I. plenipes* (cf. Fig. 10B). Telson densely covered with irregularly oriented and unevenly distributed stout spines on lateral surface only (Fig. 11A); telson not covered with stout spines on all surfaces and without posterior margin lined with posterodorsally oriented anchor-shaped spikes as in *I. plenipes* (cf. Fig. 11B). Hypoproct with two setae (Fig. 11A), not as in *I. plenipes* with > 2 seta present and arranged in a setal row (cf. Fig. 11B). Anterior gonopodal apex (podomere 7) spinose (Fig. 9C, E), with two-fold more spines than *I. plenipes* (cf. Fig. 9D, F). Anterior gonopodal podomere 3 with 2 long setae (Fig. 8E), not ringed with 6 setae, as in *I. plenipes* (cf. Fig. 8F). Posterior gonopodal apex (podomere 7) comprising a bundle of 4 styliform articles, with one article spike-shaped (Figs 11C, 12B), not bundle of 3 styliform articles as in *I. plenipes* (cf. Fig. 11D). The differential diagnosis of *I. tobini* sp. n. vs *I. plenipes* is summarized in Table 1, and a comparison of measurements between *I. tobini* sp. n. vs a male individual of *I. plenipes* (VTEC catalog # SPC000932) with an equivalent number of rings shown in Table 2.

Description of holotype (♂) (Fig. 13). Counts and measurements: p = 106. a = 2. l = 414. (106 + 2 + T). BL = 19.73. HW = 0.34. HL = 0.39. ISW = 0.21. AW =

Table 1. Differential diagnosis of *I. tobini* sp. n. versus *I. plenipes*.

Character	***I. tobini* sp. n.**	***I. plenipes***
Rings	Metazonites wider than prozonites (Fig. 10A)	Metazonites subequal in width (Fig. 10B)
Peritreme	2 large backwards projecting spines absent (Fig. 16E)	2 large backwards projecting spines present (Fig. 16F)
Metazonite posterior margin adornment	Lined with quadrate backwards projecting spines (Fig. 10C, E)	Lined with anchor-shaped backwards projecting spines (Fig 10D, F)
Metazonite posterior margin shape	Sinuate, with anteriorly curved paramedial margins (Fig. 10A)	Straight, without curvature (Fig. 10B)
Telson	Covered with stout spines on lateral surface only (Fig. 11A)	Covered with stout spines on all surfaces (Fig. 11B)
Hypoproct	2 setae present (Fig. 11A)	> 2 setae present, in a setal row (Fig. 11B)
Anterior gonopodomere 3	2 setae present (Fig. 8E)	6 setae present (Fig. 8F)
Anterior gonopodal apex	Spinose with two-fold more spines (Figs. 9C)	Less spinose (Fig. 9D)
Posterior gonopodal apex	Bundle of 4 styliform articles (Figs 11C, 12B)	Bundle of 3 styliform articles (Fig. 11D)

Table 2. Comparison of measurements between *I. tobini* sp. n. vs a male *I. plenipes* individual with an equivalent number of rings (VTEC catalog # SPC000932).

	p	**a**	**l**	**HW**	**HL**	**ISW**	**AW**	**CW**
I. tobini sp. n.	106	2	414	0.34	0.39	0.21	0.11	0.44
I. plenipes	105	2	402	0.31	0.40	0.19	0.10	0.40
	W1	**L1**	**H1**	**AS1**	**A6W**	**P6W**	**BL**	***p* + *a* + *T***
I. tobini sp. n.	0.52	0.20	0.31	0.43	0.04	0.03	19.73	106 + 2 + T
I. plenipes	0.40	0.16	0.40	0.43	0.05	0.04	17.12	105 + 2 + T

0.11. CW = 0.44. W1 = 0.52. L1 = 0.20. H1 = 0.31. AS1 = 0.43. A7W = 0.04. P7W = 0.03. Head pear-shaped, tapered anteriorly to round point at a 120° angle from antennal sockets; occiput gradually curved medially towards cervical area (Figs 2C, 5F, 13). Head covered with long, slender setae (Figs 2C, E, F; 3C, D). Gnathochilarium, labrum tightly appressed, tapered anteriorly to round point (Figs 2C, E, F; 3C, D, 6E, F). Mandibles not externally visible. Labrum with tooth-lined slit (Figs 6C, E, F; 7A–F). Labrum at base of slit with deeply-incised tridentate projection (Fig. 7E). Labrum posterior to slit with ca. 200 unevenly distributed pores, some with unidentified secretion extruded from the opening (Fig. 7F). Denticulate shelf-like carina, projecting dorsally from labrum-epistome margin (Figs 6E, 7D, 8A). Gnathochilarium, mandible, head capsule noticeably separate at base (Fig. 2E, F). Mandibular stipes concealed, commissure between gnathochilarium, head capsule visible distally (Fig. 2E, F). Gnathochilarium thin, plate-like, occupying three-quarters ventral length of head. Gnathochilarium tightly appressed to the ventral surface of the head, leaving a small opening anteriorly between labrum, gnathochilarial stipes. Lateral opening apparent be-

tween gnathochilarium and head capsule (Figs 2C, E, F; 3C, D). Gnathochilarium with reduced sclerites: stipes, mentum, lamellae linguales present; cardines absent (Fig. 3D). Stipes of gnathochilarium with inner, outer palps (Figs 7C, D; 14B). Lamellae linguales with palps (Fig. 14B). Mandibles not externally visible, mandibular cardo base noticeable between head capsule, gnathochilarium (Figs 2E, 3D, 5E). Mandible with ca. 5 flabellate external teeth, pectinate lamella with numerous rows of jagged ventrally projecting serrulae, nested in groove of endochilarial frontal body (Figs 7A–D; 14C). (Alternative description, primary homology with epipharynx: Epipharynx with distal flabellate side lobes, spiniferous keel with zipper construction. Mandibles, as in *I. plenipes* thin, stylet-like, with heavily calcified apices—not apparent externally, only visible at 400× through translucent head capsule with phase-contrast imaging on a compound microscope). Mandible (or epipharyngeal) keel nested in groove of endochilarial frontal body. Endochilarium with V-shaped frontal body (Fig. 7C, D). Endochilarium with fringed lobes (Figs 7C, D; 14B). Endochilarial fringed lobes (spatulae sensu Silvestri, 1903) protruding distally through gnathochilarial stipes and lamellae linguales (Figs 7C, 14B). Antennae sub-geniculate, elbowed between antennomeres 3, 4, comprising 7 antennomeres (Fig. 3A). Antennomeres 5, 6 enlarged. Five sensillum types: 4 apical cones (AS) oriented in a trapezoidal cluster on 7th antennomere, with longitudinally grooved outer surface and circular pore apically (Fig. 15A). Chaetiform sensilla (CS) widely spaced on antennomeres 1–7, each sensillum with 2 or 3 barbules (Fig. 3A). Trichoid sensilla (TS) oriented apically encircling antennomeres 1–7, lacking barbules (Fig. 3A). Small basiconic sensilla (Bs_2) in clusters of 3 and 4 oriented apical dorsally (retrolaterally) on antennomeres 5 and 6; smooth, capsule-shaped, 1/2 length of chaetiform sensillum (Figs 3A, 15A). Spiniform basiconic sensilla (Bs_3) in cluster of 4, oriented apical dorsally on 7th antennomere; tips facing apical cones (on longitudinal axis with Bs_2 on antennomeres 5, 6); each sensillum with 3–5 barbules (Fig. 15A). Antennae extend posteriorly to middle of 3rd tergite. Relative antennomere lengths 6>2>5>3>4>1>7. Collum not covering head, with straight cephalic edge, gradually tapering laterally (Figs 2A, C; 5E). Lateral margin of collum round, with thickened scaly carina (Figs 3D, 5E). Carina repeated serially on lateral tergal and pleural margins (absent from telson). Lateral tergal and pleural carinae jagged, pronounced on midbody segments (Fig. 15C, E). Metazonites wider than prozonites, with slightly enlarged paranota (Fig. 10A). Metazonites trapezoidal, anterior margin 3× wider than long, posterior margin 3.5× wider than long. Metazonites slightly convex (Figs 6A, 15E). Metazonite dorsally covered with long, slender setae (Figs 6A; 10A; 16A, C). Tergal setae hollow, cavity diameter at base 1/4 that of setae diameter; tipped with silk-like exudate, tangled, appearing adhered to neighboring setae (Figs 6A; 16A, C). Metazonite posterior margin (limbus) lined with quadrate posteriorly projecting spines, not anchor-shaped, with row of spines anterior to limbus on posterior rings only (Figs 10E; 15E; 16A, C, D). Limbal quadrate spikes uniform in size along margin. Ozopores oriented dorsolaterally, located near lateral metazonal margin, 1/4 length of metazonite anteriorly from limbus (Fig. 10A). Ozopores absent from collum, tergites 2–4, and telson. Ozopores elevated slightly on peritremata (porosteles absent),

without 2 large backwards projecting spines, encircled with ca. 15 robust setae (Figs 10C; 16A, C, E). Without lunate-arranged stout flat tubercles encircling ozopore. Posterior tergites more convex, covered with a greater density of long, slender setae (Figs 11A, 15F, 16C). Apodous segment lacking sternum, pleurites contiguous in midline. Apodous tergite densely setose, without vestiture of spikes (Fig. 11A). Telson covered with irregularly oriented and unevenly distributed stout spines on lateral surface only; without posterodorsally oriented anchor-shaped spikes (Fig. 11A). Prozonite highly sculptured, with ca. 12 rows of discoidal flat tubercles; anterior 9 rows aligned and posterior 2 rows staggered (Figs 15E, 16D). Prozonal posterior discoidal tubercles button-shaped protuberant, anterior tubercles flush with surface. Pleurites quadrate, flat, with jagged scaly lateral, posterior and medial margins (Fig. 15C). Pleurite medial margin broad, with scaly carina (Figs 3E; 8C; 15C; 17A, C). Pleurites plate-like, left and right combined comprising four-fifths of ventral segment area. Pleural medial margins broadly overlapping sternite, covering spiracles (Fig. 3E, 4A, 15C). Anterior, posterior sternites free, separate from pleurites; heart-shaped, wider anteriorly (Figs 17E, F; 18A). Sternum with prominent midline triangular ridge projecting ventrally, with spiracles and legs oriented ventrally (Figs 3E; 4A; 15C; 17E, F; 18A). Spiracles circular, orifice open; oriented dorsal to legs (Figs 3E, 4A, 17E). Tergites, pleurites and sternites separated by arthrodial membrane (Figs 11A; 15C, F; 17A). Arthrodial membrane between tergites and pleurites wider posteriorly, pleated (likely permitting telescoping body rings). Telson covered with long slender posteriorly curved setae (Fig. 11A). Paraprocts semihemispherical, anterior margins slightly scaly (Fig. 11A). Hypoproct small, one-eighth area of paraproct, with two posterior projecting setae. Legs with six subequally shaped podomeres, with coxa slightly shorter and tarsus slightly longer. Legs with sparse setae, appearance similar to trichoid sensilla, with 2 or 3 barbules. Coxae nearly contiguous medially, separated by thin sternal ridge. Large posteroventral D-shaped opening for eversible sac (Figs 3E, 8C, 15C, 17C). Eversible sacs membranous, bulging slightly within aperture (Figs 3E, 17C). Tarsus with pincer-like claw; dorsal claw arcuate, ventral accessory seta thick, stout (Figs 2A, C, F; 6E, 17A). 2nd leg pair with posteriorly oriented coxal gonapophyses; rounded, protuberant, one-half length of prefemur (Fig. 18B). 9th, 10th leg pairs modified into gonopods, each comprising 7 podomeres (Figs 4C, E; 8C, E; 9A, C, E; 12A, B). Anterior gonopod robust, thicker than posterior gonopod (Figs 4C, 8E, 12A). Anterior gonopodal apex (podomere 7) shovel-shaped; in repose cupped around flagelliform posterior gonopodal apex (podomere 7, Figs 4C, E; 8E; 9A, C; 12A). Posterior gonopodal podomere 7 deeply divided, comprising a bundle of 4 stylus-shaped articles (Figs 4C, E; 5A, C; 8E; 9A, E; 12B; 18C, E, F; 19B, C). 3 dorsal-most, longest articles laminate distally, recurved laterally, denticulate posterior margins (Figs 5C, 12B). Ventral-most, 4th article acuminate distally, spike-like (Figs 4E, 12B). Thin ridge-shaped sterna present between left and right gonopods, thicker between anterior gonopods. Supplementary micrographs of *I. tobini* sp. n. are archived in the Dryad Data Repository at http://dx.doi.org/10.5061/dryad.tk0b8.

Female unknown.

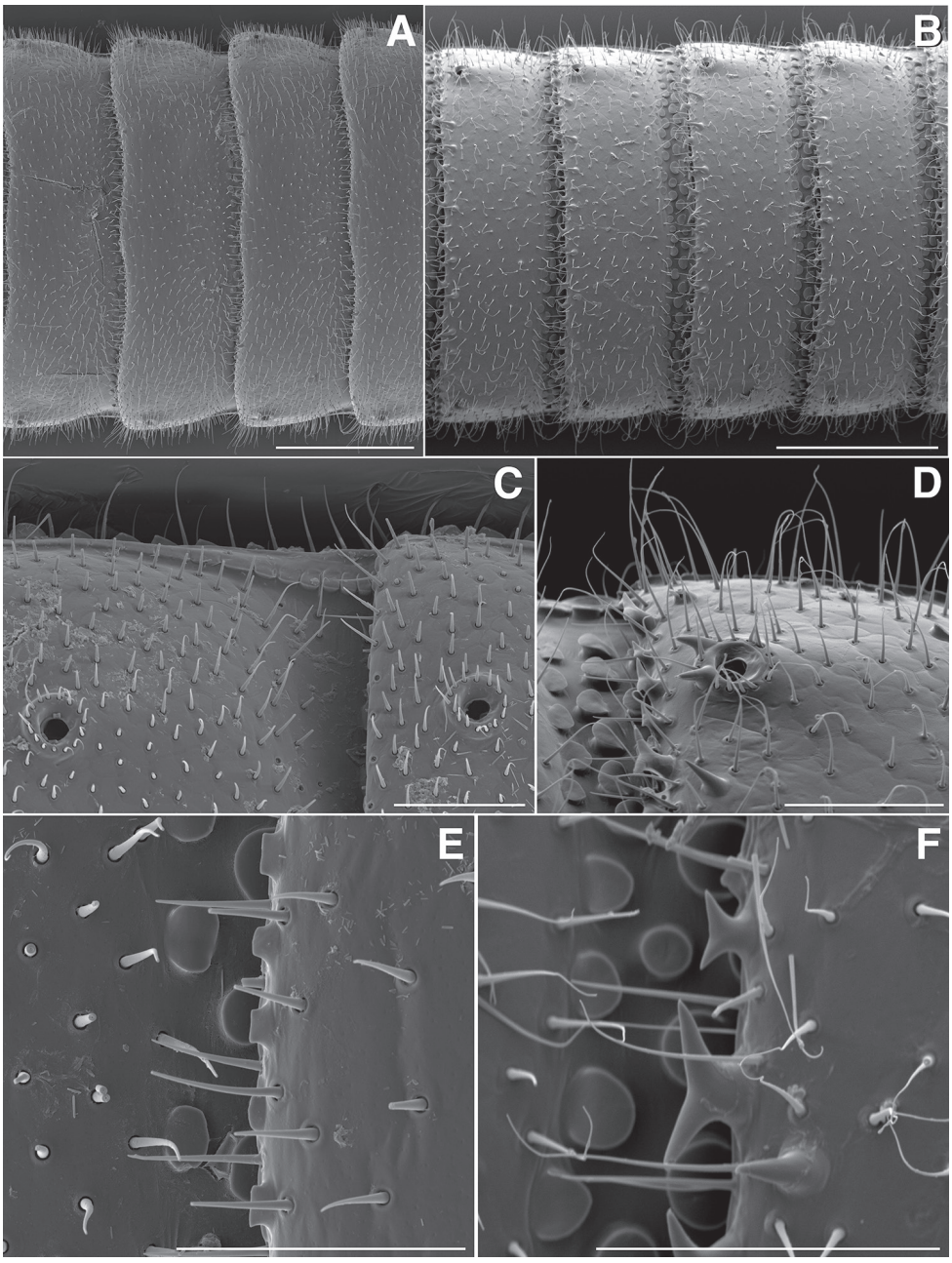

Figure 10. A Dorsal view of trunk of *I. tobini* sp. n. (scale bar 200 μm) **B** the same of *I. plenipes* (scale bar 200 μm). **C** Dorsal view of left ozopore of *I. tobini* sp. n. (scale bar 50 μm) **D** the same of *I. plenipes* (scale bar 50 μm) **E** Dorsal view of metazonite posterior margin (limbus) of *I. tobini* sp. n. (scale bar 40 μm) **F** the same of *I. plenipes* (scale bar 50 μm). (Catalog #s: *I. tobini* sp. n. MPE00735, *I. plenipes* SPC000932.)

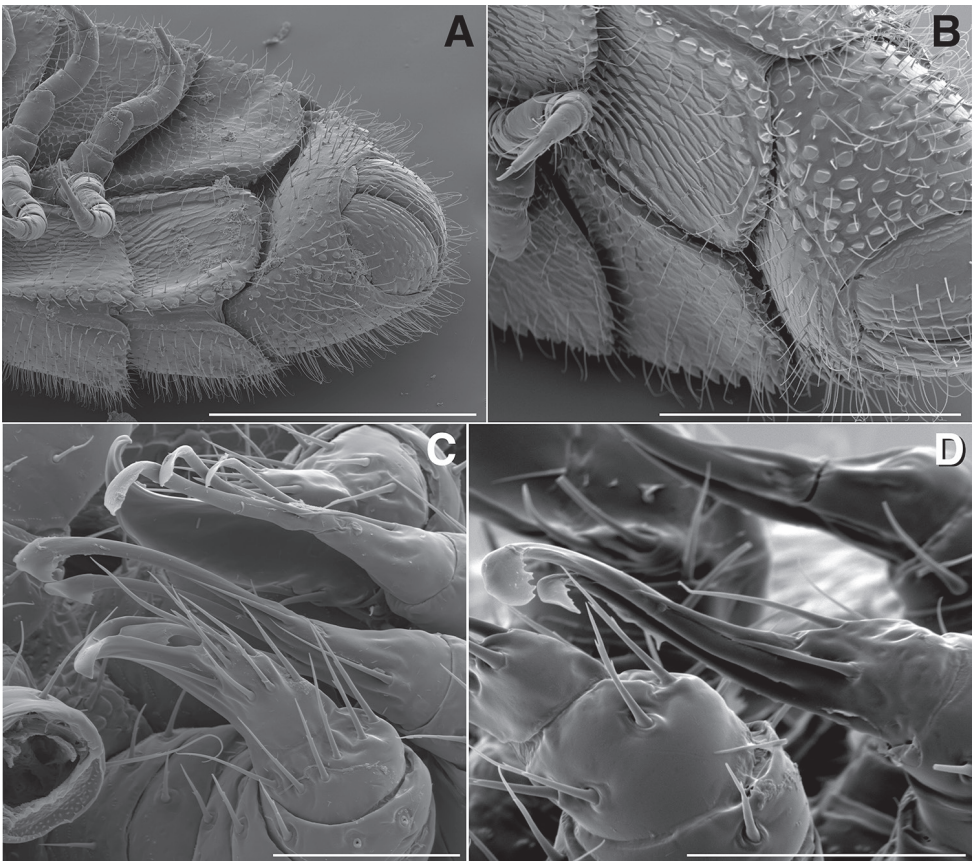

Figure 11. A Ventrolateral view of apodous ring, telson, hypoproct and paraprocts of *I. tobini* sp. n. (scale bar 300 μm) **B** the same of *I. plenipes* (scale bar 200 μm) **C** Lateral (right) view of gonopods—centered on right posterior gonopod—of *I. tobini* sp. n. (scale bar 50 μm) **D** the same of *I. plenipes* (scale bar 50 μm). (Catalog #s: *I. tobini* sp. n. MPE00735, *I. plenipes* SPC000932.)

Etymology. This new species is named for Ben Tobin, Cave Specialist and Hydrologist at Grand Canyon National Park. Ben organized and carried out numerous cave surveys in the U.S., including the field visit that uncovered *I. tobini* sp. n., and has facilitated the discovery of many new species of invertebrates and other cave fauna in Sequoia National Park. The specific name is a genitive noun derived from his surname.

Variation. Unknown. *Illacme tobini* sp. n. is known from a single male specimen (Fig. 13).

Habitat and distribution. *Illacme tobini* sp. n. is only known from a single in-cave collection, within the upper foothills of the Giant Forest in Sequoia National Park (Fig. 1B). Lange Cave is situated at the base of Yucca Mountain at the boundary of the Sierra Nevada Forest and California Interior Chaparral and Woodlands ecoregions (Fig. 20). A region characterized by a Mediterranean climate with temperature and humidity extremes encompassing cold wet winters (< 0 °C and 700 mm precipita-

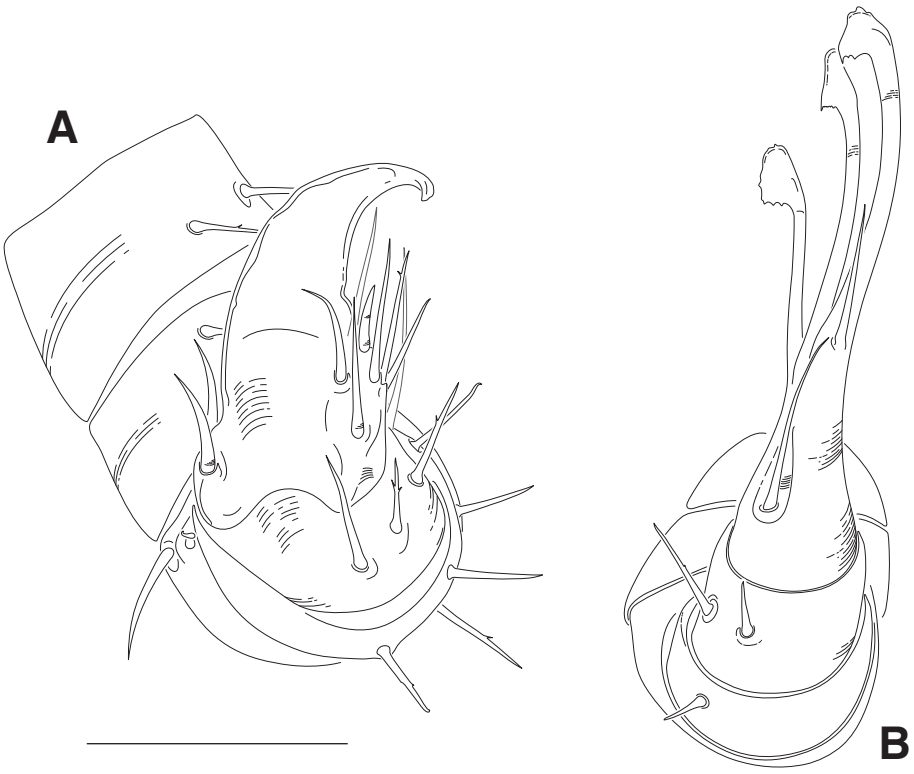

Figure 12. *Illacme tobini* sp. n.: **A** spade-shaped anterior gonopod (leg pair 9) **B** stylus-shaped posterior gonopod (leg pair 10). Scale bar 50 μm. (Catalog #: *I. tobini* sp. n. MPE00735.)

tion) and hot dry summers (> 40 °C and < 2 mm precipitation) (Tobin et al. 2013). The cave is composed of Jurassic-Triassic marble of a white, coarsely crystalline, and schistose to gneissose composition (Sisson and Moore 1994). The marble cave system is encompassed by biotite-feldspar-quartz schist rocks. The cave is ca. 90% surveyed, and has a total volume of 354.2 m^3, average diameter of 2.1 m, wall area of 733.3 m^2, and floor area of 124.6 m^2. Inside the cave, temperatures range between ca. 6 °C in the winter months (October–May) to ca. 9 °C in the summer months (June–September). The woodland habitat around the cave was primarily composed of California live-oak (*Quercus agrifolia*), California bay (*Umbellularia californica*), Giant sequoia (*Sequoiadendron giganteum*), and Mountain maple (*Acer glabrum*). Understory flora included Scouringrush horsetail (*Equisetum hymale*), California wood fern (*Dryopteris arguta*), and Thimbleberry (*Rubus parviflorus*). Other organisms encountered in the habitat included millipedes—*Parcipromus cooki*, *Californiulus yosemitensis*, *Taiyutyla loftinae*, *Amplaria muiri*; arachnids—*Yorima* sp., *Ceratinops inflatus*, *Nesticus* spp., *Pimoa* spp., *Mundochthonius* sp., *Ortholasma colossus*, *Calicina* sp.; hexapods—*Tomocerus* sp., *Amoebaleria caesia*, *Heleomyza* sp., *Hippodamia* convergens; and the salamander *Ensatina eschscholtzii platensis*.

Figure 13. *Illacme tobini* sp. n.: ♂ holotype. Scale bar 1 mm. (Catalog #: MPE00735.)

Discussion. *Illacme* species have extremely limited known geographic ranges. This feature suggests a formerly widespread, perhaps ancient, distribution, and/or membership in a larger hidden diversification in California encompassing many undiscovered taxa. *Illacme* individuals occur in the mesovoid shallow substratum (MSS), a cryptic ecosystem, which are miniscule subterranean microhabitats encompassing fissures and cracks below the soil surface (Ortuño et al. 2013). These subterranean areas are the microcaverns (< 1 mm) and mesocaverns (1 mm–20 cm) described by Howarth (1983). The fauna of the MSS likely represents a considerable fraction of unknown biodiversity, yet the habitat is unexplored and its diversity poorly known. Species discovery from these microhabitats has only recently begun, and recent advances in collecting techniques are uncovering a considerable amount of new taxa. These microhabitats are fundamentally miniature caves and many MSS taxa also include cave-restricted species (Espinasa et al. 2014). As a result, MSS organisms possess some troglomorphic features—e.g., lack of eyes, no pigment—but lack the open-space adaptations of cave animals, including long limbs and elongate sensory structures (e.g., antennae and setae). Frequently MSS taxa possess shorter legs than cave or epigean forms and a covering of thin, delicate setae on the exoskeleton (Espinasa et al. 2014). Albeit anecdotally, Manton (1961, pg. 395) associated the hirsute covering of *Siphonophora* individuals as an adaptation for maneuverability, including spiraling within narrow crevices, and

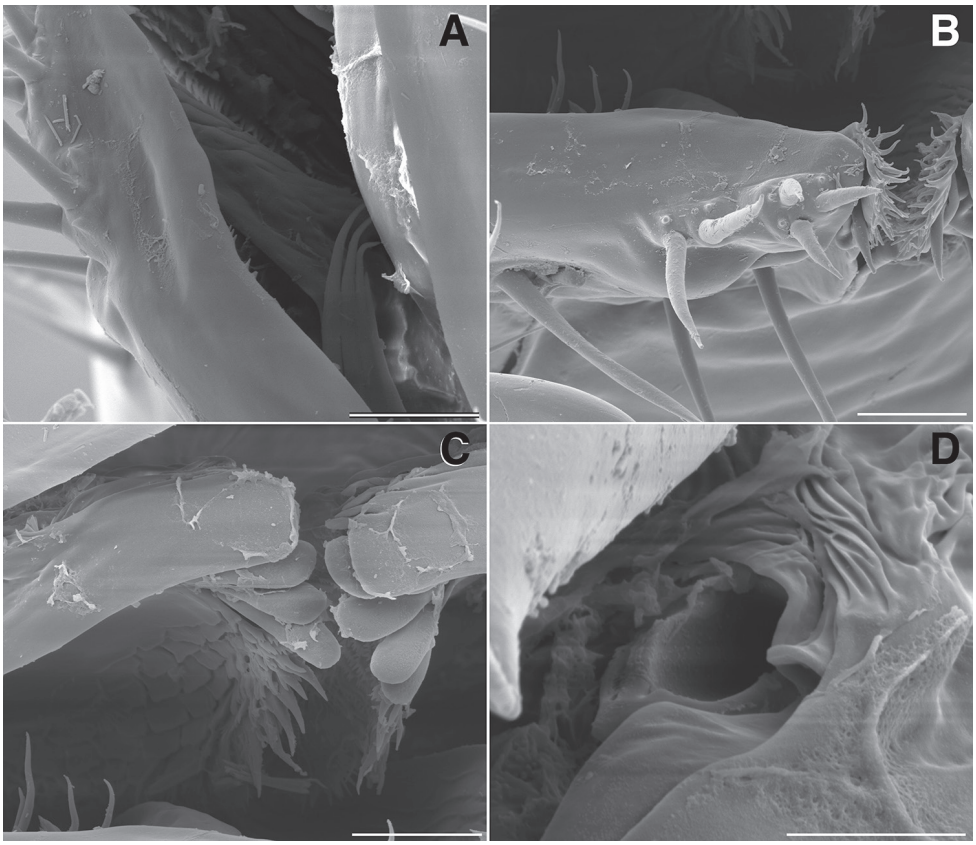

Figures 14. *Illacme tobini* sp. n.: **A** anterolateral (left) view of gnathochilarial stipes and dorsal surface of endochilarium (scale bar 10 μm) **B** anterior view of gnathochilarium with inner and outer palps (inner, outer palps with 3, 2 setae respectively) (scale bar 10 μm) **C** anterolateral (right) view of open mouth and keel-shaped pectinate lamella of the mandible (scale bar 10 μm) **D** anterolateral (right) view of mandible with base of external teeth a circular socket (scale bar 4 μm). (Catalog #: *I. tobini* sp. n. MPE00735.)

crawling upside-down on the ceilings of caverns; however, it is unclear precisely how this occurs biomechanically. *Illacme plenipes* individuals are found exclusively beneath large deep-set stones—a common place of discovery for MSS arthropods (Marek et al. 2012). In contrast, *I. tobini* sp. n. was documented solely from a marble cave. Considering that *I. plenipes* individuals were found in the MSS, and that they possess MSS adaptations (including a vestiture of setae and absence of long sensory structures and limbs), the possibility that *I. tobini* sp. n.—with similar adaptations—is cave-restricted is uncertain. Additional material of *I. tobini* sp. n. would provide evidence to address this claim. Notwithstanding the paucity of material, the significance of the discovery highlights the importance of the Sequoia caves and MSS as a habitat of distinctive biodiversity.

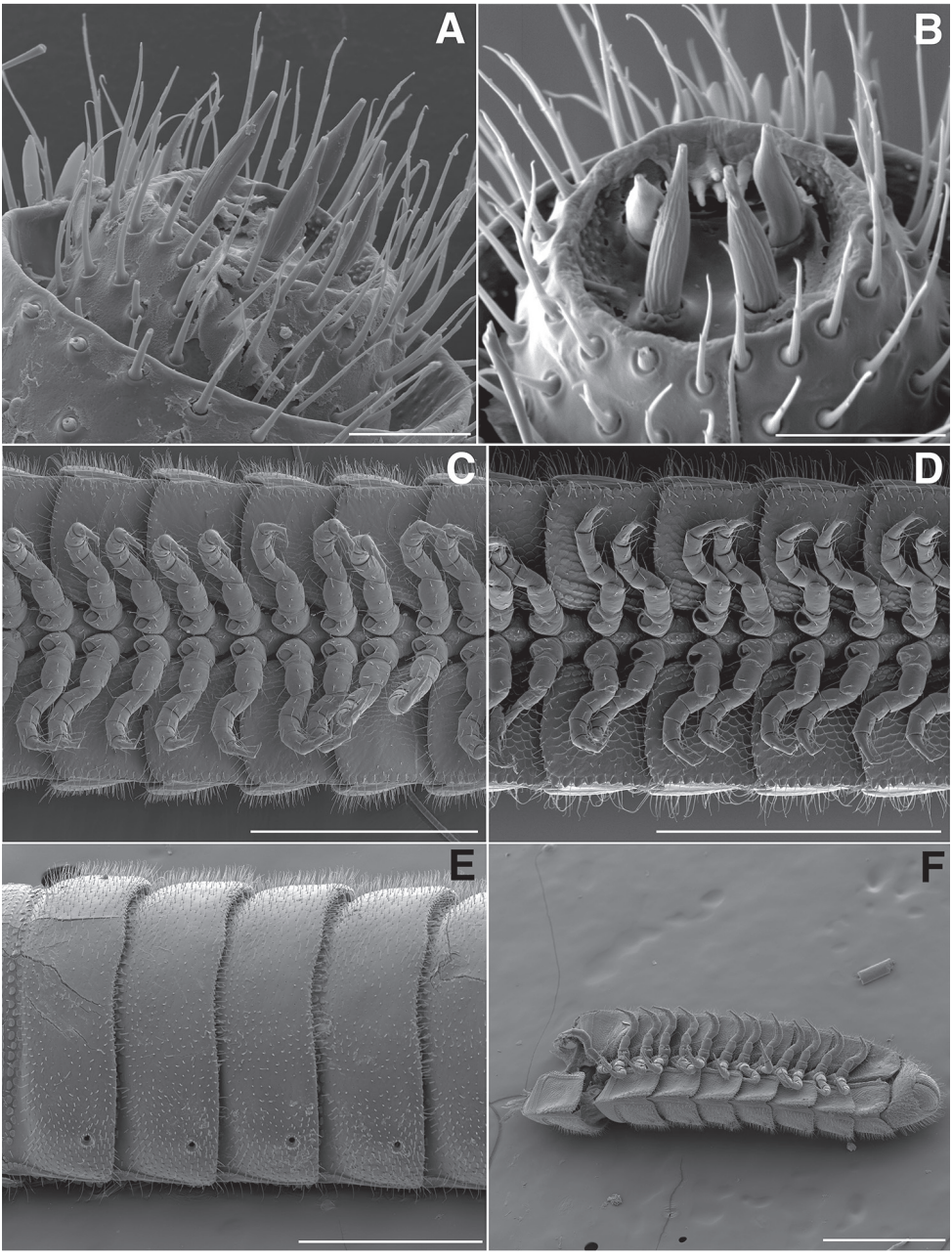

Figure 15. A Antennomere 7 of *I. tobini* sp. n. (scale bar 20 μm) **B** the same of *I. plenipes* (scale bar 20 μm). **C** Ventral view of rings of *I. tobini* sp. n. (scale bar 400 μm) **D** the same of *I. plenipes* (scale bar 400 μm). *Illacme tobini* sp. n.: **E** dorsolateral (left) view of rings 10–14 (scale bar 300 μm) **F** ventrolateral (right) view of posterior rings (scale bar 500 μm) (Catalog #s: *I. tobini* sp. n. MPE00735, *I. plenipes* SPC000932.)

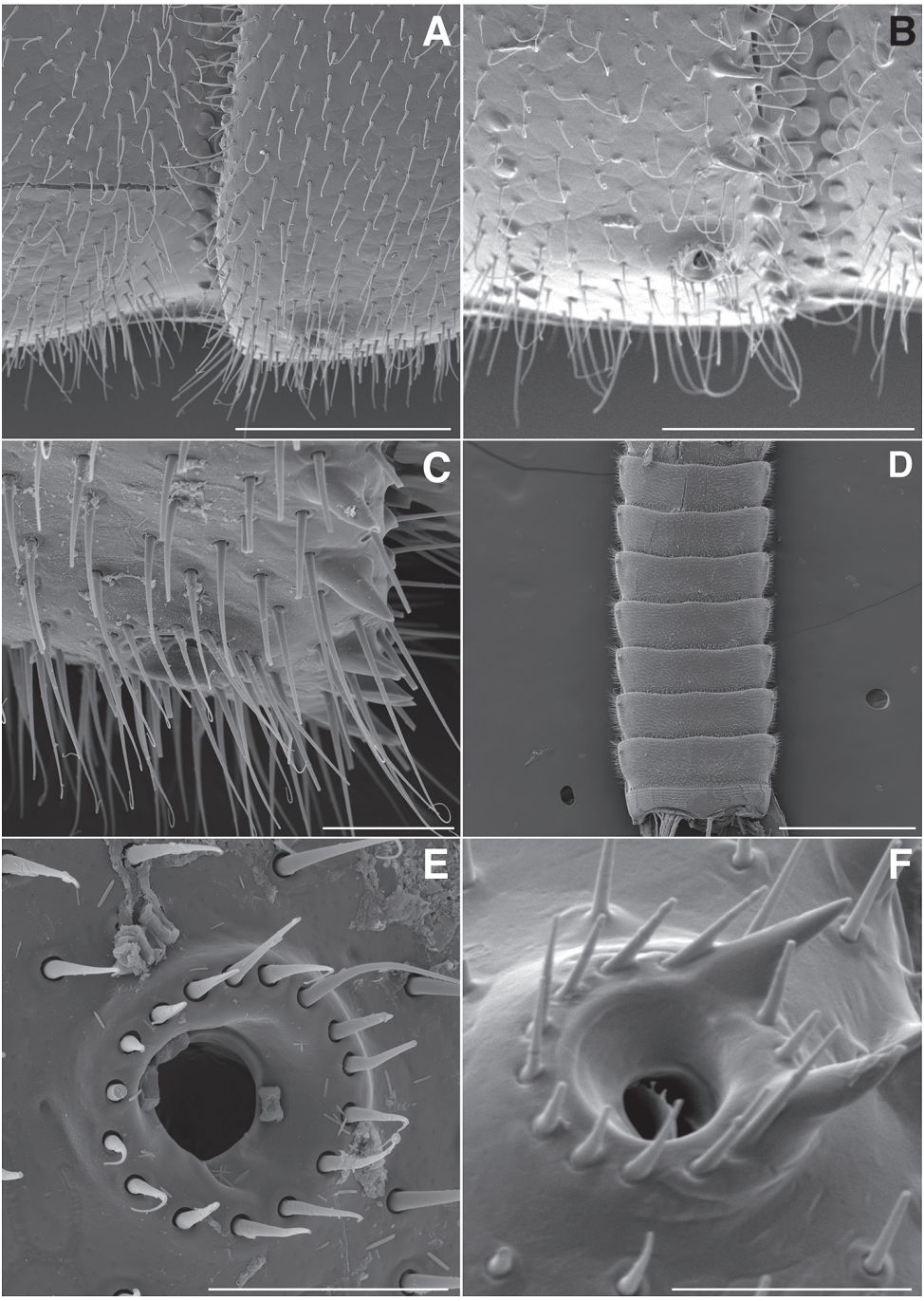

Figure 16. A dorsal view of right ozopore of *I. tobini* sp. n. (scale bar 100 μm) **B** the same of left ozopore of *I. plenipes* (scale bar 100 μm). *I tobini* sp. n.: **C** lateral (right) view of right ozopore from ring 106 (scale bar 20 μm) **D** dorsal view of trunk (scale bar 500 μm) **E** Ozopore of *I. tobini* sp. n. (scale bar 20 μm) **F** the same of *I. plenipes* (scale bar 20 μm). (Catalog #s: *I. tobini* sp. n. MPE00735, *I. plenipes* SPC000932.)

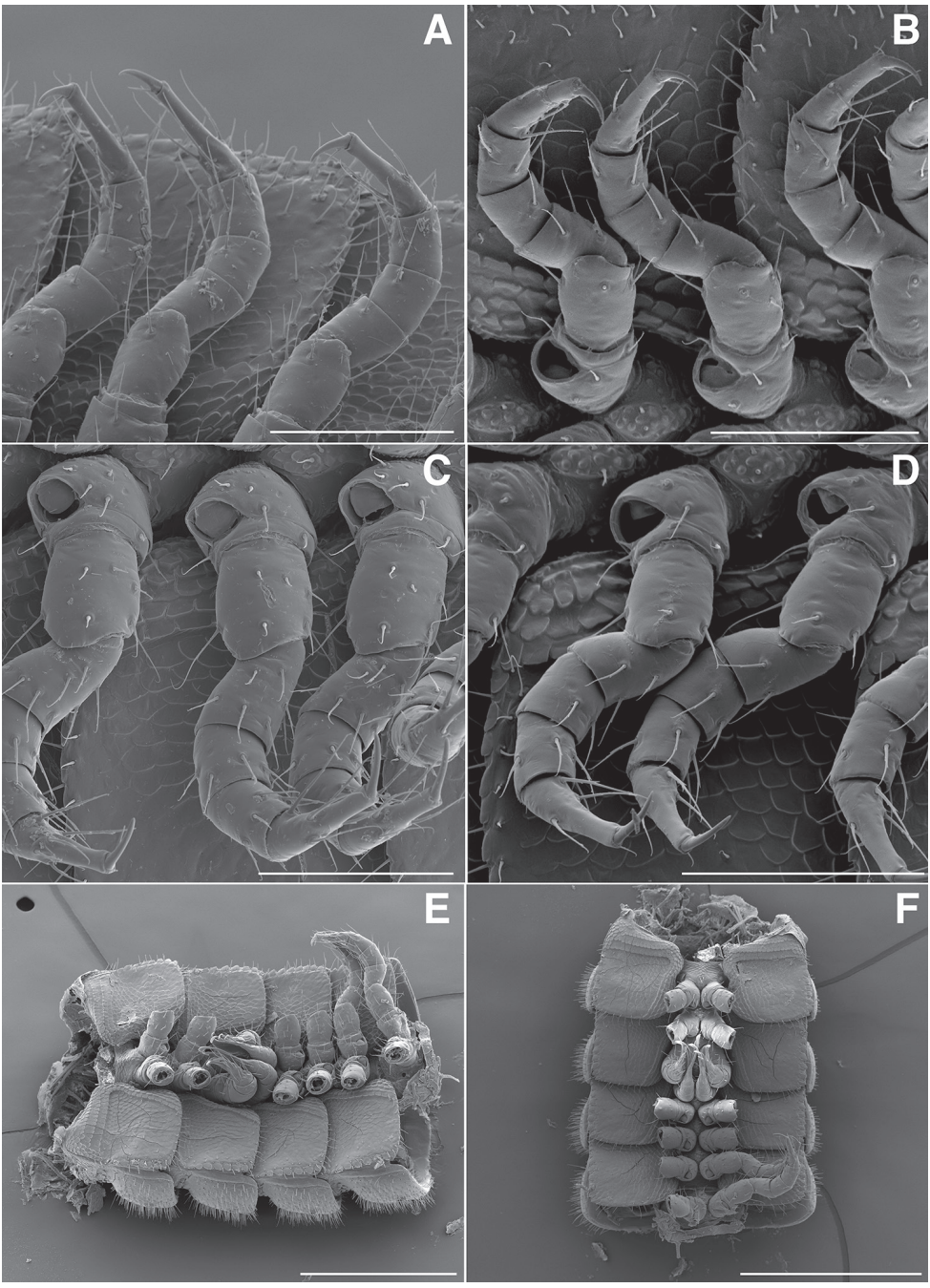

Figure 17. A Ventral view of left postgonopodal legs and claws of *I. tobini* sp. n. (scale bar 100 μm) **B** the same of *I. plenipes* (scale bar 100 μm). **C** Ventral view of left postgonopodal legs and eversible sacs of *I. tobini* sp. n. (scale bar 100 μm) **D** the same of *I. plenipes* (scale bar 100 μm). *Illacme tobini* sp. n.: **A** ventrolateral (right) view of rings 6–9 with gonopods in situ (scale bar 300 μm) **B** ventral view of the same (scale bar 400 μm). (Catalog #s: *I. tobini* sp. n. MPE00735, *I. plenipes* SPC000932.)

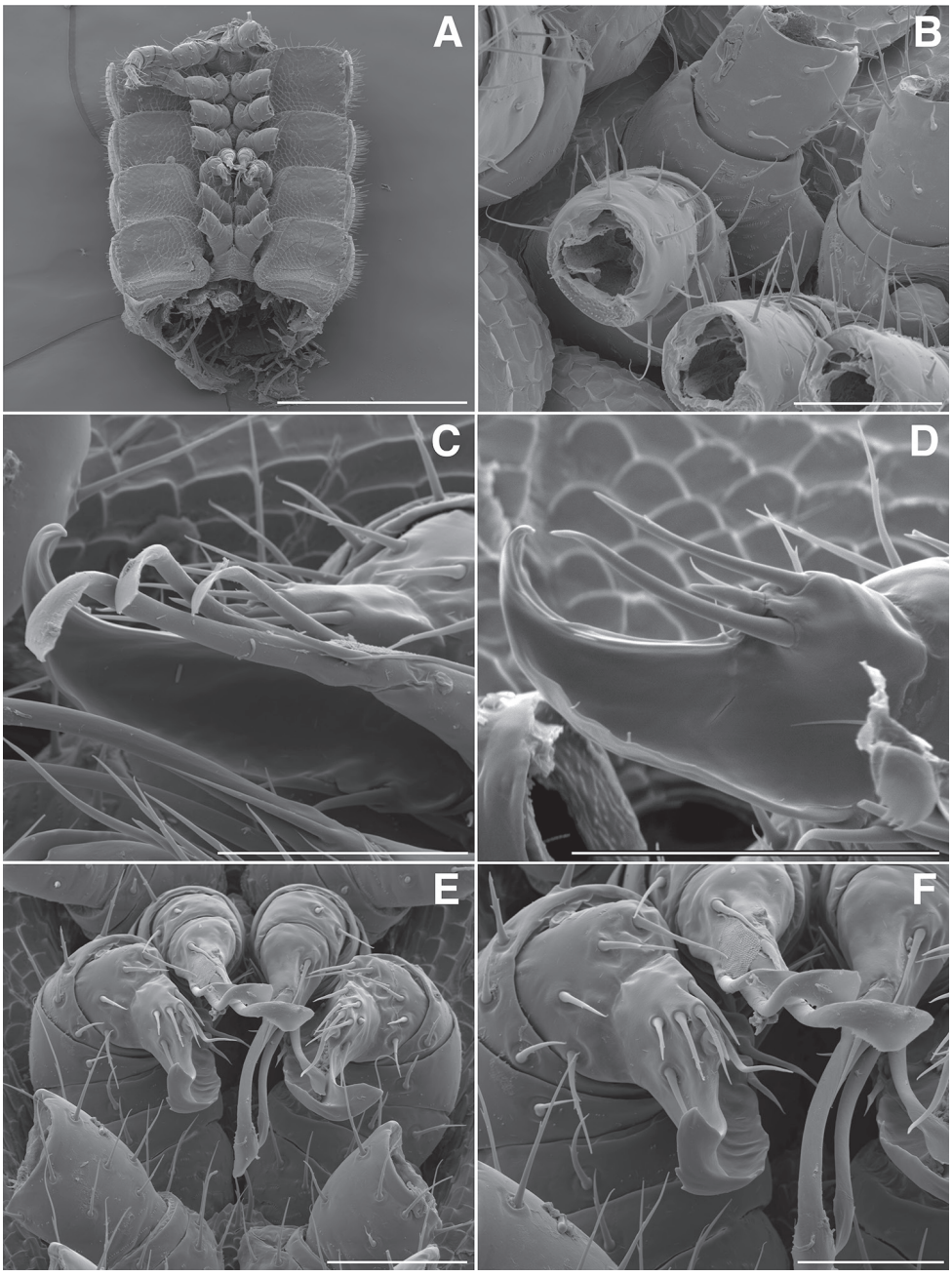

Figure 18. A Anteroventral view of rings 6–9 of *I. tobini* sp. n. with gonopods in situ (scale bar 400 μm) **B** ventrolateral (right) view of second leg pair with posteriorly oriented coxal gonapophyses (legs broken off at prefemur-femur joint) (scale bar 50 μm). **C** Medial view of right anterior gonopod of *I. tobini* sp. n. (scale bar 40 μm) **D** the same of *I. plenipes* (scale bar 50 μm). *Illacme tobini* sp. n.: **E** anteroventral view of gonopods *in situ* (scale bar 50 μm) **F** the same, close-up of right anterior gonopod (scale bar 30 μm). (Catalog #s: *I. tobini* sp. n. MPE00735, *I. plenipes* SPC000932.)

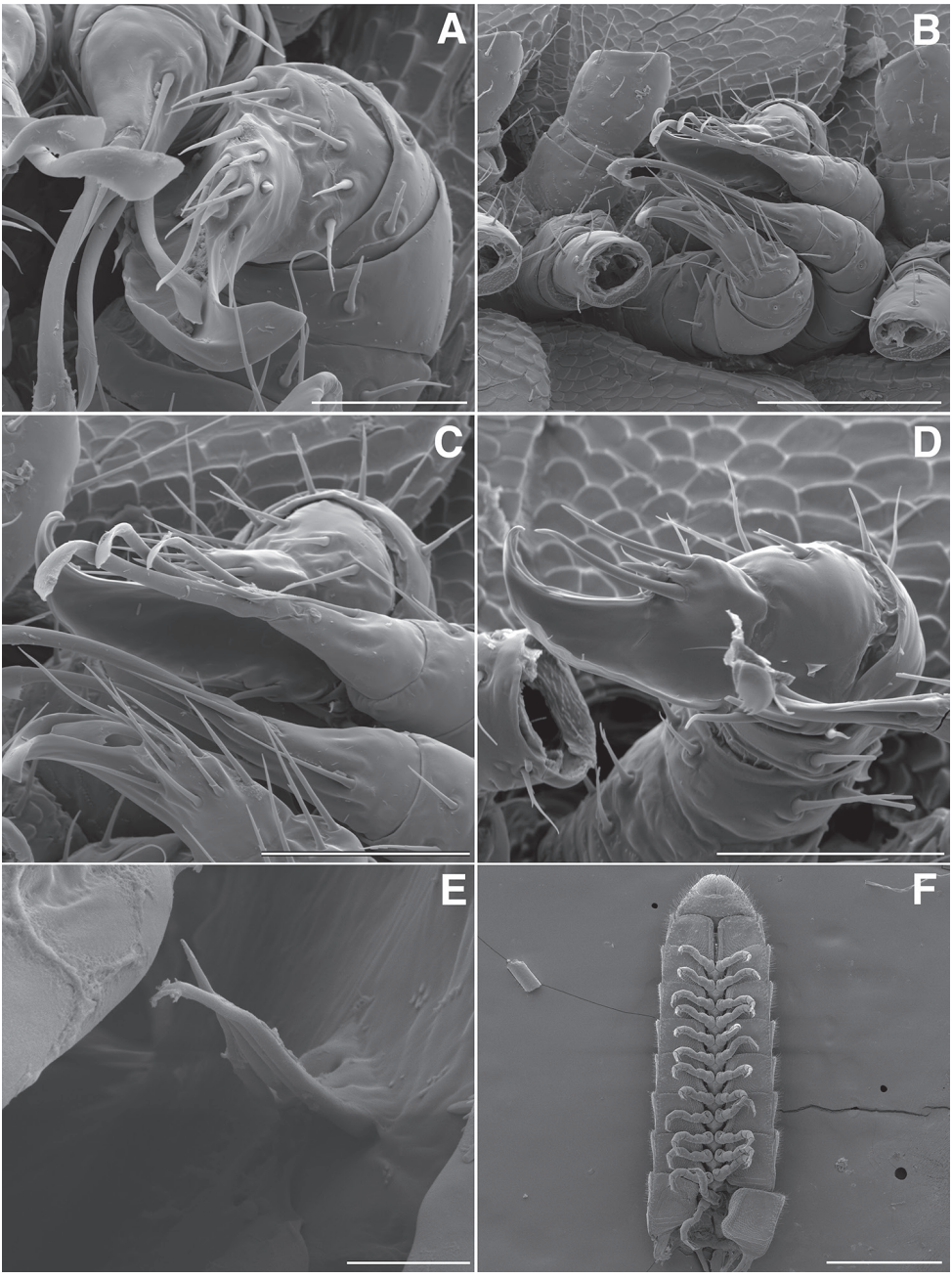

Figure 19. *Illacme tobini* sp. n.: **A** anteroventral view of left gonopod *in situ* (scale bar 30 μm) **B** ventrolateral (right) view of gonopods *in situ* (leg pairs 7, 8, 11 broken off at prefemur-femur joint) (scale bar 100 μm) **C** Medial view of right anterior gonopod of *I. tobini* sp. n. (scale bar 50 μm) **D** the same of *I. plenipes* (scale bar 50 μm). *Illacme tobini* sp. n.: **E** anterodorsal view of head with mouth open showing dorsal surface of left gnathochilarial stipe with unidentified brush-like structure (scale bar 5 μm) **F** ventral view of posterior rings (scale bar 500 μm). (Catalog #s: *I. tobini* sp. n. MPE00735, *I. plenipes* SPC000932.)

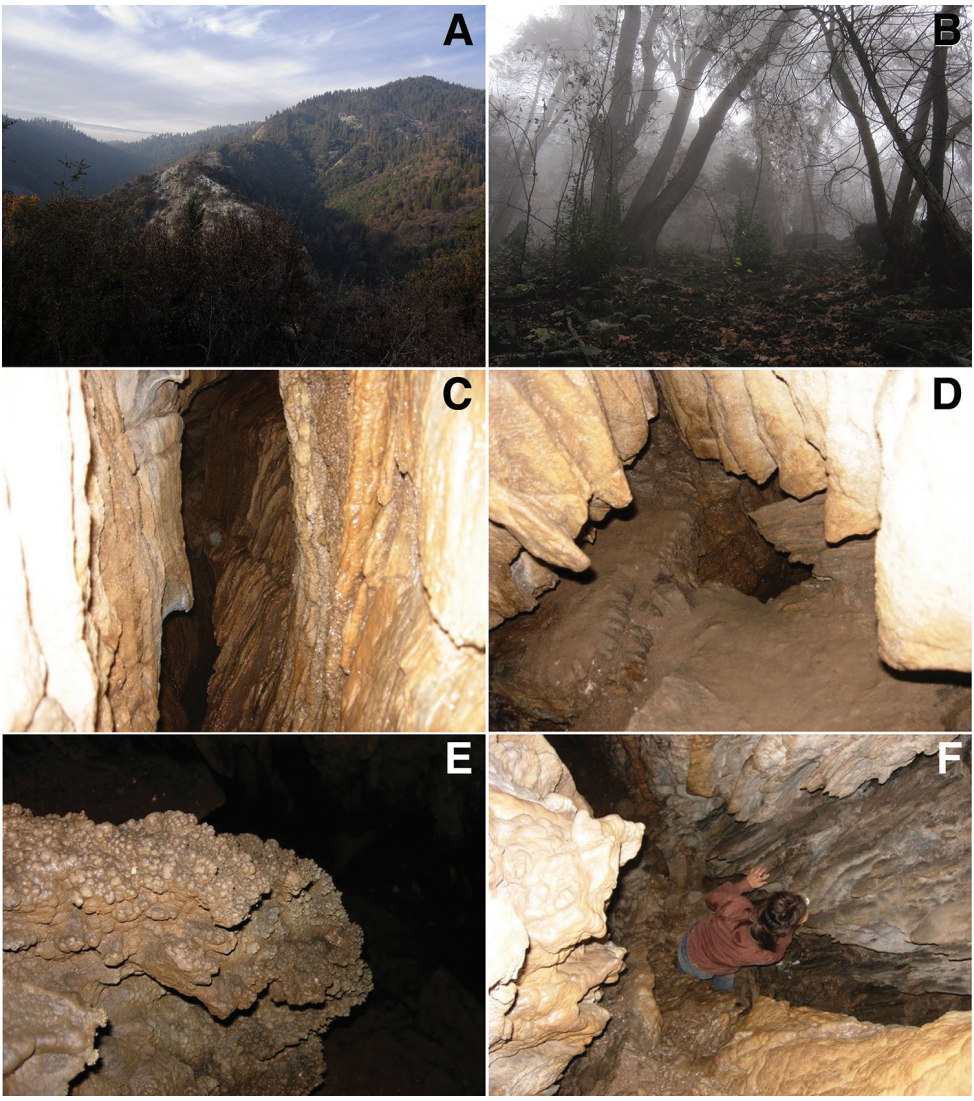

Figure 20. Habitat of *I. tobini* sp. n.: **A** Yucca Ridge, Sequoia National Park, California, with marble rocks exposed along ridge (center) **B** Woodland habitat on north facing slope of Yucca Canyon **C–F** Interior of marble cave.

The species *I. tobini* sp. n. and *I. plenipes* are the sole members of the genus and family in the Western Hemisphere. Shared morphological characters indicate the family is monophyletic, yet these features have not been considered within the context of a rigorous phylogenetic systematic framework. The features, including lack of a beak and absence of antennal pits, are broadly distributed across helminthomorph millipedes and are potentially shared ancestral traits and thereby do not indicate monophyly. The species *I. tobini* sp. n. is closely allied to *I. plenipes* based on unique shape of the head,

consistency in appearance of mouthparts, similarly shaped gonopods, and possession of many legs. However, *I. tobini* sp. n. differs from *I. plenipes* in noteworthy characters such as the shape of metazonites, ornamentation of the ozopore, and chaetotaxy and number of articles of the posterior gonopods. The divergence in these traits, considering the usual divergence in morphology between siphonorhinid taxa, suggests generic differences. Our PCR possibly failed because specimen preservation in dilute ethanol degraded the DNA (Vink et al. 2005). Pending discovery of additional individuals suitable for DNA sequencing, and phylogenetic analysis within the context of relatives in the Siphonorhinidae, a new generic designation may be justified.

Our knowledge of the cephalic morphology of the Colobognatha is limited due to their small size and derived anatomy, thereby making the generation of homology hypotheses difficult. In the current study, we revise the morphological assessment of the labrum, gnathochilarium, and mandibles. The labrum of *I. tobini* sp. n. is apically deeply divided into a slit. The dorsal margins of the slit are lined with sharp upwards-projecting spines. Moving posteriorly into the head, the labrum is further divided into a tridentate projection with additional upwards projecting spines. The remainder of the labrum posterior to the epistome is covered in a field of ca. 200 pores, half of which possess a secretion seemingly extruded from the pore openings (Fig. 7F). These labral features are not observed in other diplopods, and their homology and function is unclear. The pores appear deep and may open to the buccal cavity. The gnathochilarium of *I. plenipes* was described as "indistinguishably fused" (Marek et al. 2012, pg. 89). However, we now think the gnathochilaria of both species are composed of a mentum and pair of stipes. *Illacme tobini* sp. n. has paired lamellae linguales each with a palp (Fig. 14B), but whether this feature is present in *I. plenipes* is unclear. The mandibles of *I. tobini* sp. n. lack sharp teeth distally (as in other Chilognatha) and possess finger-like rounded teeth. The mandibular pectinate lamella are composed of numerous rows of small jagged teeth that project ventrally and nest in a groove in the frontal body of the endochilarium. It is evident that these structures are the mandibles and not the epipharynx based on the articulated nature of the articles and separation between the mandibular gnathal lobe and base. In the description of *Kleruchus olivaceus*, Attems (1938, pg. 296, fig. 195) similarly illustrates the right mandible of the male holotype. In the drawing, the finger-like mandibular teeth and pectinate lamella are strikingly similar in appearance to the equivalent structures in *I. tobini* sp. n.

Based on examination of the mouthparts of *Illacme* and other siphonophoridan species, individuals consume liquid or gelatinous foods. In Siphonophorida (and most Colobognatha), the mouthparts are drawn into a cone with a small aperture distally. The mandibles are reduced and are not divided between the cardo, stipes and galea. A suctorial feeding mode has been suggested previously, and Manton (1961, pg. 386) indicated that species of *Siphonophora* possess a "suctorial fore-gut", proboscis, skeleto-muscular features, and head movement behaviors that strongly implicate suction feeding. Manton did not elaborate upon precise modifications of the foregut for suction, but filtration devices and muscular thickening are potential features to explore in the future. The presence of a coiled hindgut and elongation of the trunk (and thereby

also the gut) for processing a nutrient poor diet are consistent with plant sap feeding (Marek et al. 2012). Dissecting individual hindguts of *I. plenipes* suggested a liquid diet since gut contents were gelatinous and homogenous, and lacking particles completely. The mouthpart morphology of *I. tobini* sp. n. is peculiar and hypothetically represents a morphology adapted for consuming fungus as they are similar in gross anatomy with some sporophagous beetles (Betz et al. 2003, Lipkow and Betz 2005, Yavorskaya et al. 2014). Specifically, *I. tobini* sp. n. possesses (1) mandibles with inner brush-like "bristle-trough" structures (Fig. 14C—mouthpart feature *ii* of Lipkow and Betz 2005) that hypothetically sweep in loose food material; (2) mandibles with outer lobes for manipulating dispersed food material and transporting it posteriorly (Figs 7A–D, 14C—feature *iii* of Lipkow and Betz 2005); and (3) a flat crushing or grinding surface of the endochilarium (Fig. 7C, D—feature *iv* of Lipkow and Betz 2005).

While the mouthparts of the Siphonophorida are more derived in morphology and function relative to other helminthomorph millipedes, the gonopods are primitive due to their leg-like structure. In contrast with gonopods of eugnathan millipedes, many of which possess two leg podomeres (coxa and telopodite), colobognaths typically have a greater number of podomeres. Although Marek et al. (2012) counted six gonopodal podomeres in *I. plenipes*, we have reexamined *I. plenipes* males and found that they, as with *I. tobini* sp. n. males, have seven gonopodal podomeres, representing the primitive complement, including a seventh tarsungulum that is the terminal article. As in other colobognaths, the tarsungulum of the posterior gonopod is stylus-like, and the anterior tarsungulum spade-shaped with a deep groove. The groove of the anterior gonopod cups the stylus, which is often observed resting within the recess, and may act as a conductor allowing the posterior gonopod to slide into the cyphopods of the female during copulation. This process may be functionally analogous to the spider embolus (=posterior gonopod in millipedes) and conductor (=anterior gonopod in millipedes).

Several groups of dispersal-limited Californian animals show a distribution in which a Sierra Nevada clade is most closely related to a clade in the Coast Ranges. Examples of this spatial pattern occur in bioluminescent millipedes (genus *Motyxia*), harvestmen (genus *Calicina*), mygalomorph spiders (*Aliatypus californicus*, *Aliatypus erebus*), and several species of salamanders (*Batrachoseps attenuatus*, *Ensatina eschscholtzii*, *Aneides lugubris*—Jockusch and Wake 2002, Martínez-Solano et al. 2007, Kuchta et al. 2009, Lapointe and Rissler 2005). Most studies that demonstrate this biogeographical pattern among taxa infer directionality of diversification from the Coast Ranges to the Sierra Nevada (reviewed in Emata and Hedin 2016). The phylogenetic studies of salamanders indicate a west-to-east pattern, relatively recent in the mid-late Pleistocene. In contrast, the studies of mygalomorphs and diplopods recover an east-to-west directionality of diversification (Satler et al. 2011, Marek and Moore 2015). Several of these taxa (e.g., *Calicina* and *Batrachoseps*) have occurred in California since the Eocene, with a "trans-valley" split occurring in the harvestman *Calicina* during mid-late Miocene (Emata and Hedin 2016). Inferred dates for the east-west splits in other taxa are unknown.

Conservation. *Illacme tobini* sp. n. is a short-range endemic restricted to the base of Yucca Mountain between the North and Marble forks of the Kaweah River in

Sequoia National Park, California. The species is only known to occur in one small cave, though its range is likely to include the MSS. Management of this species should include careful consideration of activities that may impact the surface or subsurface. Actions that include vegetation changes, ground disturbance, or alteration of drainage patterns should be restricted in scope to preserve the soil and moisture of this river basin. The abundance and composition of MSS invertebrates in most global habitats remains uncertain, and further exploration and survey of these systems, thereby building knowledge of this fauna, will help to understand more fully biodiversity that is responsible for supporting healthy forests and ecosystem services.

Species catalog of the Siphonorhinidae

Family Siphonorhinidae Cook, 1895

4 genera and 12 species: Wallacea, Sundaland, Himalayas, Indo-Burma, Madagascar, Maputaland-Pondoland-Albany, and North America.

Siphonorhinidae Cook 1895: 2. Jeekel 1971: 45. Hoffman 1980: 116. Shelley 1996b: 1808. Hoffman 1999: 195 (189 pdf). Jeekel 2001: 46. Enghoff et al. 2015: 386.

Indiozoniinae Verhoeff 1941: 220. Hoffman 1980: 116 (synonymized).

Nematozoniidae Verhoeff 1939: 218. Verhoeff 1940b: 506. Attems 1951: 197. Schubart 1966: 199. Jeekel 1971: 41. Hoffman 1980: 116 (synonymized).

Teratognathidae Attems 1951: 210. Hoffman 1980: 116 (synonymized).

Genus *Illacme* Cook & Loomis, 1928

2 species: California

Illacme Cook and Loomis 1928: 12. Type species: *Illacme plenipes* Cook & Loomis, 1928, by original designation. Chamberlin and Hoffman 1958: 189. Buckett 1964: 29. Jeekel 1971: 39. Hoffman 1980: 116. Shelley 1996b: 23. Shelley 1996a: 1808. Hoffman 1999: 195 (189 pdf). Jeekel 2001: 46. Marek and Bond 2006: 707. Shelley 2010: 45. Marek et al. 2012: 85. Wesener 2014: 415. Enghoff et al. 2015: 386.

Illacme plenipes Cook & Loomis, 1928

Illacme plenipes Cook and Loomis 1928: 12. Chamberlin and Hoffman 1958: 189. Buckett 1964: 29. Enghoff et al. 1990: 131. Hopkin and Read 1992: 1. Shelley 1996b: 23, figs 1–3. Shelley 1996a: 1808. Hoffman 1999: 195 (190 pdf). Jeekel 2001: 46. Shelley and Hoffman 2004: 221. Marek and Bond 2006: 707. Read and Enghoff 2009: 554. Shelley 2010: 45. Shelley and Golovatch 2011: 26. Marek et al. 2012: 87. Wesener 2014: 415.

Illacme tobini Marek, Krejca & Shear, 2016

Illacme tobini Marek, Krejca & Shear, 2016: herein. MALE HT (VTEC). United States: California, Tulare County, Sequoia National Park.

Genus *Kleruchus* Attems, 1938

1 species: Vietnam

Kleruchus Attems 1938: 295. Type species: *Kleruchus olivaceus* Attems, 1938, by original designation. Carl 1944: 260. Attems 1951: 211. Jeekel 1971: 40. Hoffman 1980: 116. Jeekel 2001: 46. Enghoff et al. 2015: 386.

Kleruchus olivaceus Attems, 1938

Kleruchus olivaceus Attems 1938: 296, figs 193–203. MALE HT (NMW). Vietnam: Đà Nẵng Province, Bà Nà [15.983333 N, 107.983333 W]. Lit: *Bana (C. Annam), 1.500 m., 22 IX., 31*. Marek et al. 2012: 86.

Note. Attems (1938) provided illustrations of the enlarged forelegs of *K. olivaceus* (fig. 193), head and antenna (fig. 194), mandible (fig. 195), ventral surface of head and gnathochilarium (fig. 196), pleurite (fig. 198), ventral surface of the terminal 3 segments plus telson (fig. 199), and gonopods (figs 200–203).

Genus *Siphonorhinus* Pocock, 1894

8 species: India, Indonesia, Madagascar, Vietnam

Siphonorhinus Pocock 1894: 335. Type species: *Siphonorhinus pallipes* Pocock, 1894, by original designation. Jeekel 1971: 45. Jeekel 2001: 46. Enghoff et al. 2015: 386.

Siphonorhinus angustus Pocock, 1894

Siphonorhinus angustus Pocock 1894: 336. MALE HT (BMNH). Indonesia: West Java, Bogor [-6.6 S, 106.8 W]. Lit: *Java: Buitenzorg. A single ♂ specimen.* Attems 1914: 359.

Note. With regards to *S. angustus* and *S. pallipes* (collected from the same area), Pocock (1894, pg. 336) wrote: "These two species are really so much alike that I am perfectly prepared for fresh specimens to show that the differences pointed out are merely due to individual variation. But at present there is no evidence that such is the case and the analogy of other species of the group lends no support to the view."

***Siphonorhinus cingulatus* (Attems, 1936)**

Siphonophora cingulata Attems 1936: 315, fig. 94. FEMALE HT (NMW). Vietnam: Lâm Đồng Province, Đà Lạt [11.941667 N, 108.438333 W]. Lit: *South Annam, Dalat, 5,000 feet, Langbian Province (C. Boden Kloss; iii-v.18; 1 ex)*. Attems 1938: 320. Carl 1941: 573. Carl 1944: 260. Turk 1947: 74.
Pterozonium cingulatum–Attems 1951: 231. Golovatch and Martens 1996: 167.
Zinaceps cingulatus–Chamberlin and Wang 1953: 13.
Siphonorhinus cingulatus–Jeekel 2001: 47. Golovatch and Wesener 2016: 16.

Note. Attems (1936) provided a second locality, lit: *India, Eastern Himalayas, Pashok, 1,500 and 2,600 feet, Darjeeling District (Dr. F. H. Gravely; 26.v.-14.vi.16; Dr. S. L. Hora; 16.xii.26; 2 exs.)* [27.075794 N, 88.408726 E].

***Siphonorhinus coniceps* (Attems, 1936)**

Siphonophora coniceps Attems 1936: 314, fig. 93. FEMALE HT (NMW). India: West Bengal, Darjeeling, Pashok [27.075794 N, 88.408726 W]. Lit: *India, Eastern Himalayas, Pashok, 5,000 feet, Darjeeling District (Dr. F. H. Gravely; 26.v.-14. vi.16; 1 ex.)*. Turk 1947: 74.
Indozonium coniceps–Verhoeff 1941: 215.
Siphonorhinus coniceps–Carl 1941: 573. Carl 1944: 260. Jeekel 2001: 47. Golovatch and Wesener 2016: 16.
Pterozonium coniceps–Attems 1951: 231. Attems 1953: 198, figs 117–119.
Zinaceps coniceps–Chamberlin and Wang 1953: 13.

Note. Attems (1936) described *S. coniceps* and *S. cingulata* exclusively from female material. Carl (1941, 1944) and Jeekel (2001) did not provide a justification for re-housing the species within *Siphonorhinus*. The decision was likely made from Attems's (1936, pg. 315, fig. 93a) drawing of the head of *S. coniceps* without a distinct beak.

***Siphonorhinus larwoodi* (Turk, 1947)**

Siphonophora larwoodi Turk 1947: 73, figs 18–20. FEMALE HT (BMNH). India: Uttarakhand, Almora [29.6215441 N, 79.6763696 W]. Lit: *A single female of this species was taken by Capt. H. J. Larwood occuring under stones in a micaceous sand, near the Deodar Hotel, Almora, India, 9.vii.1945*. Turk 1947: 74.
Pterozonium larwoodi–Golovatch and Martens 1996: 167.
Siphonorhinus larwoodi–Jeekel 2001: 47.

Note. Turk provided a key to six species of Indian *Siphonophora* (1947, pg. 74). Three of these species are now in *Siphonorhinus*: *S. larwoodi*, *S. coniceps*, and *S. cingulatus*.

Siphonorhinus latus Silvestri, 1895

Siphonorhinus latus Silvestri 1895: 724. MALE HT (MFS). Indonesia: North Sumatra, Si-Rambé [2.257 N, 99.1114 W]. Lit: *Sumatra: Si-Rambé (E. Modigliani).* Silvestri 1903: 53, fig. 80. Attems 1914: 359. Jeekel 2001: 47.

Siphonorhinus pallipes Pocock, 1894

Siphonorhinus pallipes Pocock 1894: 335, pl. 20, fig. 3, 3a. MALE HT (BMNH). Indonesia: West Java, Bogor [-6.6 S, 106.8 W]. Lit: *Java: Buitenzorg; several specimens (♂♀).* Carl 1912: 508, pl. 9, figs 1–3. Attems 1914: 359. Jeekel 2001: 47.

Siphonorhinus pellitus (Attems, 1930)

Siphonophora pellita Attems 1930a: 155, figs 51–61. MALE HT (NMW). Indonesia: Lesser Sunda Islands, Flores Island, Manggarai, Rana Mesé [-8.543 S, 120.713 W]. *Lit: Rana Mesé, West-Flores, 25.6.1927 (♂).* Attems 1930b: 176. Attems 1938: 319. Carl 1944: 260.
Indiozonium pellitum–Verhoeff 1941: 215.
Siphonophorella pellita–Attems 1951: 254.
Siphonorhinus pellitus–Jeekel 2001: 47.

Note. Attems (1930a) provided illustrations of the head plus five anterior segments, dorsally (fig. 51) and laterally (fig. 52); vestiture of eighth tergite (fig. 53); eighth pleurite (fig. 54); ventral view of telson, paraprocts, hypoproct (fig. 55); eighth leg tarsus (fig. 56); posterior leg tarsus (fig. 57); left anterior gonopod (fig. 58); left anterior gonopod, closeup of distal portion (fig. 59); left posterior gonopod (fig. 60); left posterior gonopod, closeup of distal portion (fig. 61).

Siphonorhinus robustus (Attems, 1938)

Teratognathus robustus Attems 1938: 299, figs 204–218. MALE HT (NMW). Vietnam: Lâm Đồng Province, Di Linh [11.581531 N, 108.076415 W]. *Lit: Djiring (S. Annam), 1.000 m., II.1933*. Attems 1953: 198.
Siphonorhinus robustus–Carl 1941: 573. Jeekel 2001: 47. Likhitrakarn et al. 2014: 475.

Note. Attems (1938) provided illustrations of the ventral surface of the gnathochilarium (fig. 204); a magnified view of the left side of the gnathochilarium, including the mentum, stipes and lamella lingualis (fig. 205); dorsal view of the head plus six anteriormost segments (fig. 206); anterior view of the tenth segment in cross-section

(fig. 207); ventral surface of the pleurite from segment 12 (fig. 208); coxa and prefemur (fig. 209); and tarsus and claw (fig. 210). Attems (1936) provided three additional localities in addition to the Djiring site: *Dalat, 1.500 m., II.1933* [11.941667 N, 108.438333 W]*; Pic de Lang Biang, 2.400 m.* [12.047222 N,108.44 W]*, 1.1931; Tayninch (Cochinchina), I.1935* [11.310043 N,106.098275 W].

Species of uncertain status in *Siphonorhinus*

Siphonorhinus sp. Wesener 2014: 417. Madagascar: Antananarivo Province, Ankaratra massif, Manjakatompo Forestry Station [-19.37083 S, 47.339 W]. *Lit: MHNG Mad 89/21; 3 ♂, 2 ♀; Madagascar, Province Antananarivo, Ankaratra massif, Station Forestière Manjakatompo, près du sommet du Anosirivo, forêt primaire, prèlévement de sol dans une vielle souch, 1980 m; 26.xi.1989, leg. B. Hauser, extraction Berlese à Genève.*

Genus *Nematozonium* Verhoeff, 1939

1 species: South Africa

Nematozonium Verhoeff 1939: 216. Type species: *Nematozonium filum* Verhoeff, 1939, by original designation and monotypy. Jeekel 1971: 41. Hoffman 1980: 116. Hamer 1998: 20. Jeekel 2001: 48. Shelley and Hoffman 2004: 218. Enghoff et al. 2015: 386.

***Nematozonium filum* Verhoeff, 1939**

Nematozonium filum Verhoeff 1939: 218, pl. 3, fig. 21, pl. 4, figs 21–28. MALE HT (ZSM). South Africa: KwaZulu-Natal Province, Cathkin Peak, Drakensberg escarpment, 1930 m [-29.06724 S, 29.35898 E]. Lit: *In 1930 m. Höhe am Cathkin Peak in den Drakensbergen.* Schubart 1966: 200. Hamer 1998: 20.

Nematozonium elongatissimum Verhoeff 1940a: 118. Schubart 1966: 200. Hamer 1998: 20. Shelley and Hoffman 2004: 218 (synonymized).

Notes. Verhoeff (1939) provided illustrations of the antenna (pl. 3, fig. 21); ventral surface of the gnathochilarium (pl. 4, fig. 22); lateral surface of the head and collum (pl. 4, fig. 23); mandibles (pl. 4, fig. 24); dorsal surface of the head, collum, and third metatergite (pl. 4, fig. 25); ventral surface of the pleurite and its margin with the tergite (pl. 4, fig. 26); dorsal surface of the telson and terminal ring (pl. 4, fig. 27); and dorsal surface of a paranota and ozopore (pl. 4, fig. 28). Hamer provided the first ever color habitus image of *N. filum* (Shelley 2015). Other localities for *N. filum* are as follows (from Shelley and Hoffman 2004): South Africa, Mpumalanga (Graskop, Barberton); KwaZulu-Natal (Bulwer, Drakensberg Mountains, Natal Drakensberg Park/Cathedral Peak, Champagne Castle, Cathkin Peak, Pietermaritzburg, Dlinza Forest Reserve nr. Eshowe).

Uncertain status in Siphonorhinidae

Undetermined genus and species Enghoff et al. 1990: 105, fig. 1. Thailand.

Undetermined genus and species Shelley and Golovatch 2011: 125. India: Meghalaya, East Khasi Hills, Cherrapunji [Sohra]. *Lit: Asia: India: Assam: 4 km (4 mi) N Cherrapiniji, 1376 m, 3 October 1961, E.S. Ross, D. Q. Cavagnaro (CASC).*

Undetermined genus and species Wesener 2014: 417. Madagascar: Fianarantsoa Province, Réserve spéciale Ivohibe and Ambalavao National Park; Toliara Province, Rèserve Naturelle Intégrale d'Andohahela.

Acknowledgements

We are grateful for the support of a National Science Foundation Systematics and Biodiversity Sciences grant to J. Bond, P. Sierwald, W. Shear, P. Marek, and T. Jones (DEB-1256139). Additional funding provided by a Virginia Tech USDA NIFA Hatch Project (VA-160028) and from the Entomology Department, College of Agriculture and Life Sciences, and Provost's Office at Virginia Tech. Thomas Wesener and two anonymous reviewers provided constructive suggestions that improved previous versions of the manuscript. The Institute for Critical Technology and Applied Science's Nanoscale Characterization and Fabrication Laboratory provided SEM beam time, and Steve McCartney facilitated equipment operation. We thank Sequoia National Park for research permits (SEKI-2009-SCI-0026, SEKI-2011-SCI-0004, SEKI-2012-SCI-0414) and Joel Despain, Ben Tobin, Koren Nydick, Alysia Schmidt, Annie Esperanza, and Harold Werner for facilitating research in the park's caves. Joel Despain and Ben Tobin provided cave dimensions and environmental data. Mary Jane Epps, Charity Hall, Kojun Kanda, and Avery Lane provided help with cave surveys.

References

Attems CG (1914) Die indo-australischen Myriopoden. Archiv für Naturgeschichte 80A: 1–398. http://www.biodiversitylibrary.org/item/173344#page/573

Attems CG (1930a) Myriopoden der Kleinen Sunda-Inseln, gesammelt von der Expedition Dr. Rensch. Mitteilungen aus dem Zoologischen Museum in Berlin 16: 117–184. doi: 10.1002/mmnz.19300160103

Attems C (1930b) Myriopoden von Java, Sumatra, und Bali. Archiv für Hydrobiologie Supplement 8: 115–192.

Attems CG (1936) Diplopoda of India. Memoirs of the Indian Museum 11: 133–323.

Attems CG (1938) Die von Dr. C. Dawydoff in französisch Indochina gesammelten Myriopoden. Mémoires du Muséum national d'histoire naturelle, N. S. 6: 187–353.

Attems CG (1951) Revision systématique des Colobognatha (Myriapodes Diplopodes) et description d'espèces nouvelles. Mémoires du Muséum national d'histoire naturelle, N. S., série A 3: 193–231.

Attems CG (1953) Myriopoden von Indochina. Expedition von Dr. C. Dawydoff (1938–1939). Mémoires du Muséum national d'histoire naturelle, N. S., série A 5: 133–230.

Betz O, Thayer MK, Newton AF (2003) Comparative morphology and evolutionary pathways of the mouthparts in spore-feeding Staphylinoidea (Coleoptera). Acta Zoologica 84: 179–238. doi: 10.1046/j.1463-6395.2003.00147.x

Brandt JF (1834) Note on Colobognatha. Oken's Isis 27: 704.

Brewer MS, Bond JE (2013) Ordinal-level phylogenomics of the arthropod class Diplopoda (millipedes) based on an analysis of 221 nuclear protein-coding loci generated using next-generation sequence analyses. PLoS ONE 8: e79935. doi: 10.1371/journal.pone.0079935

Buckett JS (1964) Annotated list of Diplopoda of California. Simmons Publishing, California, 34 pp.

Carl J (1912) Sur quelques colobognathes du Muséum du Genève. Revue suisse de zoologie 20: 507–518.

Carl J (1941) Diplopoden aus Südindien und Ceylon. 2. Teil: Nematophora und Juliformia. Revue suisse de zoologie 48: 569–714. doi: 10.5962/bhl.part.154483

Carl J (1944) K. W. Verhoeffs System der Siphonophoriden kritisch betrachtet. Revue suisse de zoologie 51: 253–465.

Chamberlin RV, Hoffman RL (1958) Checklist of the millipeds of North America. Bulletin of the United States National Museum 212: 1–236. doi: 10.5479/si.03629236.212

Chamberlin RV, Wang YHM (1953) Records of millipeds (Diplopoda) from Japan and other oriental areas, with descriptions of new genera and species. American Museum Novitates 1621: 1–13. http://digitallibrary.amnh.org/handle/2246/4890

Chung KH, Moon MJ (2006) Antennal sensory organs in the female millipede *Orthomorphella pekuensis* (Polydesmida: Paradoxosomatidae). Integrative Biosciences 10: 183–189. doi: 10.1080/17386357.2006.9647300

Cook OF (1895) Introductory note on the families of Diplopoda. In: Cook OF, Collins GN, The Craspedosomatidae of North America. Annals of New York Academy of Science 9: 1–9. doi: 10.1111/j.1749-6632.1896.tb55430.x

Cook OF, Loomis HF (1928) Millipeds of the order Colobognatha, with descriptions of six new genera and type species, from Arizona and California. Proceedings of the United States National Museum 72: 1–26. doi: 10.5479/si.00963801.72-2714.1

Emata KN, Hedin M (2016) From the mountains to the coast and back again: Ancient biogeography in a radiation of short-range endemic harvestmen from California. Molecular phylogenetics and evolution 98: 233–243. doi: 10.1016/j.ympev.2016.02.002

Enghoff H (2011) Trans-segmental serial colour patterns in millipedes and their developmental interpretation (Diplopoda). International Journal of Myriapodology 6: 1–27. doi: 10.3897/ijm.6.1949

Enghoff H, Dohle W, Blower JG (1993) Anamorphosis in millipedes (Diplopoda)–the present state of knowledge with some developmental and phylogenetic considerations. Zoological Journal of the Linnean Society 109: 103–234. doi: 10.1111/j.1096-3642.1993.tb00305.x

Enghoff H, Golovatch S, Short M, Stoev P, Wesener T (2015) Diplopoda—Taxonomic Overview. In: Minelli A (Ed.) Treatise on Zoology - Anatomy, Taxonomy, Biology. The Myriapoda, 2. Brill, Leiden, 363–453.

Espinasa L, Collins E, Botelho M (2014) Two new nicoletiid species (Insecta: Zygentoma) from the Yucatan Peninsula, México. Proceedings of the Biological Society of Washington 127: 473–482. doi: 10.2988/0006-324X-127.3.473

Fernandez R, Edgecombe GD, Giribet G (2015) Exploring phylogenomic relationships within Myriapoda: should high matrix occupancy be the goal? bioRxiv 030973. doi: 10.1101/030973

Folmer O, Black M, Hoeh W, Lutz R, Vrijenhoek R (1994) DNA primers for amplification of mitochondrial cytochrome c oxidase subunit I from diverse metazoan invertebrates. Molecular Marine Biology and Biotechnology 3: 294–299. http://www.mbari.org/wp-content/uploads/2016/01/Folmer_94MMBB.pdf

Gervais P (1844) Études sur les Myriapodes. Annales des Sciences naturelles {3} 2: 51–80. http://www.biodiversitylibrary.org/item/207457#page/11/mode/1up

Golovatch SI, Martens J (1996) On the distribution and faunogenesis of Himalayan millipedes (Diplopoda): Preliminary results. Mémoires du Muséum national d'Histoire naturelle 169: 163–174.

Golovatch SI, Wesener T (2016) A species checklist of the millipedes (Myriapoda, Diplopoda) of India. Zootaxa 4129: 1–75. doi: 10.11646/zootaxa.4129.1.1

Hamer ML (1998) Checklist of Southern African millipedes (Myriapoda: Diplopoda). Annals of the Natal Museum 39: 11–82. http://hdl.handle.net/10499/AJ03040798_145

Hebert PD, Cywinska A, Ball SL (2003) Biological identifications through DNA barcodes. Proceedings of the Royal Society of London B: Biological Sciences 270: 313–321. doi: 10.1098/rspb.2002.2218

Hoffman RL (1980 "1979") Classification of the Diplopoda. Musèum d'Histoire naturelle, Geneva, 237 pp. [date of publication 3 June 1980]

Hoffman RL (1999) Checklist of millipeds of North and Middle America. Virginia Museum of Natural History Special Publications, Martinsville, 584 pp. https://www.fieldmuseum.org/sites/default/files/hoffman_checklist_1999.pdf

Hopkin SP, Read HJ (1992) The Biology of Millipedes. Oxford University Press, Oxford, 233 pp.

Howarth FG (1983) Ecology of cave arthropods. Annual Review of Entomology 28: 365–389. doi: 10.1146/annurev.en.28.010183.002053

Jeekel C (1971) Nomenclator generum et familiarum Diplopodorum: A list of the genus and family-group names in the class Diplopoda from the 10th edition of Linneaus, 1758, to the end of 1957. Monografieën van de Nederlandse Entomologische Vereniging 5: 1–412.

Jeekel C (2001) A bibliographic catalogue of the Siphonophorida (Diplopoda). Myriapod Memoranda 3: 44–71.

Jockusch EL, Wake DB (2002) Falling apart and merging: diversification of slender salamanders (Plethodontidae: *Batrachoseps*) in the American West. Biological Journal of the Linnean Society 76(3): 361–391.

Koch M (2015) Diplopoda—General Morphology. In: Minelli A (Ed.) Treatise on Zoology - Anatomy, Taxonomy, Biology. The Myriapoda, 2. Brill, Leiden, 7–67. doi: 10.1163/978900-4188273_003

Kuchta SR, Parks DS, Mueller RL, Wake DB (2009) Closing the ring: historical biogeography of the salamander ring species *Ensatina eschscholtzii*. Journal of Biogeography 36(5): 982–995. doi: 10.1111/j.1365-2699.2008.02052.x

Lapointe FJ, Rissler LJ (2005) Congruence, consensus, and the comparative phylogeography of codistributed species in California. The American Naturalist 166(2): 290–299.

Latreille PA (1802/1804) Histoire naturelle, générale et particulière des Crustacés et des Insectes. 3+7. (= Tom 95 + 99). Dufart, Paris, 467 pp.

Likhitrakarn N, Golovatch SI, Panha S (2014) A checklist of the millipedes (Diplopoda) of Laos. Zootaxa 3754: 473–482. doi: 10.11646/zootaxa.3754.4.8

Lipkow E, Betz O (2005) Staphylinidae and fungi. Faunistisch Oekologische Mitteilungen 8: 383–411. doi: 10.1086/431283

Manton SM (1961) The evolution of arthropodan locomotory mechanisms. Part 7. Functional requirements and body design in Colobognatha (Diplopoda), together with a comparative account of diplopod burrowing techniques, trunk musculature, and segmentation. Journal of the Linnean Society of London, Zoology 44: 383–462. doi: 10.1111/j.1096-3642.1961.tb01622.x

Marek PE, Bond JE (2006) Rediscovery of the world's leggiest animal. Nature 441: 707–707. doi: 10.1038/441707a

Marek PE, Moore W (2015) Discovery of a glowing millipede in California and the gradual evolution of bioluminescence in Diplopoda. Proceedings of the National Academy of Sciences 112: 6419–6424. doi: 10.1073/pnas.1500014112

Marek P, Shear W, Bond J (2012) A redescription of the leggiest animal, the millipede *Illacme plenipes*, with notes on its natural history and biogeography (Diplopoda, Siphonophorida, Siphonorhinidae). ZooKeys 241: 77–112. doi: 10.3897/zookeys.241.3831

Marek PE, Tanabe T, Sierwald P (2014) A species catalog of the millipede family Xystodesmidae (Diplopoda: Polydesmida). Virginia Museum of Natural History Special Publications 17: 1–117.

Martínez-Solano I, Jockusch EL, Wake DB (2007) Extreme population subdivision throughout a continuous range: phylogeography of *Batrachoseps attenuatus* (Caudata: Plethodontidae) in western North America. Molecular Ecology 16(20): 4335–4355. doi: 10.1111/j.1365-294X.2007.03527.x

Nguyen Duy-Jacquemin M (1974) Les organes intracérébraux de *Polyxenus lagurus* et comparison avec organes neuraux d'autres diplopodes. Symposia of the Zoological Society of London 32: 211–216.

Olson DM, Dinerstein E, Wikramanayake ED, Burgess ND, Powell GVN, Underwood EC, D'Amico JA, Itoua I, Strand HE, Morrison JC, Loucks CJ, Allnutt TF, Ricketts TH, Kura Y, Lamoreux JF, Wettengel WW, Hedao P, Kassem KR (2001) Terrestrial ecoregions of the world: a new map of life on Earth. Bioscience 51: 933–938. doi: 10.1641/0006-3568(2001)051[0933:TEOTWA]2.0.CO;2

Ortuño VM, Gilgado JD, Jiménez-Valverde A, Sendra A, Pérez-Suárez G, Herrero-Borgoñón JJ (2013) The "alluvial mesovoid shallow substratum", a new subterranean habitat. PLoS ONE 8(10): e76311. doi: 10.1371/journal.pone.0076311

Pocock RI (1887) On the classification of the Diplopoda. Annals and Magazine of Natural History 20: 283–295. doi: 10.1080/00222938709460057

Pocock RI (1894) Chilopoda, Symphyla and Diplopoda from the Malay Archipelago. In: Weber M (Ed.) Zoologische Ergebnisse einer Reise in Niederländisch Ost-Indien 3. E.J. Brill, Leiden, 307–404, pls 19–22.

Rasband WS (2011) ImageJ. U.S. National Institutes of Health, Bethesda, Maryland, USA. Version 1.46 http://rsbweb.nih.gov/ij/

Read H, Enghoff H (2009) The order Siphonophorida - A taxonomist's nightmare? Lessons from a Brazilian collection. Soil Organisms 81: 543–556.

Regier JC, Wilson HM, Shultz JW (2005) Phylogenetic analysis of Myriapoda using three nuclear protein-coding genes. Molecular phylogenetics and evolution 34: 147–158. doi: 10.1016/j.ympev.2004.09.005

Satler JD, Starrett J, Hayashi CY, Hedin M (2011) Inferring species trees from gene trees in a radiation of California trapdoor spiders (Araneae, Antrodiaetidae, *Aliatypus*). PLoS ONE 6(9): e25355. doi: 10.1371/journal.pone.0025355

Schubart O (1966) Diplopoda III: Pselaphognatha, Opisthospermophora, Colobognatha. South African Animal Life 12: 9–227.

Shear WA (2011) Class Diplopoda de Blainville in Gervais, 1844. In: Zhang Z-Q (Ed.) Animal biodiversity: An outline of higher-level classification and survey of taxonomic richness. Zootaxa 3148: 159–164

Shear WA, Marek PE (2009) *Andrognathus hoffmani*, sp. n., A second species in the genus and the first species of Andrognathidae from México (Diplopoda, Platydesmida, Andrognathidae). In: Roble SM, Mitchell JC (Eds) A Lifetime of Contributions to Myriapodology and the Natural History of Virginia: A Festschrift in Honor of Richard L. Hoffman's 80th Birthday. Virginia Museum of Natural History Special Publication 16: 155–164.

Shelley RM (1996a) A description of *Siphonophora portoricensis* Brandt (Diplopoda: Siphonophorida: Siphonophoridae), with a catalogue of ordinal representatives in the New World. Journal of Natural History 30: 1799–1814. doi: 10.1080/00222939600771051

Shelley RM (1996b) The milliped order Siphonophorida in the United States and northern Mexico. Myriapodologica 4: 21–33. http://www.vmnh.net/content/uploads/PDF/Research_and_Collections/Myriapodologica/Myriapodologica_v4_n4.pdf

Shelley RM (2010) Rediscovery, redescription, and illustrations of the milliped, *Mitocybe auriportae* Cook and Loomis, 1928 (Colobognatha: Platydesmida: Andrognathidae). Zootaxa 2475: 39–47.

Shelley RM (2015) The myriapods, the world's leggiest animals. http://ag.tennessee.edu/EPP/Pages/Nadiplochilo/Nadiplochilo.aspx [accessed 5 June 2016]

Shelley RM, Golovatch SI (2011) Atlas of myriapod biogeography. I. indigenous ordinal and supra-ordinal distributions in the Diplopoda: perspectives on taxon origins and ages, and a hypothesis on the origin and early evolution of the class. Insecta Mundi 158: 1–134.

Shelley RM, Hoffman RL (2004) A contribution on the South African millipede genus, *Nematozonium* Verhoeff, 1939 (Siphonophorida: Siphonorhinidae). African Entomology 12: 217–222.

Sierwald P, Bond JE (2007) Current status of the myriapod class Diplopoda (millipedes): taxonomic diversity and phylogeny. Annual Review of Entomology 52: 401–420. doi: 10.1146/annurev.ento.52.111805.090210

Silvestri F (1895) I Chilopodi ed i Diplopodi di Sumatra e delle isole Nias, Engano e Mentavei. Annali del Museo civico di storia naturale di Genova, serie 2 14: 707–760.

Silvestri F (1903) Classis Diplopoda. Vol. 1a. Anatome: Pars I, Segmenta, Tegumentum, Musculi. In: Berlese A (Ed.) Acari, Myriapoda et Scorpiones huscque in Italia reperta: 1–272.

Sisson TW, Moore JG (1994) Geologic map of the giant forest quadrangle, Tulare County (No. 1751), US Geological Survey, California. http://ngmdb.usgs.gov/Prodesc/proddesc_476.htm

Tobin BW, Hutchins BT, Schwartz BF (2013) Spatial and temporal changes in invertebrate assemblage structure from the entrance to deep-cave zone of a temperate marble cave. International Journal of Speleology 42: 203–214. doi: 10.5038/1827-806X.42.3.4

Turk FA (1947) On a Collection of Diplopods from North India, both Cavernicolous and Epigaean. Proceedings of the Zoological Society of London 117: 65–78. doi: 10.1111/j.1096-3642.1947.tb00498.x

U.S. Geological Survey (2015) U.S. Topo Quadrangles–Maps for America, National Geospatial Program, 7.5-minute series, US Geological Survey, California. http://nationalmap.gov/ustopo/index.html

Verhoeff KW (1939) Polydesmoideen, Colobognathen und Geophilomorphen aus Südafrica, besonders den Drakensbergen, Natal. Annals of the Natal Museum 9: 203–224.

Verhoeff KW (1940a) Aliquid novi ex Africa. I. Polydesmoidea und Colobognatha. Zoologischer Anzeiger 130: 104–119.

Verhoeff KW (1940b) Zur vergleichenden Morphologie der Colobognathen. Archiv für Naturgeschichte, N.F. 9: 501–511.

Verhoeff KW (1941) Versuch eines Siphonophoriden-Systems und geographisch-phylogenetische Beurteilung der Gonopoden. Zoologischer Anzeiger 134: 212–224.

Vink CJ, Thomas SM, Paquin P, Hayashi CY, Hedin M (2005) The effects of preservatives and temperatures on arachnid DNA. Invertebrate Systematics 19(2): 99–104. doi: 10.1071/IS04039

Wesener T (2014) First records of the order Siphonophorida from Madagascar and Mauritius (Diplopoda). Revue suisse de Zoologie 121: 415–423.

Yavorskaya MI, Leschen RA, Polilov AA, Beutel RG (2014) Unique rostrate larvae and basidiomycophagy in the beetle family Corylophidae. Arthropod structure and development 43: 153–162. doi: 10.1016/j.asd.2013.11.001

ZooKeys 626: 45–55 (2016)
doi: 10.3897/zookeys.626.7485
http://zookeys.pensoft.net

RESEARCH ARTICLE

A peer-reviewed open-access journal
ZooKeys
Launched to accelerate biodiversity research

Two new species of the orb-weaver genus *Chorizopes* from Yunnan, China (Araneae, Araneidae)

Xiao-Qi Mi[1], Cheng Wang[1], Xian-Jin Peng[2]

1 *College of Biological, Agricultural and Forest Engineering, Tongren University, Tongren, Guizhou 554300, China* **2** *College of Life Sciences, Hunan Normal University, Changsha, Hunan 410081, China*

Corresponding author: *Xian-Jin Peng* (xjpeng@126.com)

Academic editor: *S. Li* | Received 11 December 2015 | Accepted 6 October 2016 | Published 20 October 2016

http://zoobank.org/AC23216F-E284-4344-9890-A6976C0FFFF5

Citation: Mi X-Q, Wang C, Peng X-J (2016) Two new species of the orb-weaver genus *Chorizopes* from Yunnan, China (Araneae, Araneidae). ZooKeys 626: 45–55. doi: 10.3897/zookeys.626.7485

Abstract

Two new species of the orb-weaver genus *Chorizopes* from Yunnan Province, China are described: *C. albus* **sp. n**. (male and female) from the Gaoligong Mountains and Ailao Mountains, and *C. longus* **sp. n.** (male and female) from the Gaoligong Mountains. *Chorizopes albus* **sp. n**. can be distinguished from the related species *C. shimenensis* by: 1) median apophysis widest at the middle part versus widest at the base in the latter; 2) median apophysis without the dorsal spur found in that of the latter; 3) spermathecae spherical versus ovoid in the latter; 4) having one pair of large white spots on posterior lateral area of abdomen versus having two pairs of crescent white patches with dark edges on dorsal abdomen in the latter. *Chorizopes longus* **sp. n**. can be separated from the similar species *C. tumens* by: 1) the median apophysis having a knob on the distal half versus having a knob on the basic half in the latter; 2) male palp having a spur versus absent in the latter; 3) the width of the groove between the paracymbium and cymbium as thick as the paracymbium versus two times as thick as the paracymbium in the latter; 4) copulatory duct attached on anterior ventral of the spermatheca versus on anterior dorsal in the latter. Photos of body and copulatory organs, line drawings of copulatory organs, as well as the distribution data are provided. The type specimens are deposited in the College of Life Sciences, at the Hunan Normal University (HNU) and the Museum of Tongren University (MTU).

Keywords

Diagnosis, spider, taxonomy

Introduction

The orb-weaver spider genus *Chorizopes* is characterised by an extremely elevated cephalic region and wide separation of lateral eyes from median eyes. At present, 25 species from Asia and Africa are included in this genus (World Spider Catalog 2016). Of these, eight have been reported to come from China (Schenkel 1963, Yin et al. 1990, Yin, Peng and Wang 1994, Yin, Wang and Xie 1994, Yin et al. 1997, Yin et al. 2012; Zhu et al. 1994, Song et al. 1999, Zhu and Zhang 2011). Among the eight known Chinese species, *C. khanjanes* and *C. wulingensis* have the following common characters: dorsum of opisthosoma having three pairs of lateral tubercles and three vertically arranged caudal tubercles, epigynum having a short scape, teeth of chelicerae serrated and loosely arranged. The remaining six species share the following characters: dorsum of opisthosoma having one pair of lateral tubercles and two vertically arranged posterior tubercles, scape absent, chelicerae teeth tightly arranged.

While examining specimens collected in Yunnan Province, in southwest China, two new species belonging to the genus *Chorizopes* were identified and are described in this paper.

Material and methods

Specimens are kept in 75% ethanol. The epigynum was cleared in lactic acid for examination. An Olympus SZX16 stereo microscope was used for specimen examination. Digital photographs were taken using a Canon Powershot G12 digital camera mounted on an Olympus SZX16. Compound focus images were generated using Helicon Focus software. Leg measurements are given as: total length (femur, patella + tibia, metatarsus, tarsus). All measurements are given in millimetres (mm).

Abbreviations

ALE anterior lateral eyes;
AME anterior median eyes;
C conductor;
CD copulatory ducts;
CO copulatory openings;
E embolus;
FD fertilization ducts;
HNU Hunan Normal University;
MA median apophysis;
MOA median ocular area;
MTU Museum of Tongren University;
PLE posterior lateral eyes;
PME posterior median eyes;
S spermatheca;
TA terminal apophysis.

Taxonomy

Family Araneidae Clerck, 1757

Genus *Chorizopes* O. P.-Cambridge, 1870

Type species. *Chorizopes frontalis* O. Pickard-Cambridge, 1870

***Chorizopes albus* sp. n.**
http://zoobank.org/6FAA3F69-6B44-44C9-A804-9115CE107A5E
Figs 1–12

Type material. Holotype: male, China: Yunnan Province, Jingdong County, Huashan Township, Wengang Village, 24.3389°N, 101.1410°E, 1728 m, 16 August 2015, Cheng Wang, Zhaolin Liao, Peng Luo and Gaotao Liu leg (MTU-WC20150816). Paratypes: 1 male and 2 females, same data as holotype (MTU-WC20150816); 1 male and 2 females, Yunnan Province, Jingdong County, Huashan Township, Yingpan Village, 24.2788°N, 101.0979°E, 1273 m, 15 August 2015, Cheng Wang, Zhaolin Liao, Peng Luo and Gaotao Liu leg (MTU-WC20150815); 1 female, Yunnan Province, Fugong County, Shangpa Township, 26.8620ºN, 98.8714ºE, 1177 m, 19–27 August 2005, Tang Guo leg (HNU-Tang0509).

Etymology. The specific name comes from the Latin *albus*, meaning whitish, referring to the large white spots on lateral abdomen; adjective.

Diagnosis. The new species can be distinguished from all known congeneric species by the presence of a pair of white spots on lateral abdomen (Figs 1–2), median apophysis C-shaped and widest at the middle part (Figs 5, 9), copulatory ducts short and twisted between the spermathecae, and the epigastric furrow (Figs 7–8, 11–12).

Description. Male (holotype): Carapace dark brown, hairy, elevated in cephalic region. Chelicerae dark brown, have seven promarginal teeth. Sternum triangular, pointed posteriorly, yellowish brown. Legs yellowish brown, with wide darker grey annuli. Abdomen with one pair of lateral tubercles and two vertically arranged caudal tubercles. Dorsal abdomen greyish with two white spots, ventral yellowish brown, one pair of big white spots situated on the posterior lateral (Figs 1, 3). Spinnerets yellowish brown, palp with one patellar bristle; paracymbium flattened, basally located; median apophysis prominent, widest at the middle part, with a spur at distal end; membranous conductor narrow and long, guiding the embolus; embolus slender and twisted; terminal apophysis large, pointed distally (Figs 5–6, 9–10). Total length 2.90. Carapace length 1.25, width 1.00; abdomen length 1.65, width 1.30. Eye sizes and interdistances: AME 0.13, ALE 0.08, PME 0.10, PLE 0.08, AME–AME 0.10, AME–ALE 0.48, PME–PME 0.20, PME–PLE 0.50, MOA length 0.30 with front width 0.30 and back width 0.35. Leg measurements: I 2.95 (0.90, 1.05, 0.60, 0.40), II 2.90 (0.90, 1.00, 0.60, 0.40), III 1.90 (0.60, 0.65, 0.35, 0.30), IV 2.85 (0.90, 1.05, 0.55, 0.35).

Figures 1–2. *Chorizopes albus* sp. n. **1** male habitus, dorsal view **2** female habitus, dorsal view. Scale bars 1 mm.

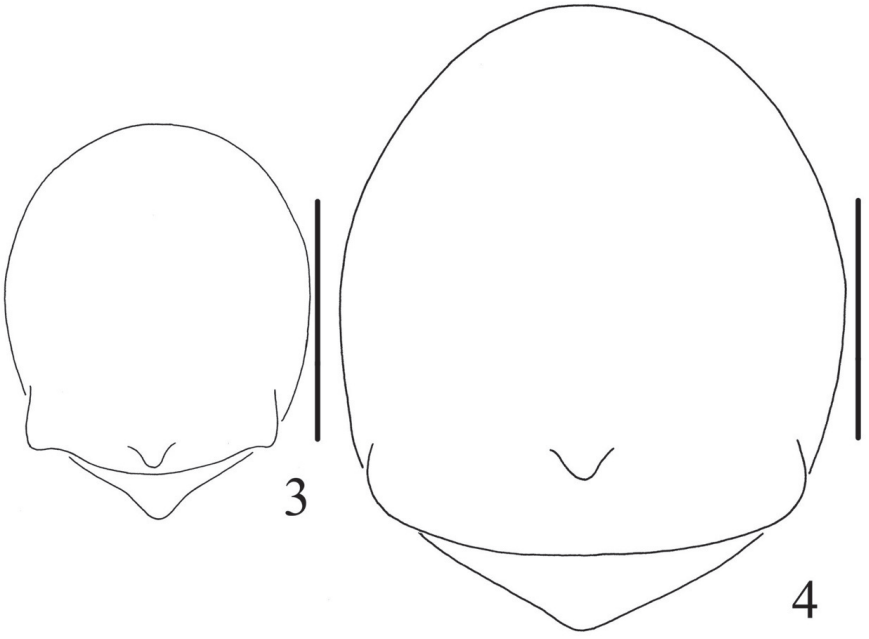

Figures 3–4. *Chorizopes albus* sp. n. **3** male abdomen, dorsal view **4** female abdomen, dorsal view. Scale bars 1 mm.

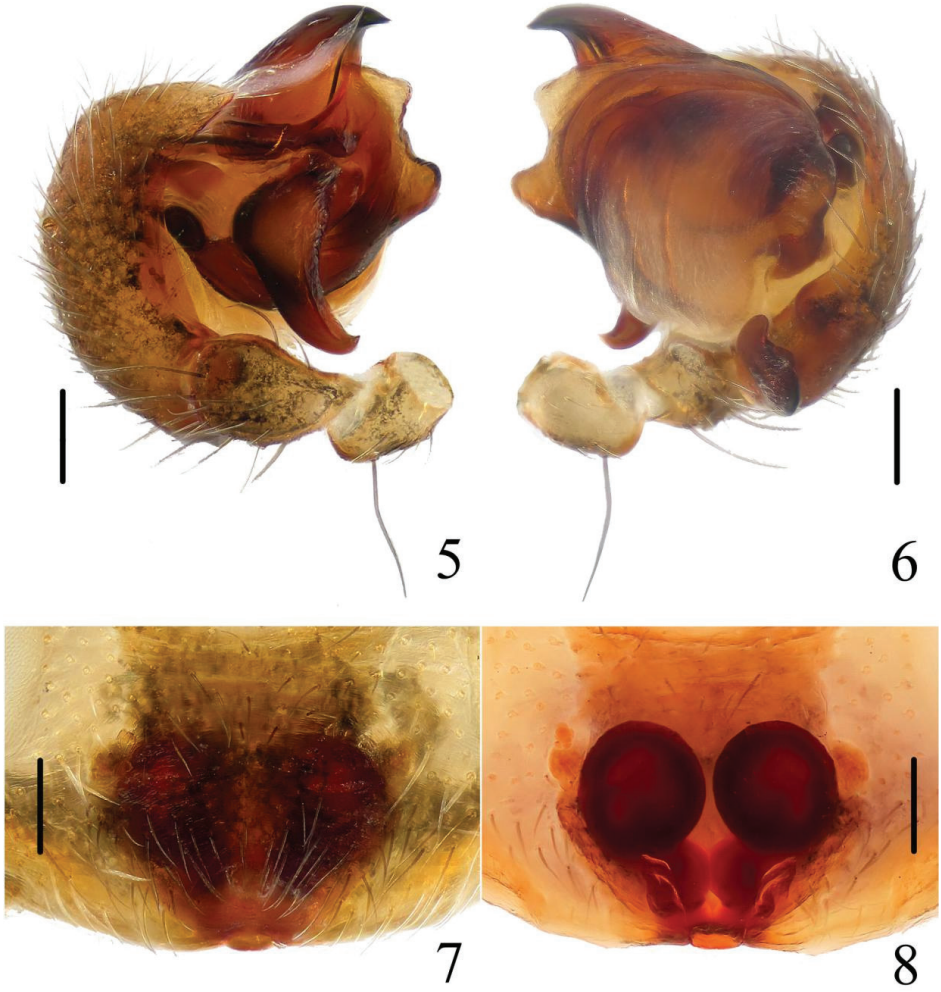

Figures 5–8. *Chorizopes albus* sp. n. **5** left palp, prolateral view **6** left palp, retrolateral view **7** epigynum, ventral view **8** vulva, dorsal view. Scale bars 0.1 mm.

Female (based on one of WC20150816): Colouration and body shape same as in male (Figs 2, 4). Epigynum is a slightly convex plate, copulatory openings posteriorly situated; copulatory ducts thick and twisted; spermathecae spherical and almost touched (Figs 7–8, 11–12). Total length 4.05. Carapace length 1.50, width 1.30; abdomen length 2.60, width 1.56. Eye sizes and interdistances: AME 0.15, ALE 0.08, PME 0.10, PLE 0.08, AME–AME 0.13, AME–ALE 0.60, PME–PME 0.25, PME–PLE 0.65, MOA length 0.35 with front width 0.35 and back width 0.43. Leg measurements: I 2.80 (0.85, 1.00, 0.55, 0.40), II 2.85 (0.90, 1.00, 0.55, 0.40), III 2.15 (0.65, 0.75, 0.40, 0.35), IV 3.15 (1.05, 1.10, 0.60, 0.40).

Variation. Males, total length 2.65–2.90, females, total length 3.35–4.05.

Distribution. China (Yunnan Province).

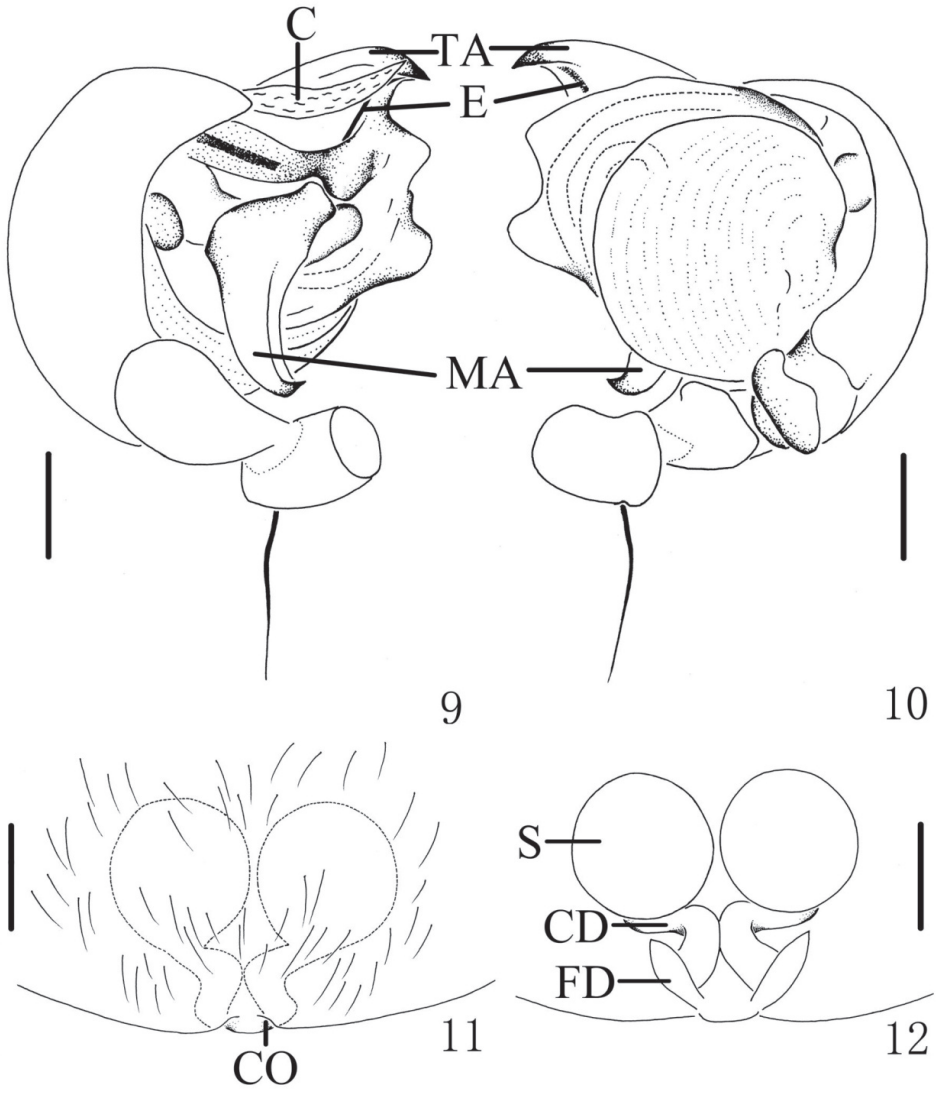

Figures 9–12. *Chorizopes albus* sp. n. **9** left palp, prolateral view **10** left palp, retrolateral view **11** epigynum, ventral view **12** vulva, dorsal view. Scale bars 0.1 mm.

***Chorizopes longus* sp. n.**
http://zoobank.org/D1E2E0F8-0881-445F-9DFC-23D772FE391D
Figs 13–24

Etymology. The specific name comes from the Latin *longus*, meaning long, referring to the long median apophysis; adjective.

Diagnosis. The new species can be separated from all known congeneric species by: the median apophysis extremely long, more than 2/5 portions beyond the edge of

Figures 13–14. *Chorizopes longus* sp. n. **13** male habitus, dorsal view **14** female habitus, dorsal view. Scale bars 1 mm.

the genital bulb in prolateral view (Figs 17–18, 21–22), and having a spur near the base (arrowed in Figs 17, 21); the copulatory ducts long and attaching the spermathecae at the anterior ventral surface (Figs 19–20, 23–24).

Type materials. Holotype, male, CHINA, Yunnan Province, Tengchong County, Houqiao Township, Yangjiatian Village, 25.3539°N, 98.2549°E, 1785 m, 28 May 2006, Xinping Wang and Peng Hu (HNU-WH060528). Paratypes: 1 male and 1 female, the same data as holotype (HNU-WH060528); 2 females, CHINA, Yunnan Province, Gongshan County, Bingzhongluo Township, Bingzhongluo Village, 30.7 air km NNW of Gongshan, in a small cave, 28.0194°N, 98.6211°E, 1760 m, 7-8 July 2000, Hengmei Yan, David Kavanaugh, Charles Griswold, Hongbin Liang, Darrell Ubick, & Dazhi Dong (HNU-00-GBC); 1 female, CHINA, Yunnan Province, Fugong County, Pihe Township, Wawa Village, 26.5903°N, 98.9082°E, 1263 m, 13 May 2004, Hengmei Yan (HNU-20040513); 1 female, CHINA, Yunnan Province, Tengchong County, Mingguang Township, Zizhi Village, Cizhuhe, 25.4560°N, 98.3703°E, 2120 m, 21 May 2006, Changmin Yin & Jiafang Hu (HNU-YHY09); 2 male and 2 female, CHINA, Yunnan Province, Tengchong Couty, Jietou Township Shaba Village, 25.3926°N, 98.7034°E, 1850 m, 25 May 2006, Xinping Wang and Peng Hu (HNU-WH060525); 1 female, CHINA, Yunnan Province, Tengchong

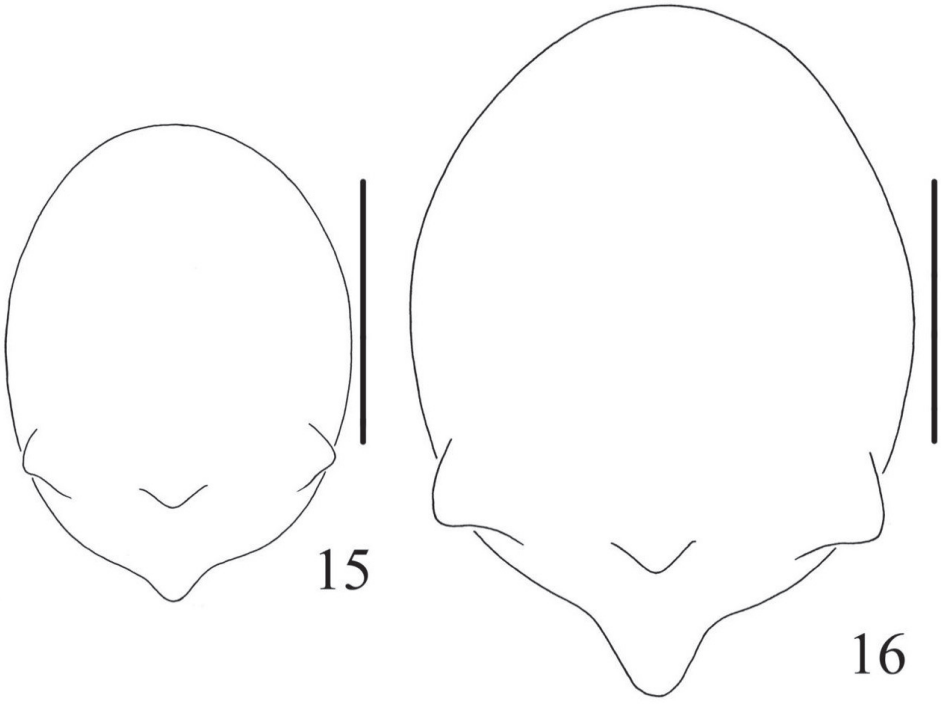

Figures 15–16. *Chorizopes longus* sp. n. **15** male abdomen, dorsal view **16** female abdomen, dorsal view. Scale bars 1 mm.

Couty, Houqiao Township, Doujiazhai Village, 25.3578°N, 98.2274°E, 1673 m, 30 May 2006, Xinping Wang and Peng Hu (HNU-WH060530).

Description. Male (holotype): Carapace dark brown, hairy, cephalic region elevated. Chelicerae dark brown, have seven promarginal teeth. Sternum triangular, dark brown. Gnathocoxae and labium yellowish brown. Legs yellowish brown with dark grey annuli. Dorsal abdomen greyish brown, cardiac pattern pale and long bar-shaped, two pairs of white spots on posterior lateral of cardiac pattern, posterior area of abdomen with one pair of lateral tubercles and two vertically arranged caudal tubercles (Figs 13, 15), ventral greyish brown with white scaly patches. Spinnerets brown. Palp with one patellar bristle; paracymbium flattened, basally located; median apophysis prominent, with a knob on the distal part; membranous conductor long and narrow; embolus slender and twisted; terminal apophysis large, pointed distally (Figs 17–18, 21–22). Total length 3.40. Carapace length 1.60, width 1.25; abdomen length 1.80, width 1.35. Eye sizes and interdistances: AME 0.10, ALE 0.08, PME 0.10, PLE 0.10, AME–AME 0.10, AME–ALE 0.50, PME–PME 0.20, PME–PLE 0.55, MOA length 0.30 with front width 0.30 and back width 0.38. Leg measurements: I 4.25 (1.30, 1.35, 1.00, 0.60), II 4.30 (1.50, 1.40, 0.85, 0.55), III 2.45 (0.80, 0.80, 0.45, 0.40), IV 3.85 (1.25, 1.20, 0.90, 0.50).

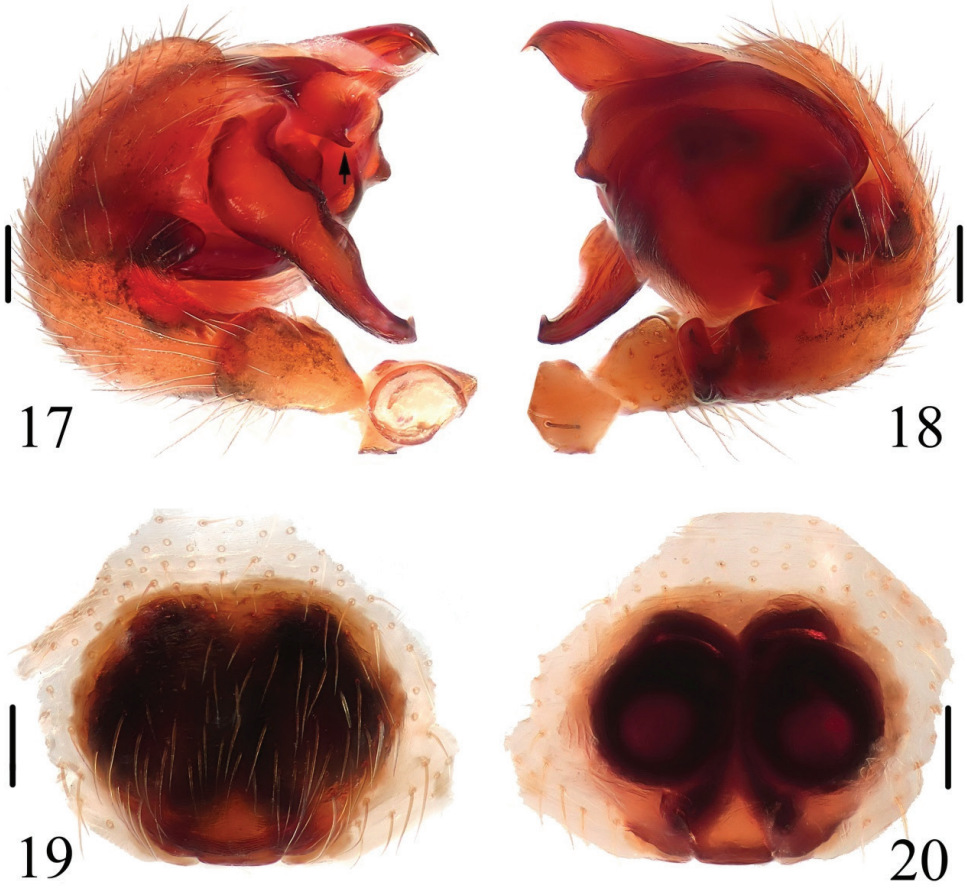

Figures 17–20. *Chorizopes longus* sp. n. **17** left palp, prolateral view **18** left palp, retrolateral view **19** epigynum, ventral view **20** vulva, dorsal view. Scale bars 0.1 mm.

Female (based on WH060528): Coloration and body shape same as in male (Figs 14, 16). Chelicerae have seven promarginal teeth. Epigynum has a slightly convex plate; copulatory openings posteriorly situated; copulatory ducts very long and twisted, attach the anterior ventral of the spermathecae; spermathecae big and spherical (Figs 19–20, 23–24). Total length 4.10. Carapace length 1.80, width 1.45; abdomen length 2.60, width 1.90. Eye sizes and interdistances: AME 0.13, ALE 0.10, PME 0.13, PLE 0.13, AME–AME 0.13, AME–ALE 0.75, PME–PME 0.23, PME–PLE 0.80, MOA length 0.38 with front width 0.33 and back width 0.40. Leg measurements: I 3.55 (1.00, 1.10, 0.90, 0.55), II 4.00 (1.15, 1.30, 1.00, 0.55), III 2.25 (0.75, 0.80, 0.50, 0.50), IV 3.10 (1.25, 1.40, 0.95, 0.50).

Variation. Males, total length 3.10–3.40 (n=4), females, total length 3.80–4.75 (n=6).

Distribution. China (Yunnan Province).

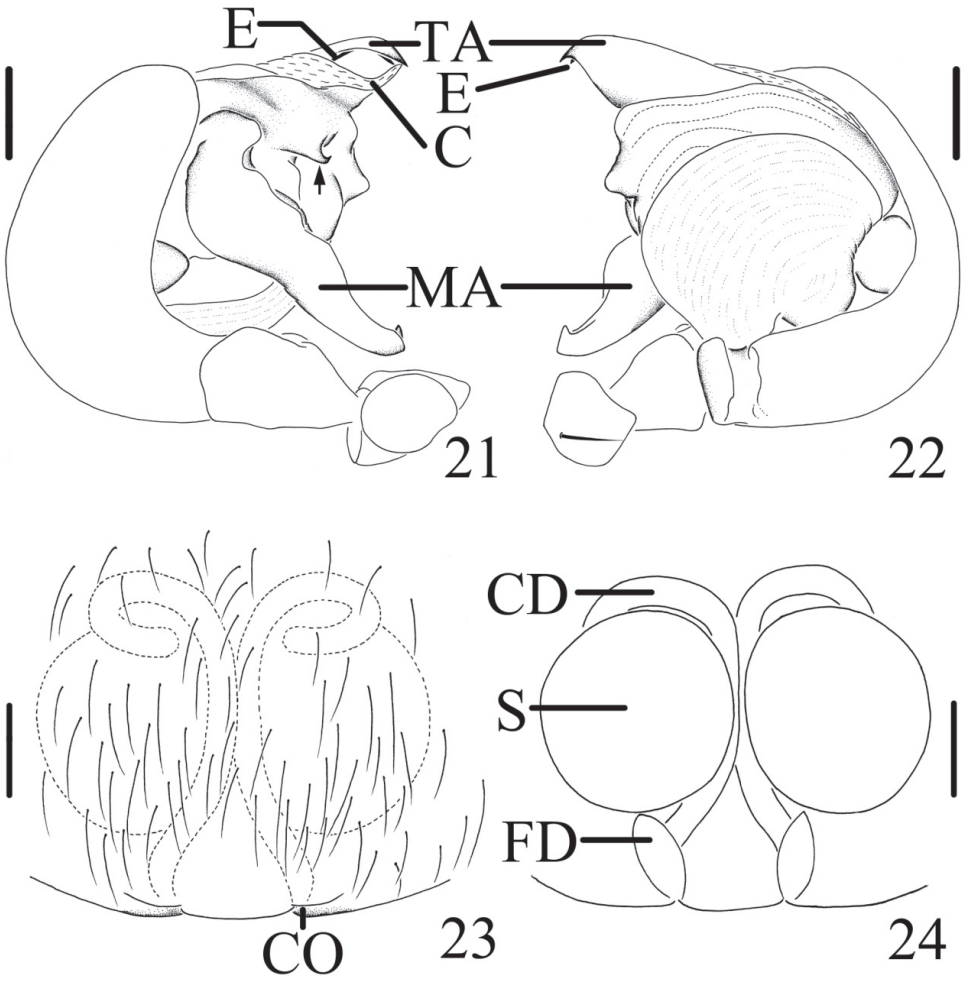

Figures 21–24. *Chorizopes longus* sp. n. **21** left palp, prolateral view **22** left palp, retrolateral view **23** epigynum, ventral view **24** vulva, dorsal view. Scale bars 0.1 mm.

Acknowledgements

We are grateful to Changmin Yin, Charles Griswold, David Kavanaugh, Darrell Ubick, Hengmei Yan, Hongbin Liang, Dazhi Dong, Xinping Wang, Guo Tang, Peng Hu, Jiafang Hu, Zhaolin Liao, Peng Luo and Gaotao Liu for collecting the specimens. This research work was sponsored by the National Science Foundation of the USA (No. DEB-0103795), the National Special Fund on Basic Research of Science and Technology of China (No. 2014FY110100) and the National Natural Sciences Foundation of China (NSFC-31272271, 31272272, 30970327, 31301861). It is also partly supported by the Science and Technology Foundation of Guizhou Province (No. J(2012)2313), and the Hunan Provincial Program for Development of Key Disciplines in Ecology.

References

Schenkel E (1963) Ostasiatische Spinnen aus dem Muséum d'Histoire naturelle de Paris. Mémoires du Muséum national d'histoire naturelle Paris (A, Zoologie) 25: 1–481.

Song DX, Zhu MS, Chen J (1999) The Spiders of China. Hebei Science and Technology Publishing House, Shijiazhuang, 640 pp.

World Spider Catalog (2016) World Spider Catalog. Natural History Museum Bern. http://wsc.nmbe.ch [version 17.0, accessed on 29 June 2016]

Yin CM, Wang JF, Xie LP, Peng XJ (1990) New and newly recorded species of the spiders of family Araneidae from China (Arachnida, Araneae). In Spiders in China: One Hundred New and Newly Recorded Species of the Families Araneidae and Agelenidae. Hunan Normal University Press, Changsha, 171 pp.

Yin CM, Peng XJ, Wang JF (1994) Seven new species of Araneidae from China (Arachnida: Araneae). Acta Arachnologica Sinica 3: 104–112.

Yin CM, Wang JF, Xie LP (1994) Two species of the gen. *Chorizopes* from China (Araneae: Araneidae). Acta Scientiarum Naturalium Universitatis Normalis Hunanensis 17(supplement): 5–8.

Yin CM, Wang JF, Zhu MS, Xie LP, Peng XJ, Bao YH (1997) Fauna Sinica: Arachnida: Araneae: Araneidae. Science Press, Beijing, 460 pp.

Yin CM, Peng XJ, Yan HM, Bao YH, Xu X, Tang G, Zhou QS, Liu P (2012) Fauna Hunan: Araneae in Hunan, China. Hunan Science and Technology Press, Changsha, 1590 pp.

Zhu MS, Zhang BS (2011) Spider Fauna of Henan: Arachnida: Araneae. Science Press, Beijing, 558 pp.

Zhu MS, Song DX, Zhang YQ, Wang XP (1994) On some new species and new records of spiders of the family Araneidae from China. Journal Hebei Normal University (Natural Sciences Edition) (supplement): 25–52.

ZooKeys 626: 57–65 (2016)
doi: 10.3897/zookeys.626.9771
http://zookeys.pensoft.net

RESEARCH ARTICLE

A peer-reviewed open-access journal
ZooKeys
Launched to accelerate biodiversity research

A new species of *Calogalesus* Kieffer from China (Hymenoptera, Diapriidae) with a key to World species

Jun Feng[1], David Notton[2], Zai-fu Xu[1]

1 *Department of Entomology, South China Agricultural University, Guangzhou 510640, P. R. China*
2 *Department of Life Sciences, Insects Division, Darwin Centre - room 315, The Natural History Museum, Cromwell Road, London, SW7 5BD, United Kingdom*

Corresponding author: *Zai-fu Xu* (xuzaifu@scau.edu.cn)

Academic editor: *N. Johnson* | Received 6 July 2016 | Accepted 10 October 2016 | Published 20 October 2016

http://zoobank.org/FBC28F3A-33E8-4E3A-9257-86023C31E820

Citation: Feng J, Notton D, Xu X-f (2016) A new species of Calogalesus Kieffer from China (Hymenoptera, Diapriidae) with a key to World species. ZooKeys 626: 57–65. doi: 10.3897/zookeys.626.9771

Abstract

A new species of *Calogalesus* Kieffer, 1912, *C. sinicus* **sp. n.**, is described and illustrated, collected from a Chinese prickly ash (*Zanthoxylum bungeanum* Maxim.) orchard in Yunnan province of China. This is the third described species of the genus in the World. The new species can be distinguished from the other two described *Calogalesus* species by the head profile, proportions of the antennal segments, tridentate mandible, and mandible length. A key to World species of the genus is provided.

Keywords

Hymenoptera, Diapriinae, *Calogalesus*, new species, Oriental region, China

Introduction

Calogalesus Kieffer, 1912 is a small genus in Diapriinae (Hymenoptera: Diapriidae), comprising two previously described species: *Calogalesus parvulus* Kieffer, 1912 from the Seychelles and *Calogalesus malabaricus* Rajmohana & Narendran, 2006 from India (Kieffer 1912a; Rajmohana and Narendran 2006). Its ecology and biology are unknown.

In recent years, during the survey of the Chinese fauna of Diapriidae funded by the National Natural Science Foundation of China, fifty-four specimens (of both sexes) belonging to *Calogalesus* were collected in Yunnan; this material is described here as a new species.

Materials and methods

All specimens were collected using yellow pan traps placed in a Chinese prickly ash (*Zanthoxylum bungeanum* Maxim.) orchard in Zhaotong, Yunnan from 10.VIII.2012 to 26.X.2012.

Specimens were examined and described under a Zeiss Stemi 2000-CS stereomicroscope. All photos were taken with a digital camera (Cool SNAP) attached to the Zeiss Stemi 2000-CS stereomicroscope and processed by using Image-Pro Plus software.

Morphological terminology mainly follows Masner and García Rodríguez (2002). The following abbreviations are used: A1, A2, … = the first, second, ... antennal segments, respectively; OOL = the shortest distance between posterior ocellus and compound eye; POL = the shortest distance between both posterior ocelli; T2 = the second (largest) tergite.

Measurements reported are relative, and refer to ratios, except for body length (head to abdominal tip, excluding antennae and ovipositor, when the body is fully extended) and fore wing length.

The holotype, 13 female and 34 male paratypes of the new species are deposited in the Hymenoptera Collection of South China Agricultural University, Guangzhou, Guangdong province, China (SCAU); three female and three male paratypes are deposited in The Natural History Museum, London, UK (NHMUK). The holotype ♀ of *C. parvulus* Kieffer, 1912 from the Seychelles (NHMUK010264968) and one male of *C. malabaricus* Rajmohana & Narendran, 2006 from India (Karnataka, Mudigere, 26.x–4.xi.1979, J. S. Noyes leg. (NHMUK010264967)) were compared with the new species.

Results

Genus *Calogalesus* Kieffer, 1912

Calogalesus Kieffer, 1912b: 6, 43. Type species: *Calogalesus parvulus* Kieffer, 1912, by monotypy; Kieffer 1912a: 73; Kieffer 1916: 10, 235; Muesebeck and Walkley 1956: 338; Johnson 1992: 145; Masner and García Rodríguez 2002: 116; Rajmohana 2006; 36.

Calicuta Rajmohana & Narendran, 2000a: 22–23, unavailable name; Rajmohana and Narendran 2000b: 193; Rajmohana & Narendran, in Rajmohana 2004: 519, 521; Rajmohana 2006: 36.

Diagnosis. Body mainly blackish-brown, brown or orange, smooth and shiny. Head with antennal shelf strongly projecting, laterally sharply angled and medially divided; frons with a curved carina on each side extending backwards, forming a ledge above upper eye orbit. Mandible bidentate or tridentate, together beak-like, projecting backwards. Antenna 12-segmented in female, 14-segmented in male; with A1 the longest segment. Female antenna without a clearly defined clava, but flagellar segments more or less thickened apically. Notauli distinct, not reaching transscutal articulation. Scutellum with two large anterior foveae. Fore wing with well-developed marginal cilia and two elongate hairless zones. Petiole strongly curved in lateral view.

Biology. This genus shows a nasiform head (elongated with frontal projections) and opisthognathous (backwards directed) beak-like mandibles, which may be associated with digging for hosts and/or bursting from host remains (Nielsen and Buffington 2011).

Distribution. The genus is known from the following biogeographic regions: Afrotropical (Masner and García Rodríguez 2002); Australian (Masner and García Rodríguez 2002); Malagasy (Kieffer 1912a, 1912b, 1916; Masner 1965; Gerlach 2013; Notton 2014; Madl 2015); Neotropical (Masner and García Rodríguez 2002; Arias-Penna 2003); Oriental (Rajmohana 2004, 2006; Rajmohana and Narendran 2000a, 2000b; Rajmohana and Bijoy 2012; Rajmohana et al. 2013).

Remarks. The genus *Calicuta* was described by Rajmohana and Narendran (2000a) without type species designation, without included species and was not explicitly indicated as new. It is therefore an unavailable name. A formal publication of the name was intended but was abandoned following the realization that it was the same genus as *Calogalesus* Kieffer (Rajmohana 2006; Rajmohana pers. comm. with Notton). The name *Calicuta* was not made available by any of the subsequent publications of Rajmohana and Narendran cited here.

Key to World species of *Calogalesus*

1 Females: 12 antennal segments; apex of metasoma pointed; ovipositor sheaths visible; apical flagellar segments more or less thickened **2**

– Males: 14 antennal segments; apex of metasoma blunt, often sunk inside T2 and not visible; no ovipositor sheaths; apical flagellar segments usually elongate, at least not thicker than basal flagellar segments **4**

2 Antenna longer than head and mesosoma (1.1:1.0), A4–A7 1.4 times as long as wide, A8–A10 1.17 times as long as wide; head profile less flattened (head length to height=1.0:1.0), subtriangular in lateral view; mandible tridentate, 0.5 times as long as eye height; POL:OOL=0.4:1.0 ..... ***C. sinicus* sp. n.**

– Antenna shorter than head and mesosoma (0.85–0.9:1.0), A4–A7 as long as wide, A8–A10 as long as wide or shorter than wide; head profile more flattened (head length to height=1.2–1.3:1.0), subrectangular in lateral view; mandible bidentate, 0.6–0.8 times as long as eye height; POL:OOL=1.2–1.3:1.0 ..... **3**

3 A2 as long as A3; A8–A10 as long as wide; mandible 0.8 times as long as eye height ..... ***C. malabaricus*** **Rajmohana & Narendran**

– A2 1.5 times as long as A3; A8–A10 distinctly shorter than wide; mandible 0.6 times as long as eye height (Fig. 10) ..... ***C. parvulus*** **Kieffer**

4 Head profile more flattened (head length to height=1.3:1.0), subrectangular in lateral view; mandible nearly as long as eye height (0.8:1.0); A4 0.9 times as long as A3 ..... ***C. malabaricus*** **Rajmohana & Narendran**

– Head profile less flattened (head length to height=1.0:1.0), subtriangular in lateral view; mandible distinctly shorter than eye height (1.0:2.0); A4 0.8 times as long as A3..... ***C. sinicus*** **sp. n.**

Calogalesus sinicus **Feng, Notton & Xu, sp. n.**
http://zoobank.org/0A2A49D5-D787-4006-A407-ED4F252B126E
Figs 1–9

Material examined. Holotype, ♀: CHINA: Yunnan, Zhaotong, Huanghua town (N27°59', E103°33'), 10.VIII.2012, Shi-wen Yang leg. Paratypes: 16 ♀♀, Yunnan, Zhaotong, Huanghua town (N27°59', E103°33'), 10.VIII–26.X.2012, Shi-wen Yang leg.; 37 ♂♂: Yunnan, Zhaotong, Huanghua town (N27°59', E103°33'), 10.VIII–26.X.2012, Shi-wen Yang leg.

Description. *Female* (Figs 1–4). Holotype. Body length 1.2 mm. Fore wing length 1.0 mm.

Colour. Head blackish-brown, mandibles brown. Antennae yellowish-brown. Mesosoma brown. Legs and tegulae yellowish-brown. Wings hyaline, with veins yellowish-brown. Metasoma brown, with apex yellowish-brown.

Head. Head subcircular in dorsal view, subtriangular in lateral view; smooth and shiny, with sparse hairs. Mandible tridentate, strongly projecting, beak-like. Labrum subtriangular. Clypeus highly convex. Eyes oval, slightly bulging laterally, with sparse hairs. Malar sulcus distinct. Frons with two sharp points and longitudinal ledges above upper eye orbit. Antennal shelf strongly projecting. Antenna 12-segmented (Fig. 3), with hairs slightly longer than width of antennal segment. Relative proportion of length to width of antennal segments: A1 (24:6); A2 (7:5); A3 (10:4); A4 (7:4); A5 (7:5); A6 (7:5); A7 (7:5); A8 (7:6); A9 (7:6); A10 (7:6); A11 (7:6); A12 (8:5). Eye 1.5 times as long as wide, 2.5 times as long as malar space. Ocelli with POL:OOL=5:12. Occipital flange moderately developed and step-like. Genal ridge with tufts of hairs.

Mesosoma. Mesosoma as wide as head in dorsal view. Cervix distinct. Pronotum smooth and shiny. Pronotal shoulders almost rounded. Epomium indistinct. Mesoscutum smooth and shiny, with sparse hairs. Notauli deep and posteriorly convergent, incomplete, reaching 0.90 length of mesoscutum, not reaching transscutal articulation. Humeral sulcus distinct. Mesoscutellum subtriangular, smooth and shiny, with two large foveae on anterior half and a row of small pits on the posterior margin. Mesopleuron smooth and shiny, with a groove beneath tegula. Sternaulus indistinct.

Figures 1–2. *Calogalesus sinicus* sp. n., ♀, holotype, habitus. **1** Lateral **2** dorsal.

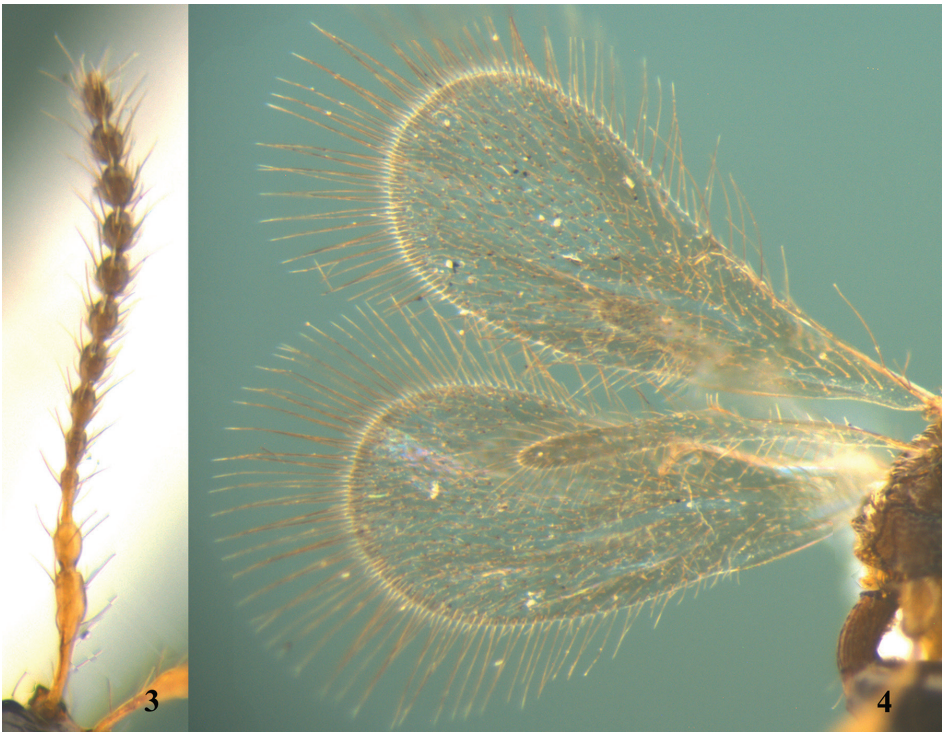

Figures 3–4. *Calogalesus sinicus* sp. n., ♀, holotype. **3** Antenna **4** wings.

Metanotum and metapleura reticulate rugose. Propodeum reticulate rugose. Dorsal surface of propodeum with one median longitudinal keel. Plica distinctly projecting posteriorly. Posterior surface of propodeum carinate and emarginated, descending

Figure 5. *Calogalesus sinicus* sp. n., ♂, paratype, habitus, lateral.

Figures 6–7. *Calogalesus sinicus* sp. n., ♂, paratype. **6** Antennae **7** wings.

Figures 8–9. Habitat of *Calogalesus sinicus* sp. n. **8** Chinese prickly ash (*Zanthoxylum bungeanum* Maxim.) orchard in Huanghua town, Zhaotong city, Yunnan province **9** *Zanthoxylum bungeanum* Maxim. (Photos by Wei Dong)

abruptly and steeply with two postero-lateral teeth in lateral view. Wings (Fig. 4) fully developed, with long marginal cilia. Fore wing with two elongate hairless zones basally; costal, subcostal, marginal and stigmal veins present, basal and postmarginal veins absent. Venation extending to half length of fore wing. Stigmal vein elongate, 0.6 times as long as marginal vein. Hind wing with submarginal vein complete. Femora and tibiae clavate. Fore tibia without an outwardly directed spine.

Metasoma. Petiole sparsely hairy, shiny, rugose with longitudinal striae, distinctly curved in lateral view; 2.6 times as long as wide in dorsal view; 2.3 times as long as high in lateral view. Gaster moderately compressed laterally. T2 enlarged, 2.6 times as long as wide in dorsal view, and covering 0.65 length of gaster in dorsal view. Anterior margin of T2 straight, without furrow or emargination. Metasomal tip conical.

Variation. Body length 1.1–1.4 mm (n=17). Fore wing length 1.0–1.3 mm (n=17).

Male (Figs 5–7). Body length 1.0–1.3 mm (n=37). Fore wing length 0.8–1.2 mm (n=37). Antenna 14-segmented (Fig. 6), with hairs slightly longer than width of antennal segment. Relative proportion of length to width of antennal segments as follows: A1 (23:4); A2 (7:4); A3 (10:3); A4 (8:3); A5 (7:4); A6 (7:4); A7 (7:4); A8 (7:4); A9 (7:4); A10 (7:4); A11 (7:4); A2 (7:4); A3 (7:4); A14 (8:4). A4 not modified. Metasomal tip blunt. Other characteristics as for females.

Biology. Host unknown. This species was collected by placing 500 yellow pan traps in a Chinese prickly ash (*Zanthoxylum bungeanum* Maxim.) orchard (Figs 8, 9) from 10.VIII.2012 to 26.X.2012. Specimens were picked up every day.

Distribution. Known from a single location in China (Yunnan).

Remarks. This new species can be separated from the two described species, *C. parvulus* Kieffer, 1912 (Fig. 10), and *C. malabaricus* Rajmohana & Narendran, 2006, by the characters given in the key. In all previous descriptions of *Calogalesus* (Masner and García Rodríguez 2002; Rajmohana et al. 2013), state that the mandible are bidentate, however the new species has tridentate mandibles, so we have revised the generic diagnosis accordingly.

Etymology. The new species is named after the country of the type locality, China.

Figure 10. *Calogalesus parvulus* Kieffer, 1912, ♀, holotype, habitus, lateral (Photo by Zi Hou, © The Trustees of the Natural History Museum, London).

Acknowledgements

We are very grateful to Shi-wen Yang for collecting the specimens, Wei Dong for providing the habitat photographs of *Calogalesus sinicus* sp. n., and Zi Hou for providing the holotype photograph of *C. parvulus* Kieffer. We are also very grateful to subject editor Dr Norman Johnson and anonymous reviewers for their comments to improve the manuscript. This study was supported by the National Natural Science Foundation of China (31272351, U0936601) and The Natural History Museum, London (NHMUK).

References

Arias-Penna TM (2003) Lista de los géneros y especies de la superfamilia Proctotrupoidea (Hymenoptera) de la región Neotropical. Biota Colombiana 4: 3–32.

Gerlach J (Ed.) (2013) Hemiptera, Hymenoptera and other insect orders of the Seychelles Islands. Manchester: Siri Scientific Press, Manchester, 400 pp.

Johnson NF (1992) Catalog of World species of Proctotrupoidea, exclusive of Platygastridae (Hymenoptera). Memoirs of the American Entomological Institute 51: v+1–825.

Kieffer JJ (1912a) Hymenoptera, Proctotrupoidea. Transactions of the Linnean Society of London, 2nd series 15(1): 45–80. doi: 10.1111/j.1096-3642.1912.tb00089.x

Kieffer JJ (1912b) Hymenoptera fam. Diapriidae. In: Wytsman P (Ed.) Genera Insectorum 124, 75 pp.

Kieffer JJ (1916) Diapriidae. Das Tierreich. Vol. 44. Walter de Gruyter & Co., Berlin, 627 pp.

Madl M (2015) A catalogue of the families Ceraphronidae, Megaspilidae (Ceraphronoidea), Diapriidae (Diaprioidea) and Proctotrupidae (Proctotrupoidea) of the Malagasy subregion (Insecta: Hymenoptera). Linzer Biologische Beiträge 47: 621–652.

Masner L (1965) The types of Proctotrupoidea (Hymenoptera) in the British Museum (Natural History) and in the Hope Department of Entomology, Oxford. Bulletin of the British Museum (Natural History): Entomology. Supplement 1: 1–154.

Masner L, García Rodríguez JL (2002) The genera of Diapriinae (Hymenoptera: Diapriidae) in the New World. Bulletin of the American Museum of Natural History 268: 1–138. doi: 10.1206/0003-0090(2002)268<0001:TGODHD>2.0.CO;2

Muesebeck CFW, Walkley LM (1956) Type species of the genera and subgenera of parasitic wasps comprising the superfamily Proctotrupoidea (order Hymenoptera). Proceedings of the United States National Museum 105: 319–419. doi: 10.5479/si.00963801.3359.319

Nielsen M, Buffington ML (2011) Redescription of *Stentorceps* Quinlan, 1984 (Hymenoptera: Figitidae), with a description of five new species. African Entomology 19: 597–613. doi: 10.4001/003.019.0305

Notton DG (2014) A catalogue of the types of Diapriinae (Hymenoptera, Diapriidae) at the Natural History Museum, London. European Journal of Taxonomy 75: 1–123. doi: 10.5852/ejt.2014.75

Rajmohana K (2004) A key to Oriental genera of Diapriinae (Hymenoptera: Proctotrupoidea: Diapriidae). In: Rajmohana K, Narendran TC (Eds) Perspectives on biosystematics and biodiversity. Prof. T.C. Narendran Commemoration Volume. Systematic Entomology Research Scholars Association, University of Calicut, Kozhikode, India 38: 519–526.

Rajmohana K (2006) Studies on Proctotrupoidea and Platygastroidea (Hymenoptera: Insecta) of Kerala. Memoirs of the Zoological Survey of India 21(1): 1–153.

Rajmohana K, Bijoy C (2012) Checklist of Diapriidae and Proctotrupidae (Hymenoptera: Insecta) of India [Online]. Zoological Survey of India. http://zsi.gov.in/checklist/Diapriidae%20and%20Proctotrupidae_Hymenoptera%20Insecta.pdf [accessed 14 Jan. 2013]

Rajmohana K, Narendran TC (2000a) Two new genera of Diapriidae (Proctotrupoidea: Hymenoptera) from India. Uttar Pradesh Journal of Zoology 20: 21–28.

Rajmohana K, Narendran TC (2000b) Descriptions of a new genus *Nigropria* and a new species of *Aneuropria* Kieffer (Diapriidae: Proctotrupoidea: Hymenoptera) from India. Entomon 25: 193–200.

Rajmohana K, Poorani J, Shweta M, Malathi C (2013) A pictorial guide to Diapriinae genera of India. Web page. Zoological Survey of India, Calicut, Kerala & National Bureau of Agricultural Insect Resources. http://www.nbair.res.in/Diapriinae/index.php [accessed 16 February 2016]

ZooKeys 626: 67–86 (2016)
doi: 10.3897/zookeys.626.8155
http://zookeys.pensoft.net

RESEARCH ARTICLE

A peer-reviewed open-access journal
ZooKeys
Launched to accelerate biodiversity research

Genetic variability of two ecomorphological forms of *Stenus* Latreille, 1797 in Iran, with notes on the infrageneric classification of the genus (Coleoptera, Staphylinidae, Steninae)

Sayeh Serri[1], Johannes Frisch[2], Thomas von Rintelen[2]

1 *Insect Taxonomy Research Department, Iranian Research Institute of Plant Protection, Agricultural Research, Education and Extension Organization, Tehran, 19395-1454, Iran* **2** *Museum für Naturkunde Berlin, Leibniz-Institut für Evolutions- und Biodiversitätsforschung, Invalidenstrasse 43, D-10115 Berlin, Germany*

Corresponding author: *Sayeh Serri* (serri@iripp.ir; sserri_2000@yahoo.com)

Academic editor: *A. Brunke* | Received 17 February 2016 | Accepted 18 September 2016 | Published 20 October 2016

http://zoobank.org/A141DF2D-F1AC-406C-A342-E78E144803E0

Citation: Serri S, Frisch J, von Rintelen T (2016) Genetic variability of two ecomorphological forms of *Stenus* Latreille, 1797 in Iran, with notes on the infrageneric classification of the genus (Coleoptera, Staphylinidae, Steninae). ZooKeys 626: 67–86. doi: 10.3897/zookeys.626.8155

Abstract

In this study, the genetic diversity of Iranian populations of two widespread *Stenus* species representing two ecomorphological forms, the "open living species" *S. erythrocnemus* Eppelsheim, 1884 and the "stratobiont" *S. callidus* Baudi di Selve, 1848, is presented using data from a fragment of the mitochondrial COI gene. We evaluate the mitochondrial cytochrome oxidase I haplotypes and the intraspecific genetic distance of these two species. Our results reveal a very low diversity of COI sequences in *S. erythrocnemus* in contrast to *S. callidus*. Moreover, the COI based phylogeny of a selection of Iranian *Stenus* support the monophyly of some species groups of *Stenus* proposed by Puthz (2008) and contradicts the traditional infrageneric classification.

Keywords

Staphylinidae, *Stenus*, genetic variability, ecomorphological forms, infrageneric classification, Iran

Introduction

Fast mutation rate and lack of recombination as well as its easy amplification and sequencing make COI a useful marker for the study of phylogeny, geographic variation and population genetics as well as species identification (Hebert et al. 2003a, b; Qian et al. 2014: 11). Many studies have demonstrated that mtDNA-COI can be used for population genetics (e.g. Szalanski et al. 2010: 8). Hajibabaei et al. (2007: 171) point out that DNA barcoding offers significant implications for the understanding of the genetic diversity of species. Here, we apply this method in the rove beetle genus *Stenus* Latreille, 1797 to test the infraspecific genetic variation of representatives of two distinct ecomorphological forms and the validity of the traditional subgeneric concept of the genus.

Stenus is well-known for its unique prey-capture behavior (e.g. Betz 1996: 15–34). The eversible labium, an apomorphy, and the variability of the tarsal structures seem to be responsible for the enormous radiation in this genus (Betz 2002: 1097). The labial features are involved in catching prey in a sudden manner despite the limited reaction ability of the beetle (Betz 1999: 1708). The variable tarsal morphology among the members of this genus also has adaptive values which are in accord with their habitat preferences (Betz 2006: 413–414). With about 2674 species (Puthz, unpublished), *Stenus* is one of the species-richest genera of animals in the world (Puthz 2012: 286). The members of this rove beetle clade mostly dwell in humid places such as river banks, swamps, bogs and wet grasslands. The multifunctional secretion of the pygidial glands is species-specific and acts as a survival factor against predators. This character has been used in illuminating several evolutionary trends (Schierling et al. 2013: 48, 51) and presumably is a character adaptive to the habitat where the species live (Lang et al. 2015: 22).

In *Stenus*, two major ecomorphological forms can be distinguished, which Kastcheev and Puthz (2011: 454) termed "open-living species" with longer legs and on average bigger bodies (Figure 1), that live in habitats with less dense, often sparse vegetation such as sandy or clayey banks, and "stratobionts" with shorter legs and compact body (Figure 2), which inhabit dense vegetation structures and organic litter. Both forms are moreover distinguished by their dispersal ability, because - unlike the open-living species - there is the evolutionary tendency in stratobionts towards flightlessness. Similar morphological adaptations were already described for many rove-beetle clades such as the paederine subtribe Scopaeina Mulsant and Rey, 1878 (Frisch et al. 2002: 30). The addressed morphological characters determine the ability of the organism to colonize particular habitats and to use their resources (Betz 2006: 413). This relation between morphological features of species and ecological characteristics of habitats seems to be descriptive for niche selection. In Iran, 68 *Stenus* species were recorded (Serri and Frisch 2016: 18), among which *S. erythrocnemus* Eppelsheim, 1884 and *S. callidus* Baudi di Selve, 1848 are the most widespread across the country and were found in most provinces of Iran. According to Kastcheev and Puthz (2011: 454), *S. erythrocnemus* is an open-living species and *S. callidus* a stratobiont. Based on Iranian populations of these species, we tested the hypothesis that open-living species show a lower infraspecific genetic diversity than stratobionts owing to their higher dispersal ability.

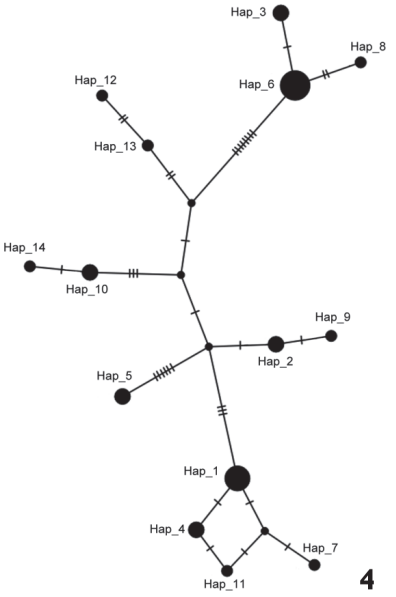

Figures 1–4. 1 *Stenus erythrocnemus* Eppelsheim, 1884. **2** *S. callidus* Baudi di Selve, 1848. **3** Haplotype network for cytochrome c oxidase subunit I (COI) DNA sequences of *S. erythrocnemus*. The circle size shows the frequency of the haplotypes. Each dashed line represents a single mutation. **4** Haplotype network for cytochrome c oxidase subunit I (COI) DNA sequences of *S. callidus*. The circle size shows the frequency of the haplotypes. Each dashed line represents a single mutation. Scale bars: 1mm.

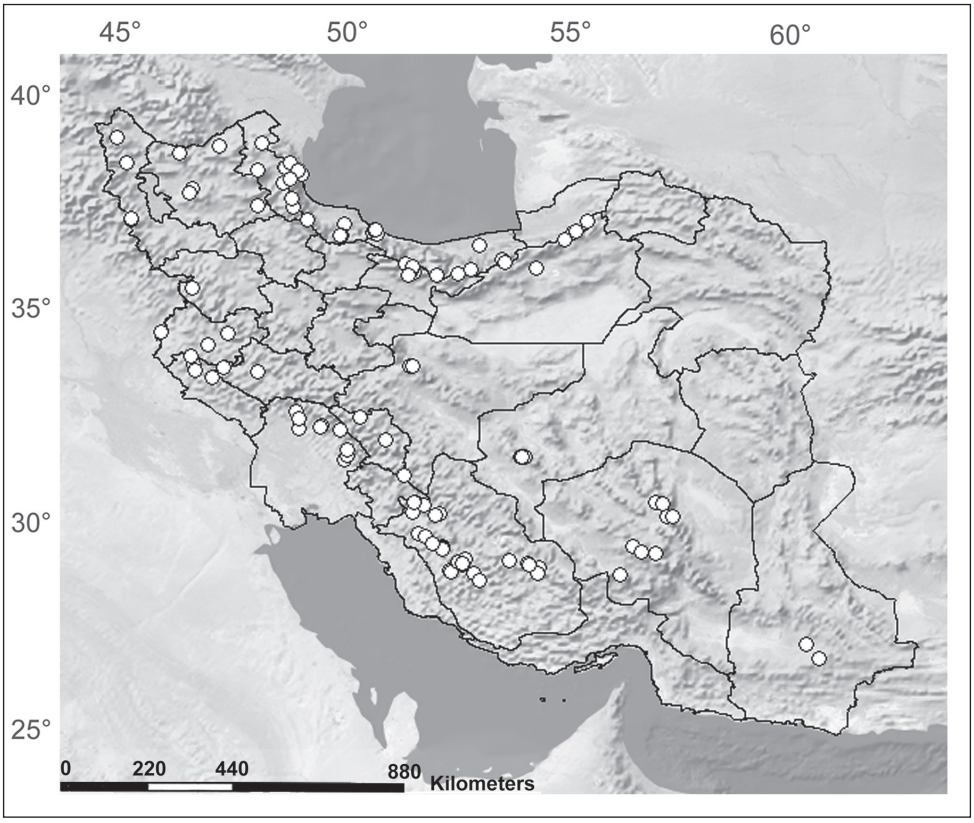

Figure 5. Distribution of *Stenus erythrocnemus* in Iran (after Serri and Frisch 2016: 28).

Stenus was traditionally divided into subgenera according to morphological characters. Based on European species only, Rey (1884: 31) introduced the six subgenera *Hemistenus*, *Hypostenus*, *Mesostenus*, *Nestus*, *Stenus*, and *Tesnus*. Later, Heyden (1905: 262) replaced *Mesostenus* with *Parastenus* because of a homonymy with a genus in the Hymenoptera. Ádám (1987: 135), however, synonymized *Parastenus* with the older name *Hemistenus* Motschulsky, 1860, because the type species of both subgenera are considered as subjective synonyms. Therefore he introduced the new subgenus *Metastenus* for a distinct species group of *Hemistenus* (Herman 2001: 2041), but later he (Ádám 2001: 126) replaced this name with *Metatesnus* because of primary homonymy with *Metastenus* Walker, 1834 in the Hymenoptera. According to Puthz (2009: 47), the genus group name *Adamostenus* Özdikmen & Darılmaz, 2008, an unnecessary replacement name for *Metatesnus*, is a junior synonym of *Metatesnus*. Puthz (2001: 35) also synonymized *Nestus* with *Stenus* s. str. based on the assumption that the tarsal characters traditionally employed for these subgenera do not define distinct monophyletic groups. In the current edition of the Catalogue of Palaearctic Coleoptera, Schülke and Smetana (2015: 802–847) still divided this genus into five subgenera, which are *Hemistenus* Motschulsky, 1860, *Hypostenus* Rey, 1884, *Stenus* Latreille, 1797,

Metatesnus Ádám, 2001 and *Tesnus* Rey, 1884. Puthz (2008: 139–148) conceived that the traditional subgeneric classification does not reflect the phylogenetic affinities within this genus and thus established 157 monophyletic species groups based on a wide range of presumed apomorphic morphological features of the species included. Ryvkin (2011: 59) argued, however, that it is better not to reject the traditional subgeneric concept prior to a comprehensive phylogenetic analysis of the subfamily. To date, there are only a few molecular studies that have investigated the phylogenetic relationships among Steninae species. The first was done recently by Koerner et al. (2013). Their results supported the monophyletic groups proposed by Puthz (2008: 139–148) and moreover revealed that some species groups of *Dianous* Leach, 1819, the second genus of the Steninae, actually constitute a monophyletic group within *Stenus*. The monophyly of some species groups proposed by Puthz (2008: 141–147) was also supported by Lang et al. (2015: 21). We performed a preliminary investigation on the intra- and interspecific genetic diversity of some Iranian *Stenus* to test the validity of the traditional classification of this genus by sequencing the "DNA Barcode" region of the mitochondrial COI gene of these species.

Material and methods

The *Stenus* specimens this study is based on were collected in the framework of the first author's research project on the diversity and biogeography of this genus in Iran (Serri and Frisch 2016), which was a part of a joint project between the Museum für Naturkunde Berlin and the Iranian Research Institute of Plant Protection on biodiversity and biogeography of selected insect taxa in Iran.

The specimens were collected in humid habitats such as river banks or grassland by hand collecting or sifting of gravelly soil, leaf litter and other phytodebris. Most specimens were killed with ethyl acetate, but some were directly fixated in 96% ethanol.

For DNA extraction, the abdomen of the larger species and the whole body of the smaller species were used and the DNA was purified by the CTAB method (Winnepenninckx et al. 1993). The polymerase chain reaction (PCR) was used to amplify a 5' end fragment of the mitochondrial cytochrome c oxidase subunit I (COI) gene using the primer pair LCO1490 5'-GGTCAACAAATCATAAAGATATTGG -3' and HCO2198 5'-TAAACTTCAGGGTGACCAAAAAATCA -3' (Folmer et al. 1994). PCR was performed in 25µl volumes including 2.5 µM PCR buffer, 1µM MgCl2, 0.5 µM dNTP, 1 µM of each forward and reverse primers, 1µM of Taq polymerase and ddH2O up to 25 µl total volumes. In the PCR thermocycles, there was an initial denaturation step at 94° for 1.5 min, followed by 6 cycles of 94° (for 30 s) denaturation, 45° (1.5 min) annealing and 72° (for 1 min) extension and subsequently 35 cycles of 94° (for 30 s) denaturation, 51° (1.5 min) annealing and 72° (for 1 min) extension. The PCR terminated at 72° (for 5 min) for final extension. The PCR products were purified on a silica membrane with Macherey and Nagel Nucleospin kits following the manufacturer's protocol. The purified PC products were sequenced using an ABI 3130 DNA

Table 1. The specimens used in this study with their location data and the GenBank association number of submitted sequences of COI. The specimen number codes the geographical origin of the specimens in the phylogenetic tree (Figures 7, 8).

Species	Specimen number	Collection site	GeneBank association number
Stenus alienigenus	147	**Kordestan:** 11 km E Sanandaj (35°20'11"N 47°09'07"E), 2100 m, 5.9.2008, leg. Serri and Frisch	KU754268
S. araxis	118	**Ardabil:** N Mt Sabalan, Gheynarjeh (38°17'18"N 47°41'22"E), 2100 m, 24.6.2008, leg. Serri	KU754251
S. araxis	121, 122	**Esfahan:** Kashan, NW Niasar, after Aznaveh (34°06'28.8"N 50°59'45.9"E), 2195 m, 19.5.2009, leg. Serri and Nasserzadeh	KU754253 KU754254
S. araxis	117	**Hamedan:** W Kabudarahang, 5 km E Goltappeh (35°12'06"N 48°14'04"E), 2210 m, 21.7.2008, leg. Serri and Nasserzadeh	KU754250
S. araxis	114	**Kordestan:** Saghez - Baneh, 27 km SW Saghez (36°08'12"N 46°02'42"E), 1600 m, 3.9.2008, leg. Serri and Frisch	KU754247
S. araxis	111	**West Azarbaijan**: W Salmas, 19 km W Kuzerash (38°11'40"N 44°33'04"E), 1960 m, 31.8.2008, leg. Serri and Frisch	KU754246
S. araxis	110	**West Azarbaijan:** Orumieh, S Silvaneh, 14 km S Ziveh (37°09'06"N 44°52'55"E), 2320 m, 1.9.2008, leg. Serri and Frisch	KU754245
S.* cf. *araxis	120	**Esfahan:** Natanz, S Karkas Mts, Taragh (33°24'39"N 51°46'14"E), 2580 m, 20.5.2009, leg. Serri	KU754252
S.* cf. *araxis	125	**Esfahan:** S Abyaneh, Bidhand (33°29'44"N 51°45'39"E), 2350 m, 18.5.2009, leg. Serri	KU754256
S.* cf. *araxis*, *S. araxis	115, 116	**Tehran**: Firouzkuh, Badroud (35°48'15"N 52°39'21"E), 2060 m, 5.8.2009, leg. Serri and Nasserzadeh	KU754248 KU754249
S. ater	136	**Semnan:** NE Chashm, Hikuh, Sheil, Parvar Protected Region (36°0'54"N 53°23'07"E), 1900 m, 7.8.2009, leg. Serri and Nasserzadeh	KU754264
S. brunnipes	151	**Mazandaran:** Sari, N Mohammadabad (36°10'09"N 53°14'08"E), 820 m, 30.5.2008, leg. Serri, Nasserzadeh and Pütz	KU754270
S. callidus	089	**Chaharmahal & Bakhtiari**: Ardel, Ghahrou, Tang-e Zeverdegan (31°59'10"N 50°51'23"E), 2350 m, 23.6.2009, leg. Serri	KU754233
S. callidus	090	**Esfahan:** Chadegan, W Zayandehrud Dam (32°43'08"N 50°44'20"E), 2070 m, 20.6.2009, leg. Serri	KU754234
S. callidus	094	**Esfahan:** Kashan, S Ghamsar, Ghazaan (33°42'20"N 51°23'48"E), 2220 m, 17.5.2009, leg. Serri	KU754236
S. callidus	045, 046	**Ghazvin:** 5 km E Abgarm (35°47'53"N 49°22'43"E), 1510 m, 21.6.2004, leg. Serri and Frisch	KU754199 KU754200
S. callidus	092	**Hamedan:** Eberou road, S Emamzadeh Abdollah (34°39'20"N 48°32'19"E), 2510 m, 22.7.2008, leg. Serri and Nasserzadeh	KU754235
S. callidus	103	**Hamedan:** Shahrestaneh (34°42'56"N 48°22'21"E), 2220 m, 23.7.2008, leg. Serri and Nasserzadeh	KU754240
S. callidus	031, 033	**Hormozgan:** Siahu, Talgerdo road, Bangolan (27°50'03"N 56°28'27"E), 890 m, 19.4.2006, leg. Serri and Frisch	KU754193 KU754194
S. callidus	034	**Kerman:** Baft, 6 km N Rabor (29°20'28"N 56°50'47"E), 2640 m, 4.5.2007, leg. Serri and Frisch	KU754195
S. callidus	084	**Khuzestan:** Baghmalek, Chamkureh (31°31'42"N 49°51'55"E), 670 m, 27-28.4.2009, leg Serri	KU754231

Species	Specimen number	Collection site	GeneBank association number
S. callidus	079–082, 085, 086	**Kordestan:**11 km E Sanandaj (35°20'11"N 47°09'07"E), 2100 m, 5.9.2008, leg. Serri and Frisch	KU754224 KU754225 KU754226 KU754227 KU754230 KU754231
S. callidus	087	**Kordestan:** 7 km S Ghorveh, Veihaj (35°06'34"N 47°45'54"E), 2060 m, 5.9.2008, leg. Serri and Frisch	KU754232
S. callidus	098, 099	**Kordestan:** Saghez - Baneh, 27 km SW Saghez (36°08'12"N 46°02'42"E), 1600 m, 3.9.2008, leg. Serri and Frisch	KU754237 KU754238
S. callidus	035, 036	**Tehran:** Firouzkuh road, Delichai (35°40'58"N 52°28'26"E), 2000 m, 21.5.2006, leg. Serri and Frisch	KU754196 KU754197
S. callidus	105–108	**Tehran**: Firouzkuh, Badroud (35°48'15"N 52°39'21"E), 2060 m, 5.8.2009, leg. Serri and Nasserzadeh	KU754241 KU754242 KU754243 KU754244
S. callidus	100	**West Azarbaijan:** 11 km E Takht-e Soleiman (36°36'43"N 47°18'48"E), 2280 m, 7.-8.9.2008, leg. Serri and Frisch	KU754239
S. callidus	083	**West Azarbaijan:** 2 km E Takht-e Soleiman N (36°38'05"N 47°14'07"E), 2270 m, 7.-8.9.2008, leg. Serri and Frisch	KU754228
S. callidus	037	**Zanjan:** Abbar - Gilvan (36°52'50"N 48°58'32"E), 430 m, 12.7.2006, leg. Serri	KU754198
S. cautus	146	**Esfahan:** S Abyaneh, Bidhand (33°29'44"N 51°45'39"E), 2350 m, 18.5.2009, leg. Serri	KU754267
S. erythrocnemus	059, 060, 062	**Ardabil:** N Mt Sabalan, Gheynarjeh (38°17'18"N 47°41'22"E), 2100 m, 24.6.2008, leg. Serri	KU754213 KU754214 KU754215
S. erythrocnemus	024	**East Azarbaijan:** Zijenab (Mt Sahand) (37°52'08"N 46°18'46"E), 2150 m, 8.8.2005, leg. Serri and Frisch	KU754192
S. erythrocnemus	134	**Esfahan:** Natanz, Taragh, Keshe, S Mt. Karkas (33°24'39.3"N 51°46'13.9"E), 2580 m, 17.5.2009, leg. Serri	KU754262
S. erythrocnemus	070	**Gilan:** E Masuleh (37°09'48"N 49°00'19"E), 820 m, 8.6.2008, leg. Serri, Nasserzadeh and Pütz	KU754219
S. erythrocnemus	009	**Kerman:** Mahan road, 3 km S pass (30°11'29"N 57°25'42"E), 2430 m, 30.4.2007, leg. Serri and Frisch	KU754189
S. erythrocnemus	051–054	**Tehran**: Dizin (36°01'53"N 51°28'52"E), 2810 m, 10.6.2008, leg. Serri, Nasserzadeh and Pütz	KU754205 KU754206 KU754207 KU754208
S. erythrocnemus	047–050	**West Azarbaijan:** SE Makou, Gharakelisa (39°05'32"N 44°32'40"E), 1860 m, 28.8.2008, leg. Serri and Frisch	KU754201 KU754202 KU754203 KU754204
S. erythrocnemus	055–058	**West Azarbaijan:** Orumieh, S Silvaneh, 14 km S Ziveh (37°09'06"N 44°52'55"E), 2320 m, 1.9.2008, leg. Serri and Frisch	KU754209 KU754210 KU754211 KU754212
S. erythrocnemus	064	**West Azarbaijan:** 18 km W Khoy, Ghotour road (38°28'45"N 44°47'08"E), 1320 m, 29.8.2008, leg. Serri and Frisch	KU754216

Species	Specimen number	Collection site	GeneBank association number
S. erythrocnemus	068, 069	**West Azarbaijan:** Siahcheshmeh - Khoy, Kordkandy (N 38°55'02" E44°27'40"), 1870 m, 28.8.2008, leg. Serri and Frisch	KU754217 KU754218
S. erythrocnemus	071–074	**West Azarbaijan:** Siahcheshmeh - Khoy, W Zarabad (N 38°44'16" E44°28'10"), 2400 m, 30.8.2008, leg. Serri and Frisch	KU754220 KU754221 KU754222 KU754223
S. erythrocnemus	011, 012	**Yazd:** Taft, Dehbala (31°35'37"N 54°07'20"E), 2550 m, 15.5.2007, leg. Serri and Frisch	KU754190 KU754191
S. fuscicornis	156	**Mazandaran:** Ramsar, Javaherdeh road, Eshkatechal (36°50'32"N 50°34'39"E), 1450 m, 6.6.2008, leg. Serri, Nasserzadeh and Pütz	KU754272
S. ganglbaueri	153	**Mazandaran:** Baladeh, Nesen, E pass (36°14'37"N 51°27'17"E), 2960 m, 1.6.2008, leg. Serri, Nasserzadeh and Pütz	KU754271
S. hypoproditor	137	**Kordestan:** N Divandarreh, SW Zarrineh, 5 km NW Ebrahimabad (35°59'10"N 46°52'11"E), 1960 m, 4.9.2008, leg. Serri and Frisch	KU754265
S. intricatus zoufali	135	**East Azarbaijan:** Tabriz - Marand, 9 km N Amand (38°17'18"N 46°08'46"E), 1520 m, 26.8.2008, leg. Serri and Frisch	KU754263
S. maculiger	133	**West Azarbaijan:** W Salmas, 10 km W Kuzerash (38°11'40"N 44°33'04"E), 1960 m, 31.8.2008, leg. Serri and Frisch	KU754261
S. martensi	166	**Mazandaran:** Kelardasht- Marzanabad road, (36°35'39"N 51°08'37"E), 1000 m, 3.6.2008, leg. Serri, Nasserzadeh and Pütz	KU754279
S. medus	161	**Mazandaran:** Rineh, S Mt Damavand (35°53'56"N 52°06'29"E), 2960 m, 3.8.2009, leg Serri and Nasserzadeh	KU754276
S. mongolicus	138	**Semnan:** Shahroud, NE Mojem, Tash (36°31'N 54°42'E), 10.8.2009, leg. Serri and Nasserzadeh	KU754266
S. ochropus	159	**Fars:** SE Sepidan, Dalkhon (30°14'40"N 52°06'09"E), 2090 m, 9.5.2007, leg. Serri and Frisch	KU754275
S. persicus	163	**Kordestan:** Saghez - Baneh, 27 km SW Saghez (36°08'12"N 46°02'42"E), 1600 m, 3.9.2008, leg. Serri and Frisch	KU754277
S. pieperi	157	**Mazandaran:** S Salmanshahr (36°38'49"N 51°10'27"E), 280 m, 4.6.2008, leg. Serri, Nasserzadeh and Pütz	KU754273
S. ressli	158	**Mazandaran:** Tonekabon, Sehezar Forest (36°32'36"N 50°49'53"E), 1090 m, 5.6.2008, leg. Serri, Nasserzadeh and Pütz	KU754274
S. schah	164	**Kohgiluye & Boyerahmad**: N Yasuj, Sepidar, Dilgan River (30°45'03"N 51°08'07"E), 2270 m, 18.6.2009, leg. Serri	KU754278
S. turk	124	**Esfahan:** S Abyaneh, Bidhand (33°29'44"N 51°45'39"E), 2350 m, 18.5.2009, leg. Serri	KU754255
S. turk	126–129	**Golestan:** NE Kalaleh, Zav, Totlitamak village (37°29'36"N 55°46'25"E), 1240 m, , 16.10.2009, leg. Serri	KU754257 KU754258 KU754259 KU754260
S. viti	148	**Mazandaran:** Kelardasht - Marzanabad (36°35'40"N 51°08'37"E), 1000 m, 3.6.2008, leg. Serri, Nasserzadeh and Pütz	KU754269

sequencer. All sequences were aligned manually and corrected for misreads using Bioedit version 7.0.5.3 (Hall 1999). Additional mitochondrial COI GenBank sequences of *Euaesthetus ruficapillus* (Lacordaire, 1835) and *E. superlatus* Peyerimhoff, 1937 were included in the dataset (GenBank accession numbers KM447120 and KM451370) as

outgroup taxa. A Maximum Parsimony Analysis was conducted with PAUP*4.0 b10 (Swofford 2002). The dataset was also analyzed in MEGA 6 (Tamura et al. 2013) with maximum likelihood using the Tamura-Nei model with uniform rates among sites. The mean *p*-distance within each species of *Stenus callidus* and *S. erythrocnemus* were calculated separately using the Kimura2-parameter model (Kimura 1980) in MEGA 6. The haplotype data files of the populations of each species and the polymorphisms indices were obtained in DnaSP 5.10 (Librado and Rozas 2009) and the nexus files were transferred to PopART version 1.7 (Leigh and Bryant 2015) in order to construct a haplotype network based on the TCS algorithm (Clement et al. 2002).

Results

The PCR amplification using LCO1490/HCO2198 primers yielded a product with a maximum length of 658 bp (excluding primers) from 91 individuals of 23 species out of a total of 157 specimens of 37 species of Iranian *Stenus*. The alignment was blasted against GenBank sequences and found to match with existing records of *Stenus*. The base composition of about 29% A, 39% T, 16% C and 16% G exhibits the common AT bias of COI.

The alignment (total of 658 bp) contained 294 variable characters, of which 246 were parsimony informative and contributed to the Maximum Parsimony (MP) Analysis. The MP Analyses produced two equally parsimonious trees with a tree length of 1197 steps, CI of 0.3768, RI of 0.8564 and RC of 0.3227 (Figure 7). Node support was estimated by bootstrap using 1000 pseudoreplicates and 100 replicates. The major clades are generally well supported (see below). All obtained sequences were submitted to GenBank (accession numbers in Table 1). The maximum likelihood tree was constructed by the heuristic search with the Nearest-Neighbor-Interchange (NNI) method, gaps treatment using all sites, the neighbor-joining (NJ) tree as the initial tree and bootstrapped with 1000 replications (Figure 8). The topology obtained from ML analyses does not deviate significantly from the MP tree. Both methods reveal a high degree of genetic homogeny among different populations of *Stenus erythrocnemus* and more pronounced heterogeny in *S. callidus*. The selected populations of *S. callidus* cluster in seven groups, but these groupings do not correspond well to the geographic distribution of the examined populations and some are not well supported in the bootstrap analysis. There are, however, some populations that form separate geographical clusters such as the populations from Kerman (specimen no. 034) with those of the Ghohrud Mountains (specimen no. 094) and the populations from Tehran Province (specimens no. 105, 107). These apparent geographical clusters are, however, not significant, because they are made up of only two populations from the same region (Figure 9). Surprisingly, the populations of *S. callidus* from Kordestan Province show a low similarity of the COI gene and appear in different clades of the cladogram (Figures 7, 8).

The haplotype networks for COI of *S. callidus* and *S. erythrocnemus* (Figures 3, 4) comprise fourteen and four haplotypes, respectively. Haplotype diversity (h) was estimated at 0.911±0.034 for *S. callidus* and 0.267±0.107 for *S. erythrocnemus*. The nucleotide diversity (π i) of each species was calculated as 0.01348±0.00074 for *S. callidus* and 0.00045±0.00019

Table 2. Kimura two-parameter pairwise genetic distances between populations of *Stenus callidus*.

	031	033	034	035	036	037	045	046	079	080	081	082	083	084	085	086	087	089	090	092	094	098	099	100	103	105	106	107	108
031																													
033	0.000																												
034	0.006	0.006																											
035	0.022	0.022	0.022																										
036	0.022	0.022	0.022	0.000																									
037	0.000	0.000	0.006	0.022	0.022																								
045	0.002	0.002	0.008	0.023	0.023	0.002																							
046	0.002	0.002	0.008	0.023	0.023	0.002	0.000																						
079	0.012	0.012	0.011	0.028	0.028	0.012	0.014	0.014																					
080	0.020	0.020	0.020	0.002	0.002	0.020	0.022	0.022	0.026																				
081	0.006	0.006	0.000	0.022	0.022	0.006	0.008	0.008	0.011	0.020																			
082	0.012	0.012	0.011	0.028	0.028	0.012	0.014	0.014	0.000	0.026	0.011																		
083	0.020	0.020	0.020	0.002	0.002	0.020	0.022	0.022	0.026	0.000	0.020	0.026																	
084	0.020	0.020	0.020	0.002	0.002	0.020	0.022	0.022	0.026	0.000	0.020	0.026	0.000																
085	0.000	0.000	0.006	0.022	0.022	0.000	0.002	0.002	0.012	0.020	0.006	0.012	0.020	0.020															
086	0.000	0.000	0.006	0.022	0.022	0.000	0.002	0.002	0.012	0.020	0.006	0.012	0.020	0.020	0.000														
087	0.003	0.003	0.009	0.022	0.022	0.003	0.005	0.005	0.015	0.020	0.009	0.015	0.020	0.020	0.003	0.003													
089	0.020	0.020	0.020	0.002	0.002	0.020	0.022	0.022	0.026	0.000	0.020	0.026	0.000	0.000	0.020	0.020	0.020												
090	0.020	0.020	0.020	0.002	0.002	0.020	0.022	0.022	0.026	0.000	0.020	0.026	0.000	0.000	0.020	0.020	0.020	0.000											
092	0.023	0.023	0.023	0.005	0.005	0.023	0.025	0.025	0.030	0.003	0.023	0.030	0.003	0.003	0.023	0.023	0.023	0.003	0.003										
094	0.008	0.008	0.002	0.023	0.023	0.008	0.009	0.009	0.012	0.022	0.002	0.012	0.022	0.022	0.008	0.008	0.011	0.022	0.022	0.022									
098	0.011	0.011	0.008	0.020	0.020	0.011	0.012	0.012	0.014	0.019	0.008	0.014	0.019	0.019	0.011	0.011	0.014	0.019	0.019	0.022	0.009								
099	0.003	0.003	0.009	0.022	0.022	0.003	0.002	0.002	0.015	0.020	0.009	0.015	0.020	0.020	0.003	0.003	0.003	0.020	0.020	0.023	0.011	0.014							
100	0.020	0.020	0.020	0.002	0.002	0.020	0.022	0.022	0.026	0.000	0.020	0.026	0.000	0.000	0.020	0.020	0.020	0.000	0.000	0.003	0.022	0.019	0.020						
103	0.020	0.020	0.020	0.002	0.002	0.020	0.022	0.022	0.026	0.000	0.020	0.026	0.000	0.000	0.020	0.020	0.020	0.000	0.000	0.003	0.022	0.019	0.020	0.000					
105	0.014	0.014	0.011	0.020	0.020	0.014	0.015	0.015	0.017	0.019	0.011	0.017	0.019	0.019	0.014	0.014	0.014	0.019	0.019	0.022	0.012	0.012	0.014	0.019	0.019				
106	0.011	0.011	0.008	0.020	0.020	0.011	0.012	0.012	0.014	0.019	0.008	0.014	0.019	0.019	0.011	0.011	0.014	0.019	0.019	0.022	0.009	0.000	0.014	0.019	0.019	0.012			
107	0.011	0.011	0.008	0.017	0.017	0.011	0.012	0.012	0.014	0.015	0.008	0.014	0.015	0.015	0.011	0.011	0.011	0.015	0.015	0.019	0.009	0.009	0.011	0.015	0.015	0.003	0.009		
108	0.012	0.012	0.009	0.022	0.022	0.012	0.014	0.014	0.015	0.020	0.009	0.015	0.020	0.020	0.012	0.012	0.015	0.020	0.020	0.023	0.011	0.002	0.015	0.020	0.020	0.014	0.002	0.011	

Table 3. Kimura two-parameter pairwise genetic distances between populations of *Stenus erythrocnemus*.

	009	**011**	**012**	**024**	**047**	**048**	**049**	**050**	**051**	**052**	**053**	**054**	**055**	**056**	**057**	**058**	**059**	**060**	**062**	**064**	**068**	**069**	**070**	**071**	**072**	**073**	**074**	**134**
009																												
011	0.000																											
012	0.000	0.000																										
024	0.002	0.002	0.002																									
047	0.000	0.000	0.000	0.002																								
048	0.000	0.000	0.000	0.002	0.000																							
049	0.002	0.002	0.002	0.003	0.002	0.002																						
050	0.000	0.000	0.000	0.002	0.000	0.000	0.002																					
051	0.000	0.000	0.000	0.002	0.000	0.000	0.002	0.000																				
052	0.000	0.000	0.000	0.002	0.000	0.000	0.002	0.000	0.000																			
053	0.000	0.000	0.000	0.002	0.000	0.000	0.002	0.000	0.000	0.000																		
054	0.000	0.000	0.000	0.002	0.000	0.000	0.002	0.000	0.000	0.000	0.000																	
055	0.000	0.000	0.000	0.002	0.000	0.000	0.002	0.000	0.000	0.000	0.000	0.000																
056	0.000	0.000	0.000	0.002	0.000	0.000	0.002	0.000	0.000	0.000	0.000	0.000	0.000															
057	0.000	0.000	0.000	0.002	0.000	0.000	0.002	0.000	0.000	0.000	0.000	0.000	0.000	0.000														
058	0.000	0.000	0.000	0.002	0.000	0.000	0.002	0.000	0.000	0.000	0.000	0.000	0.000	0.000	0.000													
059	0.000	0.000	0.000	0.002	0.000	0.000	0.002	0.000	0.000	0.000	0.000	0.000	0.000	0.000	0.000	0.000												
060	0.002	0.002	0.002	0.003	0.002	0.002	0.003	0.002	0.002	0.002	0.002	0.002	0.002	0.002	0.002	0.002	0.002											
062	0.002	0.002	0.002	0.003	0.002	0.002	0.000	0.002	0.002	0.002	0.002	0.002	0.002	0.002	0.002	0.002	0.002	0.003										
064	0.000	0.000	0.000	0.002	0.000	0.000	0.002	0.000	0.000	0.000	0.000	0.000	0.000	0.000	0.000	0.000	0.000	0.002	0.002									
068	0.000	0.000	0.000	0.002	0.000	0.000	0.002	0.000	0.000	0.000	0.000	0.000	0.000	0.000	0.000	0.000	0.000	0.002	0.002	0.000								
069	0.000	0.000	0.000	0.002	0.000	0.000	0.002	0.000	0.000	0.000	0.000	0.000	0.000	0.000	0.000	0.000	0.000	0.002	0.002	0.000	0.000							
070	0.000	0.000	0.000	0.002	0.000	0.000	0.002	0.000	0.000	0.000	0.000	0.000	0.000	0.000	0.000	0.000	0.000	0.002	0.002	0.000	0.000	0.000						
071	0.000	0.000	0.000	0.002	0.000	0.000	0.002	0.000	0.000	0.000	0.000	0.000	0.000	0.000	0.000	0.000	0.000	0.002	0.002	0.000	0.000	0.000	0.000					
072	0.000	0.000	0.000	0.002	0.000	0.000	0.002	0.000	0.000	0.000	0.000	0.000	0.000	0.000	0.000	0.000	0.000	0.002	0.002	0.000	0.000	0.000	0.000	0.000				
073	0.000	0.000	0.000	0.002	0.000	0.000	0.002	0.000	0.000	0.000	0.000	0.000	0.000	0.000	0.000	0.000	0.000	0.002	0.002	0.000	0.000	0.000	0.000	0.000	0.000			
074	0.000	0.000	0.000	0.002	0.000	0.000	0.002	0.000	0.000	0.000	0.000	0.000	0.000	0.000	0.000	0.000	0.000	0.002	0.002	0.000	0.000	0.000	0.000	0.000	0.000	0.000		
134	0.000	0.000	0.000	0.002	0.000	0.000	0.002	0.000	0.000	0.000	0.000	0.000	0.000	0.000	0.000	0.000	0.000	0.002	0.002	0.000	0.000	0.000	0.000	0.000	0.000	0.000	0.000	

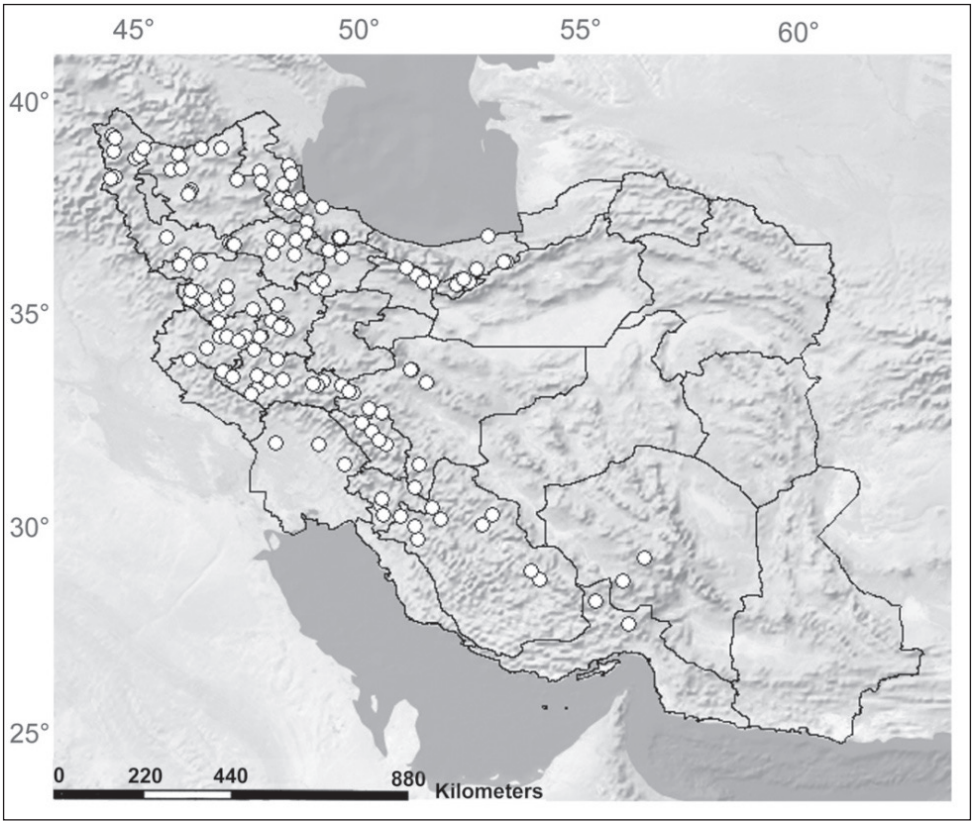

Figure 6. Distribution of *Stenus callidus* in Iran (after Serri and Frisch 2016: 28).

for *S. erythrocnemus* (Table 4). In *S. callidus*, no haplotype has an outstandingly high frequency, while *S. erythrocnemus* has a dominant haplotype (Hap_1) found in populations of the Elburz and Zagros Mountains and the central mountain ranges.

The maximum genetic distance among populations does not exceed 0.003% in *S. erythrocnemus* and is much higher in *S. callidus* with 0.028% (Tables 2, 3). The highest genetic distance as well as the highest haplotype diversity in the populations of *S. callidus* was observed in the central zone of the Zagros Mountains. In *S. erythrocnemus*, the highest genetic distance is among the populations of northwestern Iran.

Regarding the subgeneric concept of *Stenus*, our results (Figures 7, 8) do not support the traditional grouping except for *Hemistenus*, the selected species of which appear in the same clade. Our results rather support the monophyly of those species groups of Puthz (2008: 139–148), which we tested with at least two representatives. These species groups and the included species are: *S. guttula* group with *S. erythrocnemus* and *S. maculiger*, *S. cordatus* group with *S. araxis* and *S. turk*, *S. glacialis* group with *S. medus*, *S. persicus* and *S. schah*, *S. ochropus-ludyi-coarcticollis* group with *S. martensi*, *S. ochropus*, *S. pieperi* and *S. ressli*, *S. ater* group with *S. ater*, *S. hypoproditor* and *S. intricatus zoufali*.

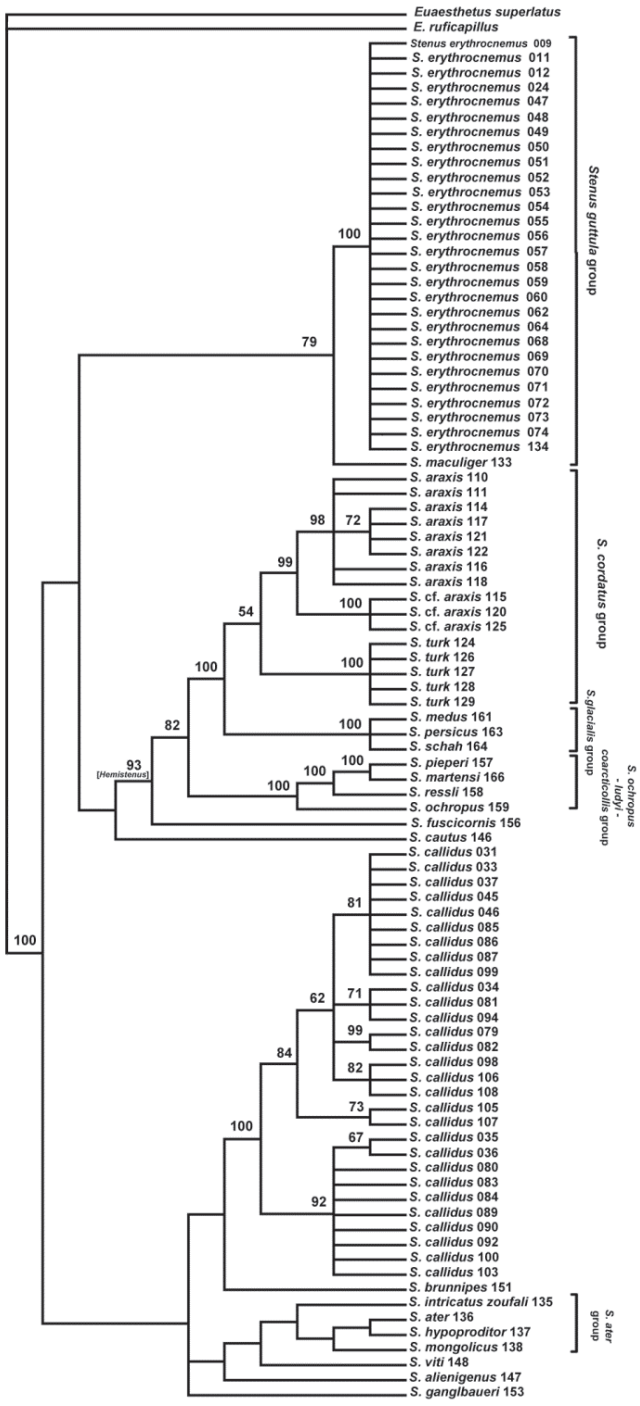

Figure 7. Strict consensus of most-parsimonious trees. Values above the branches indicate clade bootstrap support (>50) using 1000 replicates. The geographical origin of the specimens is coded by numbers behind the species name which correspond to the geographical information in Table 1.

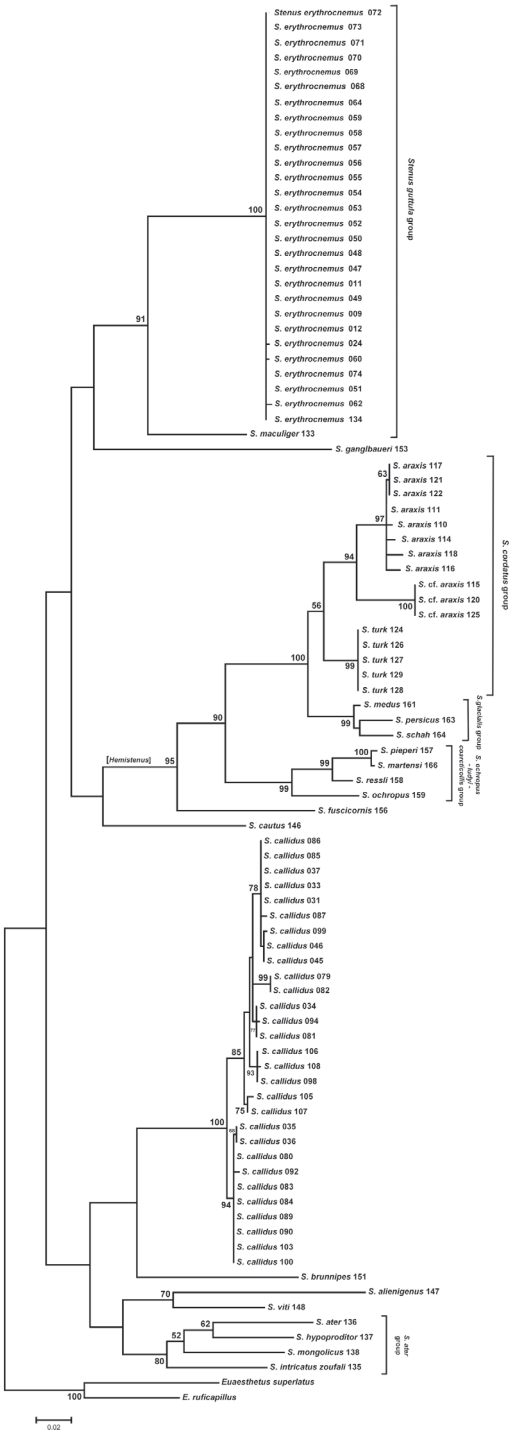

Figure 8. Maximum likelihood phylogram. Numbers on branches are bootstrap values (>50). The specimen codes correspond to the geographical information in Table 1. Scale shows number of substitutions per site.

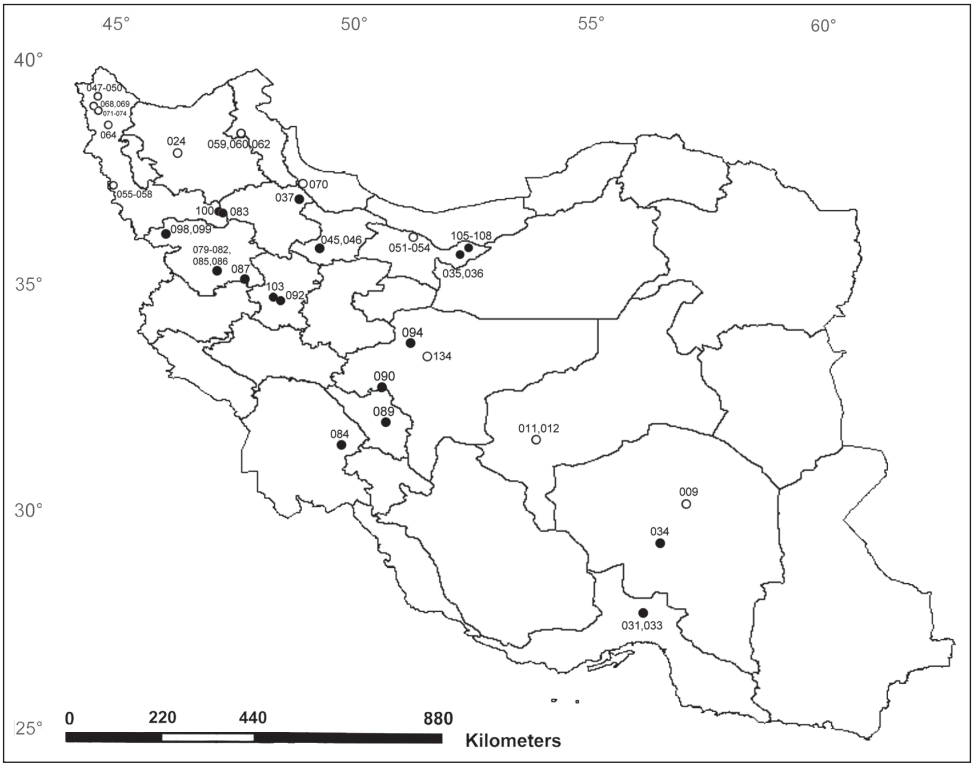

Figure 9. Distribution map of sequenced specimens of *Stenus callidus* (●) and *S. erythrocnemus* (○). Numbers are haplotype numbers (see Table 4). Sites with more than one haplotype number indicate several geographically close localities.

Discussion

With the example of Iranian populations of the open-living *Stenus erythrocnemus* and the stratobiont *S. callidus*, we demonstrate that different ecomorphological forms of congeneric species with differing dispersal ability and degree of geneflow can show a different degree of infraspecific genetic variability.

The open-living *S. erythrocnemus* is the most widespread *Stenus* in Iran. It was found in most of the country in high abundance at elevations between 250 m and 2800 m a.s. l. (Figure 5, after Serri and Frisch 2016: 27). As an example of the open-living ecomorphological form described by Kastcheev and Puthz (2011: 454), this mobile species does not show geographically structured populations. The low level of haplotype diversity as well as the low intraspecific distance of this species indicate a high level of gene flow between the populations of this species, which are connected to each other even across zoogeographic barriers due to the species' dispersal ability. This gene flow within the Iranian meta-population of *S. erythrocnemus* is probably supported by the wide ecological adaptability, which prevents geographic isolation. Unlike the remainder of Iranian *Stenus*, we repeatedly collected *S. erythrocnemus* not only

Table 4. Summary of genetic diversity indices in the mitochondrial COI gene segment of *Stenus callidus* and *S. erythrocnemus*.

Species	N	L	k	H	h (±standard deviation)	π (±standard deviation)	Haplotype no.: sequence(s) no.
Stenus callidus	29	658	30	14	0.911±0.034	0.01348±0.00074	Hap_1: 031, 033, 037, 085, 086 Hap_2: 034, 081 Hap_3: 035, 036 Hap_4: 045, 046 Hap_5: 079, 082 Hap_6: 080, 083, 084, 089, 090,100, 103 Hap_7: 087 Hap_8: 092 Hap_9: 094 Hap_10: 098,106 Hap_11: 099 Hap_12: 105 Hap_13: 107 Hap_14: 108
S. erythrocnemus	28	658	3	4	0.267±0.107	0.00045±0.00019	Hap_1: 009, 011, 012, 047, 048, 050, 051, 052, 053, 054, 055, 056, 057, 058, 059, 064, 068, 069, 070, 071, 072, 073, 074, 134 Hap_2: 024 Hap_3: 049, 062 Hap_4: 060

Abbreviations: N, number of sequences; L, sequence length (number of bases); k, number of variable sites; H, number of haplotypes; h, haplotype diversity; π, nucleotide diversity.

in natural habitats, but also in polluted sites and anthropogenic places such as watering channels of farms far from natural, permanent watercourses.

The stratobiont *S. callidus*, the second widespread *Stenus* in Iran, was collected in high abundance in most of the collecting sites all over the country (Figure 6, after Serri and Frisch 2016: 27). Our cladogram shows the separation of the tested *S. callidus* populations into six genetic units, which can be explained by the limited dispersal ability of the mostly micropterous individuals of *S. callidus*. The genetic variability of *S. callidus*, as shown by the higher genetic distance among populations and more diverse haplotypes, might moreover be increased by discontinuity of suitable habitats caused by man-made destruction, because – in contrast to *S. erythrocnemus* – the species usually avoids strongly disturbed sites.

Though our COI examination of a limited number of West Palaearctic species of *Stenus* is not extensive when it comes to understanding the supraspecific phylogeny of the entire clade, it clearly shows the monophyly of the included *Hemistenus* species and the polyphyletic relationship among the investigated members of subgenus *Stenus*. The relationships of *Tesnus* and *Metatesnus* with other species were not resolved, because we were able to extract DNA from only one species of each of these subgenera. The monophyly of the selected *Hemistenus* species is, however, consistent with the result of the analysis performed by Koerner et al. (2013: 340).

Our results, which agree with those of Koerner et al. (2013: 345) and Lang et al. (2015: 20–21), further support the monophyly of the tested infrageneric species groups proposed by Puthz (2008: 139–148). On one hand, this result is not very significant, as only few species of some of these groupings were included in this study. On the other hand, our results clearly contradict the traditional subgeneric concept, which is followed until today, and proves the morphological characters this erroneous concept is based on to be phylogenetically uninformative convergencies. The included members of one of these traditional subgenera, *Hemistenus*, constitute, however, one well supported clade (bootstrap value >90) comprising the *S. cordatus* group, the *S. glacialis* group and the *S. ochropus-ludyi-coarcticollis* group. Particularly the first two species groups are closely related sister groups (bootstrap value 100). Further investigations are necessary to show whether *Hemistenus* – unlike the other traditional subgenera - actually represents a monophyletic group or not.

Our results support the supraspecific phylogenetic concept of Puthz (2008: 139–148) and at the same time largely contradict the traditional subgenera. Therefore, these subgenera should not be used anymore in favour of the informal species groups, though the monophyly of some of them still has to be proved.

Among the collected specimens of *S. araxis*, there are specimens which show differences in the structure of the median lobe of the aedeagus and in the spermatheca. The cladogram shows that these specimens form a separate clade although they have no geographic separation. Both morphological and genetic examination of a broader basis of specimens is necessary to clarify whether this form should be considered as a distinct species.

Since we did not succeed in extracting DNA from a large number of the recently collected species or from the Iranian material in Scheerpeltz solution collected by Senglet, it was not possible to include all Iranian species into the analysis. Moreover, the paucity of fresh specimens of many rare species did not allow us to use genetic data of these species in our phylogenetic analysis. Nevertheless, this preliminary study provides benchmark data for future phylogenetic investigations that include a higher number of taxa at a wider geographic scale and additional genes. Our current analysis based on a COI fragment suggests that the 'barcoding fragment' studied here can also be used for testing the phylogenetic validity of supraspecific groups.

Acknowledgements

We thank Matthias Glaubrecht, Hamburg (formerly Museum für Naturkunde Berlin), for giving the first author the opportunity to work in the lab of the museum. Björn Stelbrink, Gießen (formerly Museum für Naturkunde Berlin), kindly supervised her in the lab and introduced her to the techniques for mitochondrial DNA analysis. We are grateful to Volker Puthz, Schlitz, who introduced the first author to *Stenus* taxonomy and never hesitated to support her over the years. The first author is thankful to Hiva Nasserzadeh, Hayk Mirzayans Insect Museum, Tehran, for her company dur-

ing collecting trips. Last but not least, we thank Lee Herman, American Museum of Natural History, New York, for proof-reading the manuscript and helpful comments. Part of field work in Iran and the whole work at the laboratory of the Museum für Naturkunde Berlin were supported by the German Research Foundation (DFG) from 2004–2011 (GZ: 446 IRN-18/1/04, 446 IRN-18/2/04, FR 2453/1-1, FR 2453/3-1).

References

Ádám L (1987) Staphylinidae of the Kiskunság National Park (Coleoptera: Staphylinidae). Natural History of the National Parks of Hungary 5: 126–168.

Ádám L (2001) In: Ádám L, Gabor H: Adatok a Zempléni-hegység, a Hernád-völgy, a Bodrogköz, a Rétköz és a Taktaköz holyvafaunájához (Coleoptera). Sátoraljaújhely, 129 pp.

Baudi di Selve F (1848) Alcune specie nuove di stafilini. Studi Entomologici 1(2): 113–148.

Betz O (1996) Function and evolution of the adhesion-capture apparatus of *Stenus* species (Coleoptera, Staphylinidae). Zoomorphology 116: 15–34. doi: 10.1007/BF02526926

Betz O (1999) A behavioral inventory of adult *Stenus* species (Coleoptera: Staphylinidae). Journal of Natural History 33: 1691–1712. doi: 10.1080/002229399299806

Betz O (2002) Performance and adaptive value of tarsal morphology in rove beetles of the genus *Stenus* (Coleoptera, Staphylinidae). The Journal of Experimental Biology 205: 1097–1113.

Betz O (2006) Ecomorphology: Integration of form, function, and ecology in the analysis of morphological structures. Mitteilungen der Deutschen Gesellschaft für Allgemeine und Angewandte Entomologie 15: 409–416.

Clement M, Snell Q, Walke P, Posada D, Crandall K (2002) TCS: estimating gene genealogies. Proc 16th Int Parallel Distrib Process Symp 2: 184. doi: 10.1109/ipdps.2002.1016585

Eppelsheim E (1884) Diagnosen neue Coleopteren aus Lenkoran. Verhandlungen des naturforschenden Vereines in Brünn 22 [1883]: 11–16.

Folmer O, Black M, Hoeh W, Lutz R, Vrijenhoek R (1994) DNA primers for amplification of mitochondrial cytochrome c oxidase subunit I from diverse metazoan invertebrates. Molecular Marine Biology and Biotechnology 3: 294–299.

Frisch J, Burckhardt D, Wolters V (2002) Rove beetles of the subtribe Scopaeina Coiffait (Coleoptera: Staphylinidae) in the West Palaearctic: Phylogeny, biogeography and species catalogue. Organisms, Diversity and Evolution 2(1): 27–53. doi: 10.1078/1439-6092-00032

Hajibabaei M, Singer GAC, Hebert PDN, Hickey DA (2007) DNA barcoding: how it complements taxonomy, molecular phylogenetics and population genetics. Trends in Genetics 23(4): 167–172. doi: 10.1016/j.tig.2007.02.001

Hall TA (1999) BioEdit: a user-friendly biological sequence alignment editor and analysis program for Windows 95/98/NT. Nucleic Acids Symposium Series 41: 95–98.

Hebert PDN, Cywinska A, Ball SL, de Waard JR (2003a) Biological identifications through DNA barcodes. Proceedings of the Royal Society of London Biological Sciences 270: 313–321. doi: 10.1098/rspb.2002.2218

Hebert PDN, Ratnasingham S, de Waard JR (2003b) Barcoding animal life: cytochrome c oxidase subunit 1 divergences among closely related species. Proceedings of the Royal Society of London Biological Sciences (270) (Suppl.): 96–99.

Herman LH (2001) Catalog of the Staphylinidae (Insecta: Coleoptera) 1758 to the end of the second millennium. IV. Staphylinine group (Part l) Euaesthetinae, Leptotyphlinae, Megalopsidiinae, Oxyporinae, Pseudopsinae, Solieriinae, Steninae. Bulletin of the American Museum of Natural History 265: 1807–2440.

Heyden L von (1905) Notiz. Wiener Entomologische Zeitung 24: 262.

Kastcheev VA, Puthz V (2011) Contribution to the knowledge of the fauna of Steninae (Coleoptera, Staphylinidae) of the Kazakhstan. 319th Contribution to the Knowledge of Steninae. Entomofauna 32: 437–460.

Kimura M (1980) A simple method for estimating evolutionary rate of base substitutions through comparative studies of nucleotide sequences. Journal of Molecular Evolution 16: 111–120. doi: 10.1007/BF01731581

Koerner L, Laumann M, Betz O, Heethoff M (2013) Loss of the sticky harpoon—COI sequences indicate paraphyly of *Stenus* with respect to *Dianous* (Staphylinidae, Steninae). Zoologischer Anzeiger 252: 337–347. doi: 10.1016/j.jcz.2012.09.002

Lang C, Koerner L, Betz O, Puthz V, Dettner K (2015) Phylogenetic relationships and chemical evolution of the genera *Stenus* and *Dianous* (Coleoptera: Staphylinidae). Chemoecology 25: 11–24. doi: 10.1007/s00049-014-0171-4

Leigh J, Bryant D (2015) POPART: full-feature software for haplotype network construction. Methods in Ecology and Evolution 6: 1110–6. doi: 10.1111/2041-210X.12410

Librado P, Rozas J (2009) DnaSP v5: a software for comprehensive analysis of DNA polymorphism data. Bioinformatics 25: 1451–1452. doi: 10.1093/bioinformatics/btp187

Puthz V (2001) Beiträge zur Kenntnis der Steninen CCLXIX. Zur Ordnung in der Gattung *Stenus* Latreille, 1796 (Staphylinidae, Coleoptera). Phillippia 10: 33–42.

Puthz V (2008) *Stenus* Latreille und die segenreiche Himmelstochter (Coleoptera, Staphylinidae). Linzer biologische Beiträge 40(1): 137–230.

Puthz V (2009) Neue und alte paläarktische *Stenus*-Arten (Col., Staphylinidae). 305. Beiträge zur Kenntnis der Steninen. Zeitschrift der Arbeitsgemeinschaft Österreichischer Entomologen 61: 29–50.

Puthz V (2012) Steninae. In: Freude H, Harde KW, Lohse A (Eds) Die Käfer Mitteleuropas. Band 4. Zweite Auflage, 286–317.

Qian L, An Y, Song J, Xu M, Ye J, Wu C, Li B, Hao D (2014) COI gene geographic variation of Gypsy moth (Lepidoptera: Lymantriidae) and a TaqMan PCR diagnostic assay. DNA Barcodes 2: 10–16. doi: 10.2478/dna-2014-0002

Rey C (1884) Tribu des brévipennes. Deuxième groupe: Micropéplides. Troisième groupe: Sténides. Annales de la Société Linnéenne de Lyon 30(2): 153–415.

Ryvkin AB (2011) Contributions to the knowledge of *Stenus* (*Nestus*) species of the *crassus* group (Insecta: Coleoptera: Staphylinidae: Steninae). 1. Four new species from the Russian Far East with taxonomic notes. Baltic Journal of Coleopterology 11(1): 57–72.

Schierling A, Seifert K, Sinterhauf SR, Rieß JB, Rupprecht JC, Dettner K (2013) The multifunctional pygidial gland secretion of the steninae (Coleoptera: Staphylinidae): ecological significance and evolution. Chemoecology 23: 45–57. doi: 10.1007/s00049-012-0118-6

Schülke M, Smetana A (2015) Staphylinidae [Omaliinae - Scydmaeninae]. In: Löbl I, Löbl D (Eds) Catalogue of Palaearctic Coleoptera Vol. 2/1. Brill, Leiden, Boston, 304–900.

Serri S, Frisch J (2016) Species diversity and biogeography of the Steninae MacLeay, 1825 of Iran, with comparative notes on *Scopaeus* Erichson, 1839 (Coleoptera: Staphylinidae). Deutsche Entomologische Zeitschrift 63(1): 17–44. doi: 10.3897/dez.63.5885

Swofford DL (2002) PAUP. Phylogenetic Analysis Using Parsimony,Version 4. 10. Sinauer Associates, Sunderland, MA.

Szalanski AL, McKern JA, Solorzano C, Austin JW (2010) Genetic Diversity of Ants (Hymenoptera: Formicidae) from the Ozark-St. Francis National Forest, Arkansas, USA. Sociobiology 56(3): 1–10.

Tamura K, Stecher G, Peterson D, Filipski A, Kumar S (2013) MEGA6: Molecular Evolutionary Genetics Analysis Version 6. Molecular Biology and Evolution 30: 2725–2729. doi: 10.1093/molbev/mst197

Winnepenninckx B, Backeljau T, De Wachter R (1993) Extraction of high molecular weight DNA from molluscs. Trends in Genetics 9: 407. doi: 10.1016/0168-9525(93)90102-N

ZooKeys 626: 87–123 (2016)
doi: 10.3897/zookeys.626.10033
http://zookeys.pensoft.net

RESEARCH ARTICLE

A peer-reviewed open-access journal
ZooKeys
Launched to accelerate biodiversity research

Taxonomic review of New World Tachyina (Coleoptera, Carabidae): descriptions of new genera, subgenera, and species, with an updated key to the subtribe in the Americas

Olivia F. Boyd[1], Terry L. Erwin[2]

1 *Department of Integrative Biology, Oregon State University, Corvallis, OR 97331 USA* **2** *Department of Entomology, National Museum of Natural History, Smithsonian Institution, P.O. Box 37012, Washington, D.C. 20013–7012 USA*

Corresponding author: *Olivia F. Boyd* (boydo@oregonstate.edu)

Academic editor: *L. Penev* | Received 30 July 2016 | Accepted 9 October 2016 | Published 20 October 2016

http://zoobank.org/3DE781B6-D48B-432B-9784-6703EA6B280B

Citation: Boyd OF, Erwin TL (2016) Taxonomic review of New World Tachyina (Coleoptera, Carabidae): descriptions of new genera, subgenera, and species, with an updated key to the subtribe in the Americas. ZooKeys 626: 87–123. doi: 10.3897/zookeys.626.10033

Abstract

The classification of the carabid subtribe Tachyina (Trechitae: Bembidiini) is reviewed in light of newly discovered diversity from Central and South America. Described herein are three new genera (*Tachyxysta* **gen. n.**, *Stigmatachys* **gen. n.**, *Nothoderis* **gen. n.**), two new subgenera of *Meotachys* (*Scolistichus* **subgen. n.**, *Hylotachys* **subgen. n.**), and two new subgenera of *Elaphropus* (*Ammotachys* **subgen. n.**, *Idiotachys* **subgen. n.**). Two names previously synonymized under *Polyderis* (*Polyderidius* Jeannel, 1962) and *Elaphropus* (*Nototachys* Alluaud, 1930) are elevated to generic and subgeneric status, respectively. Eight new species are recognized: *Tachyxysta howdenorum* (type locality: México: Chiapas: El Aguacero, 680m); *Elaphropus marchantarius* (type locality: Brazil, Amazonas, Rio Solimões, Ilha de Marchantaria), *E. acutifrons* (type locality: Brazil: Pará, Santarém) and *E. occidentalis* (type locality: Perú: Loreto, Pithecia, 74°45'W 05°28'S); *Stigmatachys uvea* (type locality: Perú: Loreto: Campamento San Jacinto, 2°18.75'S, 75°51.77'W, 175–215m); and *Meotachys riparius* (type locality: Colombia: Amazonas: Leticia, 700 ft), *M. ballorum* (type locality: Brazil: Amazonas, Rio Negro Cucui), and *M. rubrum* (type locality: Perú: Madre de Dios: Rio Manu, Pakitza, 11°56°47'S 071°17°00'W, 356m). An updated key to the genera and subgenera of Tachyina occurring in the New World is provided, with accompanying illustrations.

Resumen

La clasificación de la subtribu Tachyina (Carabidae: Trechitae: Bembidiini) se revisa luego de diversidad que ha sido nuevamente descrita del Centro y Sur América. Aquí se describen tres géneros nuevos (*Tachyxysta* **género nuevo**, *Stigmatachys* **género nuevo**, *Nothoderis* **género nuevo**), dos subgéneros nuevos del *Meotachys* (*Scolistichus* **subgénero nuevo**, *Hylotachys* **subgénero nuevo**), y dos subgéneros nuevos del *Elaphropus* (*Ammotachys* **subgénero nuevo**, *Idiotachys* **subgénero nuevo**). Dos nombres taxonómicos previamente sinonimizados con *Polyderis* (*Polyderidius* Jeannel, 1962) y *Elaphropus* (*Nototachys* Alluaud, 1930) aquí son elevados a los niveles de género y subgénero, respectivamente. Se reconocen ochos espécies nuevos: *Tachyxysta howdenorum* (localidad tipo: México: Chiapas: El Aguacero, 680m); *Elaphropus marchantarius* (localidad tipo: Brazil, Amazonas, Rio Solimões, Ilha de Marchantaria), *E. acutifrons* (localidad tipo: Brazil: Pará, Santarém) and *E. occidentalis* (localidad tipo: Perú: Loreto, Pithecia, 74°45'W 05°28'S); *Stigmatachys uvea* (localidad tipo: Perú: Loreto: Campamento San Jacinto, 2°18.75'S, 75°51.77'W, 175–215m); and *Meotachys riparius* (localidad tipo: Colombia: Amazonas: Leticia, 700 ft), *M. ballorum* (localidad tipo: Brazil: Amazonas, Rio Negro Cucui), and *M. rubrum* (localidad tipo: Perú: Madre de Dios: Rio Manu, Pakitza, 11°56°47'S 071°17°00'W, 356m). Una clave actualizada con illustraciones de los géneros y subgéneros del Tachyina que ocurren en el Nuevo Mundo está incluída.

Resumo

A classificação da subtribo Tachyina (Carabidae: Trechitae: Bembidiini) está revisto à luz da diversidade recém-descrita da América Central e do Sul. Aqui são descritos três novos gêneros (*Tachyxysta* **novo gênero**, *Stigmatachys* **novo gênero**, *Nothoderis* **novo gênero**), dois novos subgêneros de *Meotachys* (*Scolistichus* **novo subgênero**, *Hylotachys* **novo subgênero**), e dois novos subgêneros de *Elaphropus* (*Ammotachys* **novo subgênero**, *Idiotachys* **novo subgênero**). Dois nomes taxonômicos anteriormente sinonimizadas com *Polyderis* (*Polyderidius* Jeannel, 1962) e *Elaphropus* (*Nototachys* Alluaud, 1930) são elevada aos níveis de gênero e subgênero, respectivamente. Oito espécies são reconhecidas: *Tachyxysta howdenorum* (localidade tipo: México: Chiapas: El Aguacero, 680m); *Elaphropus marchantarius* (localidade tipo: Brazil, Amazonas, Rio Solimões, Ilha de Marchantaria), *E. acutifrons* (localidade tipo: Brazil: Pará, Santarém) and *E. occidentalis* (localidade tipo: Perú: Loreto, Pithecia, 74°45'W 05°28'S); *Stigmatachys uvea* (localidade tipo: Perú: Loreto: Campamento San Jacinto, 2°18.75'S, 75°51.77'W, 175–215m); and *Meotachys riparius* (localidade tipo: Colombia: Amazonas: Leticia, 700 ft), *M. ballorum* (localidade tipo: Brazil: Amazonas, Rio Negro Cucui), and *M. rubrum* (localidade tipo: Perú: Madre de Dios: Rio Manu, Pakitza, 11°56°47'S 071°17°00'W, 356m). Também está incluída uma chave atualizada com ilustrações dos gêneros e subgêneros de Tachyina que ocorrem no Novo Mundo.

Keywords

Elaphropus, *Meotachys*, *Nototachys*, *Polyderidius*, *Polyderis*, *Nothoderis*, *Stigmatachys*, *Tachyxysta*, Amazon basin

Introduction

The cosmopolitan carabid subtribe Tachyina includes about 800 described species. In the Americas, tachyine diversity is greatest in the tropics, with species documented from a wide variety of habitats (riparian, hypogean, arboreal, corticolous, myrmecophilous, etc.). Detailed accounts of New World tachyine natural history are provided in previous publications by Erwin (1974b, 1991) and Adis et al. (1986).

Among Bembidiini, tachyines are well-defined morphologically. All but a few tachyines have at least a trace of an elytral apical recurrent groove, which can vary in

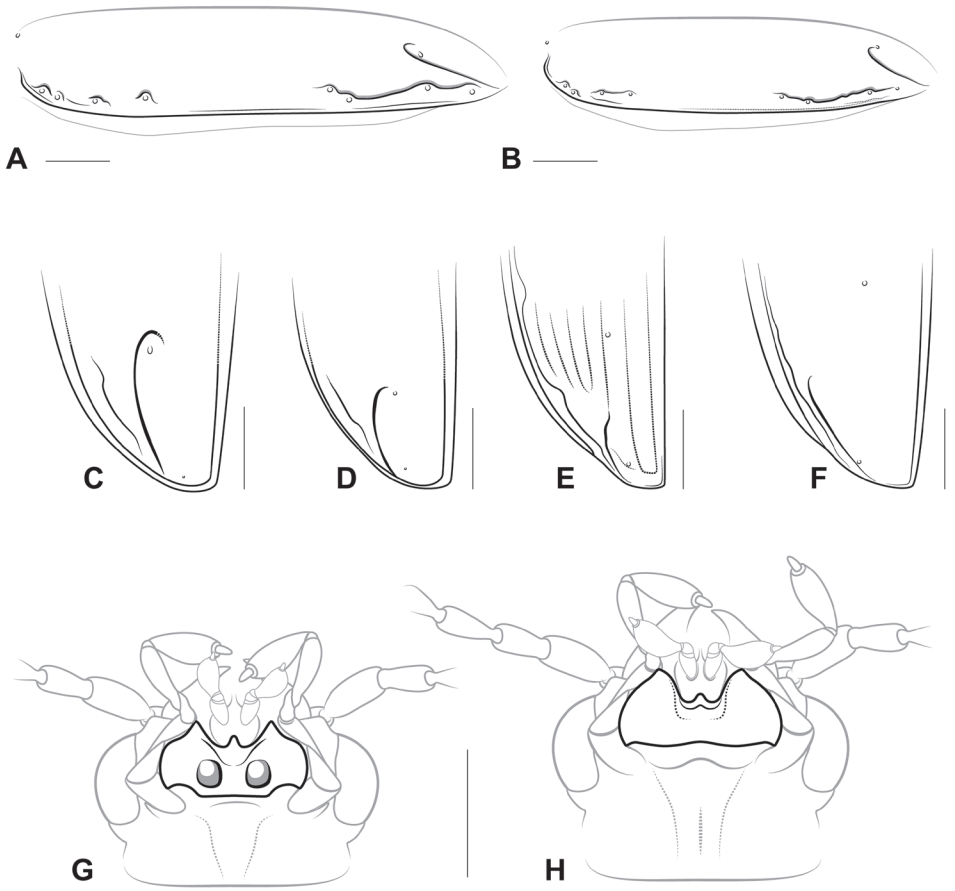

Figure 1. Basic characters for generic and subgeneric level identification of Tachyina. **A–B** Left elytron, lateral view, illustrating positions of elytral ombilicate setae and form of the 8th elytral interneur (other interneurs omitted) **A** *Paratachys fulvicollis*; **B** *Tachys vittiger* **C–F** Elytral apex **C** *Paratachys fulvicollis* **D** *Tachys vittiger*. Scale bar 0.25 mm **E** *Elaphropus* (*Ammotachys*) *marchantarius* **F** *Tachyxysta howdenorum* **G–H** Head, ventral view, illustrated to show mentum **G** *Meotachys* (*Scolistichus*) *riparius* **H** *Elaphropus* (*Barytachys*) *nebulosus*. Scale bars = 0.25 mm.

form (Fig. 1C–F). The apicolaterally notched protibiae (visible in Fig. 2D–G, I) of all Tachyina s. str. easily distinguish them from their closest relatives, the Xystosomina, which possess simpler, truncate protibiae (Erwin 1994). The mentum of a tachyine beetle may either bear paired foveae (Fig. 1G) or lack these structures (Fig. 1H), and though major taxonomic groups of tachyines can be classified broadly according to this character (see Figure 5 in Ortuño and Arillo 2015), it is unlikely to be phylogenetically informative. The scope of this review is limited to the Tachyina of the New World, including brief diagnoses of all New World genera, as well as descriptions of new genera and new taxa that serve to clarify the boundaries and definitions of existing genera. Many additional species await description. The genus *Meotachys* Erwin, 1974 includes

a small number of undescribed species (including the largest tachyine known from the New World) in addition to those representing the two new subgenera described below. This genus is of special interest due to its diversity, its potential key phylogenetic position, and the discovery of several unique external characters. Known species of *Meotachys* vary remarkably in size and form, though all share a distinctively shaped apical portion of the 8th elytral interneur. *Meotachys* is unusually heterogeneous for a group of its size; alternatively, the species richness and diversity of this group may be much larger than that which is currently represented in collections. Distributed from México to central Brazil, *Meotachys* species are associated with silty river margins, understory bamboo thickets (Erwin 1991), and the seasonal white water (várzea) and black water (igapó) inundation forests that occur throughout the Amazon basin.

Among the "non-bifoveate' Tachyina (Ortuño and Arillo 2015), the speciose and morphologically diverse genus *Elaphropus* is defined by a lack of features diagnostic for other genera (e.g., *Micratopus*, *Lymnastis*, *Anomotachys*, *Tachyta*, etc.) rather than by a convincing set of synapomorphies. Despite the suspect monophyly of *Elaphropus*, previous authors have indicated with varying degrees of certainty that its relatively well-defined subgeneric level groups belong to a "phyletic line" (Sciaky and Vigna-Taglianti 2003). Assignment of several new species described below to *Elaphropus* is done so according to historical precedent and is somewhat tentative, as these taxa may represent separate genera pending further study. The development of a molecular phylogeny of the subtribe is in progress; with a focus on deep taxon sampling in *Elaphropus* (*Tachyura*) and allies, molecular data should help illuminate natural groups among this group's numerous and disparate species.

Methods

Material examined

Codes for the institutions where type material will be deposited appear in the text as follows:

AMNH American Museum of Natural History, New York City, N.Y., USA; Lee Herman, Curator

CAS California Academy of Sciences, San Francisco, CA, USA; David H. Kavanaugh, Curator

CMNH Carnegie Museum of Natural History, Pittsburgh, PA, USA; Robert Davidson, Collection Manager

MZUSP Museum of Zoology, University of Sao Paulo, Brazil; Cleide Costa, Curator

NMNH National Museum of Natural History, Washington, D.C., USA; Terry L. Erwin, Curator

OSAC Oregon State Arthropod Collection, Oregon State University, Corvallis, OR, USA; David Maddison, Director and Curator

UNMSM Museo Historia Natural, San Marcos University, Lima Perú; Gerardo Lamas, Curator

ZSM Bavarian State Collection of Zoology (Zoologische Staatssammlung München), Munich, Germany; Martin Baehr, Curator

Morphological methods: specimen preparation and imaging

DNA voucher specimens representing some of the taxa described were available from a separate project. Males were dissected following DNA extraction. Genitalia were cleared in KOH and mounted in Euparal following the procedure described by Maddison (2014). Photo references for illustrations of genitalia were obtained using a JVC KY-F75U camera-equipped Leica DM5500 B compound microscope in bright field illumination.

External structures were examined using a Leica M165 C dissecting microscope. Measurements were taken digitally using a camera-equipped Leica Z6 and the software Cartograph (Microvision). Measurements represent a range from the smallest to largest specimen examined. Abbreviations and definitions of measurements provided are listed below. Photomicrographs obtained with this system were compiled into stacked images using the photomontage software Zerene Stacker (Zerene Systems). Digital illustrations were prepared from reference photos using Adobe Creative Cloud software tools (Adobe Systems 2015).

Descriptive terms

Morphological terms generally follow the conventions established by Erwin (1974a). Elytral ombilicate (Eo) setae are named by position according to Erwin's (1974a) chaetotaxy system. Elytral discal (Ed) setae are simply counted and referred to in ascending order from base to apex, beginning with the scutellary seta (Ed1). Arrangement of humeral setal insertions is discussed in the key as either symmetric (with notation d(1,2) = d(3,4) indicating a distance between the first and second setae which is more or less equal to the distance between setae three and four), or asymmetric (with notation d(3,4) > d(1,2) and d(3,4) > d(2,3) indicating unequal spacing among humeral setae). Several commonly used terms are abbreviated in the key and text as follows:

i1 elytral interneur 1 (closest to suture)

i8 elytral interneur 8 (closest to lateral margin)

Ed elytral discal seta

Eo elytral ombilicate seta

ABL apparent body length (labrum to elytral apex of specimen in horizontal view)

SBL standardized body length (labrum to posterior supraorbital seta + pronotum from base to apex at center line + base of scutellum to elytral apex)

TW total width across widest point of both elytra
ARG elytral apical recurrent groove

Label data are listed verbatim, with label breaks denoted as follows: "label data" / "begin new line on label" // "begin second label".

Updated Classification and Checklist of genera and subgenera of New World Tachyina

Genus (Subgenus)	# described species occurring in the Americas
Moirainpa Erwin, 1984	1
Micratopus Casey, 1914	5
Lymnastis Motschulsky, 1862	2
Costitachys Erwin, 1974	2
Tachyta Kirby, 1837	
(*Tachyta*)	6
Tachyxysta **gen. n.**	1
Elaphropus Motschulsky, 1839	
(*Tachyura* Motschulsky, 1862)	2
(*Barytachys* Chaudoir, 1868)	38
(*Ammotachys* **subgen. n.**)	1
(*Idiotachys* **subgen. n.**)	1
(*Nototachys* **subgen. n.**)	1
Porotachys Netolitsky, 1914	1
Polyderis Motschulsky, 1862	
(*Polyderis*)	1
Liotachys Bates, 1871	1
Tachysbembix Erwin, 2004	2
Tachys Dejean, 1821	15
Paratachys Casey, 1918	50
Polyderidius Jeannel, 1962	8
Stigmatachys **gen. n.**	1
Nothoderis **gen. n.**	3
Meotachys Erwin, 1974	
(*Meotachys*)	8
(*Scolistichus* **subgen. n.**)	1
(*Hylotachys* **subgen. n.**)	2
Pericompsus LeConte, 1851	
(*Pericompsus*)	49
(*Eidocompsus* Erwin, 1974)	13

Key to genera and subgenera of New World Tachyina

1 Mentum normal for Carabidae, afoveate (Fig. 1H) **2**

– Mentum with pair of paramedial, rather deep circular foveae (Fig. 1G) **13**

2(1) Elytral intervals carinate; pronotum with longitudinal carinae .... ***Costitachys*** **Erwin, 1974**

– Elytron and pronotum not carinate **3**

3(2') Labrum bilobed, covering mandibles; elytron truncate, pubescent; ARG barely impressed or absent **4**

– Labrum truncate; elytron various; ARG various **5**

4(3) Head with single pair of supraorbital setae; male and female both with two pairs apical abdominal ventral setae, lateral pair sickle-shaped..... ..... ***Micratopus*** **Casey, 1914**

– Head with two pairs of supraorbital setae; apical abdominal ventrite of male with 2 longer setae, female with 4 (Old World—adventive) .... ***Lymnastis*** **Motschulsky, 1852**

5(3') Form depressed; ARG absent; body dorsally pubescent; eyes reduced, with a few large facets ..... ***Moirainpa*** **Erwin, 1984**

– Form convex to subdepressed; ARG visible, feebly to markedly impressed; body dorsally glabrous or (rarely) sparsely setose **6**

6(5') ARG elongate, subparallel to elytral margin (Figs 5I, 1F) **7**

– ARG very short (Figs 4G, 4H, 5G, 5H), or elongate and arcuate toward midline and/or continuous with i3 (Figs 5F, 1E) **9**

7(6) Tarsal claws denticulate; prosternum plurisetose; body dorsoventrally compressed, dorsal surface coarsely microsculptured..... ***Tachyta*** **Kirby, 1837**

– Tarsal claws simple; prosternum glabrous; body convex to subdepressed; dorsal surface various..... **8**

8(7') Dorsal surface with coarse, isodiametric microsculpture; ARG straight; form subdepressed; color light brown; pronotum without basal excavation (Pantropical—adventive) ..... ***Elaphropus yunax*** **(Darlington, 1939)**

– Dorsal surface without microsculpture, except for labrum; ARG sinuate, slightly hooked anteriorly; form robust, convex (Fig. 2I); color piceous to black; basal section of pronotum with deep excavation opposite scutellum and deep, basolateral indentations (Fig. 3I)..... ***Tachyxysta*** **gen. n.**

9(6') Humeral series of elytral ombilicate punctures evenly spaced or symmetrically distributed, with d(1,2) = d(3,4) (Fig. 4F, 4G); elytra without macula(e); mesepisternum without fovea(e) **10**

– Humeral series of Eo punctures asymmetrically distributed, with Eo4 removed from closely grouped Eo1–3 such that d(3,4) > d(1,2) and d(3,4) > d(2,3) (Fig. 4H, 4I); elytra with or without macula(e); mesepisternum with or without fovea(e) **11**

10(9) Elytron with 8 micropunctulate interneurs; i4–7 not reaching apex and i4–5 converging apically (Figs 1E, 5F); pronotum subquadrate, margins not mark-

edly sinuate (Fig. 3F); ARG arcuate, continuous with i3; i8 nearly complete, with basal part parallel to elytral margin, meeting or just short of reaching humeral series of setae (Fig. 4F); apical half of i8 deeply impressed, curvy, abruptly bent around Eo5+6 and Eo7 (Figs 1E, 4F, 5F) ..... ***Elaphropus* (*Ammotachys*) subgen. n.**

– Elytron with 1–2 punctate interneurs (Fig. 2G), i2 effaced near apex and i3 only very faintly impressed; Pronotum wider than long, with sinuate margins (Fig. 3G); ARG very short, extended past Ed4; i8 reduced, interrupted, just visible near (but not passing through) Eo5 and 6 and between Eo7 and 8 (Figs 4G, 5G) ..... ***Elaphropus* (*Idiotachys*) subgen. n.**

11(9') Pronotum longer than wide, constricted at base (Fig. 3H); elytron with 5 discal setae, 1–3 closely grouped in basal third, 4th at apical third; apical half of antennae lighter than basal half, almost white (Fig. 2H); mesepisternum with 2 deep, circular foveae (Fig. 7A).... ***Elaphropus* (*Nototachys*) Alluaud, 1930**

– Pronotum subquadrate to transverse and cordiform; elytron with 4 discal setae, antennae concolorous **12**

12(11') i8 interrupted at middle; mesepisternum with one or more shallow fovea(e) or punctures ..... ***Elaphropus* (*Barytachys*) Chaudoir, 1868**

– i8 entirely impressed, subparallel to elytral margin ..... ***Elaphropus* (*Tachyura*) Motschulsky, 1862**

13(1') Head with 3 pairs supraorbital setae (Fig. 3B); ARG (if present) often hooked anteriorly (Fig. 4B); small to minute, soft-bodied; elytra translucent, flavous, usually apically truncate and rounded (southeastern USA to Argentina) (Figs 2B, 3B, 4B, 5B) ..... ***Polyderidius* Jeannel, 1962**

– Head with 2 pairs supraorbital setae..... **14**

14(13') Pronotum markedly constricted basally; i8 absent externally; form "ant-like"; apical half of antennae usually lighter than basal half, often whitish..... ***Liotachys* Bates, 1871**

– Pronotum cordiform to quadrate; i8 variable in shape and completeness; overall form not as above **15**

15(14') ARG elongate, very close to and parallel with elytral margin (see Fig. 1F)..... ***Porotachys* Netolitzky, 1914**

– ARG varied in form (very faint to markedly impressed, short to elongate, simple or hooked), but not parallel to elytral margin (directed anteriorly toward elytral disc or closer to suture than margin) (see Figs 1C–1E, 5A–5E) **16**

16(15') ARG anteriorly hooked around, into, or effaced laterad of 4th discal seta . **17**

– ARG simple, not hooked, short to elongate **19**

17(16) ARG hooked into or effaced laterad of 4th discal seta (Fig. 1D), IF effaced, specimen from sea coast and with granulate microsculpture; i8 subsulcate, not incurved at Eo5–6 (Fig. 1B) ..... ***Tachys* s. str. Stephens, 1829**

– Hook of ARG either surrounding or produced laterad of 4th discal seta; i8 medially incurved, diverted from elytral margin at Eo5–6..... **18**

18(17') ARG hooked around 4th discal seta (Fig. 1C); width across eyes at widest point less than greatest width of pronotum; i8 subsulcate posterior to midpoint of elytron (Fig. 1A); elytra with transverse, linear microsculpture ..... ***Paratachys* Casey, 1918**

– Hook of ARG produced laterad of 4th discal seta; width across eyes at widest point about equal to greatest width of pronotum; i8 shallow; surface dull, with coarse, granulate microsculpture; specimen from sea coast ..... ***Tachysbembix* Erwin, 2004**

19(16') Pronotum convex, with barely rounded hind angles; i8 reduced, faintly visible apically, not redirected around elytral ombilicate setae ..... ***Polyderis* s. str Motschulsky, 1862**

– Pronotum shallowly convex to subdepressed, with square to acute posterior angles; i8 partially to completely impressed, apically diverted around Eo5–6, Eo7 OR interneurs deeply punctate and reduced in number..... **"*Pericompsus*/*Meotachys* complex" 20**

20(19') Pronotum with continuous, punctate transverse impression, usually arcuate (forming crescent-shaped basal section), sometimes bilobed; i8 with conspicuous posthumeral foveae or fovea, usually at basal fourth or midpoint OR elytron with 8 entirely punctate interneurs; elytra with or without color pattern or macula(e) ..... ***Pericompsus* 25**

– Pronotum with punctate or subsulcate transverse impressions converging at medial furrow, forming triangular basal section (see Fig. 3A–E); i8 visible or not, without posthumeral foveae; elytron with up to 8 micropunctulate or striatiopunctate interneurs OR with 6 or fewer punctate interneurs; elytra unicolorous..... **21**

21(20') Elytral humeri obliquely rounded (possibly brachypterous), margins serrate; elytron with at most 6 deeply punctate interneurs (Fig. 5A), i8 not visible (Fig. 4A); ARG very small, just visible at elytral apex (Figs 4A, 5A); eyes reduced; body dorsally opaque, red-brown (Peruvian Amazon) (Figs 2A, 3A, 5A) ..... ***Stigmatachys* gen. n.**

– Elytral humeri squarely rounded, margins smooth or serrate (Fig. 5C–E); i8 at least visible apically, medially incurved at Eo5–6 (Fig. 4C–E) and ARG rudimentary (see Fig. 1E) to distinct and markedly engraved; eyes large; degree of dorsal infuscation variable..... **22**

22(21') Elytral interneurs distinctly punctate, fewer than 8 entirely visible..... ***Meotachys* s. str. Erwin, 1974**

– Elytral interneurs micropunctulate to striatiopunctate, up to 8 entirely visible **23**

23(22') Pronotum transversely cordate, margins sinuate, posterior angles prominent and slightly acute (Fig. 3E); mesepisternum with single small, deep, reniform pit (Fig. 7B); i1 deeply impressed basally at level of scutellum; ARG short, faintly impressed, not connected to i3 (Fig. 5E); interval between ARG and i8 not raised..... ***Meotachys* (*Hylotachys*) subgen. n.**

– Pronotum transversely quadrate, margins subparallel to slightly sinuate, posterior angles approximately square (Fig. 3C–D); mesepisternum without pit; i1 without deep basal impression; ARG continuous with i3 (see Fig. 1E); elytral apex with raised interval between ARG and i8 ..... **24**

24(23') Elytral margin partially to entirely serrate; i8 feebly to moderately impressed from Eo5 to apex, separated from elytral margin by Eo5–8 but not markedly curved in apical half (Fig. 4C)..... ***Nothoderis* gen. n.**

– Elytral margin smooth (Fig. 5D); i8 curvy and deeply impressed in apical half, abruptly bent at Eo5–6 and around Eo7 (Fig. 4D) .... ***Meotachys* (*Scolistichus*) subgen. n.**

25(20) i8 with a deep, nearly perforate fovea at or just anterior to middle of elytron; elytron with two additional subhumeral foveae of varied size; pronotum often narrowed at base; body typically elongate; elytra often with dark markings... ..... ***Pericompsus* s. str. LeConte, 1852**

– i8 not foveate at or near middle of elytron; if foveate posterior to humerus, then fovea shallow and bearing seta OR small, perforate, and located at basal fourth near seta Eo4c; pronotum usually quadrate, with base and apex subequal in width; body typically compact, robust, unicolorous..... ..... ***Pericompsus* (*Eidocompsus*) Erwin, 1974**

Diagnoses and descriptions of genera and subgenera of New World Tachyina

Genus *Moirainpa* Erwin, 1984

Type species. *Moirainpa amazona* Erwin, 1984.

Diagnosis. Mentum without foveae; eyes reduced and pubescent, with a few large facets; labrum not covering mandibles; foretibia notched apicolaterally; elytron entire, with serrate humeral margin; ARG absent; body subdepressed, pubescent. ABL = 1.0 mm.

Distribution. Known from várzea white water inundation forests of the upper to middle Amazon River drainage (Erwin 1984).

Genus *Micratopus* Casey, 1914

Type species. *Blemus aenescens* (LeConte, 1848).

Diagnosis. Mentum without foveae; labrum bilobed, covering mandibles; head with single pair of supraorbital setae; elytra truncate; terminal abdominal ventrite of both male and female with four long setae, the lateral pair sickle-shaped. ABL = 1.2–3.0 mm.

Distribution. Often abundant at lights, this speciose and underdescribed genus is known from southern North America to northern South America and the Caribbean (Erwin 1991, Erwin et al. 2002).

Genus *Lymnastis* Motschulsky 1862

Type species. *Lymnaeum indicum* (Motschuslky, 1851).

Diagnosis. Mentum without foveae; labrum bilobed, covering mandibles; head with two pairs of supraorbital setae; elytra slightly truncate; terminal abdominal ventrite of male with two long, straight setae, female with four long, straight setae; body densely to sparsely setose.

Distribution. This Old World genus is adventive in Hawaii and the Caribbean (Erwin et al. 2002).

Genus *Costitachys* Erwin, 1974

Type species. *Costitachys inusitatus* Erwin, 1974.

Diagnosis. Mentum without foveae; foretibia with apicolateral notch; body subdepressed, flavotestaceous, shiny; head with single pair of supraorbital setae; basal protarsomere of male dilated, medially dentiform; head (3), pronotum (5), and elytron (8) with prominent longitudinal carinae; ABL = 1.7–2.6 mm.

Distribution. Known from sandy riparian habitats throughout the Amazon basin, from the eastern Andes of Ecuador and Perú to the Atlantic coast of South America (Erwin 1974; Erwin and Kavanaugh 1999, 2007).

Genus *Tachyta* Kirby, 1837

Type species. *Tachyta picipes* Kirby, 1837.

Diagnosis. Elongate, subdepressed; mentum lacking foveae; dorsal surface (excluding Old World taxa) with coarse, isodiametric microsculpture; prosternum plurisetose; tarsal claws denticulate; basal two protarsomeres of male dilated, medially dentiform; ARG elongate, slightly hooked anteriorly, close and subparallel to lateral margin of elytron. ABL = 1.8–3.3 mm.

Distribution. Widely distributed from the boreal Nearctic to Central America and the Caribbean, associated with fallen logs (Erwin 1975).

Genus *Tachyxysta* Boyd & Erwin, gen. n.

http://zoobank.org/316DFAA8-D484-4AD1-A2B5-1380C9CED42D

Type species. *Tachyxysta howdenorum* Boyd & Erwin, sp. n.

Diagnosis. Pronotum with distinctly inflated basal section separated from pronotal disc by subsulcate transverse impression; basal section interrupted at midpoint by prominent, deep excavation opposite scutellum; overall form robust, convex.

Description. Size. ABL = 2.4–2.5 mm; SBL = 2.5–2.7 mm; TW = 1.15–1.25 mm.

Form. Compact, robust, convex.

Color. Dorsally piceous, unicolorous (Fig. 2I); antennae and legs lighter, rufotestaceous except for darker basal half of coxae; dorsally glabrous and without microsculpture except for labrum.

Head. Two pairs of supraorbital setae within channeled longitudinal frontal furrows; frons not raised between furrows, often with subtle transverse wrinkles (Fig. 3I); mentum without foveae.

Prothorax. Base of pronotum (Fig. 3I) with deep lateral depression near posterior angle; posterior angle of pronotum raised, prominent; basal section of pronotum convex, interrupted by deep medial excavation opposite scutellum; male without dilated basal protarsomere(s); protibia notched apicolaterally (Fig. 2I); tarsal claws simple, not denticulate.

Pterothorax.Elytral margin reflexed; i1 entire, subsulcate or faintly impressed; i2–i7 not visible; i8 striatiopunctate from humerus to Eo5, apically subsulcate (Fig. 4I); recurrent groove elongate, slightly sinuate, subparallel to elytral margin, and recurved anteriorly (Fig. 5I); surface without spots; elytral ombilicate setae 2, 6, and 8 more than twice as long as next longest seta.

Genitalia. male aedeagus robust, elongate, with unequally sized, apically 3- or 4-setose parameres (Fig. 6E).

Distribution. The Mexican specimens were collected near or in El Ocote Preserve; the Honduran specimen was collected in an area near Comayagua National Park. Based on collection data from a limited number of specimens, *T. howdenorum* may be restricted to higher altitudes.

Derivation of name. Feminine. Derived from *Tachys*, the nominate genus of the subtribe Tachyina, and the Greek *xustos* (="smooth/polished"), in reference to this species' unmicrosculptured, glabrous dorsal surface and alluding to its general resemblance to some members of the subtribe Xystosomina, particularly those of the genus *Erwiniana*.

Tachyxysta howdenorum sp. n.

http://zoobank.org/62D8132A-524B-4C03-A219-3BC8B2FEBB3A
Figs 2I, 3I, 4I, 5I, 6E

Type material. Holotype: male (UASM) with following label data: "MEXICO. Chiapas, / El Aguacero, 16 km / W Ocozocoautla / 680m 5.[?]13.VI.1990 / H. & A. Howden FIT". Paratypes: 6 (2 male, 4 female) in CNC, FSCA, UASM, from type locality [1♀, UASM], "MEX.,Jnct.Rts. / 190&195,Chis. / VI-6-1969 / J.M.Campbell" [2♂, one with second label, "At Black / Light", CNC], "HONDURAS / Comayagua Dept. / Rancho Chiquito / Km 64 / 29 May 1964 // Blanton, Broce, / & Woodruff Coll. / Light:UV, trap" [1♀, FSCA], "Jct.Hwys 190-195, / Chis.Mex.VI.6, / 1969 H.F.Howden" [2♀, UASM].

Type locality. México: Chiapas: El Aguacero.

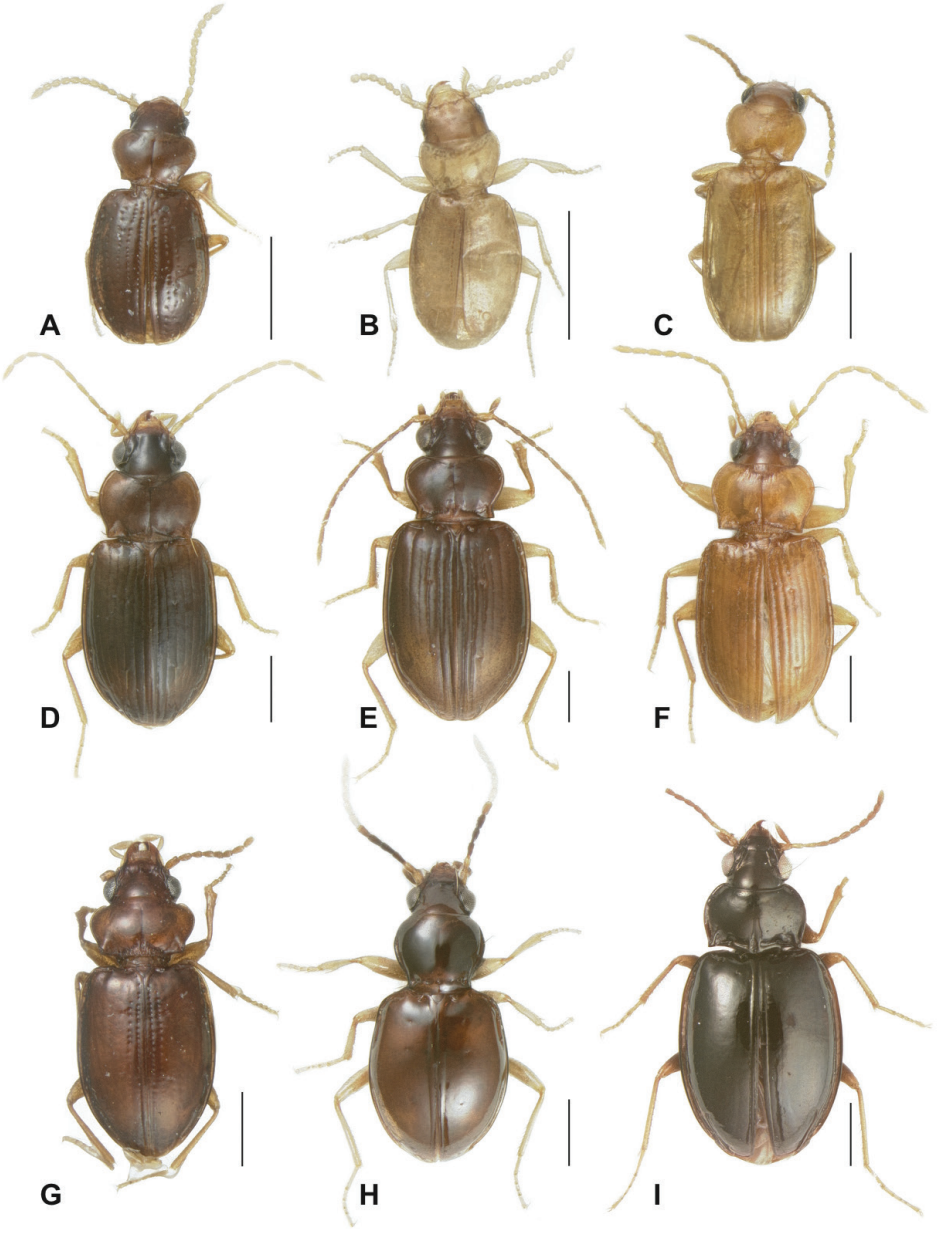

Figure 2. New Tachyina. **A** *Stigmatachys uvea* (holotype, ♀), Perú, Loreto, Campamento San Jacinto **B** *Polyderidius* sp., México, San Luis Potosí; **C** *Nothoderis rufotestacea*, USA, Arizona, Cochise Co. **D** *Meotachys* (*Hylotachys*) *ballorum* (paratype, ♀), Brazil, Amazonas, Tapurucuara **E** *Elaphropus* (*Ammotachys*) *marchantarius* (paratype, ♂), Venezuela, San Carlos de Rio Negro **F** *Meotachys* (*Scolistichus*) *riparius* (paratype, ♀), Brazil, Amazonas, Rio Solimões, Ilha de Marchantaria; **G** *Elaphropus* (*Idiotachys*) *acutifrons* (holotype, ♀), Brazil, Santarem **H** *Elaphropus* (*Nototachys*) *occidentalis* (paratype, ♂), Perú, Madre de Dios, Pakitza **I** *Tachyxysta howdenorum* (holotype, ♂), México, Chiapas, El Aguacero. Scale bars = 0.5 mm.

Description. Size, form, color, head, prothorax, pterothorax, abdomen, genitalia, and distribution as in description of the genus.

Derivation of specific epithet. The patronym *howdenorum* honors Henry and Anne Howden, collectors of the holotype. The Howdens collected several examples included in the type series of *T. howdenorum* two decades apart in different locations.

Remarks. Despite its superficial resemblance to the genus *Xystosomus*, *T. howdenorum* possesses a combination of characters that support its placement among the Tachyina but discourage its membership in any previously described tachyine genus; *T. howdenorum* has an apicolaterally notched protibia and an apical recurrent groove reminiscent of *Tachyta*, but lacks the denticulate tarsal claws diagnostic for that genus (Erwin, 1975).

Genus *Elaphropus* Motschulsky, 1839

Type species. *Elaphropus caraboides* Motschulsky, 1862.

Diagnosis. Mentum lacking foveae; claws simple; prosternum glabrous; elytron with 2 to 8 visible interneurs, complete or not, and variable in form; i8 impressed entirely or effaced at midpoint or visible only near apex; ARG short, straight or medially arcuate or if elongate and parallel to elytral margin, not recurved anteriorly.

Subgenus *Tachyura* Motschulsky, 1862

Type species. *Elaphrus quadrisignatus* Duftschmidt, 1812.

Diagnosis. i8 impressed from base to apex, subparallel to elytral margin, inserted anteriorly between Eo2 and Eo3; humeral series of elytral ombilicate setal insertions asymmetrically distributed, with Eo4 removed from closely grouped Eo1–3 such that d(3,4) > d(1,2) and d(3,4) > d(2,3); ARG short, straight to medially arcuate or elongate, straight, and parallel to elytral margin (*E. yunax*).

Distribution. Old World, Australia; adventive in the Americas.

Subgenus *Barytachys* Chaudoir, 1868

Type species. *Bembidium incurvum* Say, 1834.

Diagnosis. i8 visible near base and apex, middle section effaced; humeral series of elytral ombilicate setal insertions asymmetrically distributed, with Eo4 removed from closely grouped Eo1–3 such that d(3,4) > d(1,2) and d(3,4) > d(2,3); ARG short, straight or medially arcuate.

Distribution. North and Central America, the Caribbean islands.

Figure 3. Pronotum, dorsal aspect. **A** *Stigmatachys uvea* (holotype, ♀), Perú, Loreto, Campamento San Jacinto **B** *Polyderidius* sp., México, San Luis Potosí **C** *Nothoderis rufotestacea*, USA, Arizona, Cochise Co. **D** *Meotachys* (*Hylotachys*) *ballorum* (paratype, ♀), Brazil, Amazonas, Tapurucuara **E** *Elaphropus* (*Ammotachys*) *marchantarius* (paratype, ♂), Venezuela, San Carlos de Rio Negro **F** *Meotachys* (*Scolistichus*) *riparius* (paratype, ♀), Brazil, Amazonas, Rio Solimões, Ilha de Marchantaria; **G** *Elaphropus* (*Idiotachys*) *acutifrons* (holotype, ♀), Brazil, Santarem **H** *Elaphropus* (*Nototachys*) *occidentalis* (paratype, ♂), Perú, Madre de Dios, Pakitza **I** *Tachyxysta howdenorum* (holotype, ♂), México, Chiapas, El Aguacero. Scale bars = 0.25 mm.

Subgenus *Ammotachys* subgen. n.
http://zoobank.org/2A384793-FA57-4E0B-823B-A16D69167739

Type species. *Elaphropus marchantarius* sp. n.

Diagnosis. Mentum lacking foveae; elytron (Fig. 5F) with 8 micropunctulate interneurs; elytral humeral margin serrate; basal half of i8 (Fig. 4F) parallel to elytral margin, meeting or nearly reaching humeral series of setal insertions; humeral setae symmetrically distributed; apical half of i8 curvy, abruptly bent around Eo5+6 and Eo7; apical recurrent groove (Fig. 1E) rudimentary, continuous with i3.

Description. Size. ABL = 2.25–2.8 mm; SBL = 2.35–2.9 mm; TW = 0.95–1.15 mm

Form. Elongate, parallel-sided, subdepressed.

Color. Uniformly yellow-brown to flavous.

Microsculpture. Head and anteromedial part of pronotum with coarse, scaly, isodiametric microsculpture; remainder of pronotum and elytron with linear, transverse microsculpture.

Head. Mentum without foveae.

Prothorax. Basal section of pronotum (Fig. 3F) triangular, rugose, with basal transverse impressions not well-defined; pronotum with dark, medial furrow that does not reach anterior margin; pronotal furrow with shallow basal excavation; convergent transverse impressions barely visible along anterior margin of pronotum; basal protarsomere of male with prominent medial dentiform expansion.

Pterothorax. Elytral margin serrate; humeral margin (Fig. 4F) with four symmetrically spaced setal insertions; elytron with 8 micropunctulate interneurs; i4–7 not reaching apex and i4–5 converging apically (Fig. 1E); basal half of i8 parallel to elytral margin, meeting or nearly reaching humeral series of setae; apical half of i8 deeply impressed, abruptly curved around Eo5+6 and Eo7 and somewhat deviated medially from elytral margin; ARG (Fig. 1E) rudimentary, continuous with i3.

Genitalia. Not examined.

Distribution. Widely distributed in the Amazon basin. Known from several localities along the Rio Negro (S. Venezuela), Rio Solimões (S. Colombia and Pará, Brazil), and their confluence, and the Rio Xingu (NE Mato Grosso, Brazil).

Derivation of name: Masculine. Greek noun, *ammos* (= "sand"), in reference to the habitat and coloration of the known species of this genus, and *Tachys*, the nominate genus of the subtribe Tachyina.

Remarks. Though these beetles are tentatively placed within *Elaphropus* due to the afoveate mentum, their remarkable (though perhaps homoplasious) resemblance to the foveae-bearing species *Meotachys* (*Scolistichus*) *riparius*, calls into question the long-assumed taxonomic value and phylogenetic distribution of this character. These two species have similarly broad, pan-Amazonian, apparently overlapping distributions. Molecular data should help to clarify whether their shared morphologies are due to convergence of separate lineages or the loss or gain of foveae within a lineage.

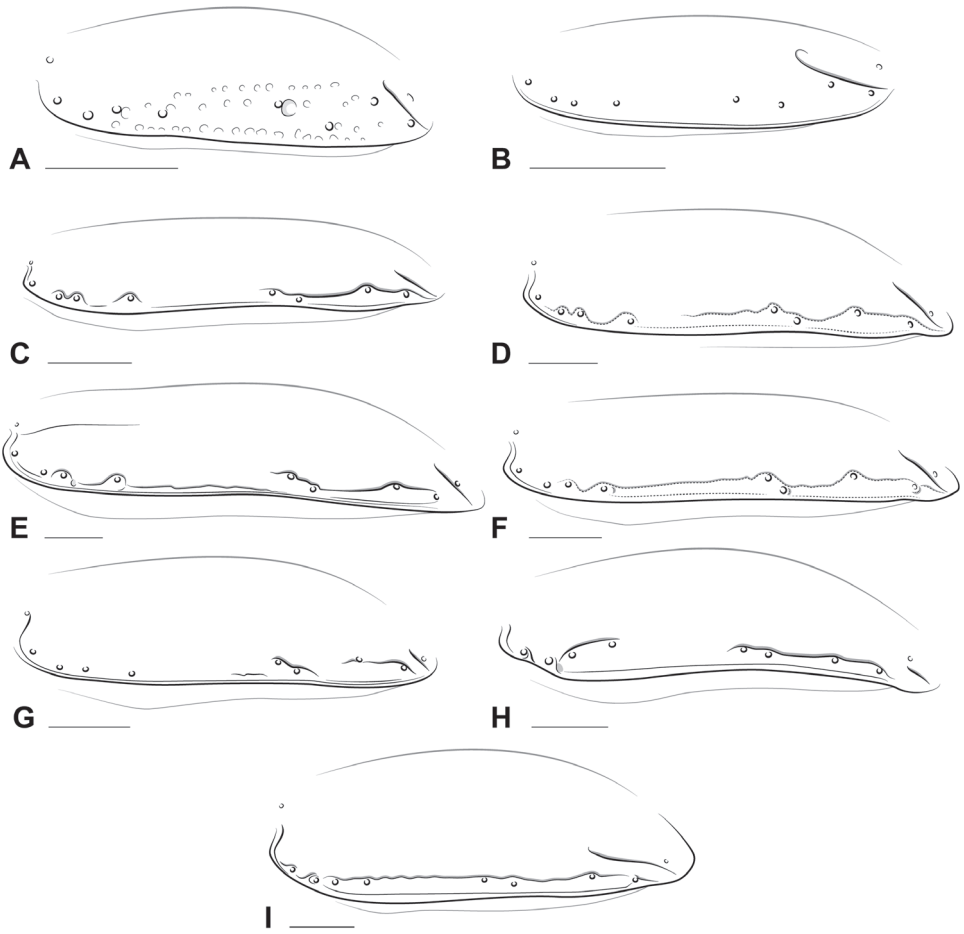

Figure 4. Illustrations of left elytron, lateral view, showing variation in the form of the 8th elytral interneur (other interneurs not shown) among newly described taxa. **A** *Stigmatachys uvea* (holotype, ♀) **B** *Polyderidius* sp. **C** *Nothoderis* sp. **D** *Meotachys* (*Scolistichus*) *riparius*; **E** *Meotachys* (*Hylotachys*) *ballorum*; **F** *Elaphropus* (*Ammotachys*) *marchantarius* **G** *Elaphropus* (*Idiotachys*) *acutifrons* **H** *Elaphropus* (*Nototachys*) *occidentalis* **I** *Tachyxysta howdenorum*. Scale bars = 0.25 mm.

Elaphropus (*Ammotachys*) *marchantarius* sp. n.

http://zoobank.org/DEB2BADC-BEEC-430D-B80D-735BB7407ADC
Figs 1E, 2F, 3F, 4F, 5F

Type material. Holotype: male (NMNH) with following label data: "BRAZIL/AM-(Rio Solimões) / Ilha de Marchantaria / 59°58'W 3°15'S;Várzea / J. Adis leg. 22 I 1982". Paratypes: 8 (6 male, 2 female) in NMNH, ZSM from "BRAZIL/AM-(Rio Solimões) / Ilha de Marchantaria / 59°58'W 3°15'S;Várzea / J. Adis leg. 1.10.81" [1♂, NMNH], "BRAZIL/AM-(Rio Solimões) / Ilha de Marchantaria / 59°58'W 3°15'S;Várzea / J. Adis leg 20-2.[?] [handwritten] 1989A" // Lago Camaleão: light trap

/ 3.60 m above ground on / *Macrolobium acaciifolium* / leg. C Martius/A Rebello" [1♂, NMNH], handwritten label: "Jacareacanga / Para Brasie / XII-1968 / M. Alvarenga" [1♂, NMNH], "VENEZUELA, T.F.Amaz. / San Carlos de Rio / Negro, 23 Jan. 1985 / P. & P. Spangler, / R.Faitoute,W.Steiner" [1♂, NMNH], "LETICIA,Amazonas / Colombia 700 ft. / Feb.23-Mar.2/74 / H. & A. Howden" [2♂, UASM], "BRAZIL/ AM-(Rio Solimões) / Ilha de Marchantaria / 59°58'W 3°15'S;Várzea / J. Adis leg. 22.XII 1981[?]" [1♀, NMNH], "Jacaré P.N.Xingu / M.Grosso- Bras. / XI.1961 / leg.M.Alvarenga" [1♀, ZSM].

Type locality. Brazil: Amazonas: Rio Solimões, Ilha de Marchantaria, 59°58'W 3°15'S.

Description. Size, form, color, microsculpture, head, prothorax, mesothorax, and distribution as in description of the subgenus.

Derivation of specific epithet. The specific epithet *marchantarius* is a toponym referring to Ilha de Marchantaria, the collection locality of the majority of type material, located near Manaus, Brazil.

Subgenus *Idiotachys* subgen. n.
http://zoobank.org/F61DBD6D-C37B-4643-AA9E-15632116072C

Type species. *Elaphropus acutifrons* sp. n.

Diagnosis. Mentum without foveae; head with prominent keel-like frontoclypeal carina; elytral interneurs punctate, incomplete in length, and reduced in number; i8 visible only in apical half, interrupted and reduced.

Description. Size. ABL = 2.15–2.2 mm; SBL = 2.25–2.325; TW = 0.95–1.0 mm.

Form. (Fig. 2G) Oval, compact, somewhat dorsoventrally compressed.

Color. Dark reddish brown, glabrous with some small punctules.

Microsculpture. Apparently absent, but difficult to see due to specimen condition.

Head. Mentum without deep foveae but with very faint, shallow impressions at base; frons (Fig. 3G) without longitudinal furrows but with keel-like medial carina between deep lateral depressions at clypeus; margin above antennal insertion prominent, with deep sinuate groove extending to midpoint of eye; labrum coarsely microsculptured; gula densely pitted.

Prothorax. Pronotum (Fig. 3G) transversely cordiform with sinuate, somewhat reflexed margins; pronotum nearly twice as wide as long at widest point; basal section sculpted with deep longitudinal wrinkles; posterior angles prominent, square, upturned; transverse impression dividing basal section from pronotal disc punctate, interrupted medially by deep, narrow excavation; medial furrow emerging from basal excavation, not reaching anterior margin; anterior transverse impressions lightly impressed, medially convergent; prosternum sulcate, with pair of prominent longitudinal ovoid bumps; procoxae separated by broad, apically rounded prosternal process; protibial apicolateral notch (Fig. 2G) oblique, rounded, not abrupt as is typical across Elaphropus, not bearing spine.

Pterothorax. Mesepisternum neither foveate nor perforate; elytral interneurs 1–2 punctate, with second effaced near apex; i3 only very faintly impressed (Figs 2G, 5G); ARG very

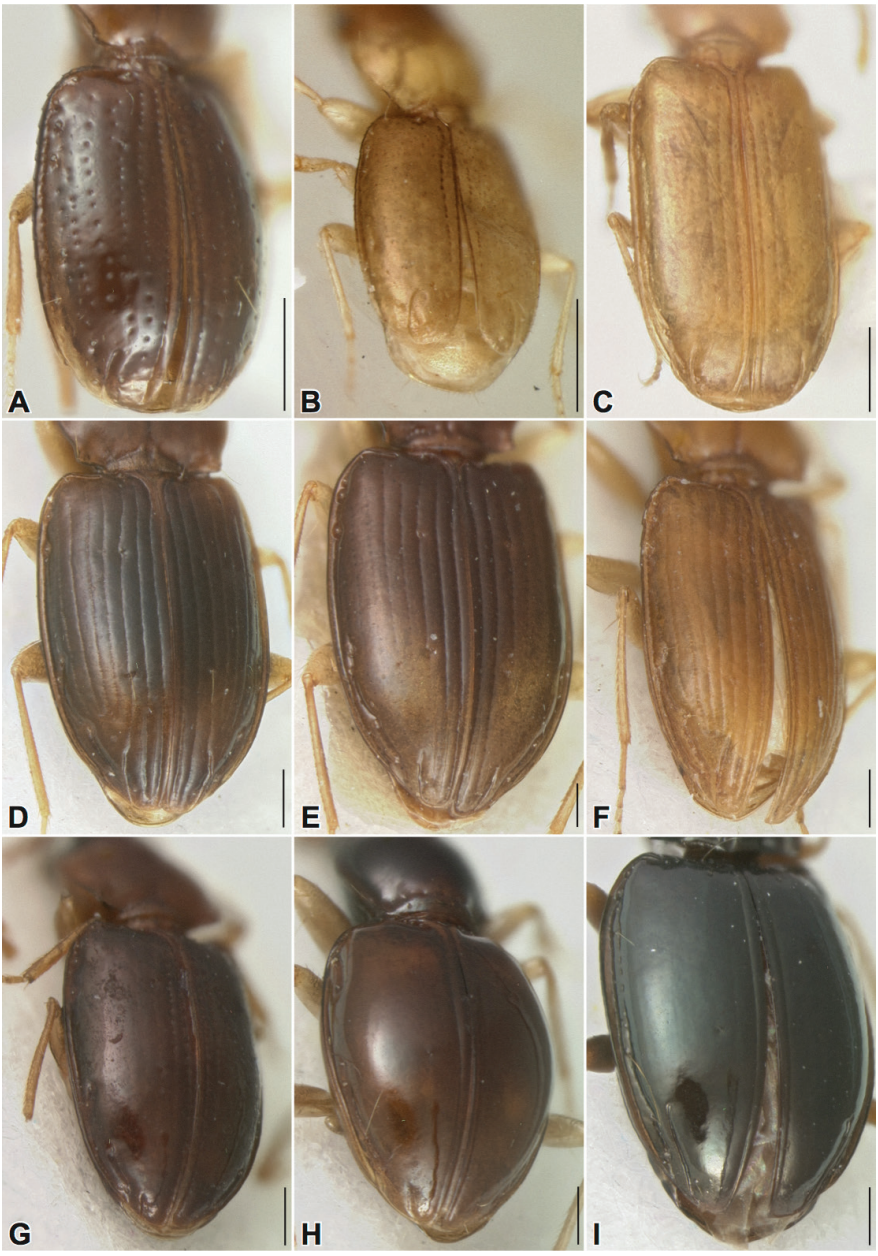

Figure 5. Elytral apex, left dorsal oblique view. **A** *Stigmatachys uvea* (holotype, ♀), Perú, Loreto, Campamento San Jacinto **B** *Polyderidius* sp., México: San Luis Potosí **C** *Nothoderis rufotestacea*, USA: AZ: Cochise Co. **D** *Meotachys* (*Hylotachys*) *ballorum* (paratype, ♀), Brazil, Amazonas, Tapurucuara **E** *Elaphropus* (*Ammotachys*) *marchantarius* (paratype, ♂), Venezuela, San Carlos de Rio Negro **F** *Meotachys* (*Scolistichus*) *riparius* (paratype, ♀), Brazil, Amazonas, Rio Solimões, Ilha de Marchantaria **G** *Elaphropus* (*Idiotachys*) *acutifrons* (paratype, ♀), Brazil, Santarem **H** *Elaphropus* (*Nototachys*) *occidentalis* (paratype, ♂), Perú, Madre de Dios, Pakitza **I** *Tachyxysta howdenorum* (holotype, ♂), México, Chiapas, El Aguacero. Scale bars = 0.25 mm.

short, extending past Ed4; i8 (Fig. 4G) interrupted, partially impressed, just visible near (but not passing through) Eo5 and 6, and between Eo7 and 8; elytron with 9 ombilicate and 4 discal setae; humeral setal insertions widely spaced along basal third of elytral margin.

Genitalia. Not examined.

Distribution. Known only from the type locality of Santarém, Pará, Brazil.

Derivation of name: Masculine. From the Greek adjective *ídios* (="self/peculiar"), in reference to its unique combination of characters, and *Tachys*, the nominate genus of the subtribe Tachyina.

Remarks. Based on its afoveate mentum and apicolaterally notched protibiae, the only known species of *Idiotachys* is considered to be part of the greater *Elaphropus* complex. The overall proportions, reduced and punctate elytral strial interneurs, reduced 8th interneur, and arrangement of humeral elytral ombilicate setae diagnostic for the species described below preclude its placement in any existing *Elaphropus* subgenus. These, along with unique external characters, support *Idiotachys* as a lineage distinct from either *Tachyura* or *Barytachys*, the two subgenera it most closely resembles.

Elaphropus (*Idiotachys*) *acutifrons* sp. n.

http://zoobank.org/9DDB4A8E-DE04-4868-805A-3F02903391E6
Figs 2G, 3G, 4G, 5G

Type material. Holotype: female (AMNH) with following label data: "Santarem". Paratypes: 1 female in NMNH, from type locality.

Type locality. Brazil: Pará, Santarém.

Description. Form, size, color, head, prothorax, pterothorax, and distribution as in description of the subgenus.

Derivation of specific epithet. Derived from the Latin *acutus* (="sharp") and *frons* (="front"), in reference to this species' distinctive raised frons.

Subgenus *Nototachys* Alluaud, 1930, stat. n.

Type species. *Tachys comptus* Andrewes, 1922

Diagnosis. Mentum without paired foveae; antennae apically lighter than at base (Fig. 2H); dorsal surface glabrous, without microsculpture; pronotum (Fig. 3H) narrowed at base, with posterior angle approximately square or projecting slightly laterad and produced slightly anterior to base of pronotum; foretibia with apicolateral notch; elytron with two pale maculae; i8 inserted basally into deep pit between Eo2 and Eo3; i8 (if complete) distant from elytral margin at midpoint, or (if interrupted) (Fig. 4H) deeply impressed basally and apically; mesepisternum (Fig. 7A) with one or two deep pits; elytron with 4 or 5 discal setae (if 5, 2 basal setae positioned close together); only i1 and i8 visibly impressed; Eo4 distant from Eo3; ARG short, simple.

Distribution. Southern Africa, South Asia, and South America.

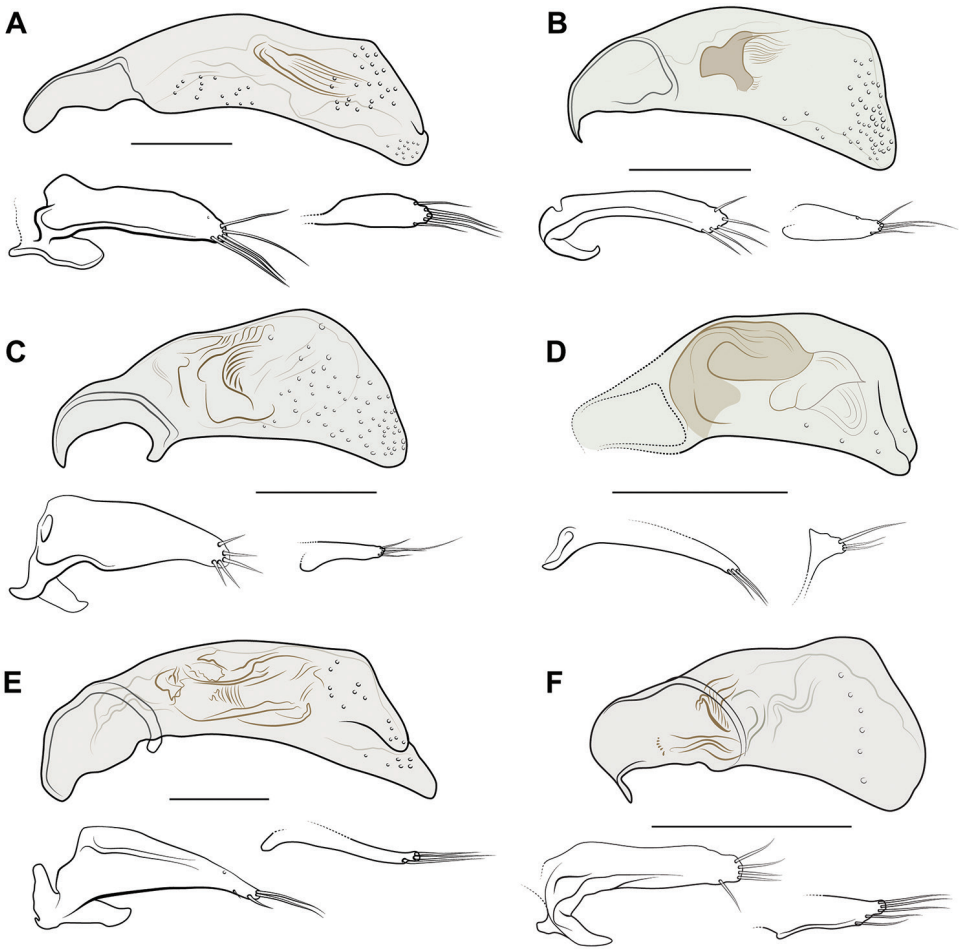

Figure 6. Illustrations of aedeagus, left lateral aspect, with parameres (left and right) shown below median lobe. **A** *Meotachys* (*Hylotachys*) *ballorum*, DRM voucher DNA2854 **B** *Nothoderis* sp., DRM voucher DNA2870 **C** *Nothoderis sp.*, DRM voucher DNA2935 **D** *Polyderis laeva*, DRM voucher DNA2913 **E** *Tachyxysta howdenorum*, DRM voucher 4881 **F** *Nothoderis rufotestacea*, DRM voucher DNA0718. Scale bars = 0.1 mm.

***Elaphropus* (*Nototachys*) *occidentalis* sp. n.**
http://zoobank.org/D1442F62-1AD0-45B4-985C-A7E913943CE9
Figs 2H, 3H, 4H, 5H, 7A

Type material. Holotype: male (NMNH) with following label data: "PERU: LORETO / Pithecia 16May90 / 74°45'W 05°28'S / T.L. Erwin Coll. // At light on Launch / in evening after / sunset'. Paratypes: 12 (4 male, 8 female) in AMNH, CAS, CMNH, MZUSP, NMNH, from "PERU: LORETO 1km SW Boca / del Rio Samira Vigilante Post / No. 1 130m 31 Aug 1991 / 04°40.5'S 074°18.9'W // Treading margins of open / grassy

marsh, no water / T.L. Erwin & M.G. Pogue / Lot 73" [1♂, NMNH], "Rio Cauaburi / AM, Brasil / 9.XII.1962 / J.Bechyné col." [1♂, MZUSP], "COLOMBIA:Amazonas / Leticia, 15-VI-65 / P. R. Craig / and J. Robb" [1♂, CAS], "PERU: MADRE DE DIOS / Pakitza, Rio Manu / 6&9Feb90 T.L. Erwin / 70°58'W 12°07'S // Treading and / quaking river edge / fine silt/sand, / sparse vegetation" [1♂, 1♀, NMNH], "PERU: MADRE DE DIOS / Pakitza, Varzea / 18&21Feb90 TL Erwin / 70°58'W 12°07'S // In leaf litter on / upper flood margin / of Cocha Chica / Tr. Pacal /57" [1♀, NMNH], "PERU: MADRE DE DIOS / Pakitza, quebrada / 06Feb90 T.L. Erwin / 70°58'W 12°07'S // Under leaves at / edge of stream / behind lab, silt" [1♀, NMNH], PERU: LORETO, San / Regis, Rio Maranon / 73°57'W 04°32'S / 04May90, dusk // river margin, at / light on Launch / T.L. Erwin Coll." [1♀, NMNH], PERU: Madre de Dios / Rio Tambopata Res. / 30km (air) sw Pto. / Maldonato, 290m / 12°50'S 069°20'W // B.M. 1983-455 / N.E.Stork / 3.x.-15.xi.1983 / riverbank" [1♀, NMNH], "BRASIL:Barra do / Tapirape, Mato Grosso, / I:1-15:1966 / B.Malkin leg." [1♀, CMNH], ARGENTINA,Tucuman: / 15 Km.N.Tucuman, / Rio Sali. / Dec.30,1971 833 / Lee Herman" [1♀, AMNH], handwritten: "Rep Arg / Tucuman / Ciudad 111-59" [1♀, NMNH].

Type locality. Perú: Loreto, Pithecia, 74°45'W, 05°28'S.

Diagnosis. Mentum without foveae; elytron smooth, with two pale maculae and 5 discal setae, Ed1–3 closely grouped in basal third (Fig. 2H); pronotum (Fig. 3H) narrowed at base; mesepisternum (Fig. 7A) with two deep pits; apical half of antennae (Fig. 2H) lighter than basal half.

Description. Size. ABL = 2.0–2.4 mm; SBL = 2.4–2.7 mm; TW = 1.0–1.2 mm.

Form. (Fig. 2H) Convex, shiny, glabrous; pronotum distinctly narrowed at base.

Microsculpture. Absent except for isodiametrically microsculptured labrum.

Color. Glabrous, rufotestaceous to piceous; elytron with two pale maculae.

Head. Mentum without foveae; frons without longitudinal depressions; frontoclypeal suture with very short lateral subfoveate grooves extending posteriad; apical half of antennae abruptly lighter that basal half, nearly white in many specimens.

Prothorax. Pronotum (Fig. 3H) narrowed at base, margins sinuate; posterior angle approximately square; lateral margin of pronotum narrowly explanate, with flange about 2× wider at midpoint than at base or apex and bordered by lateral groove; lateral groove extending to posterior angle; shallow, transverse basal impressions reduced to a series of several small, shallow punctules; basal two protarsomeres of male dilated, medially dentiform.

Pterothorax. Mesepisternum (Fig. 7A) with two deep, circular pits; elytral interneur 8 (Fig. 4H) very deeply impressed from Eo2–4, completely effaced between Eo4 and Eo5, deeply impressed from Eo5 to apex; dorsal surface glabrous and without microsculpture; elytral margin smooth; elytra apically narrowed after Eo5+6; each elytron with two pale spots; i1 subsulcate, 2–7 only visible as subcuticular dots; elytron with 5 discal setae, Ed1–4 in basal ⅔, Ed5 near tip of ARG (Fig. 2H); humeral setal insertions (Fig. 4H) asymmetrically distributed, with 4th removed from 1–3; elytral ombilicate setae 2, 6, and 8 very long, 2–3× the length of the next longest ombilicate seta; ARG (Fig. 5H) short, shallow, extending just past Ed5.

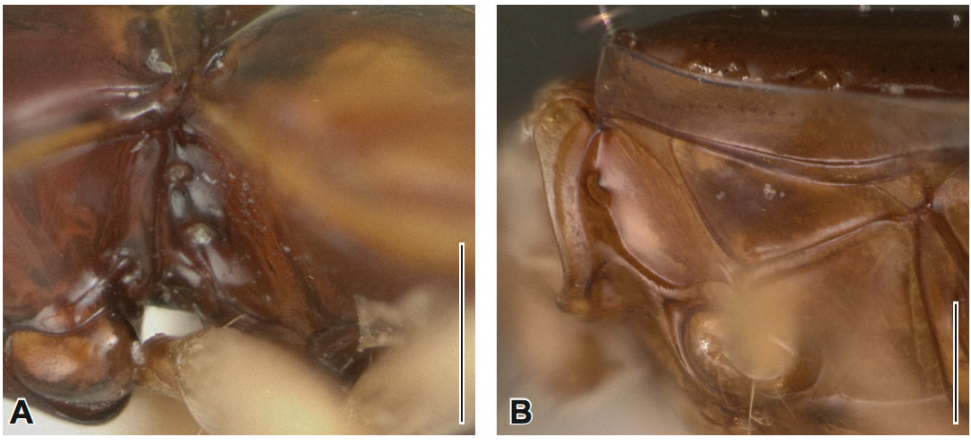

Figure 7. Mesepisternal pits of new Tachyina. **A** *Elaphropus* (*Nototachys*) *occidentalis* (paratype, ♂) Perú, Loreto **B** *Meotachys* (*Hylotachys*) *ballorum* (paratype, ♀), Brazil, Amazonas, Rio Demiti. Scale bars = 0.25 mm.

Genitalia. Not examined.

Distribution. Known from Perú, Brazil, and Argentina. Widespread and apparently abundant in—though not restricted to—riparian habitats.

Derivation of specific epithet. Derived from the Latin *occidens* (="west"), in reference to the New World precinctiveness of this species. This subgenus was previously only described from the Old World.

Genus *Porotachys* Netolitzky, 1914

Type species. *Trechus bisulcatus* Nicolai, 1822

Diagnosis. Large in size (> 4 mm); mentum bearing paired foveae; pronotum quadrate, with square to acute hind angles; base of elytra wider than pronotum; elytra round, convex, with width across elytra conspicuously greatest at midpoint; ARG elongate, straight, very close to and subparallel with lateral margin of elytron.

Distribution. Palearctic—adventive in North America.

Genus *Polyderis* Motschulsky, 1862

Type species. *Tachys brevicornis* Chaudoir, 1846

Diagnosis. Very small (< 2 mm), mentum bearing paired foveae; pronotum convex, posterior angles squarely rounded or slightly obtuse; antennae short, submoniliform; i8 reduced, barely impressed, visible apically; ARG very short.

Distribution. Old World and Australia, with a single species (*P. laeva*) in the Americas.

Genus *Liotachys* Bates, 1871

Type species. *Liotachys antennatus* Bates, 1871.

Diagnosis. Overall form "ant-like"; antennae lighter apically than at base; pronotum pedunculate, slender at base and lacking produced hind angles; mentum bearing paired foveae; elytron smooth, with only i1 visible (subsulcate); i8 not visible; ARG short and arcuate.

Distribution. Amazon basin.

Genus *Tachysbembix* Erwin, 2004

Type species. *Tachysbembix sirena* Erwin, 2004.

Diagnosis. Mentum bearing paired foveae; anterior tibia with apicolateral notch; dorsal surface dull, with coarse, granulate microsculpture; head and eyes large; head and pronotum subequal in greatest width; pronotum round, subcordiform; pronotal hind angles tiny, laterally produced; i8 slightly bent around Eo5–6; ARG elongate, anterior hook laterally remote from 4th discal seta. ABL = 3.3–3.9 mm.

Distribution. Known from shoreline habitats along the Pacific coast of Costa Rica (Erwin 2004) and undescribed species from México to Colombia (Erwin in prep).

Genus *Tachys* Dejean, 1821

Type species. *Tachys scutellaris* Stephens, 1828.

Diagnosis. Mentum bearing paired foveae; protibia with apicolateral notch; dorsal surface typically with isodiametric microsculpture; pronotum subquadrate; i8 not markedly diverted around Eo5–6 (Fig. 1B); ARG elongate, hooked anteriorly into or effaced laterad of Ed4 (Fig. 1D).

Distribution. Typically halophilic (Erwin et al. 2002), cosmopolitan.

Genus *Paratachys* Casey, 1918

Type species. *Tachys austinicus* Casey, 1918.

Diagnosis. Mentum bearing paired foveae; protibia with apicolateral notch; dorsal surface typically with transverse linear microsculpture and slight iridescence; pronotum subquadrate; i8 conspicuously bent around Eo5–6 (Fig. 1A); ARG elongate, anteriorly hooked around Ed4 (Fig. 1C) (Erwin et al. 2002).

Distribution. Diverse habitats, cosmopolitan.

Genus *Polyderidius* Jeannel, 1962
Figs 2B, 3B, 4B, 5B

Type species. *Polyderidius rapoporti* Jeannel, 1962 by original designation.

Diagnosis. Mentum with paired, circular foveae; head with three pairs of supraorbital setae (Fig. 3B), antennae submoniliform; elytral apices rounded/truncate (Fig. 2B), apical recurrent groove hooked anteriorly (Fig. 4B). Many species have reduced eyes and some are brachypterous.

Description. Size. ABL = 1.0–1.2 mm; SBL = 1.1–1.3 mm; TW = 0.45–0.5 mm.

Form. Minute, delicate, dorsolaterally compressed.

Color. (Fig. 2B) Uniformly flavous, flavous with darker head, or uniformly testaceous.

Microsculpture. Varied, from coarse/scaly/isodiametric to fine/linear/transverse.

Head. Head with three pairs of supraorbital setae (Fig. 3B); mentum with paired circular or oval-shaped foveae, or with pair of shallow impressions; eyes reduced in most members; antennae submoniliform and densely setose; subapical labial palpomere conspicuously large and bulbous.

Prothorax. (Fig. 3B) Basal section of pronotum triangular; posterior angles of pronotum bluntly square to rounded and slightly obtuse; procoxae narrowly separated by apically pointed prosternal process; male without dilated basal protarsomere(s).

Pterothorax. Elytral interneurs (if visible) punctate to striatiopunctate and very faintly impressed; i1 often entire, striatiopunctate; no trace of i8; apical recurrent groove (Fig. 4B) thin, well-impressed, and hooked anteriorly; elytral apex (Fig. 2B) rounded and truncate; flight wing with fringed margin, or reduced to a minute pad.

Abdomen. Terminal ventrite with two (male) or four (female) elongated setae.

Genitalia. See Jeannel 1962.

Distribution. Known from across South and Central America, México, the southeast United States (Alabama, Mississippi), Hawaii, and islands of the Caribbean (Puerto Rico, Cuba) with the greatest species diversity in the Amazon basin (Adis et al. 1986).

Genus *Stigmatachys* gen. n.
http://zoobank.org/E49F39AB-8125-48DF-9125-7DA310CB72FA

Type species. *Stigmatachys uvea* sp. n.

Diagnosis. Mentum bifoveate; antennae submoniliform; eyes reduced; labial subulate palpomere absent or reduced; lateral margin of pronotum sinuate; elytral humerus rounded; elytral interneurs punctate and reduced in number, with punctures becoming irregular near apex; abdominal sclerites densely and irregularly punctate.

Description. Size. ABL = 1.2 mm; SBL = 1.35 mm; TW = 0.6 mm.

Form. (Fig. 2A) Minute, compact, convex.

Color. Reddish brown, with lighter appendages.

Microsculpture. Mostly absent, with local patches of isodiametric microsculpture at base of head and around eyes.

Head. (Fig. 3A) Antennae submoniliform; mentum with shallow foveae; head with two pairs of supraorbital setae; eyes reduced, each with about 12 large facets; frontoclypeal suture with small lateral subfoveate depressions; frons without longitudinal depressions; margin above antennal insertion prominent, with longitudinal bead; small dark puncture between gular sutures; labial palps very small, with subulate palpomere reduced or absent.

Prothorax. (Fig. 3A) Pronotum markedly cordiform; posterior lateral margin slightly crenulate; basal section triangular and shallowly pitted/sculptured; basal transverse impressions and medial furrow sulcate, meeting at a point to form triangular basal section; prosternal process very narrow.

Pterothorax. Mesepisternum without pits or foveae; humeral angles obliquely rounded; elytra oval, convex, each elytron (Fig. 5A) with 9 ombilicate and 4 discal setae and 6 visible punctate interneurs, with punctures scattered near apex; lateral channel lined with evenly spaced punctures; i8 not visible (Fig. 4A); elytral margin serrate; elytral disc with a few short, fine setae between i4 and margin; ARG (Figs 4A, 5A) short and deeply engraved, slightly curved medially near apex, directed toward i3.

Abdomen. Ventrites densely punctate and moderately setose.

Genitalia. Not examined.

Distribution. Known only from the type locality in Loreto, Perú.

Derivation of name: Masculine. Derived from the Greek noun *stigma* (="mark" or "puncture"), in reference to the coarsely punctate elytra of the lone representative of this genus, and *Tachys*, the nominate genus of the subtribe Tachyina.

Stigmatachys uvea sp. n.

http://zoobank.org/A8FAF4A3-EEA5-4616-BCC8-DE2DD586B564
Figs 2A, 3A, 4A, 5A

Type material. Holotype: female (NMNH) with following label data: "PERU: Dept. Loreto / Campamento San Jacinto / 2°18.75'S, 75°51.77'W / 6 July 1993, 175-215 m / Richard Leschen #39 / ex. rainforest berlese". Paratypes: none.

Type locality. Perú: Loreto: Campamento San Jacinto, 2°18.75'S, 75°51.77'W, 175–215m.

Description. Size, form, color, microsculpture, head, prothorax, pterothorax, abdomen, and distribution as in description of the genus.

Derivation of specific epithet. Derived from the Latin noun *uvea* (="grape"), referring to the ovate shape of the elytra of the holotype in dorsal view.

Genus *Nothoderis* gen. n.
http://zoobank.org/AAD450AD-FC22-45D8-93D4-B1B6F7C0090D
Figs 2C, 3C, 4C, 5C, 6B, C, F

Type species. *Tachys rufotestacea* Hayward, 1900.

Diagnosis. Mentum with paired circular foveae; posterior angles of pronotum square to slightly acute (Fig. 3C); elytral interneurs striatiopunctate to micropunctulate, number visible varied; elytral margin partially to entirely serrate; i8 effaced anteriad of Eo5, separated from elytral margin by Eo5–8 (Fig. 4C); apical recurrent groove slightly arcuate, moderately impressed (Fig. 5C); elytral apex with raised plicate interval between i8 and ARG.

Description. Size. ABL = 1.5–2.4 mm; SBL = 1.6–2.5 mm; TW = 0.6–1.0 mm.

Form. Small to minute, compact to elongate and subdepressed.

Color. Flavotestaceous to rufotestaceous.

Microsculpture. Varied; head and pronotum usually with isodiametric microsculpture; elytra with linear/transverse microsculpture or (rarely) glabrous.

Head. Mentum bifoveate; head with two pairs of supraorbital setae.

Prothorax. (Fig. 3C) Pronotum with prominent, square to slightly acute posterior angles; basal section of pronotum triangular, with straight or curved transverse impressions meeting at base of median furrow; basal protarsomere of male dilated, medially dentiform.

Pterothorax. (Fig. 5C) Elytron with one or more striatiopunctate to micropunctulate interneurs; Eo1 at sharpest point of humeral angle; i8 (Fig. 4C) effaced anteriad of Eo5, medially curved and moderately impressed near apex, separated from margin by Eo5–8; elytral margin partially to entirely serrate, serrations inconspicuous to prominent and individually setigerous; apical recurrent groove slightly arcuate, moderately impressed, continuous with or directed toward i3; elytral apex with raised interval between i8 and ARG.

Genitalia. (Based on male genitalia dissected and examined from single individuals of four different species) Male (Fig. 6B, C, F): overall form varied, median lobe with comb-like internal sclerites; both right and left parameres wedge-shaped, stout at base; left paramere large and broad with dark, sclerotized basal hook and 5 apical setae; right paramere smaller, with 4 or 5 apical setae. Female genitalia not examined.

Distribution. Known from North, Central, and Amazonian South America.

Derivation of name: Feminine. Greek adjective *nothos* (="false/spurious"), in reference to this diverse and New World-restricted group's misleading taxonomic history, and *deris* (="fight" (Bousquet 2012)), from the name *Polyderis*. Members of this genus were previously classified within *Polyderis* based on a lack of useful and distinctive characters owing to their diminutive size; species of *Nothoderis* are restricted to the New World and are morphologically distinct from *Polyderis* (an old world genus with one species, *P. laeva*, widely distributed in North America).

Remarks. Species of *Nothoderis* are united by the shape of the pronotum, course of the eighth elytral interneur, features of male genitalia, form of the elytral apical recurrent groove, and preliminary molecular evidence. Male genitalia of *Polyderis laeva* were

also examined and illustrated, and differ notably from all examples of *Nothoderis* in the form of the internal sclerite(s) and parameres (Fig. 6D). *Polyderis laeva* remains the sole new world representative of *Polyderis* s.str. based on external morphology; in addition, preliminary molecular evidence suggests that *P. laeva* belongs to a lineage phylogenetically distinct from that of *N. rufotestacea* and other representatives of *Nothoderis*. Rather, members of this gen. n. are affiliated with the *Meotachys*/*Pericompsus* complex (Maddison et al. in prep.).

Genus *Meotachys* Erwin, 1974

Type species. *Tachys ampicollis* Bates, 1882.

Diagnosis. Subdepressed to dorsally convex; testaceous to rufous; mentum bearing paired circular foveae; foretibia notched apicolaterally; basal protarsomere of male dilated, medially dentiform; mesepisternum with or without small fovea; elytral strial interneurs varied in form, punctate to striatiopunctate; i8 apically curvy, diverted medially at Eo5–6 and Eo7; ARG short and arcuate or rudimentary and continuous with i3. ABL = 1.2–4.6 mm.

Distribution. Meotachys species occupy diverse habitats and are described from México to southern Brazil (Erwin 1974, 1991).

Subgenus *Scolistichus* subgen. n.

http://zoobank.org/98C5C6F4-3858-46D4-81A0-24B8FC42256A

Type species. *Meotachys riparius* sp. n.

Diagnosis. Pronotum and elytra with fine, linear, transverse microsculpture; pronotum quadrate; mesepisternum without fovea(e); elytron with smooth margin and 8 micropunctulate interneurs, 4–7 not extended to apex; apical recurrent groove rudimentary, continuous with i3.

Description. Size. ABL = 2.3–2.35; SBL = 2.475–2.55; TW = 1.05–1.075 mm.

Form. Elongate, subdepressed.

Color. (Fig. 2D) Dark rufous to piceous or bicolored, with head and pronotum lighter.

Microsculpture. Microsculpture of anterior part of head coarse, scaly, isodiametric; pronotal and elytral microsculpture transverse, linear; elytral surface with slight iridescence.

Head. Mentum bifoveate; frontoclypeal suture very faint, with shallow lateral impressions.

Prothorax. (Fig. 3D) Pronotum quadrate; basal section triangular, posterior margin with short rugae; basal transverse impressions well-defined, punctate, interrupted by shallow basal excavation; thin medial furrow emerging from basal excavation not reaching anterior margin of pronotum; anterior convergent impressions short, thin, effaced medially; basal protarsomere of male with prominent dentiform medial expansion.

Pterothorax. Elytral margins smooth; elytron (Fig. 5D) with 8 micropunctulate interneurs; i4–7 not reaching apex; i8 (Fig. 4D) curvy and deeply impressed in apical half, abruptly bent around Eo5+6 and Eo7; ARG (see Fig. 1E) rudimentary, continuous with i3; elytral apex with raised interval between i8 and ARG.

Genitalia. Not examined.

Distribution. Known from localities across the Amazon basin, from the upper Rio Negro system to the Rio Napo in Ecuador and northeastern Perú, and the lower Solimões River near Manaus.

Derivation of name: Masculine. From the Greek *skolios* (="crooked"), and *stíchos* (="line"/"row"), in reference to the diagnostic curved 8th interneur.

***Meotachys* (*Scolistichus*) *riparius* sp. n.**
http://zoobank.org/9C5C03C9-A541-46DB-8C06-DC1CC12F4AAF
Figs 2D, 3D, 4D, 5D

Type material. Holotype: male (UASM) with following label data: "LETICIA, Amazonas / Colombia 700 ft. / Feb.23-Mar.2/74 / H. & A. Howden". Paratypes: 5 (1 male, 4 female) in NMNH, UASM, from same locality as holotype [1♀, UASM], "BRASIL Amazonas / Rio Demiti, ca. / 0°37'N 66°48'W / below "Highland / Camp" varzea for. / Sept. 11, 1978 // BRASIL EXP. / 1978 / G.E.& K.E. Ball / Collectors" [1♂, UASM], "BRASIL Amazonas / Rio Demiti, near / Little Homestead / 0°35'N 66°41'W / varzea for. Loc. 1 / Sept. 4, 1978 // BRASIL EXP. / 1978 / G.E.& K.E. Ball / Collectors" [1♀, UASM], BRASIL/AM-(Rio Solimões) / Ilha de Marchantaria / 59°58'W 3°15'S;Várzea / J. Adis leg 13-17.5 [handwritten] 1991 // Lago Camaleão: light trap / 3.60 m above ground on / *Macrolobium acaciifolium* / leg. C Martius/A Rebello" [1♀, NMNH], "ECUADOR Napo Prov. / Laguna Jatuncocha / 20 km s Nuevo Roca- / fuerte on Rio Yasuni / sweep, 8.II.1986 / A.T. Finnamore" [1♀, UASM].

Type locality. Colombia: Amazonas: Leticia, 700 ft.

Description. Form, color, head, prothorax, mesothorax, and abdomen as in description of the subgenus.

Derivation of specific epithet. Derived from Latin *ripa* (="river bank/edge"), in reference to the riparian habitats throughout the Amazon basin from which this species is known.

Subgenus *Hylotachys* subgen. n.
http://zoobank.org/F38109B2-B8B9-436A-A715-E66EFF4EA72B

Type species. *Meotachys ballorum* sp. n.

Diagnosis. Mentum bifoveate, antennae long and slender, pronotal margins sinuate, mesepisternum with single small, deep, reniform pit (Fig. 7B), i1 deeply impressed at base, apical recurrent groove (Fig. 5E) short, faintly impressed.

Description. Size. ABL = 2.7–3.3 mm; SBL = 2.8–3.4 mm; TW = 1.2–1.5 mm.

Form. (Fig. 2E) Elongate, elytra subdepressed to convex.

Color. Matte and dark brown to piceous or glabrous and dark red-brown.

Microsculpture. Varied.

Head. Mentum bifoveate; antennae long, about 2/3 ABL; frons (Fig. 3E) with shallow lateral depressions at clypeus extending posteriad; margin above antennal insertion with shallow groove/channel.

Prothorax. Pronotum (Fig. 3E) transversely quadrate or narrowed near base, with base and apex about equal in width, but greatest width about 1.5× as wide as narrowest width; lateral margin of pronotum markedly sinuate; anterior convergent impressions boldly impressed, not reaching medial furrow; basal transverse impressions deeply punctate, interrupted by small but deep medial excavation; basal section of pronotum opposite scutellum smooth, inflated; thin, medial furrow emerging from basal excavation not meeting anterior margin of pronotum; prosternum smooth, not sulcate.

Pterothorax. Mesepisternum with single, small, reniform pit/fovea, with opening directed slightly posteriad (Fig. 7B); elytron (Fig. 5E) with 3–6 striate interneurs; i1 complete (reaching apex), subsulcate, originating near apex of scutellum, deeply impressed at base; i3–7 incomplete or absent, i3 abruptly bent around Ed2 and Ed3; i5 (either visible as strial interneur or shallow depression) originating at tip of elytral basal margin and clearly separating elytral disc from humeral region; i8 (Fig. 4E) basally effaced and separated from margin by Eo5–8; apical recurrent groove simple, short, faintly impressed.

Distribution. Known from the type locality in Ecuador, as well as 4 localities along the Rio Negro, northern Amazonas, Brazil, and southern Perú.

Derivation of name: Masculine. From the Greek *hyle* (="wood/forest", "matter/substance"), in reference to the association of species of this genus with Amazonian inundation forest habitats and the unique suite of characters uniting the two species, and *Tachys*, the nominate genus of the subtribe Tachyina.

Meotachys (*Hylotachys*) *ballorum* sp. n.

http://zoobank.org/5EFB9951-AD8A-49A1-90AB-8ED61241E65F

Figs 2E, 3E, 4E, 5E, 6A, 7B

Type material. Holotype: male (UASM) with following label data: "BRASIL Amazonas / Rio Negro Cucui / varzea forest / Sept. 17, 1978 // BRASIL EXP. / 1978 / G.E.& K.E. Ball / Collectors". Paratypes: 5 (2 male, 3 female) in UASM, ZSM from the type locality [1♂, UASM], "Brasilien / Tapurucuara am / Rio Negro/Amazonas / 7 11.1963 / C. Lindemann" [1♂, 1♀, ZSM], "BRASIL Amazonas / Rio Demiti, ca. / 0°53'N 66°57'W / "La Laguna" / Varzea forest / Sept. 13, 1978 // BRASIL EXP. / 1978 / G.E.& K.E. Ball / Collectors" [1♀, UASM], BRASIL Amazonas / ca. 10 km. n.e. / São Gabriel da / Cachoeira, stream / margin, forest / Sept. 20, 1978 // BRASIL EXP. / 1978 / G.E.& K.E. Ball / Collectors" [1♀, UASM].

Type locality. Brazil: Amazonas, Rio Negro Cucui.

Description. Head and abdomen as in description of the genus.

Size. ABL = 3.2–3.3 mm; SBL = 3.3–3.4 mm; TW = 1.4–1.5 mm.

Form. (Fig. 2E) Large, elongate, subdepressed.

Color. Uniformly dark brown and slightly iridescent.

Microsculpture. Pronotum and elytron with very fine, linear, transverse microsculpture; head with coarse, isodiametric microsculpture.

Prothorax. Pronotum (Fig. 3E) transversely quadrate, wider than long.

Pterothorax. Elytra broad and parallel-sided, narrowed beginning at apical third, 5–6 visible strial interneurs, first two complete (Fig. 2E); i5 originating at tip of elytral basal margin and separating basal elytral disc from humeral region; otherwise as in description of the genus.

Genitalia. Male (Fig. 6A): median lobe elongate, with slender brush-shaped internal sclerite; left and right parameres both broad and paddle-shaped apically, each with 5 long apical setae; right paramere smaller. Female: not examined.

Distribution. Known from Brazil, Ecuador, and Colombia.

Derivation of specific epithet. Patronym in honor of George and Kay Ball, who collected the major part of the type series on their 1978 expedition to Brazil.

Remarks. The habitat of this species was mistakenly regarded as várzea. In fact the specimens were collected in igapó forest (Ball, personal communication, 2016)

***Meotachys* (*Hylotachys*) *rubrum* sp. n.**

http://zoobank.org/C153738B-61A6-4D63-B269-FBAA9498C2E7

Type material. Holotype: male (NMNH) with following label data: "PERU: MADRE DE DIOS / Rio Manu, BIOLAT Biol. Sta. / Pakitza, 356m, 16 Oct. 1989 / 11°56°47'S 071°17°00'W / T.L. Erwin Trocha Pacal /21". Paratypes: 1 female, in NMNH, from "PERU: MADRE DE DIOS / Rio Manu, BIOLAT Biol. Sta. / Pakitza, 356m, 25 June 1993 / 11°56°47'S 071°17°00'W / T.L. Erwin & F. Pfuno // Treading red-colored leaf litter / at edge of lake shore in sunny / area Tr. Gallareta Lot 524'.

Type locality. Perú: Madre de Dios: Rio Manu, BIOLAT Biol. Sta., Pakitza, 11°56°47'S 071°17°00'W, 356m.

Description. Head and abdomen as in description of the genus.

Size. ABL = 2.7–2.85 mm; SBL = 2.8–2.9 mm; TW = 1.2–1.3 mm.

Form. Head and prothorax slender, elytra rounded and convex.

Color. Uniformly rufotestaceous, shiny.

Microsculpture. Head, pronotum and elytron smooth, glabrous.

Prothorax. Pronotum subequal in length and width.

Pterothorax. Elytra somewhat round and convex, each with 2–3 visible strial interneurs, only i1 completely impressed; i5 position without visible stria, but with gently sloping "shelf" which originates at tip of elytral basal margin and separates basal elytral disc from humeral region.

Genitalia. Not examined.

Distribution. Known only from the type locality in the Madre de Dios region of southeastern Perú.

Derivation of specific epithet. Latin *rubrum* (="red/crimson"), in reference to the deep red-brown color of this species.

Note: The holotype will be deposited in UNMSM and is currently held in trust until the completion of studies at NMNH.

Genus *Pericompsus* LeConte, 1851

Type species. *Bembidium ephippiatum* Say, 1834.

Diagnosis. Mentum with paired foveae; pronotum with continuous, punctate transverse impression; basal transverse impression arcuate or lobed, forming crescent-shaped or bilobed basal section; elytron either with one to two conspicuous subhumeral fovea(e) along i8 in basal fourth or with 8 entirely punctate interneurs; elytra with or without color pattern. ABL = 1.72–3.72 mm. (Erwin 1974a; Erwin et al. 2002).

Distribution. Australia and the Americas.

Subgenus *Pericompsus* sensu stricto

Type species. *Bembidium ephippiatum* Say, 1834.

Diagnosis. Typically elongate, subcylindrical in form; pronotum quadrate to narrowed in basal fourth; elytral i8 with a deep fovea at or just anterior to midpoint of elytron and two smaller, subhumeral foveae of variable size; elytral interneurs punctate to striatiopunctate; elytra usually testaceous with darker markings resembling ink blotches. ABL = 1.88–3.72 mm. (Erwin 1974a; Erwin et al. 2002).

Distribution. Species of this subgenus are numerous and described from across the New World between the temperate mid-latitudes of North and South America and some of the Caribbean islands.

Subgenus *Eidocompsus* Erwin, 1974

Type species. *Trechus brasiliensis* Sahlberg, 1844.

Diagnosis. Broad and robust, depressed to subcylindrical in form; pronotum quadrate, subequal in width at base and apex; elytra usually unicolorous; elytral interneurs punctate; i8 subsulcate and not bearing fovea(e) at or near middle of elytron; i8 with or without subhumeral fovea: if present, then fovea shallow and bearing seta or small, perforate, and located at basal fourth near seta Eo4; if i8 lacking posthumeral foveae, elytron with 8 entirely punctate interneurs. ABL = 1.84–3.04 mm. (Erwin 1974a; Erwin et al. 2002).

Distribution. Species of this subgenus are restricted to the New World, described from México south to Argentina and some of the Caribbean islands.

Discussion

Both species of the *Meotachys* subgenus *Hylotachys* described above are the first "bifoveate' (Ortuño and Arillo 2015) tachyines discovered to possess mesepisternal pits. These structures are highly varied in form and are found in "non-bifoveate" species throughout *Elaphropus* (*Tachyura*) and allied subgenera (incl. *Tachylopha*, *Barytachys*, *Nototachys*, and *Sphaerotachys*) (Erwin 1970), as well as a small subgenus of South American *Bembidion* (Maddison 2014) and certain Oodini (Spence 1982). Nearly all species known to possess these structures are hygrophilous. The waxy substance noted by Maddison (2014) in ethanol-preserved specimens was not observed in any of the specimens of *Hylotachys* examined, which were likely not ethanol-killed.

Previously synonymized under *Polyderis* (Erwin 1974b) and later considered a subgenus, *Polyderidius* Jeannel 1962 should be considered a separate genus, united by consistent morphological characters and distinct from *Polyderis* s.str. Species of *Polyderidius* are instead probably allied with *Paratachys* and *Tachys* s.str., based on the form of the elytral apical recurrent groove.

Nototachys Alluaud, 1930 is a small but distinctive group whose name has been considered a subjective synonym of *Elaphropus* (Erwin 1974) or the *Elaphropus* subgenus *Sphaerotachys* (Sciaky and Vigna-Taglianti 2003), as a subgenus of *Elaphropus* (Bousquet 2012) or *Tachyura* (Kópecky 2003), or as a separate genus (Lorenz 2005). The newly described South American species, *Elaphropus* (*Nototachys*) *occidentalis*, expands the known distribution of this previously Old World-restricted subgenus. *Elaphropus occidentalis* shares aspects of its overall form with *E. comptus* (Andrewes 1922), the type species of *Nototachys*, and its aberrant discal elytral chaetotaxy with *E.* (*Nototachys*) *comptus borealis* (Andrewes 1925).

Relationships among groups within the subtribe Tachyina, in particular *Elaphropus*, remain a subject of contention and have been reviewed by several authors in recent decades. The conflicting taxonomic concepts proposed in previous reviews, classifications, and checklists (Lindroth 1966, Erwin 1974b, Shilenkov 2002, Kopecký 2003, Sciaky and Vigna-Taglianti 2003, Lorenz 2005, Bousquet 2012) represent alternative hypotheses waiting to be tested in a molecular context.

Due to their small size and a lack of resources for their identification, tachyines are easy to overlook or misidentify. A good deal of undescribed tachyine diversity is likely hidden in uncurated material, stored bycatch, and existing collections (Baehr 2016). In the Amazon Basin, ecosystem level processes are thought to have generated the rapid diversification apparent in this and other groups (Erwin and Adis 1978). Detailed collection data and large sample sizes exist for a number of New World species discovered through long term, bulk collecting efforts employing passive traps, leaf litter sampling, and canopy fogging (Erwin 1983, 1984, 1991). Much less is understood of the way of life, intraspecific diversity, and distribution of species described from small series and with limited representation in collections. Conservation status is difficult to estimate for such rarely collected taxa as *Costitachys* and *Tachyxysta*, especially for those known only from unique collecting events (e.g., *Stigmatachys* and *Elaphropus* (*Idiotachys*)). Moreover, anthropogenic impact to rapid-

ly developing regions such as the Atlantic coast of South America has likely already affected the distribution and abundance of both described and undiscovered tachyine species.

Acknowledgements

In addition to the individuals mentioned under *Material examined* above, the authors thank all the collectors and curators who provided specimens for this work: George Ball (UASM), Yves Bousquet (CNC), Warren Steiner (NMNH), Brian Farrell (MCZ), R.C. Graves, and the late Henry Howden, as well as curators Thierry Deuve (MNHN) and Cleide Costa (MZUSP) for loaning critical specimens from the collections of the late J. Negré and Hans Reichardt, respectively. Charyn Micheli provided much support and assistance with the NMNH Tachyina collections during this project, including processing of large loans and acquisition of literature and specimen data. Thanks to D.H. Kavanaugh and G.E. Ball for their comments on the manuscript. We especially thank David Maddison for his many hours of advice and encouragement throughout the project and for his valuable comments on drafts of the manuscript. This work was funded in part from the Harold E. and Leona M. Rice Endowment Fund at Oregon State University, through David Maddison. Funding for article processing charges was provided by the National Museum of Natural History, Smithsonian Institution, Department of Entomology.

References

Adis J, Paarmann W, Erwin TL (1986) On the Natural History and Ecology of Small Terrestrial Ground-Beetles (Col.: Bembidiini: Tachyina: Polyderis) from an Amazonian Black-Water Inundation Forest. In: Carabid Beetles, 413–427.

Alluaud C (1930) Étude des *Tachys* Africains. II. *Nototachys* subg. nov. Afra 2: 14–15.

Andrewes HE (1922) Papers on Oriental Carabidae. The Annals and Magazine of Natural History 9: 161–169. doi: 10.1080/00222932208632757

Andrewes HE (1925) A Revision of the Oriental Species of the Genus *Tachys*. Annali del Museo Civico di Storia Naturale di Genova 51: 372–502.

Baehr M (2016) A peculiar gen. n. of the Bembidiine subtribe Tachyina from northern Queensland, Australia (Insecta, Coleoptera, Carabidae, Bembidiini, Tachyina). Transactions of the Royal Society of South Australia 35: 99–110. doi: 10.1080/03721426.2016.1147116

Bates HW (1871) Notes on Carabidae, and descriptions of new species (No. 2). The Entomologist's Monthly Magazine 7: 244–248.

Bates HW (1882) Insecta, Coleoptera, Carabidae. In Godman and Salvin, Biologia Centrali-Americana 1(1): 40–152.

Bousquet Y (2012) Catalogue of Geadephaga (Coleoptera, Adephaga) of America, north of Mexico. ZooKeys 245: 1–1722. doi: 10.3897/zookeys.245.3416

Casey TL (1918) A review of the North American Bembidiinae. Memoirs on the Coleoptera VIII, 1–223.

Chaudoir M de (1846) Enumération des Carabiques et Hydrocanthares, recueillis pendant un voyage au Caucase et dans les provinces transcaucasiennes par Baron M. de Chaudoir et le Baron A. de Gotsch. J. Wallner, Kiew, 1–268.

Chaudoir M de (1868) Observations synonymiques sur les Carabiques de l'Amérique septentrionale et descriptions d'espèces nouvelles de ce pays. Revue et Magasin de Zoologie Pure et Appliquée II 20: 212.

Dejean PFMA (1821) Catalogue de la collection de coléoptères de M. le Baron Dejean. Crevot, Paris, 1–136. doi: 10.5962/bhl.title.11259

Duftschmid CE (1812) Fauna Austriae, oder Beschreibung der österreichischen Insekten für angehende Freunde der Entomologie. Zweyter Theil. Akademie Buchhandlung, Linz und Leipzig.

Erwin TL (1970) Unique structures in members of *Tachys* sensu lat. (Coleoptera: Carabidae). The Pan-Pacific Entomologist 46: 231–232.

Erwin TL (1974a) Studies of the subtribe Tachyina (Coleoptera: Carabidae: Bembidiini), Part II: A Revision of the New World-Australian Genus *Pericompsus* LeConte. Smithsonian Contributions to Zoology, 1–96. doi: 10.5479/si.00810282.162

Erwin TL (1974b) Studies of the Subtribe Tachyina (Coleoptera: Carabidae: Bembidiini) Supplement A: Lectotype designations for new world species, two new genera, and notes on generic concepts. Proceedings of the Entomological Society of Washington 76: 123–155.

Erwin TL (1975) Studies of the Subtribe Tachyina (Coleoptera: Carabidae: Bembidiini), Part III: Systematics, Phylogeny, and Zoogeography of the Genus *Tachyta* Kirby. Smithsonian Contributions to Zoology. doi: 10.5479/si.00810282.208

Erwin TL (1983) Beetles and other insects of tropical forest canopies at Manaus, Brazil, sampled by insecticidal fogging. In: Tropical Rainforest Ecology, 59–75.

Erwin TL (1984) Small terrestrial ground-beetles of the Amazon basin (Coleoptera: Bembidiini: Tachyina and Anillina). Amazoniana 8: 511–518.

Erwin TL (1991) Natural history of the carabid beetles at the BIOLAT Biological Station, Rio Manu, Pakitza, Peru. Revista Peruana de Entomologia 33: 1–85.

Erwin TL (1994) Arboreal beetles of tropical forests: the Xystosomi group, subtribe Xystosomina (Coleoptera: Carabidae: Bembidiini). Part I. Character analysis, taxonomy, and distribution. The Canadian Entomologist 126: 549–666. doi: 10.4039/Ent126549-3

Erwin TL (2004) The beetle family Carabidae of Costa Rica and Panamá: Descriptions of four new genera and six new species with notes on their way of life (Insecta: Coleoptera). Zootaxa 18: 1–18.

Erwin TL, Adis J (1978) Amazonian Inundation Forests: Their Role as Short-Term Refuges and Generators of Species Richness and Taxon Pulses. In: Prance GT (Ed.) Biological Diversification in the Tropics, 358–371.

Erwin TL, Kavanaugh DH (1999) Studies of the Subtribe Tachyina (Coleoptera: Carabidae: Bembidiini), Supplement D: Description of a male of *Costitachys inusitatus* Erwin, with notes on distribution of this species. The Coleopterists Bulletin 53: 52–55.

Erwin TL, Kavanaugh DH (2007) Studies of the Subtribe Tachyina (Coleoptera: Carabidae: Bembidiini). Supplement E: A Revision of Genus *Costitachys* Erwin 1974. Proceedings of the California Academy of Sciences 58: 331–338.

Erwin TL, Kavanaugh DH, Moore W (2002) The Family Carabidae: Key to the Tribes and Genera known to occur in Costa Rica. http://www.inbio.ac.cr/papers/carabidae/esp/images/CR_carabid_key.doc

Hayward R (1900) A study of the species of Tachys of boreal America. Transactions of the American Entomological Society 24: 32–143.

Kirby W (1837) The insects. In: Richardson J (Ed.) Fauna Boreali-Americana. J. Fletcher, Norwich, 325 pp.

Jeannel R (1962) Les Trechides do la Paléantarctide Occidentale. In: Biologie de l°Amérique australe. Volume I. Paris, 527–655.

Kopecký T (2003) Subtribe Tachyina Motschulsky, 1862. In: Löbl I, Smetana A (Eds) Catalogue of Palaearctic Coleoptera l: Archostemata - Myxophaga - Adephaga. Apollo Books, Stenstrup, 273–280.

LeConte JL (1848) A descriptive catalogue of the geodephagous Coleoptera inhabiting the United States east of the Rocky Mountains. Annals of the Lyceum of Natural History of New York 4: 173–474. doi: 10.1111/j.1749-6632.1848.tb00277.x

LeConte JL (1851) Descriptions of new species of Coleoptera, from California. Annals of the Lyceum of Natural History of New York 5: 125–184. doi: 10.1111/j.1749-6632.1852.tb00123.x

Lindroth CH (1966) The ground-beetles (Carabidae, exdl. Cicindelinae) of Canada and Alaska. Part 4. Opuscula Entomologica, Supplementa 29, 409–648.

Lorenz W (2005) Systematic list of extant ground beetles of the world. W. Lorenz, privately published by the author. Tutzing, Germany.

Maddison DR (2014) An unexpected clade of South American ground beetles (Coleoptera, Carabidae, Bembidion). ZooKeys 155: 113–55. doi: 10.3897/zookeys.416.7706

Motschulsky V de (1839) Coléoptères du Caucase et des provinces transcaucasiennes. Bulletin de la Société Impériale des Naturalistes de Moscou 12: 68–93.

Motschulsky V de (1851) Enumération des nouvelles espèces de coléoptères rapportés par M. Victor Motschoulsky de son dernier voyage. Bulletin de la Société Impériale des Naturalistes de Moscou 24: 479–511.

Motschulsky V de (1862) Entomologie spéciale. Remarques sur la collection d°insectes de V. de Motschulsky. Coléoptères. Études Entomologiques 11: 15–55.

Netolitzky F (1914) Die Bembidiini in Winklers Catalogus. Entomologische Blätter 10: 164–176.

Nicolai EA (1822) Dissertatio inauguralis medica sistens Coleopterorum species agri Halensis. Grunert, Halae, 1–48.

Ortuño VM, Arillo A (2015) Fossil carabids from Baltic amber–III–*Tarsitachys bilobus* Erwin, 1971: an interesting fossil ground beetle from Baltic amber (Coleoptera: Carabidae: Trechinae): Redescription and comments on its taxonomic placement. Zootaxa 4027: 578–586. doi: 10.11646/zootaxa.4027.4.7

Sahlberg RF (1844) Coleoptera diebus 15–27 Decembris anni 1839 ad Rio Janeiro lecta. Acta Societatis Scientiarum Fennicae 2(1): 499–522.

Say T (1834) Descriptions of New North American Insects and Observations on Some Already Described. Transactions of the American Philosophical Society 4: 409–470. doi: 10.2307/1004840

Sciaky R, Vigna-Taglianti A (2003) Observations on the systematics of the tribe Tachyini (Coleoptera Carabidae). Bollettino della Societa Entomologica Italiana 2: 79–96.

Shilenkov VG (2002) New data on the taxonomy of the carabid tribe Tachyini (Coleoptera, Carabidae). Entomologicheskoe Obozrenie 81(1): 31–4.

Spence JR (1982) Taxonomic status, relationships, and biogeography of *Anatrichis* LeConte and *Oodinus* Motschulsky (Carabidae: Oodini). The Coleopterists Bulletin 36: 567–580.

ZooKeys 626: 125–135 (2016)
doi: 10.3897/zookeys.626.7918
http://zookeys.pensoft.net

RESEARCH ARTICLE

A peer-reviewed open-access journal
ZooKeys
Launched to accelerate biodiversity research

Three spider species of the genus *Mimetus* Hentz, 1832 (Araneae, Mimetidae) from China

Chen Zeng[1], Cheng Wang[2], Xian-Jin Peng[1]

1 *College of Life Sciences, Hunan Normal University, Changsha, Hunan 410081, China* **2** *College of Biological, Agricultural and Forest Engineering, Tongren, Guizhou 554300, China*

Corresponding author: *Xian-Jin Peng* (xjpeng@126.com)

Academic editor: *Shuqiang Li* | Received 1 February 2016 | Accepted 6 October 2016 | Published 25 October 2016

http://zoobank.org/F11D0387-AF43-4DA4-8DC4-C48B67FD9E04

Citation: Zeng C, Wang C, Peng X-J (2016) Three spider species of the genus *Mimetus* Hentz, 1832 (Araneae, Mimetidae) from China. ZooKeys 626: 125–135. doi: 10.3897/zookeys.626.7918

Abstract

The present paper deals with three species of the genus *Mimetus* from China, including *M. echinatus* Wang, 1990, *M. lamelliformis* **sp. n.** (male), and *M. wangi* **sp. n.** (female and male). *M. lamelliformis* differs from the related species *M. echinatus* Wang, 1990 by: cymbial tip with several slender long macrosetae; cymbium boat-shaped, length/width ratio about 3/1 in retrolateral view; vexillum about 1/2 length of cymbium in retrolateral view. *M. wangi* **sp. n.** differs from the related species *M. sinicus* Song & Zhu, 1993 by: the opisthosoma with a pair of distinct outgrowths in the dorsum; sperm duct nearly horizontal; spermathecae kidney shaped and contiguous. Photos of body and copulatory organs, line drawings of copulatory organs, as well as the locality map are provided.

Keywords

Taxonomy, new species, Asia, diagnosis, redescription

Introduction

The genus *Mimetus* was established by Hentz (1832) with the type species *M. syllepsicus* Hentz, 1832. A total of 54 species have been described from all over the world except Australia and Antarctica. Up to now, only six species have been recorded from China by Wang (1990), Liang and Wang (1991), Song and Zhu (1993) (World Spider Catalog 2016). *Mimetus* species can be distinguished from members of other genera by the male

bearing a "shovel" (a shovel-like appendage on the dorsal edge of the cymbium), and a "vexillum" (the distal sclerotized extension of the shovel) (Heimer 1986), in combination with a bulb possessing sclerites S2–S5 and three longitudinal lines of spines on the carapace (Harms and Dunlop 2009). Female epigyne simple but distinct, with two inconspicuous copulatory opening, spermatheca strongly sclerotized (Harms and Harvey 2009a, b).

While examining specimens collected from Hunan, Guizhou and Yunnan Provinces, two members of *Mimetus* were identified as new species and one was identified to be *M. echinatus* Wang, 1990. Descriptions and diagnoses of the new species and a redescription of *M. echinatus* have been presented in this paper.

Material and methods

All specimens were kept in 75% ethanol, examined and measured with an Olympus SZX16 stereomicroscope and an Olympus BX53 compound microscope, respectively. Photos were taken with a digital camera Canon Powershot G12 mounted on an Olympus SZX16 and compound focus images were generated using Helicon Focus Software (3.10).

Specimens are deposited in the College of Life Sciences, Hunan Normal University, Changsha, China. All measurements are given in millimeters (mm). Leg measurements are given as: total length (femur, patella + tibia, metatarsus, tarsus). The abbreviations used in text including:

AER anterior eye row;
ALE anterior lateral eye;
AME = anterior median eye;
CD copulatory duct;
CO copulatory opening;
E embolus;
FD fertilization duct;
M membrane;
MOA median ocular area;
P paracymbium;
PER posterior eye row;
PLE posterior lateral eye;
PME posterior median eye;
S spermatheca;
SH shovel;
ST subtegulum;
VE vexillum.

Taxonomy

***Mimetus* Hentz, 1832**

***Mimetus echinatus* Wang, 1990**
Figs 1–4

Mimetus echinatus Wang, 1990: 44, fig. IV.6–10 (male and female).

Type material examined. 2♂, 1♀, **China, Hunan,** Changsha City, Yuelu Mountain, 20 April 1981, Jiafu Wang leg.;

Figure 1. *Mimetus echinatus* Wang, 1990, one of the males. **A** habitus, dorsal view **B** palp, prolateral view **C** palp, retrolateral view. Scale bars: **A**, 1.0; **B–C**, 0.2.

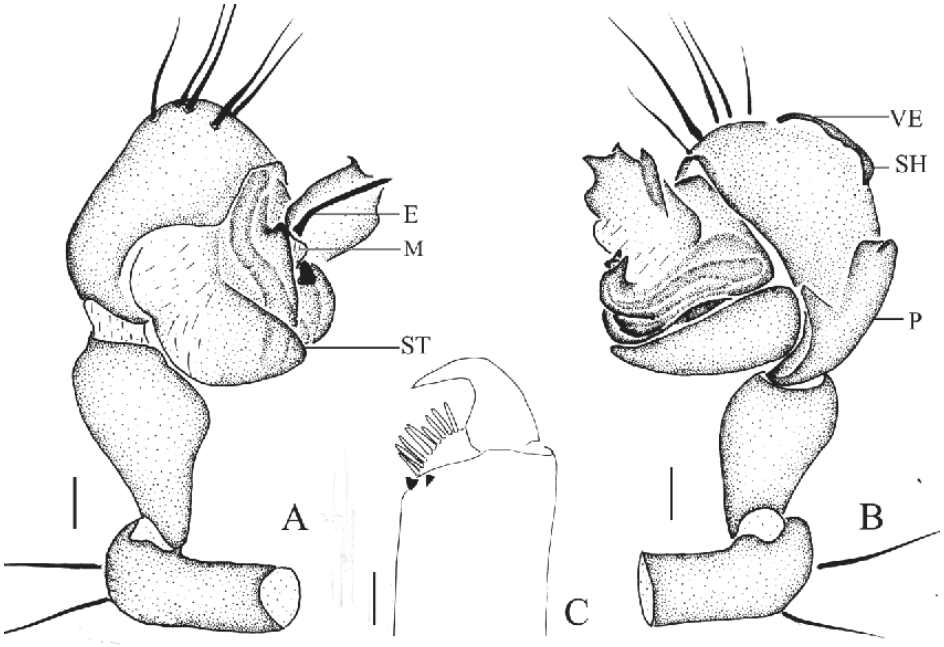

Figure 2. *Mimetus echinatus* Wang, 1990, one of the male. **A** palp, prolateral view **B** palp, retrolateral view **C** left chelicera, ventral view. Scale bars: **A–B**, 0.2; **C**, 0.1.

Other material examined. 6♂, 2♀, **China, Hunan,** Shimen County, Huping Township, Daling Village, 30.02175°N, 110.37455°E, 710m, 19 June 2014, Cheng Wang, Bing Zhou, Jiahui Gan and Yuhui Gong leg.

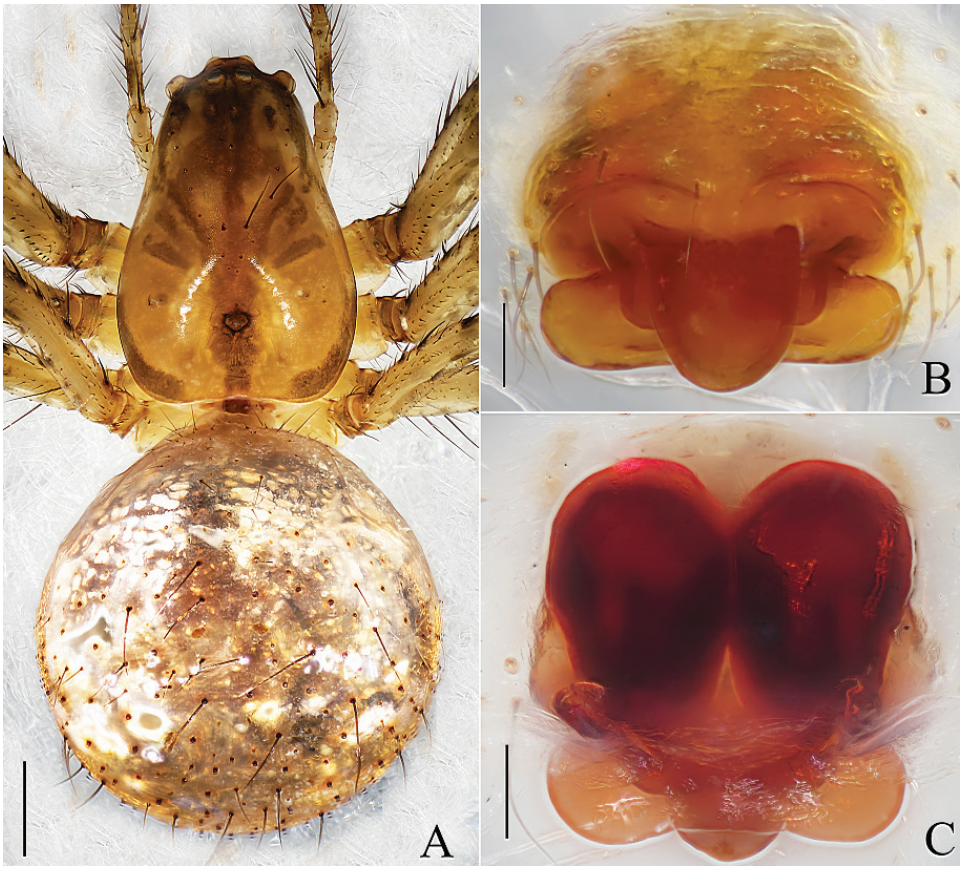

Figure 3. *Mimetus echinatus* Wang, 1900, from Shimen. **A** habitus, dorsal view **B** epigyne, ventral view **C** vulva, dorsal view. Scale bars: **A**, 1.0; **B–C**, 0.1.

Redescription. Male. Carapace (Fig. 1A) bright yellow, long oval, widest at coxae II and III. Fovea circular, deep, its surrounding area reddish brown. Sternum light yellow, pear-shaped, the surrounding with seven gray circular patches, margin with long scopulae, median glabrous. AER slightly recurved, PER nearly straight, ALE and PLE contiguous. Chelicerae reddish brown, with 9 promarginal peg setae and 2 retromarginal teeth (Fig. 2C). Color of endites and labium similar. Legs spiniferous, femora with reddish brown patches. Dorsum of opisthosoma (Fig. 1A) suboval, light yellow-brown, with white patches on both sides, covered with long macrosetae. Venter grayish-white, with round white patches.

Male palp (Figs 1B–C, 2A–B): Patella strong, the dorsum with two thick and long macrosetae. Cymbium wedge, length/width ratio about 2/1, tip with several robust macro-setae Paracymbium distinct, distal black and strongly sclerotized. Distal division of the bulb rolls up as sulciform to protect embolus and serves as a functional conducter. Embolus relatively slender, distal division reaches the position of 2:00 o'clock approximately with a membrane covering its proximal area in prolateral view.

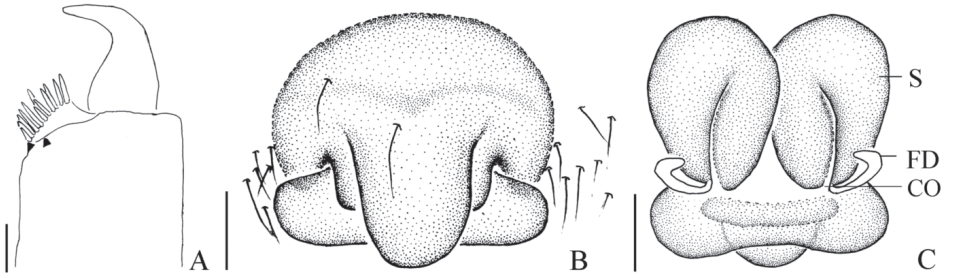

Figure 4. *Mimetus echinatus* Wang, 1990, from Shimen. **A** left chelicerae, ventral view **B** epigynum, ventral view **C** vulva, dorsal view. Scale bars: **A–C**, 0.1.

Female. Carapace (Fig. 3A) yellowish brown, pear-shaped, with several reddish brown diagonal patches, posterior margin reddish brown, fovea and sternum similar to male. ALE and PLE contiguous, AER and PER nearly straight. Endite, labium and sternum similar to male but darker. Chelicerae stronger than male with 12 promarginal peg setae and 2 retromarginal teeth (Fig. 4A). Legs femur with reddish annuli basely, other area with small reddish brown patches, patella brown, metatarsus with brown annuli. Opisthosoma (Fig. 3A) subcircular, slightly wider than long. Dorsum of opisthosoma (Fig. 3A) yellowish brown, with long macrosetae and white patches. The markings of venter similar to male. Spinnerets reddish brown, anterior spinnerets longest.

Epigyne (Figs 3B–C, 4B–C) slightly wider than long, with three parts, including lingulate scape, rectangular basal plate and a laminar layer covering the venter of the basal plate. Scape and basal plate cross shaped, scape about 1/2 length of Epigyne, width of basal plate approximately equal to Epigyne. Spermathecae ovoid, about 2/3 length of epigynum. Copulatory ducts indistinct in dorsal view.

Distribution. China (Hunan).

***Mimetus lamellaris* sp. n.**

http://zoobank.org/F3A39691-1AAA-41EA-B389-9538A19E0274

Figs 5–6

Type material. Holotype ♂, China, Guizhou: Yanhe County, Daheba Township, Mayanhe National Nature Reserve 28.65839°N, 108.26033°E, 364m, 28 July 2014, Xianjin Peng, Cheng Wang, Bing Zhou, Ping Liu, Yi Huang and Mingyong Liao leg.

Etymology. The specific name comes from the Latin word *lamellaris*, meaning flaky and referring to the flaky vexillum on the cymbial tip; adjective.

Diagnosis. The new species can be distinguished from all known congeneric species by: cymbial tip with several slender long macrosetae (Fig. 5B–C); cymbium boat-shaped, length/width ratio about 3/1 in retrolateral view (Figs 5C, 6B); the angle between the basal and apical of embolus about 110° (Figs 5B, 6A); vexillum about 1/2

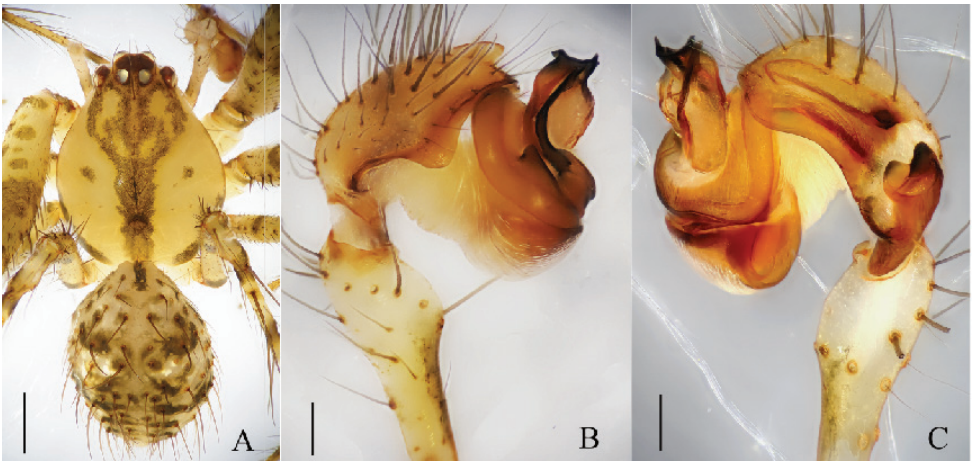

Figure 5. *Mimetus lamellaris* sp. n., holotype male. **A** habitus, dorsal view **B** palp, prolateral view **C** palp, retrolateral view. Scale bars: **A**, 0.5; **B–C**, 0.1.

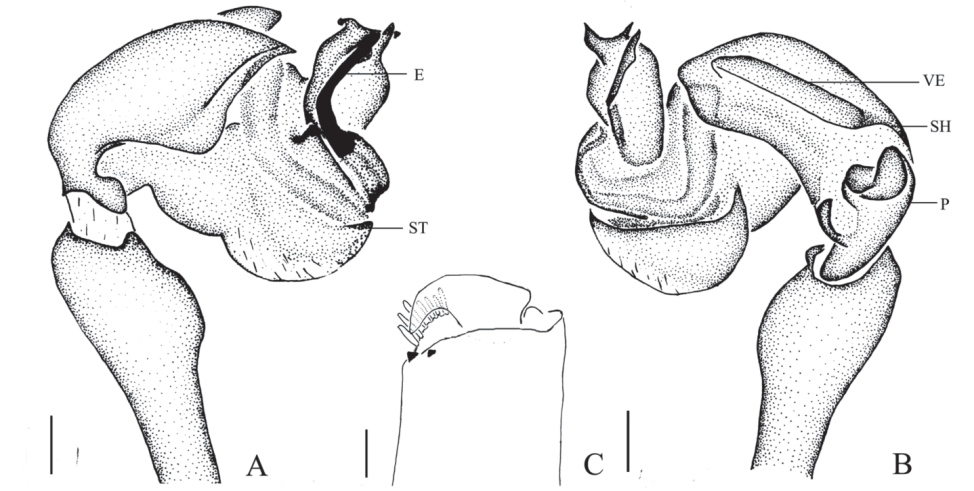

Figure 6. *Mimetus lamellaris* sp. n., holotype male. **A** palp, prolateral view **B** palp, retrolateral view **C** left chelicerae, ventral view. Scale bars: **A–C**, 0.1.

length of cymbium in retrolateral view (Figs 5B–C, 6B–C); apical part of paracymbium broaden to rotund, with two hornlike outgrowths (Figs 5C, 6B).

Description. Male: Total length 3.05. Prosoma 1.65 long, 1.30 wide. Opisthosoma 1.40 long, 1.13 wide. Clypeus 0.20 high. Carapace (Fig. 5A) yellow, long oval, widest at coxae II and III, with a longitudinal brown patch medially, posterior partion reddish brown. Fovea circular, deep, surrounding area reddish brown. AER recurved, PER nearly straight, ALE and PLE continuous. Eye sizes and interdistances: AME 0.13, ALE 0.08, PME 0.11, PLE 0.05, AME–AME 0.06, ALE–AME 0.07, PME–PME 0.06, PME–PLE 0.13. MOA anterior width 0.34, posterior 0.28, length 0.35. Chelicerae red-

dish brown, with 7 promarginal peg setae and 2 retromarginal teeth (Fig. 6C), distal area with long hairs. Endites light yellow, longer than wide. Labium reddish brown, wider than long. Sternum yellow, long oval, each side with two brown patches, margins with long scopulae, centrally glabrous. Legs light yellow, spiniferous, with reddish brown patches equidistributed. Length of legs: I 10.35 (2.73, 3.52, 2.60, 1.50), II 7.78 (2.43, 2.72, 12.6, 1.01), III 4.53 (1.10, 1.53, 1.00, 0.90), IV 5.66 (1.12, 2.03, 1.11, 0.60). Leg formula: 1243. Dorsum of opisthosoma (Fig. 5A) light yellow, long oval, with long macrosetae and brown patches. Venter gray white, with white patches in middle.

Male palp (Figs 5B–C, 6A–B): tibia long and thin, distally swollen, with several long macrosetae. Cymbium boat-shaped, widest in middle in prolateral view, with slender macrosetae on the tip. Vexillum flaky, about 1/2 length of cymbium in retrolateral view, visible in prolateral view. Distal of paracymbium broaden to rotund, with two hornlike outgrowths. Basal division of the bulb visible, distal division of the bulb rolls up as sulciform to protect embolus. Embolus hook-shaped, and the angle between its basal and apical about 110°.

Female. Unknown.

Distribution. China (Guizhou).

***Mimetus wangi* sp. n.**
http://zoobank.org/35717222-6AAA-402E-800C-1E4C46CFE6CF
Figs 7–10

Type material. Holotype ♂**, China, Yunnan:** Gaoligong Mountains, Dulongjiang Township, Xianjiudang Village, 27.93682°N, 98.3260°E, 1634m, 5 April 2004, Guo Tang leg. **Paratypes**: 5♀, same data as holotype.

Etymology. The specific name is a patronym in honor of Professor Jiafu Wang, a well known spider taxonomist in China; noun.

Diagnosis. The new species can be distinguished from all known congeneric species by: the dorsum of the opisthosoma with a pair of distinct outgrowths (Fig. 7A); the ratio of cymbium length/width about 2/1 in retrolateral view (Figs 7C, 8B); spermathecae kidney shaped (Figs 9C, 10C) and contiguous (Figs 9B, 10B); the width of spermathecae slightly narrower than basal plate (Figs 9B, 10B).

Description. Male: Total length 3.34. Prosoma 1.50 long, 1.20 wide. Opisthosoma 1.84 long, 1.40 wide. Clypeus 0.05 height. Carapace (Fig. 7A) yellow brown, long oval, widest at coxae II and III, with longitudinal brown patches at median area and three brown patches on both sides of the lateral margins. Fovea circular. AER slightly recurved, PER nearly straight, ALE and PLE contiguous. Eye sizes and interdistances: AME 0.13, ALE 0.08, PME 0.10, PLE 0.06, AME–AME 0.08, ALE–AME 0.05, PME–PME 0.05, PME–PLE 0.13, MOA anterior width 0.28, posterior width 0.25, length 0.31. Chelicerae yellow, with 7 promarginal peg setae and 2 retromarginal teeth. Endites light yellow, longer than wide. Labium light yellow, longer than wide. Sternum pear-shaped, glabrous, colored as labium except margin with few macrose-

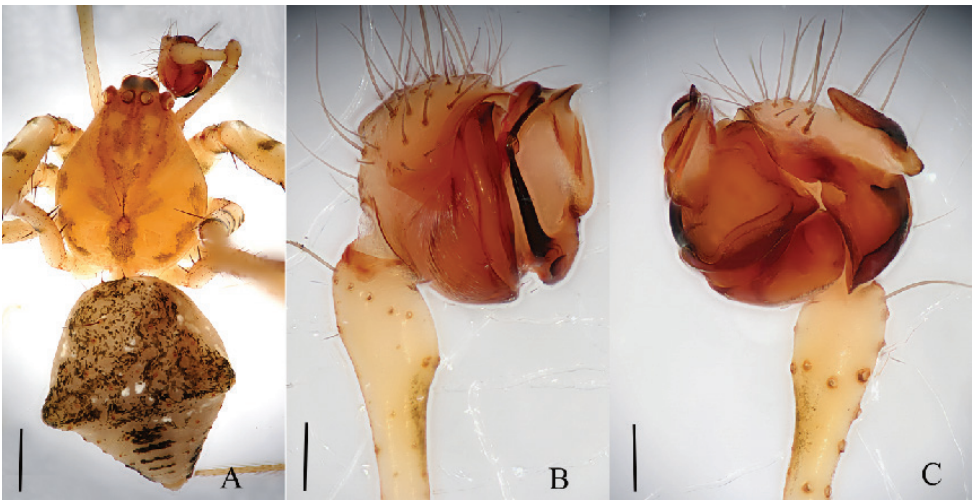

Figure 7. *Mimetus wangi* sp. n., holotype male. **A** habitus, dorsal view **B** palp, prolateral view **C** palp, retrolateral view. Scale bars: **A**, 0.5; **B–C**, 0.1.

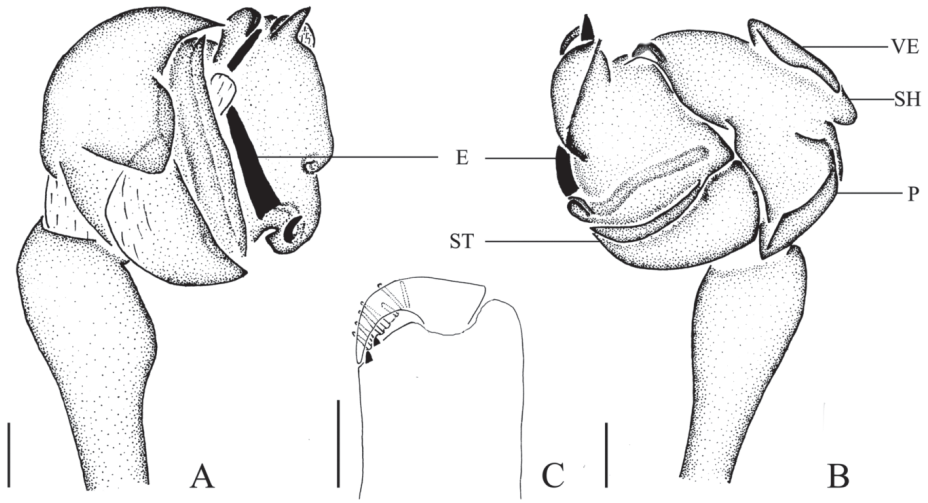

Figure 8. *Mimetus wangi* sp. n., holotype male. **A** palp, ventral view **B** palp, prolateral view **C** left chelicera, ventral view. Scale bars: **A–B**, 0.1; **C**, 0.1.

tae. Legs slim, spiniferous, with brown patches. Length of legs: I 11.23 (3.31, 3.82, 2.80, 1.30), II 9.00(2.48, 2.91, 2.40, 1.21), III 4.58 (1.01, 1.68, 1.00, 0.0.88), IV 6.05 (1.90, 2.00, 1.40, 0.75). Leg formula: 1243. Opisthosoma (Fig. 7A) long oval, filled with small black spots and few white patches, anterior area with few macrosetae, middle portion widest, with two outgrowths in both sides, posterior portion sloping, with five transverse black stripes. Venter with three brown patches, median area grey, glabrous, with white spots on both sides.

Figure 9. *Mimetus wangi* sp. n., one of the female paratypes. **A** habitus, dorsal view **B** epigyne, ventral view **C** vulva, dorsal view. Scale bars: **A**, 0.5; **B–C**, 0.1.

Male palp (Figs 7C–D, 8B–C): tibia slim, with several macrosetae. Cymbial length/width ratio about 2/1 in retrolateral view, distal end extending to vexillum, shovel obvious, with dense long setae. Sperm duct nearly horizontal. Embolus with a membrane covering its terminal 2/3 portion in prolateral view. Paracymbium massive.

Female. Total length 3.65. Prosoma 1.55 long, 1.10 wide. Opisthosoma 1.95 long, 2.05 wide. Clypeus 0.10 high. Carapace (Fig. 9A) yellowish brown, long oval. AER recurved, PER slightly procurved. ALE and PLE continuous. Eye sizes and interdistances: AER 0.10, ALE 0.13, PME 0.13, PLE 0.15, AME–AME 0.04, AME–ALE 0.06, PME–PME 0.05, PME–PLE 0.10. MOA anterior width 0.28, posterior width 0.21, length 0.31. Chelicerae, endites and labium coloured as in male, labium slightly wider than long. Chelicerae with 8 promarginal peg setae and 2 retromarginal teeth. Sternum similar to male except for lightly colored. Leg patches and spines similar to male.

Length of legs: I 12.92 (3.51, 4.30, 3.60, 1.50), II 9.55 (2.87, 2.91, 2.38, 1.38), III 5.93 (1.82, 1.91, 1.21, 1.00), IV 6.75 (2.10, 2.30, 1.35, 1.00). Dorsum of opisthosoma (Fig. 9A) similar to male, except for fewer black spots and more white spots, and

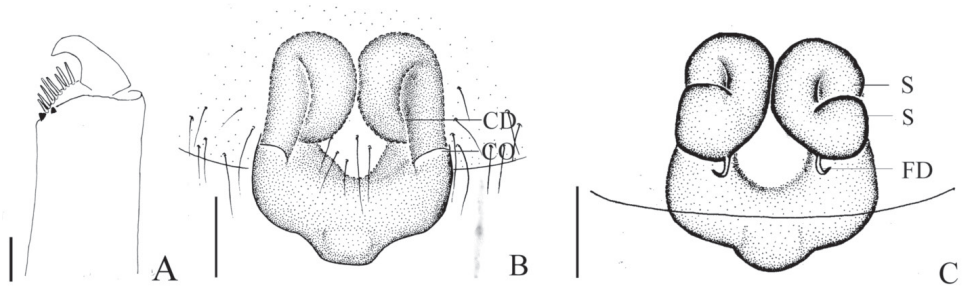

Figure 10. *Mimetus wangi* sp. n., one of the female paratypes. **A** left chelicerae, ventral view **B** epigynum, ventral view **C** vulva, dorsal view. Scale bars: **A–C**, 0.1.

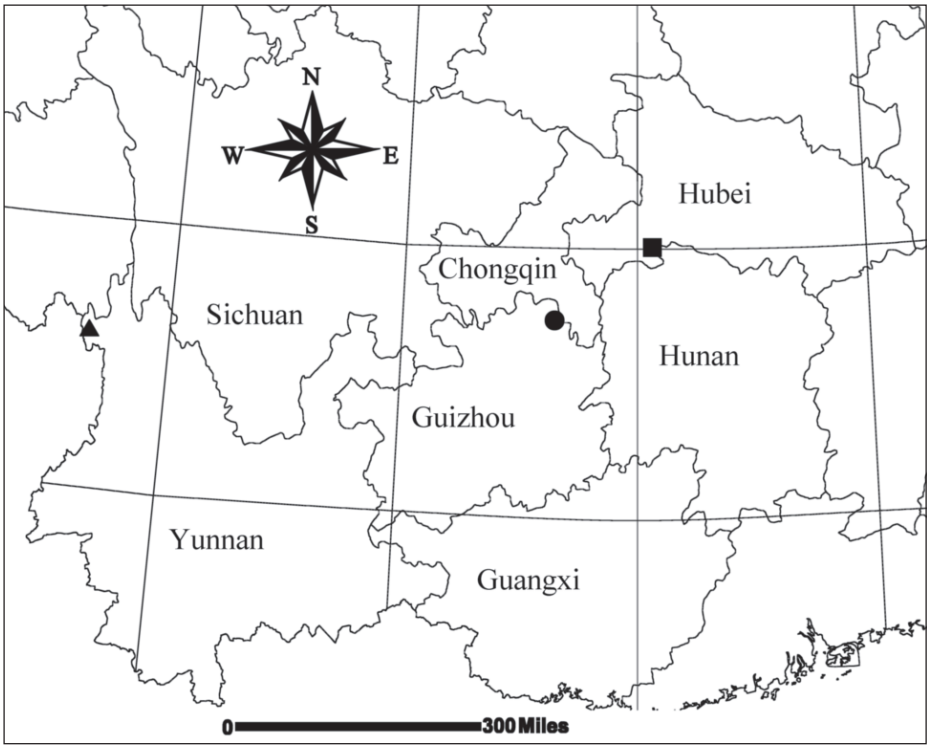

Figure 11. Collecting localities of three *Mimetus* species. ■ *M. echinatus*; ● *M. lamellaris* sp. n.; ▲ *M. wangi* sp. n.

between the two outgrowths is a transverse black wide stripe. Venter similar to male except three patches darker.

Epigyne (Figs 9B–C, 10B–C) slightly longer than wide, with a yellowish brown labiate outgrowth at the bottom of the base plate, copulatory openings visible, close to epigastric furrow. Spermathecae kidney shaped, contiguous, slightly narrower than basal plate. Basal plate scalloped. Copulatory ducts indistinct in dorsal view

Distribution. China (Yunnan).

Acknowledgements

We are grateful to Yi Huang, Ping Liu, Bing Zhou, Jiahui Gan, Yuhui Gong Mingyong Liao and Guo Tang for collecting the specimens. This research was sponsored by the National Science Foundation of the USA through the grant Biotic survey of the Gaoligongshan, a biodiversity hotspot in western Yunnan, China (No. DEB-0103795). It is also partly supported by the National Natural Sciences Foundation of China (NSFC-30970327, 31272271, 31272272), the National Special Fund on Basic Research of Science and Technology of China (No. 2014FY110100), Hunan Provincial Natural Science Foundation of China (No.11JJ1004/12JJ3028), Program for New Century Excellent Talents in University (NCET-12-0717), China Postdoctoral Science Foundation (No. 20100471221/201104506), the program of Hunan Provincial Science and Technology Plans (No. 2010RS4006) and the Hunan Provincial Program for Development of Key Disciplines in Ecology.

References

Harms D, Dunlop JA (2009) A revision of the fossil pirate spiders (Arachnida: Araneae: Mimetidae). Palaeontology 52: 779–802. doi: 10.1111/j.1475-4983.2009.00890.x

Harms D, Harvey MS (2009a) A review of the pirate spiders of *Tasmania* (Arachnida, Mimetidae, Australomimetus) with description of a new species. Journal of Arachnology 37: 188–205. doi: 10.1636/A08-35.1

Harms D, Harvey MS (2009b) Australian pirates: systematics and phylogeny of the Australasian pirate spiders (Araneae: Mimetidae), with a description of the Western Australian fauna. Invertebrate Systematics 23: 231–280. doi: 10.1071/IS08015

Heimer S (1986) Notes on the spider family Mimetidae with description of a new genus from Australia (Arachnida, Araneae). Entomologische Abhandlungen, Staatliches Museum für Tierkunde Dresden 49: 113–137.

Hentz NM (1832) On North American spiders. Silliman's Journal of Science and Arts 21: 99–122.

Liang TE, Wang JF (1991) A new species of spiders of the genus *Mimetus* in Xinjiang (Araneae: Mimetidae). Journal of the August 1st Agricultural College 14: 61–62.

Song DX, Zhu MS (1993) A new species of the genus *Mimetus* from China (Araneae: Mimetidae). Acta Zootaxonomica Sinica 18: 421–423.

Wang JF (1990) Study on the spiders of family Mimetidae from south China (Arachnida: Araneae). Acta Zootaxonomica Sinica 15: 36–47.

World Spider Catalog (2016) World Spider Catalog. Natural History Museum Bern. http://wsc.nmbe.ch, version 15.5 [accessed on 12 Sep. 2016]

ZooKeys 626: 137–154 (2016)
doi: 10.3897/zookeys.626.9633
http://zookeys.pensoft.net

RESEARCH ARTICLE

A peer-reviewed open-access journal
ZooKeys
Launched to accelerate biodiversity research

Two complete mitochondrial genomes from *Praticolella mexicana* Perez, 2011 (Polygyridae) and gene order evolution in Helicoidea (Mollusca, Gastropoda)

Russell L. Minton[1], Marco A. Martinez Cruz[2], Mark L. Farman[3], Kathryn E. Perez[2]

1 *School of Science and Computer Engineering, University of Houston Clear Lake, 2700 Bay Area Boulevard MC 39, Houston, Texas 77058 USA* **2** *Department of Biology, University of Texas Rio Grande Valley, 1201 West University Drive, Edinburg, Texas 78539 USA* **3** *UK Healthcare Genomics, 225 Plant Science Building, 1405 Veteran's Drive, University of Kentucky, Lexington, Kentucky 40546 USA*

Corresponding author: *Russell L. Minton* (minton@uhcl.edu)

Academic editor: *T. Backeljau* | Received 21 June 2016 | Accepted 16 October 2016 | Published 25 October 2016

http://zoobank.org/344AB9CB-0143-4C2E-87EB-FEAA037552E2

Citation: Minton RL, Martinez Cruz MA, Farman ML, Perez KE (2016) Two complete mitochondrial genomes from *Praticolella mexicana* Perez, 2011 (Polygyridae) and gene order evolution in Helicoidea (Mollusca, Gastropoda). ZooKeys 626: 137–154. doi: 10.3897/zookeys.626.9633

Abstract

Helicoidea is a diverse group of land snails with a global distribution. While much is known regarding the relationships of helicoid taxa, comparatively little is known about the evolution of the mitochondrial genome in the superfamily. We sequenced two complete mitochondrial genomes from *Praticolella mexicana* Perez, 2011 representing the first such data from the helicoid family Polygyridae, and used them in an evolutionary analysis of mitogenomic gene order. We found the mitochondrial genome of *P. mexicana* to be 14,008 bp in size, possessing the typical 37 metazoan genes. Multiple alternate stop codons are used, as are incomplete stop codons. Mitogenome size and nucleotide content is consistent with other helicoid species. Our analysis of gene order suggested that Helicoidea has undergone four mitochondrial rearrangements in the past. Two rearrangements were limited to tRNA genes only, and two involved protein coding genes.

Keywords

Gene rearrangement, mitochondria, tRNA, homoplasy, convergence, phylogeny

Introduction

Helicoidea (Mollusca, Gastropoda) is a globally distributed and diverse superfamily of terrestrial mollusks (reviewed in Razkin et al. 2015). It is part of the larger Stylommatophora, a clade that accounts for around 80% of all terrestrial mollusks (Klussmann-Kolb et al. 2008) and encompasses over 100 families. Helicoid snails possess a typical pulmonate body plan with two pairs of tentacles, a usually dextrally coiled shell, and a vascularized pallial cavity that functions as a lung (Beesley et al. 1998). Taxonomic and systematic classifications of Helicoidea have differed based on morphological, ecological, and molecular characters including select mitochondrial markers (Steinke et al. 2004, Manganelli et al. 2005, Groenenberg et al. 2011). Phylogenies based on entire mitochondrial genomes (Wang et al. 2014a, Deng et al. 2016) are limited in size and scope due to the paucity of helicoid data relative to other mollusk groups (e.g. Caenogastropoda).

The mitogenome serves as a powerful evolutionary tool given its small size and fast mutation rate relative to the nuclear genome (Avise et al. 1987, Saccone et al. 1999, Funk and Omland 2003). Mitogenome organization has several qualities that make it a valuable phylogenetic marker. For example, mitochondrial gene order and content can be highly variable in metazoans (Black and Roehrdanz 1998, Mindell et al. 1998, Weigert et al. 2016). Transposition of tRNA genes is more common than movement of protein coding or ribosomal RNA genes (Xu et al. 2006) and may be weighted accordingly during analysis (Bader et al. 2008). Variability in gene length, arrangement, and strand assignment can be examined as sets of phylogenetically informative characters (Gissi et al. 2008). Many mitochondrial gene order rearrangements also represent rare events that serve as homoplasy-free evidence of common ancestry (Boore and Brown 1998, Rokas and Holland 2000, Gribaldo and Philippe 2002) provided they carry sufficient phylogenetic information (Yang 1998). In mollusks, these classes of genetic variation can occur within the same family or genus (Milbury and Gaffney 2005, Rawlings et al. 2010). Helicoideans possess typical metazoan mitogenomes, with 37 genes organized among ribosomal (16S and 12S) and transfer RNA (22, including two each for leucine and serine) genes and 13 protein coding genes (Boore 1999). The degree of genetic rearrangements and variability within and among helicoid mitogenomes, however, is poorly understood.

Within Helicoidea, only three of the constituent 19 families (Bouchet et al. 2005) are represented by complete mitogenomes on GenBank: Bradybaenidae, Camaenidae, and Helicidae. Currently unrepresented is Polygyridae, a helicoid family endemic to the Americas. Many of the most visible and commonly encountered land snails in North America are polygyrids. Nearly 300 species are described in the family, including five that are considered problematic invasives (Perez et al. 2014). We focused our efforts on *Praticolella mexicana* Perez, 2011, a small, globe-shaped snail (Figure 1) most likely native to Mexico and introduced to the Caribbean and the United States gulf coast (Perez 2011). The United States Department of Agriculture reports finding this species in shipments of fruit, furniture, and ornamental plants (USDA pers. comm.). Our study had two primary research aims: to sequence and annotate the mitochondrial genome of *P. mexicana* to examine gene order and arrangement in Polygyridae; and to

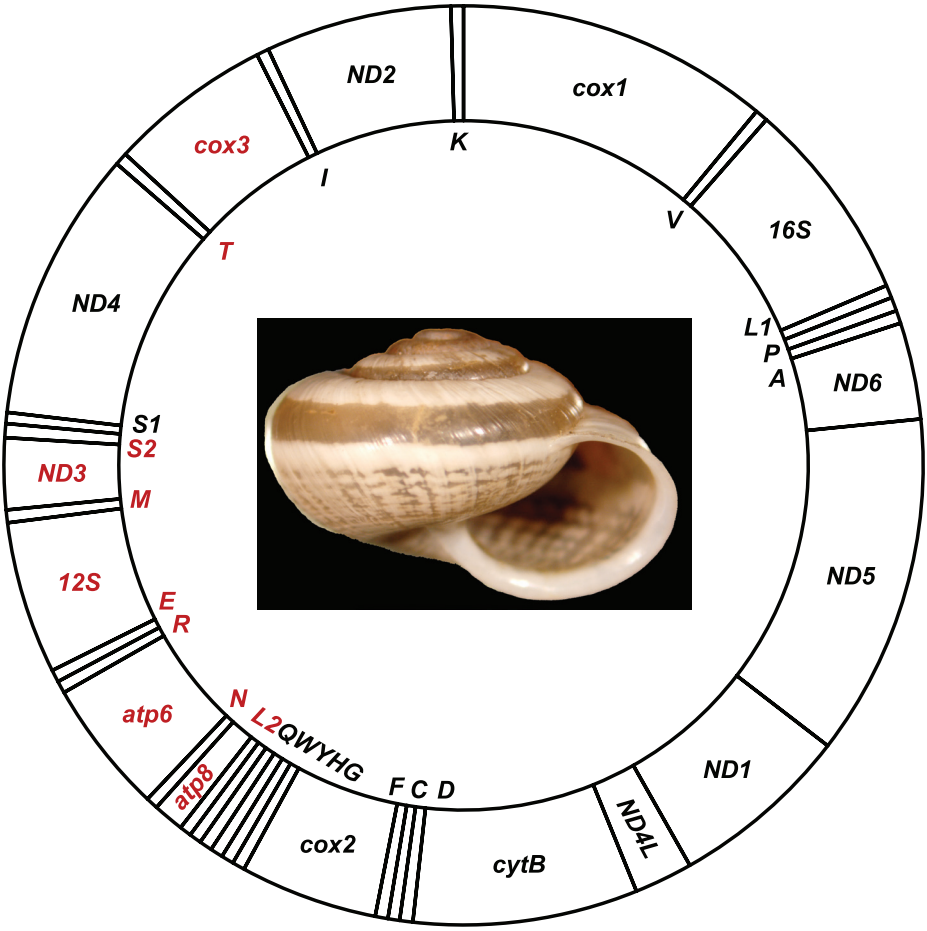

Figure 1. Mitochondrial genome of *Praticolella mexicana* UTRGV and McAllen illustrated with an image of the species holotype (ANSP 426031). Gene order and sizes are shown relative to one another, not including non-coding regions. Genes are color coded by H (black) or L (red) strand. IUPAC single letter codes are used to identify tRNA genes.

explore gene order evolution in Helicoidea. Results from both aspects of the study will increase our knowledge of these gastropod groups and provide a better understanding of land snail mitochondrial genome evolution.

Materials and methods

Specimen collection and DNA extraction

We collected one adult *P. mexicana* each from the UTRGV campus in Edinburg, Texas (26.30726; -98.1714), and from a residential neighborhood in McAllen, Texas

(26.2085; -98.2254). We immersed foot tissue from each snail in reconstituted BupH™ phosphate buffered saline (Thermo Scientific) and homogenized it with a Dounce homogenizer. We used EDTA-free Protease Inhibitor Cocktail (Thermo Scientific) and the Mitochondrial Isolation Kit for Tissue (Thermo Scientific) to isolate intact mitochondria from the homogenates. Mitochondrial DNA was extracted using the Mitochondrial DNA Isolation Kit (BioVision) followed by application of Plasmid-Safe™ ATP-dependent DNase (Epicenter) to remove any remaining nuclear DNA.

Genome sequencing and assembly

We purified enriched mitochondrial DNA using the Zymoclean Genomic DNA Clean and Concentrator kit (Zymo Research) and quantified it using a BioAnalyzer (Agilent Technologies). Approximately 50 ng of total DNA was used for barcoded library construction using the Nextera DNA library prep kit (Illumina), precisely following the manufacturer's instructions. We pooled the *P. mexicana* samples on one flowcell and sequenced them on the MiSeq (Illumina) platform using the 2x250 bp run mode. Barcodes and deconvolution of the pooled reads was performed automatically in the BaseSpace (Illumina) server and used their native format. The CLCBio 8.0.2 *de novo* genome assembly tool was used to assemble the reads using default parameter settings. Genomic contigs representing mitochondrial DNA segments were subsequently identified using the CLCBio assembly Fasta files to query a BLAST database comprising the *Achatina fulica* mitochondrial genome (GenBank: KJ744205).

Genome annotation

We loaded the assembly for each individual into Geneious 8 (http://www.geneious.com, Kearse et al. 2012) and used the built-in ORF finder function to identify putative coding regions. We compared the output to that generated in MITOS (Bernt et al. 2013) to determine the location and orientation of 13 protein-coding genes. ARWEN (Laslett and Canbäck 2008) and tRNAscan-SE 1.21 (Lowe and Eddy 1997) were used to identify the 22 tRNAs, and MITOS and BLAST (Altschul et al. 1990) were used to locate the two ribosomal genes. Nucleotide and codon composition analyses were conducted in DAMBE (Xia and Xie 2001).

Phylogenetic analysis of mitochondrial genes

To determine the position of Polygyridae within Helicoidea, we extracted the amino acid sequences for all 13 protein-coding genes from the two new genomes. These were combined with mitochondrial genome sequences from eight other helicoid taxa, and eight stylommatophoran and one non-stylommatophoran outgroup (Table 1). Genome

Table 1. Taxonomic list of mitochondrial genomes used in the study.

Taxonomy	GenBank	Reference
Clade Systellommatophora		
Superfamily Onchidioidea		
Family Onchidiidae		
Onchidella celtica	AY345048	Grande et al. 2004
Clade Stylommatophora		
Superfamily Achatinoidea		
Family Achatinidae		
Achatina fulica	KJ744205	He et al. 2016
Superfamily Clausilioidea		
Family Clausiliidae		
Albinaria caerulea	X83390	Hatzoglou et al. 1995
Superfamily Helicoidea		
Family Bradybaenidae		
Aegista aubryana	KT192071	Yang et al. 2016
Aegista diversifamilia	KR002567	Huang et al. 2016
Dolicheulota formosensis	KR338956	Huang et al. 2016
Mastigeulota kiangsinensis	KM083123	Deng et al. 2016
Family Camaenidae		
Camaena cicatricosa	KM365408	Wang et al. 2014a
Family Helicidae		
Cepaea nemoralis	U23045	Terrett et al. 1996
Cylindrus obtusus	JN107636	Groenenberg et al. 2012
Cornu aspersum	JQ417194	Gaitán-Espitia et al. 2013
Family Polygyridae		
Praticolella mexicana McAllen	KX259343	this study
Praticolella mexicana UTRGV	KX278421	this study
Superfamily Orthalicoidea		
Family Cerionidae		
Cerion incanum	KM365085	unpublished
Family Orthalicidae		
Naesiotus nux	KT821554	Hunter et al. 2016
Superfamily Pupilloidea		
Family Pupillidae		
Gastrocopta cristata	KC185403	Marquardt 2013
Pupilla muscorum	KC185404	Marquardt 2013
Family Vertiginidae		
Vertigo pusilla	KC185405	Marquardt 2013
Superfamily Succineoidea		
Family Succineidae		
Succinea putris	JN627206	White et al. 2011

fragments of *Euhadra herklotsi* (Z71693-701) were excluded because the gene order data (see below) could not be coded. Data for each gene were aligned separately in MUSCLE (Edgar 2004). We used IQTREE 1.4.2 (Nguyen et al. 2014) to determine

that all alignments fit the mtZOA+F+I+G4 model (Rota-Stabelli et al. 2009) optimally. We assembled all alignments into a single data matrix and analyzed it in IQTREE under maximum likelihood, allowing each gene to be optimized separately. We assessed branch support using 10,000 ultra-fast bootstrap replicates (Minh et al. 2013).

Gene order analysis and phylogeny

For all included mitogenomes, we determined the gene order and strand assignment. Using *Cornu aspersum* (JQ417194) as reference (Gaitán-Espitia et al. 2013), we numbered the genes consecutively in a 5' to 3' direction on the H strand starting with *cox1* as gene number one. With each of the genes now numbered, we proceeded to generate gene order for the other mitogenomes, using positive numbers for H strand and negative numbers for L strand. The resulting data matrix was analyzed under maximum likelihood using MLGO (Hu et al. 2014). MLGO uses a binary encoding method with probabilistic models (Lin et al. 2013) to infer gene duplications, genome rearrangements, and branch support through bootstrapping. We compared our amino acid phylogeny to the gene order tree using the Kishino-Hasegawa test (Kishino and Hasegawa 1989) as implemented in IQTREE. We also used our protein sequence phylogeny with MLGO to reconstruct ancestral genomes to study the evolution of gene order in Helicoidea.

Results

Approximately 12 million sequences reads derived from the UTRGV *P. mexicana* sample assembled into over 450,000 contigs, the largest of which was 14,275 bp in length. A BLAST search against the *A. fulica* mitogenome revealed that the largest contig was comprised entirely of mitochondrial sequence. The McAllen *P. mexicana* sample comprised 26 million reads that assembled into more than 300,000 contigs. The largest contig spanned 14,259 bp and was also composed entirely of mitochondrial sequence. After final sequence editing, both *P. mexicana* mitogenomes were found to be 14,008 bp in length.

The complete *P. mexicana* mitochondrial genomes (KX278421 UTRGV, KX259343 McAllen; Figure 1) possess the same genes in the same orders and orientations (Table 2). The smallest tRNA is 54 bp (*tRNA-Ser1*), while the largest is 68 bp (*tRNA-Ser2*). Non-coding regions make up 1.4% (194 bp) of the *P. mexicana* mitogenome. The genome has three large non-coding regions. The first region is 25 bp and sits between *cox3* and *tRNA-Ile*. The second region is 56 bp long and exists between the two serine tRNAs. The third region is a GC-rich 89 bp segment between the *tRNA-Trp* and *tRNA-Gln* genes. Searches using BLAST (Altschul et al. 1990) found no significant matches in any database for these three non-coding regions.

Genome size for *P. mexicana* is comparable with the other helicoid and stylommatophoran taxa available (Table 3). The majority of the genes (nine protein-coding,

Table 2. Mitochondrial genome annotation for *P. mexicana* UTRGV.

Gene	Start	Stop	Length	Strand	Start codon	Stop codon	Anticodon
cox1	1	1525	1525	H	TTG	T	
tRNA-Val	1526	1587	62	H			TAC
16S	1589	2579	991	H			
tRNA-Leu1	2580	2642	63	H			TAG
tRNA-Pro	2640	2706	67	H			TGG
tRNA-Ala	2706	2768	63	H			TGC
ND6	2769	3239	471	H	GTG	TAA	
ND5	3223	4893	1671	H	TTG	TAG	
ND1	4887	5768	882	H	ATC	TAG	
ND4L	5768	6052	285	H	GTG	TAA	
cytB	6054	7148	1095	H	ATT	TAG	
tRNA-Asp	7149	7212	64	H			GTC
tRNA-Cys	7209	7265	57	H			GCA
tRNA-Phe	7270	7331	62	H			GAA
cox2	7332	8003	672	H	ATG	TAG	
tRNA-Gly	8007	8068	61	H			TCC
tRNA-His	8063	8123	61	H			GTG
tRNA-Tyr	8131	8192	62	H			GTA
tRNA-Trp	8186	8248	63	H			TCA
tRNA-Gln	8338	8396	59	L			TTG
tRNA-Leu2	8397	8454	58	L			TAA
atp8	8458	8608	151	L	ATG	T	
tRNA-Asn	8612	8670	59	L			GTT
atp6	8671	9322	652	L	ATG	T	
tRNA-Arg	9323	9382	60	L			TCG
tRNA-Glu	9383	9442	60	L			TTC
12S	9443	10186	744	L			
tRNA-Met	10187	10248	62	L			CAT
ND3	10250	10597	348	L	TTG	TAA	
tRNA-Ser2	10598	10665	68	L			TGA
tRNA-Ser1	10723	10776	54	H			GCT
ND4	10777	12100	1324	H	ATG	T	
tRNA-Thr	12010	12162	62	L			TGT
cox3	12163	12958	796	L	ATT	T	
tRNA-Ile	12985	13044	60	H			GAT
ND2	13048	13954	907	H	ATG	T	
tRNA-Lys	13955	14008	61	H			TTT

one rRNA, 15 tRNA) are located on the H strand (Figure 1). Gene overlap exists among protein coding and tRNA genes. The overall base composition of all taxa based on the H strand shows anti-cytosine bias along with excesses of thymine and guanine (Table 3). Protein-coding genes comprise 76.2% of the total *P. mexicana* genome, and

Table 3. Nucleotide and skew statistics for the mitochondrial genomes used.

		Whole genome composition						
Species	**Size (bp)**	**A%**	**C%**	**G%**	**T%**	**A+T%**	**AT skew**	**GC skew**
Achatina fulica	15057	0,280	0,171	0,195	0,355	0,634	-0,118	0,064
Aegista aubryana	14238	0,313	0,145	0,164	0,379	0,692	-0,095	0,062
Aegista diversifamilia	14039	0,325	0,133	0,157	0,386	0,711	-0,086	0,083
Albinaria caerulea	14130	0,328	0,138	0,155	0,379	0,707	-0,073	0,059
Camaena cicatricosa	13843	0,319	0,135	0,167	0,379	0,698	-0,086	0,108
Cepaea nemoralis	14100	0,262	0,189	0,213	0,336	0,598	-0,125	0,058
Cerion incanum	15177	0,298	0,158	0,185	0,360	0,657	-0,095	0,077
Cylindrus obtusus	14610	0,258	0,166	0,219	0,358	0,615	-0,162	0,137
Dolicheulota formosensis	14237	0,284	0,131	0,167	0,418	0,702	-0,191	0,120
Gastrocopta cristata	14060	0,308	0,136	0,172	0,384	0,692	-0,110	0,116
Helix aspersa	14050	0,307	0,136	0,165	0,392	0,699	-0,121	0,097
Mastigeulota kiangsinensis	14029	0,295	0,144	0,182	0,379	0,674	-0,125	0,118
Naesiotus nux	15197	0,336	0,120	0,147	0,397	0,733	-0,083	0,100
Praticolella mexicana McAllen	14008	0,289	0,126	0,188	0,398	0,686	-0,159	0,198
Praticolella mexicana UTRGV	14008	0,288	0,126	0,188	0,398	0,686	-0,160	0,198
Pupilla muscorum	14149	0,325	0,129	0,153	0,393	0,718	-0,094	0,083
Succinea putris	14092	0,339	0,109	0,122	0,430	0,769	-0,113	0,055
Vertigo pusilla	14078	0,326	0,123	0,155	0,397	0,722	-0,098	0,116

five start (ATC, ATG, ATT, GTG, TTG) and two stop (TAA, TAG) codons are used. Incomplete stop codons (T) are used for *atp6*, *atp8*, *cox1*, *cox3*, *ND2*, and *ND4* (Table 2). No downstream stop codons were found for those six genes.

Maximum-likelihood analysis of our protein sequence dataset of 19 taxa and 4,011 aligned amino acid positions yielded a single tree (Figure 2). Helicoidea, Bradybaenidae, and Helicidae were recovered as well-supported monophyletic groups (100% bootstrap support), as were Pupilloidea and Pupillidae. Bradybaenidae and *Camaena* were well-supported sister taxa, and *P. mexicana* was positioned as sister to the remaining helicoid taxa. A maximum likelihood phylogeny of gene order again supported the monophyly of Bradybaenidae, Helicidae and Pupillidae, and suggested a sister relationship of Bradybaenidae with *P. mexicana* (Figure 3). Helicoidea, well-supported in the analysis of protein sequences, was not recovered as monophyletic though branch support was low (Figure 2). The gene order phylogeny represented a significantly less likely topology than the protein phylogeny (Δ likelihood = 1246.275, $p << 0.01$).

Given the protein topology represented the more likely relationships among our included taxa, we reconstructed ancestral gene orders predicted by MLGO with that topology. The results suggested a pattern of four rearrangements in the helicoid mitochondrial genome (Figure 4), assuming the fewest number of gene rearrangements. Starting with the hypothetical ancestral helicoid mitogenome (Figure 2 node A), *P. mexicana* had (*tRNA-Tyr*, *tRNA-Trp*) transposing with (*tRNA-Gly*, *tRNA-His*). The Helicidae+*Camaena*+Bradybaenidae ancestor maintained the same order as the hypothetical ancestral helicoid. Two unique rearrangements followed in Helicidae (Figure 2

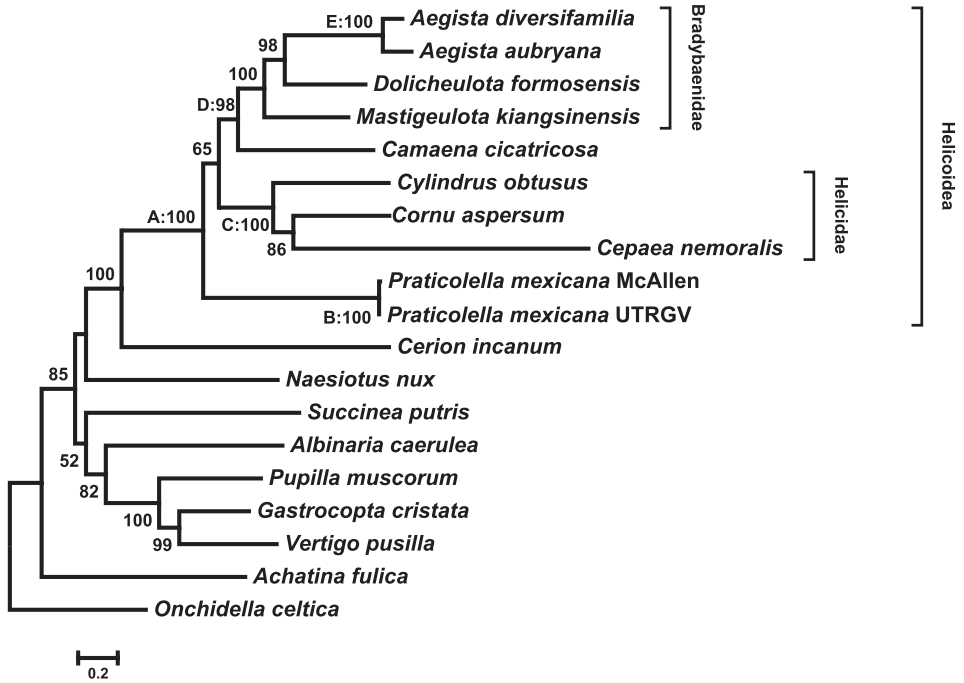

Figure 2. Maximum likelihood phylogeny of Stylommatophora protein coding genes. Analysis in IQTREE yielded a single tree (log likelihood = -89104.188) under the mtZOA+F+I+G4 model. Branch support >50% is shown based on 10,000 ultra-fast bootstrap replicates. Helicoidea, Bradybaenidae, and Helicidae were recovered as monophyletic. Nodes A-E refer to rearrangements shown in Figure 4.

node C); *tRNA-Pro* moved from between *tRNA-Leu1* and *tRNA-Ala* to between *ND6* and *ND5*, and (*tRNA-Ser2*, *ND4*) transposed with *(tRNA-Thr, coxIII*). The ancestor of *Camaena*+Bradybaenidae (Figure 2 node D) showed the same (*tRNA-Tyr*, *tRNA-Trp*) and (*tRNA-Gly*, *tRNA-His*) rearrangement as *P. mexicana*. Finally, a unique rearrangement is seen in *Aegista* (Figure 2 node E) The *ND3* gene moved from between *tRNA-Met* and *tRNA-Ser1* to between *tRNA-Tyr* and *tRNA-Trp*.

Discussion

Gastropod mitogenomes tend to be compact (Boore 1999) even while carrying non-coding regions of varying sizes (Grande et al. 2008). Both mitogenomes sequenced from *P. mexicana* encode the standard 37 metazoan genes and possess intergenic non-coding regions. We believe that the 56 bp non-coding region between *tRNA-Ser1* and *Ser2* may represent the putative mitochondrial origin of replication (POR) and control region for *P. mexicana*. The POR is usually an AT-rich sequence that may contain palindromic stretches of nucleotides. The 56 bp region in *P. mexicana* is comparable in size to the presumed POR in *Camaena* and Bradybaenidae and is similarly AT-rich, though it is

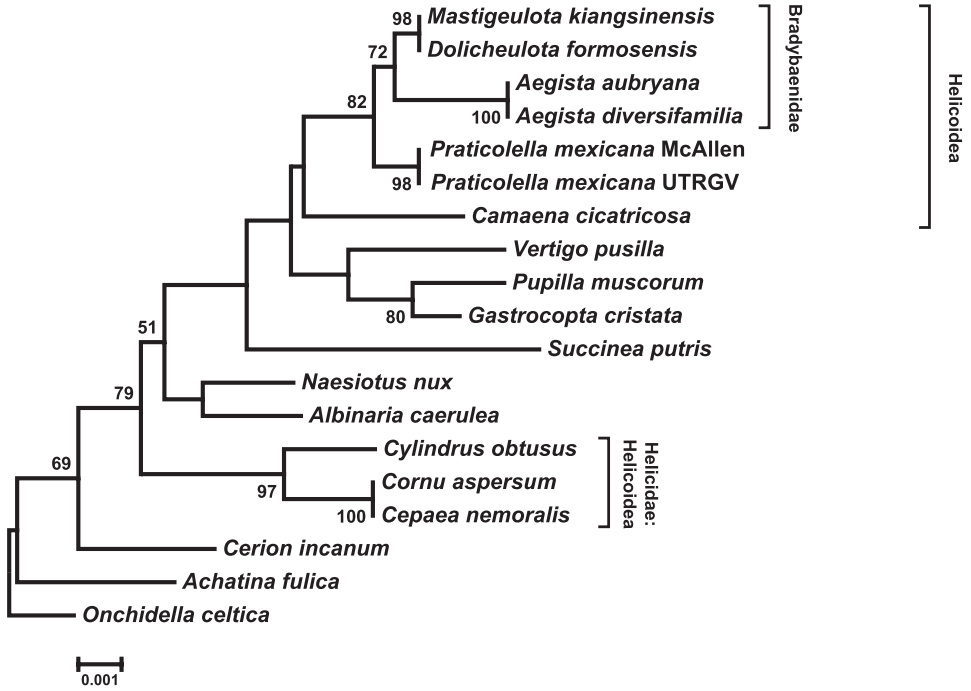

Figure 3. Maximum likelihood phylogeny of gene order. Analysis in MLGO yielded a single tree. Branch support >50% is shown based on 100 bootstrap replicates. Bradybaenidae and Helicidae were recovered as monophyletic, but Helicoidea was not.

often adjacent to *cox3* in pulmonate snails (Gaitán-Espitia et al. 2013). Both new mitogenomes have the same gene order and strand orientations, and have the highest GC skew and third highest AT skew (Perna and Kocher 1995) among the species examined. Strand-specific bias in nucleotide composition is a common feature among metazoan mitogenomes (Hassanin et al. 2005) and may be a constraint of organellar function (Asakawa et al. 1991).

The two *P. mexicana* mitogenomes differ by 71 bp, which was fewer differences than seen in *Cornu aspersum* from Chile (107-149 bp), the only other stylommatophoran with more than one mitogenome available (Gaitán-Espitia et al. 2013). Our preliminary intraspecific mitogenome divergence in *P. mexicana* (0.5%) is comparable to that seen in other metazoans such as butterfly (Vanlalruati et al. 2015) and catfish (Wang et al. 2014b) species. The majority of the differences represent substitutions in non-coding regions or third codon positions. Our results also show that *P. mexicana* uses six different start codons and incomplete stop codons for mitochondrial gene expression. The invertebrate mitochondrial genetic code uses multiple alternate start codons (Osawa et al. 1992, Jukes and Osawa 1993), and partial stop codons are found in other land snail mitogenomes (Groenenberg et al. 2012, Wang et al. 2014a, Yang et al. 2015). Post-transcriptional adenylation is predicted to complete incomplete stop codons (Ojala et al. 1981).

A	B	C	D	E
coxI	*coxI*	*coxI*	*coxI*	*coxI*
V	*V*	*V*	*V*	*V*
16S	*16S*	*16S*	*16S*	*16S*
L1	*L1*	*L1*	*L1*	*L1*
P	***P***	*A*	***P***	***P***
A	*A*	*ND6*	*A*	*A*
ND6	*ND6*	***P***	*ND6*	*ND6*
ND5	*ND5*	*ND5*	*ND5*	*ND5*
ND1	*ND1*	*ND1*	*ND1*	*ND1*
ND4	*ND4*	*ND4*	*ND4*	*ND4*
cytB	*cytB*	*cytB*	*cytB*	*cytB*
D	*D*	*D*	*D*	*D*
C	*C*	*C*	*C*	*C*
F	*F*	*F*	*F*	*F*
coxII	*coxII*	*coxII*	*coxII*	*coxII*
Y	***G***	*Y*	***G***	***G***
W	***H***	*W*	***H***	***H***
G	*Y*	***G***	*Y*	*Y*
H	*W*	***H***	*W*	***ND3***
Q	*Q*	*Q*	*Q*	*W*
L	*L*	*L*	*L*	*Q*
atp8	*atp8*	*atp8*	*atp8*	*L*
N	*N*	*N*	*N*	*atp8*
atp6	*atp6*	*atp6*	*atp6*	*N*
R	*R*	*R*	*R*	*atp6*
E	*E*	*E*	*E*	*R*
12S	*12S*	*12S*	*12S*	*E*
M	*M*	*M*	*M*	*12S*
ND3	***ND3***	***ND3***	***ND3***	*M*
S	*S*	*S*	*S*	*S*
S	***S***	*T*	***S***	***S***
ND4	*ND4*	*coxIII*	*ND4*	*ND4*
T	*T*	***S***	*T*	*T*
coxIII	*coxIII*	*ND4*	*coxIII*	*coxIII*
I	*I*	*I*	*I*	*I*
ND2	*ND2*	*ND2*	*ND2*	*ND2*
K	*K*	*K*	*K*	*K*

Figure 4. Ancestral gene order reconstructions for Helicoidea. Columns (**A–E**) correspond to labeled nodes in Figure 2. IUPAC single letter codes are used to identify tRNA genes. Rearrangements in red and blue are unique to Helicidae. The convergent rearrangement seen in Bradybaenidae, *Camaena*, and *Praticolella* is shown in yellow. The green rearrangement is unique to *Aegista*.

Mitochondrial gene rearrangements are common across Metazoa (Black and Roehrdanz 1998, Boore et al. 2004, Mwinyi et al. 2009, Wang et al. 2016) often including the movement of tRNA genes (Mueller and Boore 2005, Dowton et al. 2009). In Helicoidea, two of the four rearrangements we observed involve tRNA genes only. These tRNA rearrangements are the most common type seen in mitogenomes (Xu et al. 2006) The (*tRNA-Tyr*, *tRNA-Trp*) and (*tRNA-Gly*, *tRNA-His*) rearrangement seen in bradybaenids, camaenids, and polygyrids represents a convergent restructuring of the genome. These homoplastic events involving tRNA genes were first observed in insects (Flook et al. 1995) and have been reported across Arthropoda. The fourth rearrangement we observed is unique to *Aegista*, involving the movement of the *ND3* protein coding gene. While less frequent than tRNA rearrangements, those involving protein coding genes without multiple gene inversions or transpositions have been shown in other mollusks (Grande et al. 2008, Osca et al. 2015).

Our protein sequence data support previous works showing the monophyly of Helicoidea, Helicidae, and Bradybaenidae. Previous work has suggested close relationships between Bradybaenidae, Camaenidae, and Polygyridae, but the monophyly of the former two families remains in question (Wade et al. 2001, Cuezzo 2003, Wade et al. 2006, Wade et al. 2007, Razkin et al. 2015). Unfortunately, with the relatively small number of mitogenomes available, our data were unable to resolve these issues. Our gene order phylogeny further supported the monophyly of Helicidae and Bradybaenidae, suggested close relationships between Bradybaenidae, *Camaena*, and *P. mexicana*, but did not suggest a monophyletic Helicoidea despite its consistent recovery elsewhere (Wade et al. 2001, Grande et al. 2004, Wade et al. 2007, Razkin et al. 2015). This finding was unexpected, since comparisons of gene trees to gene order phylogenies tend to produce similar results across the tree of life when using whole nuclear genomes (Wolf et al. 2001). Differences that do arise have been attributed to the phylogenies deriving from uncorrelated datasets, with gene sequence trees being driven by point mutations in the coding DNA sequence while the gene orders vary through rearrangement (Sankoff et al. 1992). While many studies examine mitochondrial gene order in the context of sequence phylogenies (e.g. Aguileta et al. 2014, Weigert et al. 2016), we found no studies that used MLGO or similar older programs (e.g. MGRA, Alekseyev and Pevzner 2009) to generate mitochondrial gene order phylogenies. More thorough and inclusive analyses are needed to determine to what extent the two types of phylogenies can be congruent and how that congruence speaks to mitogenomic evolution (Leigh et al. 2011).

Acknowledgements

RLM is supported in part by faculty research and development funds and a Barrios fellowship from UHCL. MAMC and KEP would like to acknowledge UTRGV Science Education Grant #52007568 funded by the Howard Hughes Medical Institute, ADVANCE Institutional Transformation Grant (NSF# 1209210), UTRGV Faculty Research Council, and College of Sciences for financial support. This work was sup-

ported in part by the National Science Foundation (under grant HRD-1463991). Any opinions, findings, and conclusions or recommendations are those of the authors and do not necessarily reflect the views of NSF. Jolanta Jaromczyk at UK Healthcare Genomics assisted with genome assembly.

References

Aguileta G, de Vienne DM, Ross ON, Hood ME, Giraud T, Petit E, Gabaldon T (2014) High variability of mitochondrial gene order among fungi. Genome Biology and Evolution 6: 451–465. doi: 10.1093/gbe/evu028

Alekseyev M, Pevzner PA (2009) Breakpoint graphs and ancestral genome reconstructions. Genome Research 19: 943–957. doi: 10.1101/gr.082784.108

Altschul SF, Gish W, Miller W, Myers EW, Lipman DJ (1990) Basic local alignment search tool. Journal of Molecular Biology 215: 403–410. doi: 10.1016/S0022-2836(05)80360-2

Asakawa S, Kumazawa Y, Araki T, Himeno H, Miura K-i, Watanabe K (1991) Strand-specific nucleotide composition bias in echinoderm and vertebrate mitochondrial genomes. Journal of Molecular Evolution 32: 511–520. doi: 10.1007/bf02102653

Avise JC, Arnold J, Ball RM, Bermingham E, Lamb T, Neigel JE, Reeb CA, Saunders NC (1987) Intraspecific phylogeography: the mitochondrial DNA bridge between population genetics and systematics. Annual Review of Ecology and Systematics 18: 489–522. doi: 10.1146/annurev.ecolsys.18.1.489

Bader M, Abouelhoda MI, Ohlebusch E (2008) A fast algorithm for the multiple genome rearrangement problem with weighted reversals and transpositions. BMC Bioinformatics 9: 516. doi: 10.1186/1471-2105-9-516

Beesley PL, Ross GJ, Wells A (1998) Mollusca: the southern synthesis. CSIRO publishing, 1250 pp.

Bernt M, Donath A, Jühling F, Externbrink F, Florentz C, Fritzsch G, Pütz J, Middendorf M, Stadler PF (2013) MITOS: Improved de novo metazoan mitochondrial genome annotation. Molecular Phylogenetics and Evolution 69: 313–319. doi: 10.1016/j.ympev.2012.08.023

Black W, Roehrdanz RL (1998) Mitochondrial gene order is not conserved in arthropods: prostriate and metastriate tick mitochondrial genomes. Molecular Biology and Evolution 15: 1772–1785. doi: 10.1093/oxfordjournals.molbev.a025903

Boore JL (1999) Animal mitochondrial genomes. Nucleic Acids Research 27: 1767–1780. doi: 10.1093/nar/27.8.1767

Boore JL, Brown WM (1998) Big trees from little genomes: mitochondrial gene order as a phylogenetic tool. Current Opinion in Genetics and Development 8: 668–674. doi: 10.1016/s0959-437x(98)80035-x

Boore JL, Medina M, Rosenberg LA (2004) Complete sequences of the highly rearranged molluscan mitochondrial genomes of the scaphopod *Graptacme eborea* and the bivalve Mytilus edulis. Molecular Biology and Evolution 21: 1492–1503. doi: 10.1093/molbev/msh090

Bouchet P, Rocroi J-P, Frýda J, Hausdorf B, Ponder W, Valdés Á, Warén A (2005) Classification and nomenclator of gastropod families. Malacologia 47: 1–397. doi: 10.4002/040.052.0201

Cuezzo MG (2003) Phylogenetic analysis of the Camaenidae (Mollusca: Stylommatophora) with special emphasis on the American taxa. Zoological Journal of the Linnean Society 138: 449–476. doi: 10.1046/j.1096-3642.2003.00061.x

Deng P-J, Wang W-M, Huang X-C, Wu X-P, Xie G-L, Ouyang S (2016) The complete mitochondrial genome of Chinese land snail *Mastigeulota kiangsinensis* (Gastropoda: Pulmonata: Bradybaenidae). Mitochondrial DNA 27: 1441–1442. doi: 10.3109/19401736.2014.953083

Dowton M, Cameron SL, Dowavic JI, Austin AD, Whiting MF (2009) Characterization of 67 mitochondrial tRNA gene rearrangements in the Hymenoptera suggests that mitochondrial tRNA gene position is selectively neutral. Molecular Biology and Evolution 26: 1607–1617. doi: 10.1093/molbev/msp072

Edgar RC (2004) MUSCLE: multiple sequence alignment with high accuracy and high throughput. Nucleic Acids Research 32: 1792–1797. doi: 10.1093/nar/gkh340

Flook P, Rowell H, Gellissen G (1995) Homoplastic rearrangements of insect mitochondrial tRNA genes. Naturwissenschaften 82: 336–337. doi: 10.1007/bf01131531

Funk DJ, Omland KE (2003) Species-level paraphyly and polyphyly: frequency, causes, and consequences, with insights from animal mitochondrial DNA. Annual Review of Ecology, Evolution, and Systematics 34: 397–423. doi: 10.1146/annurev.ecolsys.34.011802.132421

Gaitán-Espitia JD, Nespolo RF, Opazo JC (2013) The complete mitochondrial genome of the land snail *Cornu aspersum* (Helicidae: Mollusca): intra-specific divergence of protein-coding genes and phylogenetic considerations within Euthyneura. PLOS ONE 8: e67299. doi: 10.1371/journal.pone.0067299

Gissi C, Iannelli F, Pesole G (2008) Evolution of the mitochondrial genome of Metazoa as exemplified by comparison of congeneric species. Heredity 101: 301–320. doi: 10.1038/hdy.2008.62

Grande C, Templado J, Cervera JL, Zardoya R (2004) Molecular phylogeny of euthyneura (Mollusca: Gastropoda). Molecular Biology and Evolution 21: 303–313. doi: 10.1093/molbev/msh016

Grande C, Templado J, Zardoya R (2008) Evolution of gastropod mitochondrial genome arrangements. BMC Evolutionary Biology 8: 61. doi: 10.1186/1471-2148-8-61

Gribaldo S, Philippe H (2002) Ancient phylogenetic relationships. Theoretical Population Biology 61: 391–408. doi: 10.1006/tpbi.2002.1593

Groenenberg DS, Neubert E, Gittenberger E (2011) Reappraisal of the "Molecular phylogeny of Western Palaearctic Helicidae sl (Gastropoda: Stylommatophora)": when poor science meets GenBank. Molecular Phylogenetics and Evolution 61: 914–923. doi: 10.1016/j.ympev.2011.08.024

Groenenberg DS, Pirovano W, Gittenberger E, Schilthuizen M (2012) The complete mitogenome of *Cylindrus obtusus* (Helicidae, Ariantinae) using Illumina next generation sequencing. BMC Genomics 13: 114. doi: 10.1186/1471-2164-13-114

Hassanin A, Léger N, Deutsch J (2005) Evidence for multiple reversals of asymmetric mutational constraints during the evolution of the mitochondrial genome of Metazoa, and consequences for phylogenetic inferences. Systematic Biology 54: 277–298. doi: 10.1080/10635150590947843

Hatzoglou E, Rodakis GC, Lecanidou R (1995) Complete sequence and gene organization of the mitochondrial genome of the land snail *Albinaria coerulea*. Genetics 140: 1353–1366.

He Z-P, Dai X-B, Zhang S, Zhi T-T, Lun Z-R, Wu Z-D, Yang T-B (2016) Complete mitochondrial genome of the giant African snail, *Achatina fulica* (Mollusca: Achatinidae): a novel location of putative control regions (CR) in the mitogenome within Pulmonate species. Mitochondrial DNA 27: 1084–1085. doi: 10.3109/19401736.2014.930833

Hu F, Lin Y, Tang J (2014) MLGO: phylogeny reconstruction and ancestral inference from gene-order data. BMC Bioinformatics 15: 1. doi: 10.1186/s12859-014-0354-6

Huang C-W, Lin S-M, Wu W-L (2016) Mitochondrial genome sequences of landsnails *Aegista diversifamilia* and *Dolicheulota formosensis* (Gastropoda: Pulmonata: Stylommatophora). Mitochondrial DNA 27: 2793–2795. doi: 10.3109/19401736.2015.1053070

Hunter SS, Settles ML, New DD, Parent CE, Gerritsen AT (2016) Mitochondrial genome sequence of the Galápagos endemic land snail *Naesiotus nux*. Genome Announcements 4: e01362–01315. doi: 10.1128/genomea.01362-15

Jukes T, Osawa S (1993) Evolutionary changes in the genetic code. Comparative Biochemistry and Physiology Part B: Comparative Biochemistry 106: 489–494. doi: 10.1016/0305-0491(93)90122-l

Kearse M, Moir R, Wilson A, Stones-Havas S, Cheung M, Sturrock S, Buxton S, Cooper A, Markowitz S, Duran C (2012) Geneious Basic: an integrated and extendable desktop software platform for the organization and analysis of sequence data. Bioinformatics 28: 1647–1649. doi: 10.1093/bioinformatics/bts199

Kishino H, Hasegawa M (1989) Evaluation of the maximum likelihood estimate of the evolutionary tree topologies from DNA sequence data, and the branching order in Hominoidea. Journal of Molecular Evolution 29: 170–179. doi: 10.1007/bf02100115

Klussmann-Kolb A, Dinapoli A, Kuhn K, Streit B, Albrecht C (2008) From sea to land and beyond–new insights into the evolution of euthyneuran Gastropoda (Mollusca). BMC Evolutionary Biology 8: 57. doi: 10.1186/1471-2148-8-57

Laslett D, Canbäck B (2008) ARWEN: a program to detect tRNA genes in metazoan mitochondrial nucleotide sequences. Bioinformatics 24: 172–175. doi: 10.1093/bioinformatics/btm573

Leigh JW, Lapointe F-J, Lopez P, Bapteste E (2011) Evaluating phylogenetic congruence in the post-genomic era. Genome Biology and Evolution 3: 571–587. doi: 10.1093/gbe/evr050

Lin Y, Hu F, Tang J, Moret BM (2013) Maximum likelihood phylogenetic reconstruction from high-resolution whole-genome data and a tree of 68 eukaryotes. In: Pacific Symposium on Biocomputing Pacific Symposium on Biocomputing. NIH Public Access, 285 pp.

Lowe TM, Eddy SR (1997) tRNAscan-SE: a program for improved detection of transfer RNA genes in genomic sequence. Nucleic Acids Research 25: 955–964. doi: 10.1093/nar/25.5.0955

Manganelli G, Salomone N, Giusti F (2005) A molecular approach to the phylogenetic relationships of the western palaearctic Helicoidea (Gastropoda: Stylommatophora). Biological Journal of the Linnean Society 85: 501–512. doi: 10.1111/j.1095-8312.2005.00514.x

Marquardt JD (2013) Mitochondrial genome evolution in pupillid land snails. MS thesis, University of New Mexico, Albuguerque, New Mexico. http://hdl.handle.net/1928/23195

Milbury CA, Gaffney PM (2005) Complete mitochondrial DNA sequence of the eastern oyster *Crassostrea virginica*. Marine Biotechnology 7: 697–712. doi: 10.1007/s10126-005-0004-0

Mindell DP, Sorenson MD, Dimcheff DE (1998) Multiple independent origins of mitochondrial gene order in birds. Proceedings of the National Academy of Sciences 95: 10693–10697. doi: 10.1073/pnas.95.18.10693

Minh BQ, Nguyen MAT, von Haeseler A (2013) Ultrafast approximation for phylogenetic bootstrap. Molecular Biology and Evolution 30: 1188–1195. doi: 10.1093/molbev/mst024

Mueller RL, Boore JL (2005) Molecular mechanisms of extensive mitochondrial gene rearrangement in plethodontid salamanders. Molecular Biology and Evolution 22: 2104–2112. doi: 10.1093/molbev/msi204

Mwinyi A, Meyer A, Bleidorn C, Lieb B, Bartolomaeus T, Podsiadlowski L (2009) Mitochondrial genome sequence and gene order of *Sipunculus nudus* give additional support for an inclusion of Sipuncula into Annelida. BMC Genomics 10: 27. doi: 10.1186/1471-2164-10-27

Nguyen L-T, Schmidt HA, von Haeseler A, Minh BQ (2014) Iq-tree: A fast and effective stochastic algorithm for estimating maximum-likelihood phylogenies. Molecular Biology and Evolution 32: 268–274. doi: 10.1093/molbev/msu300

Ojala D, Montoya J, Attardi G (1981) tRNA punctuation model of RNA processing in human mitochondria. Nature 290: 470–474. doi: 10.1038/290470a0

Osawa S, Jukes T, Watanabe K, Muto A (1992) Recent evidence for evolution of the genetic code. Microbiological Reviews 56: 229–264.

Osca D, Templado J, Zardoya R (2015) Caenogastropod mitogenomics. Molecular Phylogenetics and Evolution 93: 118–128. doi: 10.1016/j.ympev.2015.07.011

Perez KE (2011) A new species of *Praticolella* (Gastropoda: Polygyridae) from northeastern Mexico and revision of several species of this genus. Nautilus 125: 113–126.

Perez KE, Defreitas N, Slapcinsky J, Minton RL, Anderson FE, Pearce TA (2014) Molecular phylogeny, evolution of shell shape, and DNA barcoding in Polygyridae (Gastropoda: Pulmonata), an endemic North American clade of land snails. American Malacological Bulletin 32: 1–31. doi: 10.4003/006.032.0103

Perna NT, Kocher TD (1995) Patterns of nucleotide composition at fourfold degenerate sites of animal mitochondrial genomes. Journal of Molecular Evolution 41: 353–358. doi: 10.1007/bf00186547

Rawlings TA, MacInnis MJ, Bieler R, Boore JL, Collins TM (2010) Sessile snails, dynamic genomes: gene rearrangements within the mitochondrial genome of a family of caenogastropod molluscs. BMC Genomics 11: 440. doi: 10.1186/1471-2164-11-440

Razkin O, Gómez-Moliner BJ, Prieto CE, Martínez-Ortí A, Arrébola JR, Muñoz B, Chueca LJ, Madeira MJ (2015) Molecular phylogeny of the western Palaearctic Helicoidea (Gastropoda, Stylommatophora). Molecular Phylogenetics and Evolution 83: 99–117. doi: 10.1016/j.ympev.2014.11.014

Rokas A, Holland PW (2000) Rare genomic changes as a tool for phylogenetics. Trends in Ecology and Evolution 15: 454–459. doi: 10.1016/s0169-5347(00)01967-4

Rota-Stabelli O, Yang Z, Telford MJ (2009) MtZoa: a general mitochondrial amino acid substitutions model for animal evolutionary studies. Molecular Phylogenetics and Evolution 52: 268–272. doi: 10.1016/j.ympev.2009.01.011

Saccone C, De Giorgi C, Gissi C, Pesole G, Reyes A (1999) Evolutionary genomics in Metazoa: the mitochondrial DNA as a model system. Gene 238: 195–209. doi: 10.1016/s0378-1119(99)00270-x

Sankoff D, Leduc G, Antoine N, Paquin B, Lang BF, Cedergren R (1992) Gene order comparisons for phylogenetic inference: Evolution of the mitochondrial genome. Proceedings of the National Academy of Sciences 89: 6575–6579. doi: 10.1073/pnas.89.14.6575

Shao R, Campbell NJ, Schmidt ER, Barker SC (2001) Increased rate of gene rearrangement in the mitochondrial genomes of three orders of hemipteroid insects. Molecular Biology and Evolution 18: 1828–1832. doi: 10.1093/oxfordjournals.molbev.a003970

Steinke D, Albrecht C, Pfenninger M (2004) Molecular phylogeny and character evolution in the Western Palaearctic Helicidae *s.l.* (Gastropoda: Stylommatophora). Molecular Phylogenetics and Evolution 32: 724–734. doi: 10.1016/j.ympev.2004.03.004

Terrett J, Miles S, Thomas R (1996) Complete DNA sequence of the mitochondrial genome of *Cepaea nemoralis* (Gastropoda: Pulmonata). Journal of Molecular Evolution 42: 160–168. doi: 10.1007/bf02198842

Vanlalruati C, De Mandal S, Guruswami G, Nachimuthu SK (2015) Illumina based whole mitochondrial genome of *Junonia iphita* reveals minor intraspecific variation. Genomics Data 6: 280–282. doi: 10.1016/j.gdata.2015.10.016

Wade CM, Hudelot C, Davison A, Naggs F, Mordan PB (2007) Molecular phylogeny of the helicoid land snails (Pulmonata: Stylommatophora: Helicoidea), with special emphasis on the Camaenidae. Journal of Molluscan Studies 73: 411–415. doi: 10.1093/mollus/eym030

Wade CM, Mordan PB, Clarke B (2001) A phylogeny of the land snails (Gastropoda: Pulmonata). Proceedings of the Royal Society of London B: Biological Sciences 268: 413–422. doi: 10.1098/rspb.2000.1372

Wade CM, Mordan PB, Naggs F (2006) Evolutionary relationships among the Pulmonate land snails and slugs (Pulmonata, Stylommatophora). Biological Journal of the Linnean Society 87: 593–610. doi: 10.1111/j.1095-8312.2006.00596.x

Wang P, Yang H-F, Zhou W-C, Hwang C-C, Zhang W-H, Qian Z-X (2014a) The mitochondrial genome of the land snail *Camaena cicatricosa* (Müller, 1774) (Stylommatophora, Camaenidae): The first complete sequence in the family Camaenidae. ZooKeys 451: 33–48. doi: 10.3897/zookeys.451.8537

Wang Q, Xu C, Xu C, Wang R (2014b) Complete mitochondrial genome of the Southern catfish (*Silurus meridionalis* Chen) and Chinese catfish (*S. asotus* Linnaeus): Structure, phylogeny, and intraspecific variation. Genetics and Molecular Research 14: 18198–18209. doi: 10.4238/2015.december.23.7

Wang Z-L, Li C, Fang W-Y, Yu X-P (2016) The complete mitochondrial genome of two *Tetragnatha* spiders (Araneae: Tetragnathidae): Severe truncation of tRNAs and novel gene rearrangements in Araneae. International Journal of Biological Sciences 12: 109. doi: 10.7150/ijbs.12358

Weigert A, Golombek A, Gerth M, Schwarz F, Struck TH, Bleidorn C (2016) Evolution of mitochondrial gene order in Annelida. Molecular Phylogenetics and Evolution 94: 196–206. doi: 10.1016/j.ympev.2015.08.008

White TR, Conrad MM, Tseng R, Balayan S, Golding R, de Frias Martins A, Dayrat BA (2011) Ten new complete mitochondrial genomes of pulmonates (Mollusca: Gastropoda) and their impact on phylogenetic relationships. BMC Evolutionary Biology 11: 295. doi: 10.1186/1471-2148-11-295

Wolf YI, Rogozin IB, Grishin NV, Tatusov RL, Koonin EV (2001) Genome trees constructed using five different approaches suggest new major bacterial clades. BMC Evolutionary Biology 1: 8. doi: 10.1186/1471-2148-1-8

Xia X, Xie Z (2001) DAMBE: software package for data analysis in molecular biology and evolution. Journal of Heredity 92: 371–373. doi: 10.1093/jhered/92.4.371

Xu W, Jameson D, Tang B, Higgs PG (2006) The relationship between the rate of molecular evolution and the rate of genome rearrangement in animal mitochondrial genomes. Journal of Molecular Evolution 63: 375–392. doi: 10.1007/s00239-005-0246-5

Yang X, Xie G-L, Wu X-P, Ouyang S (2016) The complete mitochondrial genome of Chinese land snail *Aegista aubryana* (Gastropoda: Pulmonata: Bradybaenidae). Mitochondrial DNA 27: 3538–3539. doi: 10.3109/19401736.2015.1074207

Yang Z (1998) On the best evolutionary rate for phylogenetic analysis. Systematic Biology 47: 125–133. doi: 10.1080/106351598261067